

**EVALUATING THE EXPRESSION PROFILE
AND DEVELOPMENTAL POTENTIAL OF
MOUSE KIDNEY-DERIVED STEM CELLS**

Thesis submitted in accordance with the
requirements of the University of Liverpool for the
degree of Doctor in Philosophy

by

Egon Jacopo Ranghini

February 2011

Acknowledgements

My first and biggest acknowledgement is for my Supervisor, Dr. Patricia Murray, for leading my work during my PhD always with true enthusiasm, for her endless support, for her precious advices and for all the opportunities I was given since I arrived in Liverpool. The progresses I have made and the scientist I have become have been possible thanks to her supervision.

I would like to sincerely acknowledge Dr. Bettina Wilm, Mr. Simon Kenny and Prof. David Edgar for following my work with deep interest, for their accurate suggestions and their helpful criticisms that have profoundly contributed to improve my work.

I feel very grateful to Prof. Giovanni Camussi and Prof. Benedetta Bussolati, as I was given the opportunity to work and complete a crucial part of my project under their supervision in Torino. Many thanks to Dr. Stefania Bruno for her support and for the time and energy she dedicated to my work during my stay in Torino.

I would like to deeply thank Mr. Sokratis Theocharatos for providing the EGFP-expressing vector, but mostly for being a great and truthful friend. Your company and friendship was very important for me and I already know I will miss you, my friend, when I leave Liverpool.

I would like to express all my gratitude to my sincere friend Abs for his company and for sharing with me nearly 4 years in Liverpool. I'm also very grateful to all my friends in Liverpool, in particular to Maurycy, Deepak, Ale, Nicole, Milos, Laurence and Jonathan for making me feel like I was at home. I cannot find the right words to explain how that was important for me! Last, but not least, I would like to thank all my colleagues in Liverpool, my relatives and anyone who gave me support, advices and criticisms during these years. Grazie!

ABSTRACT

The mammalian kidney develops through a series of complex interactions between two embryonic tissues - the metanephric mesenchyme (MM) and the ureteric bud (UB). It has been demonstrated that all cell types present in the main body of the nephron, the functional unit of the adult kidney, derive from a population of progenitor cells present in the cap mesenchyme, a domain of the MM adjacent to the UB tips. It is therefore plausible that a fraction of these progenitor cells might remain undifferentiated as the kidney develops, in order to give rise to the resident kidney stem/progenitor cells present in the adult organ. The main objective of the present study was to compare the expression profile and nephrogenic potential of *in vitro* cultured MM cells with that of a kidney-derived stem cell clonal line (H6 clone), isolated from postnatal mouse kidney. The rationale of this study was that a comparable expression profile and nephrogenic ability between *in vitro* cultured MM cells and H6 cells would suggest that the H6 clonal line might represent a remnant of the embryonic MM present in the adult kidney.

The initial part of this study aimed to optimize culture conditions that could support the expansion of MM cells, isolated from E11.5 mouse kidney rudiments, *in vitro* for several days. It was found that when cultured in the presence of BMP7 and FGF2 and on uncoated tissue culture dishes, MM cells could undergo expansion and maintained an MM-like phenotype for several days, as indicated by the expression of many MM-specific markers, such as *Wt1*, *Osr1*, *Sall1*, *Gdnf* and *Vim*. The nephrogenic potential of *in vitro* cultured MM cells was investigated using the chimera

formation assay, which consisted of recombining MM cells, labelled with quantum dots, with E11.5 reaggregated kidney rudiments. If MM cells following *in vitro* culture retained a nephrogenic potential, then it would be expected that they would be able to participate nephrogenesis and integrate into nephron-like developing structures. The chimera formation assay demonstrated that *in vitro* cultured MM cells retained a nephrogenic potential, as following recombination with E11.5 reaggregated kidney rudiments, cultured MM cells were able to integrate into nephron-like developing structures, but not into the UB. In the second part of this study the expression profile and nephrogenic potential of the H6 clonal line was investigated and compared with that of cultured MM cells. The H6 clonal line showed limitless proliferative capacity and the ability to spontaneously generate renal-like cell types in culture, such as podocyte-like and proximal tubule-like cells. Besides, H6 cells could also differentiate into non renal cell types, such as osteocytes and adipocytes. H6 cells expressed many stem cell markers and, except for *Sall1*, the same set of MM-specific genes already found in freshly isolated and cultured MM cells. In addition, H6 cells expressed many markers normally found in fully differentiated renal cells, such as *synaptopodin*, *megalyn*, *desmin* and *aquaporin1*. *In vitro* megalin functionality assay demonstrated that the H6 clonal line could generate functional proximal tubule-like cells, as a subset of H6 cells was able to uptake albumin through the megalin receptor. Following recombination with E11.5 reaggregated kidney rudiments, H6 cells integrated into nephron-like developing structures at a comparable ratio with that of 4 days cultured MM cells. In addition, H6 cells participated in the formation of developing renal-like structures, such as developing glomeruli and proximal tubules. Similar to the embryonic MM, the

H6 clonal line did not integrate into UB. In the last part of this study the nephrogenic potential of the H6 clonal line was investigated in a mouse model of acute renal tubular failure (ARF), induced by intramuscular injection of glycerol. When injected into the tail vein of ARF-induced mice at the peak of renal injury, H6 cells were able to reach the kidney and engraft mainly, if not exclusively, into damaged proximal tubules. The cells persisted in the kidney for up to 9 days, which was the latest time point investigated. Engrafted cells displayed apical localization of megalin, suggesting that they had differentiated to proximal tubule cells *in vivo*. However, it was found that the H6 clonal line could not accelerate the recovery of ARF-induced kidney, compared with PBS-injected animals. Finally, it was found that the H6 clonal line did not integrate into non-target organs, such as lung, spleen and liver, and did not show any tumorigenic potential. In conclusion, the results of this study suggest that the H6 clonal line might represent a remnant of the embryonic MM present in the postnatal organ. The H6 clonal line might act as a bi-potent stem cell population, since it is able to generate podocyte-like cells and proximal tubule-like cells in culture.

TABLE OF CONTENTS

List of Figures and Tables	Page X
Glossary	XVIII
Chapter 1	1
1.1 The kidney	2
1.1.1 The nephron	3
1.1.2 Kidney development	7
1.1.2.1 <i>The pronephros</i>	9
1.1.2.2 <i>The mesonephros</i>	9
1.1.2.3 <i>The metanephros</i>	10
1.1.3 Mechanisms of induction in the metanephrogenic mesoderm	12
1.2 Chronic kidney disease and end-stage renal disease	24
1.3 Stem cells	28
1.3.1 Stem cells in development and homeostasis	28
1.3.2 Stem cells for the treatment of acute renal failure	31
1.3.2.1 <i>Stem cells from rodent kidney</i>	32
1.3.2.2 <i>Stem cells from human kidney</i>	39
1.3.2.3 <i>Stem cells from fetal kidney</i>	42
1.3.2.4 <i>Mesenchymal stem cells</i>	45
1.3.2.5 <i>Human amniotic fluid stem cells</i>	49
1.4 Aims of the project	56

Chapter 2	58
2.1 Dissection	59
2.1.1 Animal husbandry	59
2.1.2 Dissection of organs from adult mice	59
2.1.2.1 <i>Dissection of kidneys from postnatal mice</i>	60
2.1.3 Dissection of embryonic kidney rudiments	60
2.1.4 Dissection of metanephric mesenchyme	60
2.1.5 Dissection of spinal cord	61
2.2. Tissue culture	61
2.2.1 Culture of the kidney-derived H6 and E5 clonal lines	61
2.2.2 Freezing of the kidney-derived H6 and E5 clonal lines	62
2.2.3 Thawing of the kidney-derived H6 and E5 clonal lines	63
2.2.4 Culture of metanephric mesenchyme	63
2.2.5 Co-culture of metanephric mesenchyme and spinal cord	63
2.2.6 Culture of metanephric mesenchyme in the presence of GSK-3 inhibitor IX	65
2.2.7 Culture of kidney rudiments	67
2.2.8 Culture of kidney rudiments chimeras	67
2.2.8.1 <i>Culture of metanephric mesenchyme with embryonic kidney rudiments</i>	67
2.2.8.2 <i>Culture of the H6 clonal line with embryonic kidney rudiments</i>	69
2.2.9 <i>In vitro</i> differentiation of the H6 clonal line	69
2.2.10 Cell expansion assay	70

2.3 Cell labelling	71
2.3.1 Lentiviral transduction to generate H6 EGFP ⁺ cells	71
2.3.2 Quantum dots labelling	72
2.4 Fixation and preparation of tissue sections	73
2.4.1 Fixation of cultured cells	73
2.4.2 Fixation of cultured cells for osteogenic and adipogenic differentiation assays	73
2.4.3 Fixation of cultured cells for megalin functionality assay	73
2.4.4 Fixation of samples cultured on membrane filter	74
2.4.4.1 <i>Fixation of chimeras containing H6 EGFP⁺ cells</i>	74
2.4.5 Fixation of kidneys for paraffin-embedded sections	74
2.4.6 Fixation of frozen organ sections	74
2.4.7 Preparation of paraffin-embedded kidney sections	75
2.4.8 Preparation of adult organs frozen sections	76
2.4.9 Preparation of microscope subbed slides	76
2.5 Proximal tubule cell functionality assay	76
2.5.1 Megalin functionality assay	76
2.5.2 Competitive inhibition of BSA uptake	77
2.5.3 Organic anion transport functionality assay	77
2.6 Renal injury model	78
2.6.1 Animal husbandry	78
2.6.2 Induction of renal injury	79

2.6.3 H6 EGFP ⁺ cell inoculation	79
2.6.4 Determination of blood urea nitrogen and serum creatinine levels	80
2.6.5 Proliferative activity of kidney tubular cells	80
2.6.6 Tumorigenic assay	81
2.7 Flow cytometry	81
2.7.1 Flow cytometry on cultured cells	81
2.7.2 Flow cytometry on ARF-induced disaggregated kidneys	82
2.8 Immuno- and histological staining	83
2.8.1 Immunofluorescence staining of cultured cells	83
2.8.2 Immunofluorescence staining of samples cultured on membrane filter	84
2.8.3 Evaluation of differentiation assays	84
2.8.4 Deparaffinization of paraffin-embedded kidney sections	85
2.8.5 Haematoxylin and eosin staining	85
2.8.6 Immunohistochemistry of paraffin- embedded kidney sections	86
2.8.7 Immunohistochemistry of frozen lung, spleen and liver sections	87
2.9 Molecular biology	88
2.9.1 RNA extraction	88
2.9.2 DNA extraction	89
2.9.3 DNase treatment	89
2.9.4 cDNA synthesis	89
2.9.5 Oligonucleotide primers	90
2.9.6 PCR reaction	90
2.9.7 Gel electrophoresis	91
2.10 Statistical analysis	91

3.3 Discussion	128
Chapter 4	132
4.1 Introduction	133
4.2 Results	141
4.2.1 Investigating the ability of cultured MM cells to undergo induction using Grobstein's assay	141
4.2.2 Investigating the ability of cultured MM cells to undergo induction following BIO incubation	147
4.2.3 Investigating the <i>in vitro</i> nephrogenic potential of MM cells	153
4.2.3.1 <i>Recombination of freshly isolated MM cells with E11.5 reaggreated kidney rudiments</i>	155
4.2.3.2 <i>Recombination of 4 days cultured MM cells with E11.5 reaggreated kidney rudiments</i>	157
4.2.4 Comparing the ability of freshly isolated and cultured MM cells to integrate into developing nephrons	159
4.3 Discussion	161
Chapter 5	169
5.1 Introduction	170
5.2 Results	174
5.2.1 Ability of H6 cells to form renal-like cell types <i>in vitro</i>	174
5.2.1.1 <i>Morphology of the H6 clonal line</i>	174
5.2.1.2 <i>Renal cell-specific gene expression in the H6 clonal line</i>	175

5.2.1.3	<i>Cytofluorimetric analysis of the H6 clonal line</i>	179
5.2.1.4	<i>Renal cell-specific protein expression in the H6 clonal line</i>	181
5.2.2	Evaluating the ability of H6 cells to differentiate into non-renal cell types	183
5.2.2.1	<i>Ability of H6 cells to differentiate into osteocytes and adipocytes</i>	184
5.2.2.2	<i>Ability of H6 cells to differentiate into endothelial cells</i>	185
5.2.3	Determining the growth rate of the H6 cell population	187
5.3	Discussion	189
Chapter 6		197
6.1	Introduction	198
6.2	Results	205
6.2.1	Investigating the <i>in vitro</i> nephrogenic potential of the H6 clonal line	205
6.2.1.1	<i>H6 cells expressing enhanced green fluorescent protein</i>	206
6.2.1.2	<i>Recombination of the H6 clonal line with E11.5 reaggregated kidney rudiments</i>	208
6.2.2	Determining the percentage of H6 cells integrated into nephron-like developing structures	212
6.2.3	Investigating the functionality of the H6 clonal line <i>in vitro</i>	214
6.2.3.1	<i>The H6 clonal line expressed functional megalin</i>	214

6.2.3.2	<i>Co-localization of megalin with fluorescent BSA</i>	216
6.2.3.3	<i>Investigating organic anion transporter functionality in the H6 clonal line</i>	217
6.2.3.4	<i>Investigating the expression of OAT genes in H6 cells</i>	220
6.3	Discussion	221
Chapter 7		227
7.1	Introduction	228
7.2	Results	233
7.2.1	Establishing the acute renal tubular injury model in CD1 mice	233
7.2.1.1	<i>Determining the presence of the gene Sry in the H6 clonal line</i>	233
7.2.1.2	<i>Optimization of glycerol dose in mice</i>	235
7.2.2	Investigating the ability of the H6 clonal line to engraft into ARF-induced mouse kidneys	238
7.2.2.1	<i>Immunohistochemical staining to detect the presence of H6 cells in host kidney</i>	239
7.2.2.2	<i>Cytofluorimetric analysis to confirm the ability of H6 cells to engraft into host kidney</i>	241
7.2.3	Investigating the unspecific engraftment of the H6 clonal line	242
7.2.4	Investigating the ability of the H6 clonal line to differentiate into renal tubular cells	243
7.2.5	Evaluating the renal function of ARF-induced mice following H6 EGFP ⁺ cell inoculation	245
7.2.6	Determining the proliferative activity of ARF-induced mouse kidney tubular cells	249

7.2.7 Investigating the tumorigenic potential of the H6 clonal line	251
7.3 Discussion	252
Chapter 8	261
8.1 Final discussion	262
8.2 Future works	280
References	283

LIST OF FIGURES AND TABLES

Figure 1. Section of human kidney.	Page 2
Figure 2. Representation of nephron.	3
Figure 3. Scanning electron micrograph of a podocyte with cytoplasmic and foot processes surrounding glomerular capillaries.	5
Figure 4. Transverse section of human embryo (E21.0) showing the three embryonic germ layers.	7
Figure 5. Schematic representation of mesoderm layers and their derivative tissues.	8
Figure 6. Schematic representation of mammalian kidney development.	9
Figure 7. Representation of reciprocal induction between metanephric blastema and epithelium during kidney development.	11
Figure 8. Representation of <i>Gdnf</i> (red) and <i>Ret</i> and <i>Gfra1</i> expression during kidney development.	14
Figure 9. Proposed molecular cascade for metanephric mesenchyme induction.	23
Figure 10. Projection of prevalence of ESRD using data available through 2000 and data available through 2006.	26
Figure 11. Representation of stem cell self-renewal and differentiation into different specialized cell types.	28
Figure 12. Schematic representation of the Bowman's capsule.	41
Figure 13. Schematic representation of transfilter culture.	64

Figure 14. Strategy adopted to induce freshly isolated (t=0) MM and MM following 24h, 48h and 72 hours of culture by stimulation with spinal cord.	65
Figure 15. Strategy followed to induce freshly isolated (t=0) MM and MM following 24h, 48h and 72 hours of culture by stimulation with BIO.	66
Figure 16. Chimera formation assay protocol	69
Figure 17. Diagram of the EGFP-expressing vector used to transfect the H6 clonal line.	71
Figure 18. E11.5 embryonic kidney rudiments.	103
Figure 19. Metanephric mesenchyme and ureteric bud after separation.	103
Figure 20. MM cells cultured for 24, 48 and 96 hours in control medium and in the presence of 50 ng/ml BMP7 and 50ng/ml BMP7 + 100ng/ml FGF2.	105
Figure 21. MM cells cultured for 96 hours in the presence of FGF2 only, FGF2 + 25ng/ml BMP7 and FGF2 + 50ng/ml BMP7.	108
Figure 22. Strategy followed to subculture MM cells.	109
Figure 23. Metanephric mesenchyme cells subcultured at passage 1 in MM medium supplemented with 25 ng/ml BMP7 and 100 ng/ml FGF2.	110
Figure 24. Metanephric mesenchyme cells subcultured at passage 2 in MM medium supplemented with 25 ng/ml BMP7 and 100 ng/ml FGF2.	110
Figure 25. MM cells cultured at passage 3 in MM medium supplemented with 25 ng/ml BMP7, 100 ng/ml FGF2 and 100 ng/ml SCF.	112
Figure 26. Growth curves of P0, P1 and P2 MM cells cultured in MM medium supplemented with 25 ng/ml BMP7 and 100 ng/ml FGF2.	113

Figure 27. Freshly isolated MM cells cultured in MM medium supplemented with 25 ng/ml BMP7 and 100 ng/ml FGF2 stained for Wt1 and Pax2.	117
Figure 28. MM cells cultured for 24 hours in MM medium supplemented with 25 ng/ml BMP7 and 100 ng/ml FGF2 stained for Wt1 and Pax2.	118
Figure 29. MM cells cultured for 48 hours in MM medium supplemented with 25 ng/ml BMP7 and 100 ng/ml FGF2 stained for Wt1 and Pax2.	119
Figure 30. MM cells cultured for 72 hours in MM medium supplemented with 25 ng/ml BMP7 and 100 ng/ml FGF2 stained for Wt1 and Pax2.	120
Figure 31. MM cells cultured for 96 hours in MM medium supplemented with 25 ng/ml BMP7 and 100 ng/ml FGF2 stained for Wt1 and Pax2.	121
Figure 32. Immunofluorescence staining of MM cells cultured at passage 1 and passage 2 for Wt1.	122
Figure 33. Negative control for the immunostaining.	123
Figure 34. Expression profile of freshly isolated and cultured MM cells.	127
Figure 35. Schematic representation of the canonical Wnt signalling pathway.	137
Figure 36. Induction of freshly isolated metanephric mesenchyme with embryonic spinal cord.	143
Figure 37. Induction of 24 hours cultured metanephric mesenchyme with embryonic spinal cord.	144
Figure 38. Induction of 48 hours cultured metanephric mesenchyme with embryonic spinal cord.	145
Figure 39. Freshly isolated metanephric mesenchyme cultured without spinal cord did not undergo induction.	146

Figure 40. Induction of freshly isolated metanephric mesenchyme with 5 μ M BIO.	149
Figure 41. Induction of 24 hours cultured metanephric mesenchyme with 5 μ M BIO.	150
Figure 42. Induction of 48 hours cultured metanephric mesenchyme with 5 μ M BIO.	151
Figure 43. Freshly isolated metanephric mesenchyme cultured in the absence of BIO (Control) did not undergo induction.	152
Figure 44. E11.5 reagggregated kidney rudiments could form organotypic renal structures after 3 days of culture.	154
Figure 45. Immunofluorescence staining of E11.5 reagggregated kidney rudiments showed the correct spatial expression of Wt1 and Pax2.	155
Figure 46. Immunostaining of freshly isolated MM cells labeled with quantum dots and recombined with E11.5 reagggregated kidney rudiments.	156
Figure 47. Immunostaining for Pax2 of QD-labelled freshly isolated MM cells recombined with E11.5 reagggregated kidney rudiments.	157
Figure 48. Immunostaining of 4 days cultured MM cells labeled with quantum dots and recombined with E11.5 reagggregated kidney rudiments.	158
Figure 49. Immunostaining for Pax2 of cultured MM cells, labeled with quantum dots, recombined with E11.5 reagggregated kidney rudiments.	159
Figure 50. Percentage of freshly isolated and cultured MM cells, labeled with quantum dots, integrated into nephron-like developing structures.	160

Figure 51. Phase contrast micrographs of H6 cells.	174
Figure 52. Gene expression profile of the H6 clonal line cultured in KSC medium.	177
Figure 53. Cytofluorimetric analysis of the H6 clonal line cultured in KSC medium.	180
Figure 54. Immunostaining for Wt1, Msi1 and Pax2.	182
Figure 55. Immunostaining for megalin and synaptopodin.	183
Figure 56. Light micrographs of osteogenic and adipogenic differentiation assays.	184
Figure 57. Cytofluorimetric analysis of H6 cells cultured in Endothelial Basal Medium supplemented with 10 ng/ml VEGF.	185
Figure 58. Confocal images of H6 cells stained for Vwf and Wt1	186
Figure 59. Growth curve of the H6 clonal line, determined with a colorimetric reaction based on the activity of cellular dehydrogenases.	187
Figure 60. Schematic representation of megalin and cubulin receptors in the apical membrane of kidney proximal tubules.	201
Figure 61. Schematic representation of OAT family members in kidney proximal tubules.	203
Figure 62. Micrographs of H6 cells transfected with EGFP vector.	207
Figure 63. Cytofluorimetric analysis performed on H6 EGFP ⁺ cells.	207
Figure 64. Immunostaining of H6 cells recombined with E11.5 reagggregated kidney rudiments.	208
Figure 65. Immunostaining for Pax2 and Wt1.	210
Figure 66. The H6 clonal line could participate to the formation of developing proximal tubules.	211

Figure 67. The H6 clonal line could participate to the formation of developing glomeruli.	212
Figure 68. Percentage of freshly isolated MM (n=3), 4 days cultured MM cells (n=3) and H6 cells (n=3) labelled with quantum dots, integrated into nephron-like developing structures.	213
Figure 69. <i>In vitro</i> megalin functionality assay.	215
Figure 70. Co-localization of megalin and FBSA.	216
Figure 71. Organic anion transporters functionality assay performed on E11.5 intact kidney rudiment.	218
Figure 72. Organic anion transporters functionality assay performed on E11.5 reaggregated kidney rudiments.	219
Figure 73. RT-PCR performed on H6 cells and postnatal mouse kidney.	220
Figure 74. PCR performed on genomic DNA isolated from H6 cells.	234
Figure 75. Haematoxylin and eosin staining of paraffin-embedded kidney sections.	236
Figure 76. Blood urea nitrogen and serum creatinine concentration measured in healthy mice and in ARF-induced mice three days after injection of 9 ml/Kg/body weight of glycerol.	237
Figure 77. Strategy followed to investigate the ability of the H6 clonal line to engraft into and participate in the recovery of ARF-induced mouse kidneys.	239
Figure 78. Immunohistochemical staining for EGFP performed on paraffin-embedded kidney sections of ARF-induced mice.	240
Figure 79. Flow cytometry analysis performed on single cell disaggregated ARF-induced mouse kidneys.	241

Figure 80. Immunohistochemical staining for EGFP performed on frozen sections of lung, spleen and liver of ARF-induced mice.	243
Figure 81. Immunohistochemical staining for EGFP and megalin performed on consecutive paraffin-embedded kidney sections of ARF-induced mice.	244
Figure 82. Evaluation of renal function in healthy and ARF-induced mice.	247
Figure 83. Immunohistochemical staining for BrdU and PCNA performed on paraffin-embedded kidney sections of ARF-induced mice.	249
Figure 84. Evaluation of tubular cell proliferation in ARF-induced mice.	250
Table 1. Classification of CKD into 5 stages of increasing severity.	24
Table 2. Non renal stem cell populations used in animal models of acute renal failure.	52
Table 3. Renal stem cell populations used in animal models of acute renal failure.	53
Table 4. List of primary antibodies used for cytofluorimetric analysis.	92
Table 5. List of primary antibodies used for immunostaining.	92
Table 6. List of secondary antibodies used for immunostaining.	93
Table 7. Primer sequences and amplicons size.	93
Table 8. Effect of serum concentration on MM cell growth.	106
Table 9. Expansion of P0 MM cells.	113
Table 10. Expansion of P1 MM cells.	113

Table 11. Expansion of P2 MM cells.	113
Table 12. List of markers selected for the RT-PCR analysis.	124
Table 13. Integration ability of MM cells.	160
Table 14. List of markers selected for the RT-PCR analysis.	176
Table 15. Genes expressed in freshly isolated metanephric mesenchyme (MM), MM cells following 4 days of <i>in vitro</i> culture (4d MM) and in the H6 clonal line.	178
Table 16. Expansion of H6 cells.	187
Table 17. Principal differences between MM cells and the H6 clonal line	188
Table 18. Integration ability of freshly isolated MM (fresh MM) (n=3), MM cells following 4 days of <i>in vitro</i> culture (4d MM cells) (n=3) and H6 cells (n=3).	213
Table 19. Blood urea nitrogen and serum creatinine concentrations measured in healthy and ARF-induced mice.	246

GLOSSARY

- 6-CF: 6-carboxyfluorescein.
- ARF: acute renal failure.
- BIO: glycogen synthase kinase-3 inhibitor.
- BM: basement membrane.
- BrdU: 5-bromo-2-deoxyuridine.
- BSA: bovine serum albumin.
- BUN: blood urea nitrogen.
- CB: comma shaped body.
- CKD: chronic kidney disease.
- DAPI: 4',6-diamidino-2-phenylindole, dihydrochloride.
- DMEM: Dulbecco's modified eagle medium.
- EGFP: enhanced green fluorescent protein.
- EMB: Endothelial Basal Medium.
- ES cells: embryonic stem cells.
- ESRD: End-Stage Renal Disease.
- FA: folic acid.
- FBSA: fluorescent bovine serum albumin.
- FCS: fetal calf serum.
- GMB: glomerular basement membrane.
- GSK-3: glycogen synthase kinase-3.
- hAFSC: human amniotic fluid stem cells.
- HSC: hemopoietic stem cells.
- KSC: kidney-derived stem cells.
- LIF: leukemia inhibitory factor.
- LRTC: label-retaining tubular cells.
- MET: mesenchymal-to-epithelial transition.
- MM: metanephric mesenchyme.

- MKPC: mouse kidney progenitor cells.
- MRPC: multipotent renal progenitor cells.
- MSC: mesenchymal stem cells.
- ND: nephron-like developing structure.
- OAT: organic anion transporter.
- OCT: organic cation transporter
- PBS: phosphate buffered saline.
- PCNA: proliferating cell nuclear antigen.
- PD: population doubling.
- PFA: paraformaldehyde.
- PNA: peanut agglutinin.
- PS: penicillin/streptomycin.
- QD: quantum dots.
- RAP: receptor-associated protein.
- REC: renal embryonic cells.
- RT: room temperature.
- RT-PCR: reverse transcriptase-polymerase chain reaction.
- RV: renal vesicle.
- SC: spinal cord.
- SCF: stem cell factor.
- SCID mice: severe combined immunodeficiency mice.
- SD: standard deviation.
- SP cells: side population cells.
- ST: stroma.
- UB: ureteric bud.
- VEGF: vascular endothelial growth factor.

To my family

*“It is not birth, marriage or death, but gastrulation,
which is truly the most important time in your life”*

Lewis Wolpert

CHAPTER 1

1.1 The Kidney

The kidneys are important organs that regulate the level of water and solutes in the blood and contribute to maintain the homeostasis of the body by eliminating waste products in the form of urine. In humans the kidneys are located on each side of the vertebral column, in the posterior part of the abdomen. Because of the asymmetry of the abdominal cavity, the right kidney is situated slightly lower than the left one, which is located slightly more medially. In a normal adult human, each kidney is bean-shaped and is about 11 to 12 cm long, 5 to 7.5 cm width and 2.5 to 3 cm thick. The weight of each adult kidney ranges from 115 g to 170 g, thus representing 0.5% of the total weight of the body (Brenner, 2000).

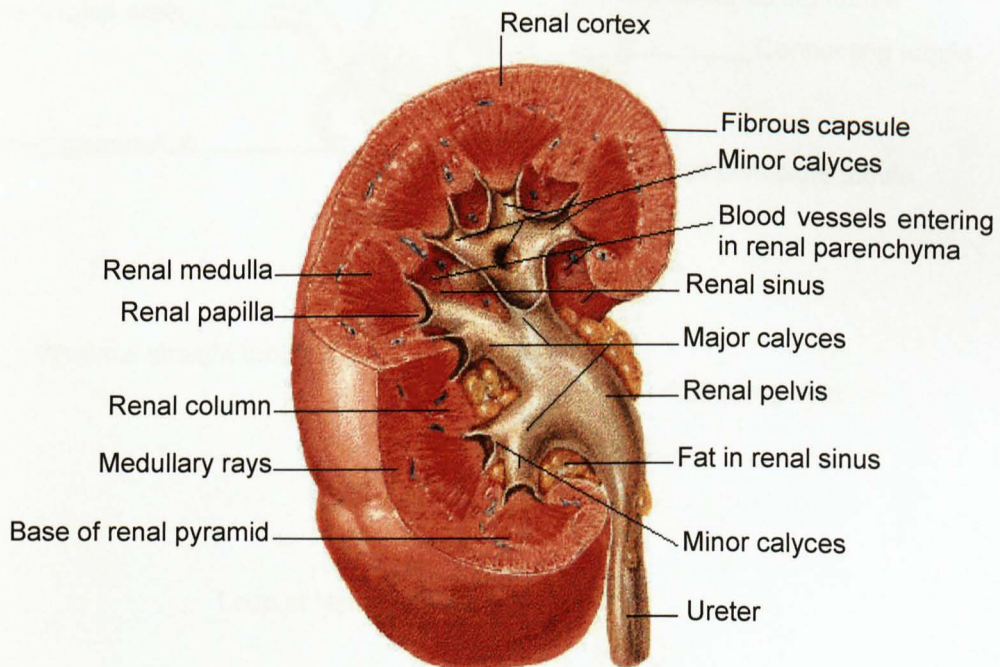


Figure 1. Section of human kidney (Modified from www.novartis.com).

A tough fibrous tissue, called the renal capsule, surrounds the kidney. The external portion of the kidney is called the renal cortex. Beneath the renal cortex lies the renal medulla, an area that in humans contains up to 18 cone-shaped sections called the renal pyramids (Brenner, 2000). The tip of each renal pyramid points towards the centre of the kidney and empties into a calyx which in turn empties into the renal pelvis (Fig. 1). Unlike in humans, the rodent kidney contains only one renal pyramid, which empties into the renal pelvis (Brenner, 2000). The function of the pelvis is to transmit the urine into the bladder through the ureter.

1.1.1 The nephron

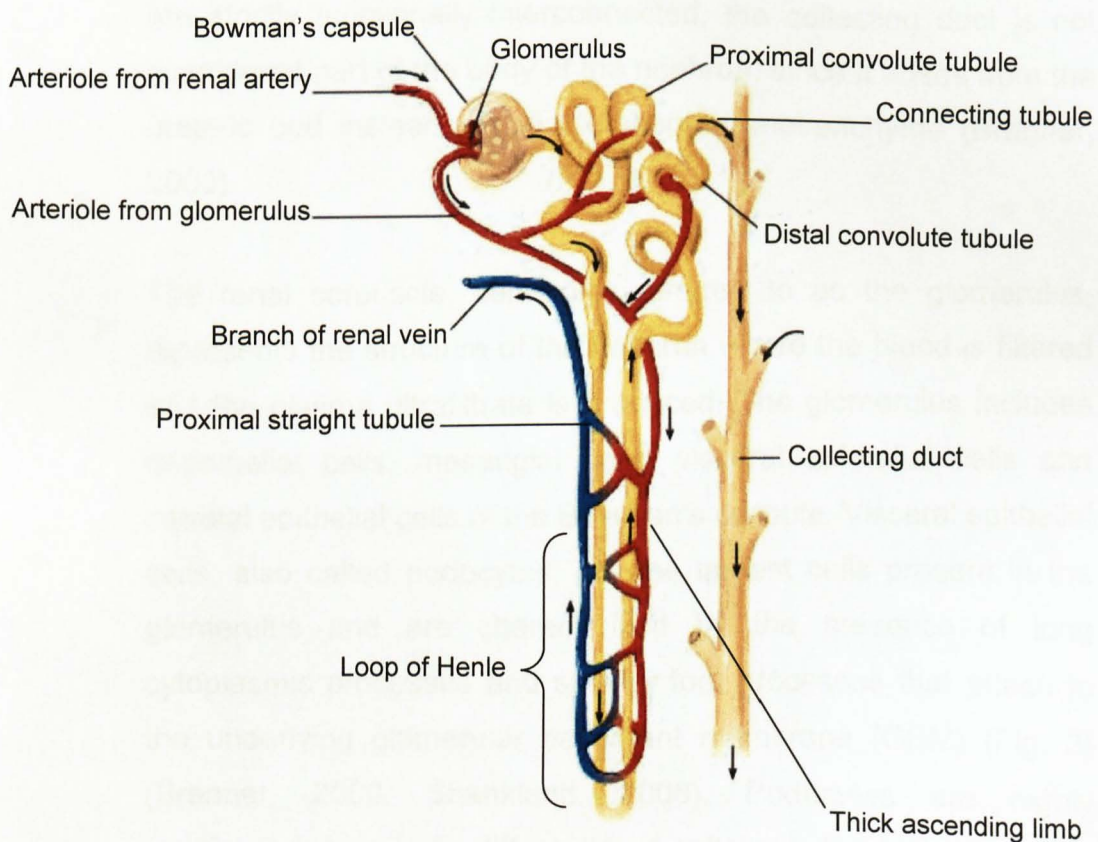


Figure 2. Representation of nephron (Modified from www.anselm.edu).

The nephron represents the functional unit of the kidney. Each human kidney contains approximately $6 \times 10^5 - 1.4 \times 10^6$ nephrons, whereas the rat and mouse kidney contain about 3×10^4 and 1.1×10^4 nephrons, respectively (Brenner, 2000; Dickinson et al., 2005). The nephron consists of five distinct structures, namely the renal corpuscle (which includes the glomerulus and Bowman's capsule), the proximal tubules, the thin limbs, the distal tubules and the connecting segment (Fig. 2) (Brenner, 2000). As demonstrated by Kobayashi and colleagues, all these structures arise from a domain within the metanephric mesenchyme called the cap mesenchyme (Kobayashi et al., 2008). At the most distal end, the nephron is connected with the collecting duct system: although the nephron and collecting duct are strictly functionally interconnected, the collecting duct is not considered part of the body of the nephron, since it arises from the ureteric bud instead of the metanephric mesenchyme (Brenner, 2000).

The renal corpuscle, commonly referred to as the glomerulus, represents the structure of the nephron where the blood is filtered and the plasma ultrafiltrate is produced. The glomerulus includes endothelial cells, mesangial cells, visceral epithelial cells and parietal epithelial cells of the Bowman's capsule. Visceral epithelial cells, also called podocytes, are the largest cells present in the glomerulus and are characterized by the presence of long cytoplasmic processes and smaller foot processes that attach to the underlying glomerular basement membrane (GBM) (Fig. 3) (Brenner, 2000, Shankland, 2006). Podocytes are highly specialized, terminally differentiated cells with the task of filtering the blood: they form a size barrier and charge barrier to proteins, maintain the glomerular loop shape, secrete vascular endothelial

growth factor (VEGF) and synthesize and maintain the GBM (Shankland, 2006). Podocytes are critically important for the development of kidney disease: depletion of podocytes due to infection, genetic, immune and toxic insults leads to proteinuria, a condition which might lead to glomerulosclerosis and ultimately to kidney failure (Shankland, 2006; Ronconi et al., 2009).

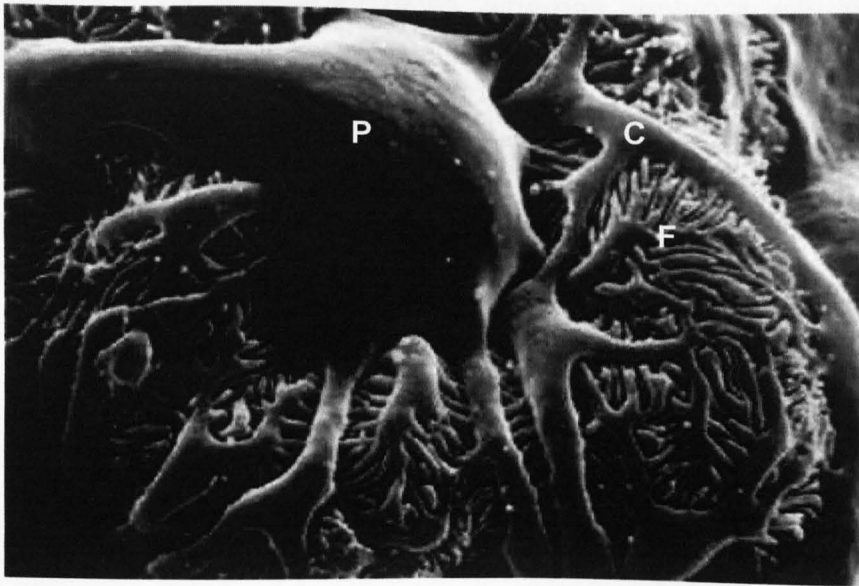


Figure 3. Scanning electron micrograph of a podocyte (P) with cytoplasmic (C) and foot (F) processes surrounding glomerular capillaries (Modified from Smoyer and Mundel, 1998).

Once formed, the ultrafiltrate is collected in the urinary space of the Bowman's capsule, and then enters the renal tubules. The proximal tubule represents the first part of the renal tubule: it is formed by a convoluted portion (pars convoluta), which is a protrusion of the parietal epithelium of the Bowman's capsule, and a straight portion (pars recta), which is connected with the thin limb of the loop of Henle (Brenner, 2000). Proximal tubules play a pivotal role in maintaining body homeostasis, as the reabsorption and secretion of an immensely broad spectrum of inorganic and

organic molecules occurs within these segments (see section 6.1 for more details) (Brenner, 2000; Christensen and Gburek, 2004, Sweet, 2005; Sweet et al., 2006). The descending thin limb of the loop of Henle connects the pars recta of the proximal tubule with the thick ascending limb of the distal tubule (Brenner, 2000). Generally, nephrons with short loops of Henle originate from superficial or mid-cortical locations, whereas nephrons with long loops of Henle originate from the corticomedullary boundary (Brenner, 2000). The distal tubule represents the terminal segment of the nephron: it is formed by the thick ascending limb (pars recta) and the distal convoluted tubule (pars convoluta). The distal convoluted tubule extends to the connecting tubule, which couples the nephron with the collecting duct (Brenner, 2000). The ultrafiltrate produced in the Bowman's capsule moves through the proximal and distal tubules towards the collecting duct, then into the ureter where it is finally drained into the bladder in the form of urine.

Mammalian nephrogenesis is completed by birth or during the early postnatal period. In humans, for instance, the full endowment of nephrons is formed during intrauterine life (Dickinson et al., 2005); conversely, in rodents, such as in mouse and rat, nephrogenesis continues until approximately postnatal day (P) 7 and P10, respectively (Dickinson et al., 2005). Since the mammalian kidney cannot form new nephrons following postnatal life, an extensive loss of nephrons due to damage or disease leads to chronic kidney disease, which might ultimately result in end-stage renal disease (ESRD).

1.1.2 Kidney development

The three embryonic germ layers, the endoderm, the mesoderm and the ectoderm, are generated during gastrulation, which occurs at approximately embryonic day (E) 6.5 in mouse and at E15 in humans (Fig. 4).

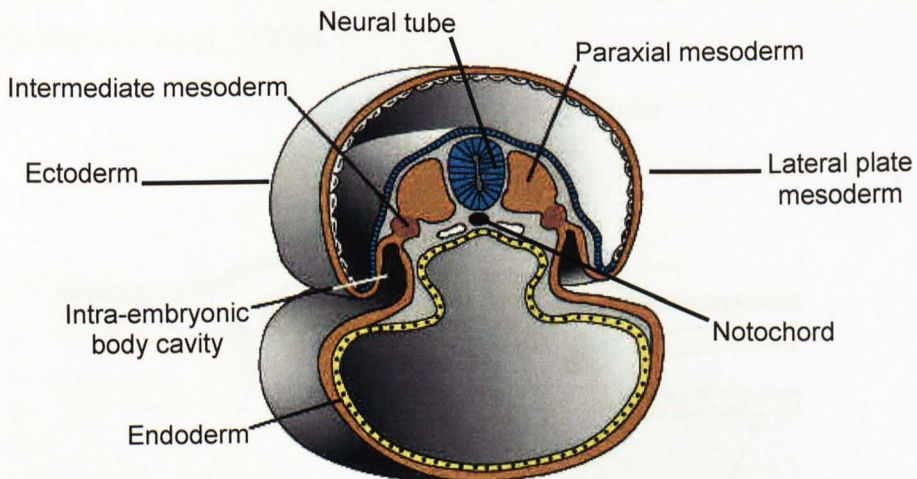


Figure 4. Transverse section of human embryo (E21.0) showing the three embryonic germ layers (Modified from <http://connection.lww.com>).

The mesoderm gives rise to three sub-populations: the paraxial mesoderm, the lateral plate mesoderm and the intermediate mesoderm. Besides, the mesoderm gives rise to the notochord, which defines the primitive axis of the embryo. The paraxial mesoderm gives rise to the head tissues and the somites, which forms the cartilage of the vertebrae and ribs, the muscles of the rib cage, back and limbs, and the dermis of the dorsal skin. The lateral plate mesoderm generates some extra embryonic tissues and the somatic (parietal) and splanchnic (visceral) mesoderm. The somatic mesoderm forms the future body wall, and the splanchnic layer forms the circulatory system and the gut wall. The intermediate mesoderm gives rise to the kidney and the gonads and their respective duct systems, forming the urogenital system

(Gilbert, 2006; Risbud et al., 2010). Nevertheless, more recent studies have suggested that kidney development might depend on integration mechanisms between intermediate and paraxial mesoderm: in fact it has been demonstrated that epithelial structures of the nephron arise from the intermediate mesoderm, whereas renal stromal cells derive from the paraxial mesoderm (Guillaume et al., 2009).

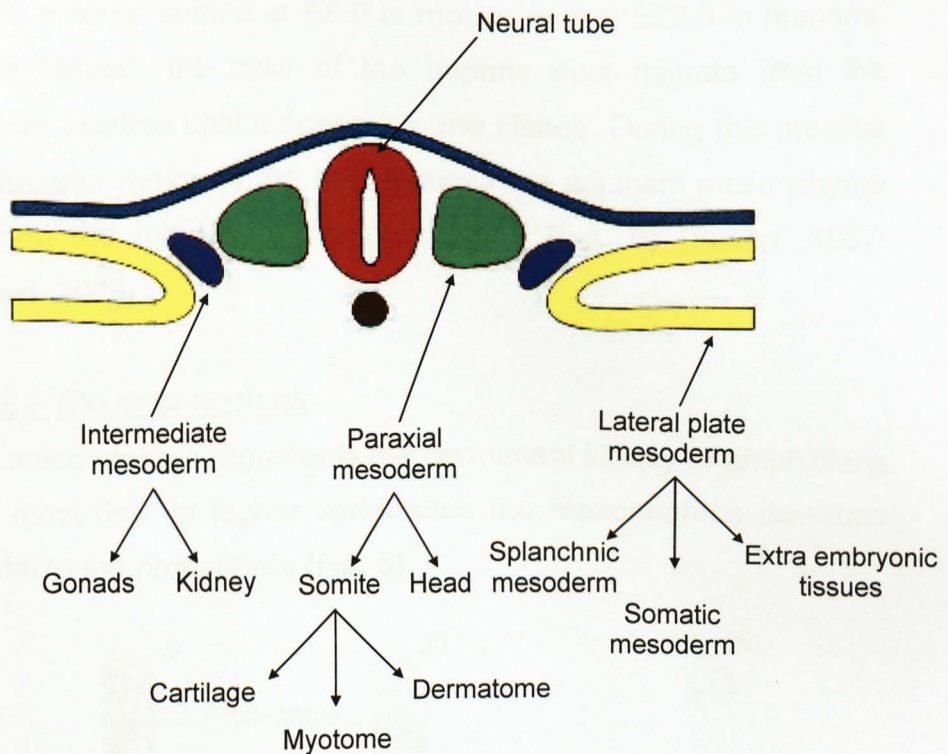


Figure 5. Schematic representation of mesoderm layers and their derivative tissues (Modified from <http://www.dls.ym.edu.tw>).

The development of the mammalian kidney proceeds through three subsequent stages in which the intermediate mesoderm generates three distinct excretory organs: the pronephros, the mesonephros and the metanephros. Both the pronephros and the mesonephros are only transient in mammals, while the metanephros develops into the permanent kidney.

1.1.2.1 The pronephros

The development of the pronephros into a functional excretory organ is limited to some lower vertebrates such as primitive fish (lampreys and hagfish), and to the larval stage of teleost fish (e.g. zebrafish) and amphibians. The pronephric duct, which constitutes the central component of the excretory system throughout development, originates in the intermediate mesoderm just ventral to the anterior somite at E8.0 in mouse and at E22.0 in humans. Once formed, the cells of the nephric duct migrate from the anterior location until it opens into the cloaca. During this process the anterior region of the duct induces the adjacent mesenchyme to form the tubules of the pronephros (Fig. 6) (Saxén, 1987; Gilbert, 2006).

1.1.2.2 The mesonephros

The mesonephros represents the permanent kidney of amphibians and most fish. In higher vertebrates the mesonephros develops caudal to the pronephros (Fig. 6).

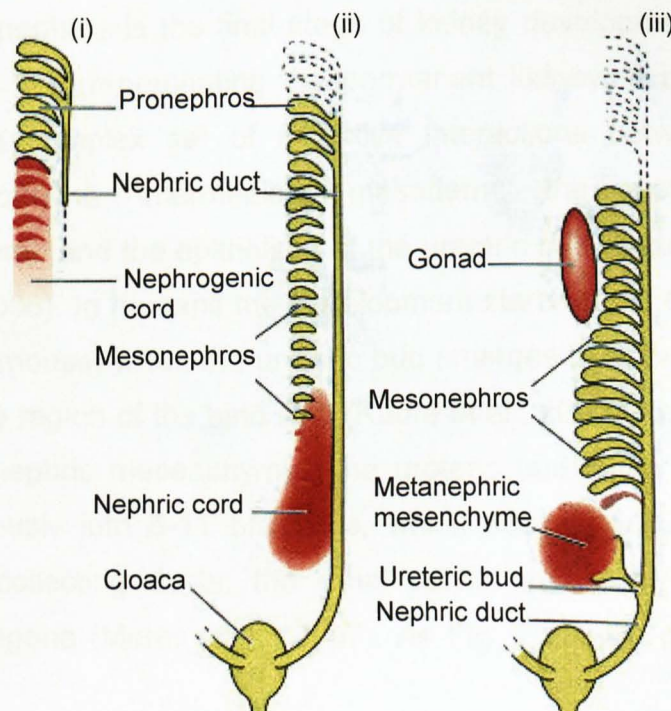


Figure 6. Schematic representation of mammalian kidney development. The excretory system develops throughout three subsequent organs, the pronephros (i), the mesonephros (ii), and the metanephros (iii) (Modified from Gilbert, 2006).

As the mesonephros is developing, the pronephric tubules and the anterior part of the pronephric duct start to degenerate. The remaining portion of the pronephric duct is often called the nephric or Wolffian duct (after CF Wolff described it in 1759). In humans the mesonephros starts to develop around E25.0. Although it consists of a large number of mesonephric tubules (around 30) that might have a filtering function during embryonic life, the mesonephros does not function as a working kidney (Brenner, 2000). However, the mesonephros provides important developmental functions: for example in male mammals some mesonephric tubules give rise to the *vas deferens* and *efferent* ducts of the testes (Saxén, 1987; Gilbert, 2006).

1.1.2.3 The metanephros

The metanephros is the final stage of kidney development for all amniotes, thus representing the permanent kidney. It originates through a complex set of inductive interactions between two tissues of the intermediate mesoderm: the metanephric mesenchyme and the epithelium of the ureteric bud (Saxén, 1987; Gilbert, 2006). In humans the development starts at the fifth week (E10.5 in mouse) when the ureteric bud emerges from the nephric duct in the region of the hind limb (Kuure et al., 2000) and invades the metanephric mesenchyme. The ureteric bud starts to divide dichotomously into 6-11 branches, which subsequently develop into the collecting ducts, the renal pelvis, the ureter and the bladder trigone (Murer et al., 2007). As Fig. 7 shows, the tips of

the branches induce the mesenchymal cells of the metanephric mesenchyme to condense and differentiate around them into epithelial aggregates called the renal vesicles. These aggregates start to proliferate and elongate into an intricate structure that first gives rise to a “comma” shaped body and then generates an S-shaped tube.

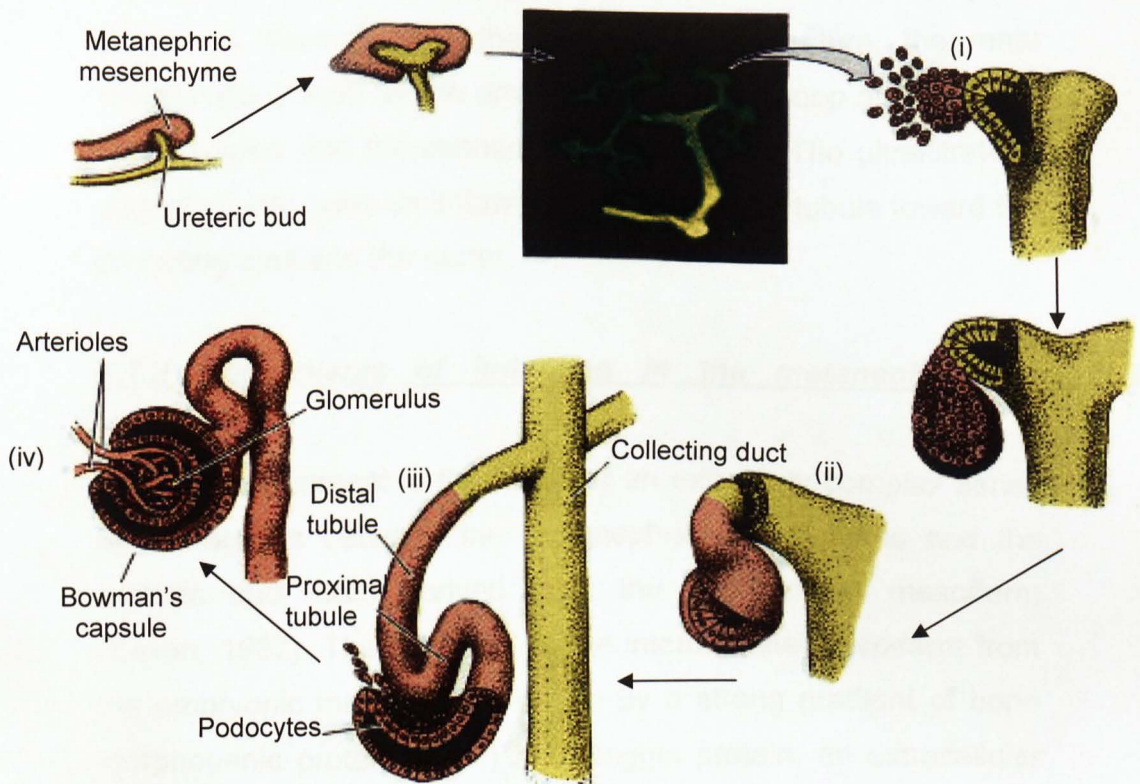


Figure 7. Representation of reciprocal induction between metanephric blastema and epithelium during kidney development. The tips of the UB branches induce the condensation of mesenchymal cells into epithelial aggregate (i); subsequently a “comma” shaped body forms (ii), develops into an S-shaped tube (iii), and finally differentiates into the renal tubules and the glomerulus (iv) (Modified from Gilbert, 2006).

The cells of this structure begin to differentiate into specific cell types, the proximal and distal tubule cells, and into the glomerulus

(Saxén, 1987; Gilbert, 2006). The portion of the nephric duct that lies between the ureter and the primitive bladder undergoes apoptosis, thus permitting the ureter to start its incorporation into the bladder (Murer et al., 2007).

As mentioned previously, the nephron is the functional unit of the kidney. It is composed of a glomerulus that is surrounded by the Bowman's capsule, and the renal tubules. In turn, the renal tubules are formed by the proximal tubules, the loop of Henle, the distal tubules and the connecting duct (Fig. 2). The ultrafiltrate is converted into urine as it flows through the renal tubule toward the collecting duct and the ureter.

1.1.3 Mechanisms of induction in the metanephrogenic mesoderm

Kidney development is the result of an extremely complex series of interactions between the metanephric mesenchyme and the ureteric bud, both derived from the intermediate mesoderm (Saxén, 1987). The induction of the intermediate mesoderm from the embryonic mesoderm is driven by a strong gradient of bone morphogenic protein (BMP) and Noggin protein, an extracellular antagonist of BMP signalling. In detail, the intermediate mesoderm is formed when the BMP gradient predominates; conversely, a high gradient of Noggin protein specifies the paraxial mesoderm (Vize et al. 2003).

Among different BMP factors, BMP7 seems to be required for the survival of the metanephric mesenchyme *in vivo*. Loss of *Bmp7* expression results in impaired nephrogenesis which becomes evident by E16.5: null embryos display small kidneys that lack condensed mesenchyme and contain many cystic structures

(Dudley and Robertson, 1997). *Bmp7* is expressed in the metanephric mesenchyme when the contacts between the ureteric bud and the metanephric mesenchyme are established, and it is maintained throughout kidney development (Dudley et al., 1999). Another factor involved in maintaining the metanephric mesenchyme survival is fibroblast growth factor 2 (FGF2), which is expressed by the UB (Barasch et al., 1997). It seems to act in conjunction with BMP7 to promote cell survival by inhibiting apoptosis. FGF2 also promotes the condensation of mesenchymal cells, and mediates the transcriptional activation of *Wilms' tumour suppressor gene-1*, *Wt1* (Perantoni et al., 1995; Gilbert, 2006).

The formation of metanephric mesenchyme is dependent on the expression of *Wt1*. This gene is initially expressed in the intermediate mesoderm and then restricted to the metanephric mesenchyme, gonads and mesothelium (Brodbeck and Englert, 2004). The expression of *Wt1* is low in non-induced metanephric mesenchyme, but it increases after mesenchymal condensation and induction (Donovan et al., 1999). In adult kidney, *Wt1* expression is restricted to podocytes (Dressler, 2006). In mice lacking *Wt1*, the metanephric mesenchyme cells undergo apoptosis at E11.0, leading to renal agenesis. However, in *Wt1* null embryos, the expression of other genes crucial for MM development, such as *Pax2*, *Six1* and *Gdnf*, is still detectable (Donovan et al., 1999).

Once it has formed, the metanephric mesenchyme stimulates the outgrowth of the ureteric bud (UB) from the Wolffian duct. The TGF- β family member, glial cell-line-derived neurotrophic factor (*Gdnf*), stimulates the ureteric bud outgrowth through the receptor tyrosine kinase, *Ret*, and the GPI-linked cell surface co-receptor,

Gfra1 (Takahashi, 2001; Arighi et al., 2005). *Gdnf* is only expressed in the metanephric mesenchyme, adjacent to the caudal portion of the Wolffian duct. On the other hand, both *Ret* and *Gfra1* are expressed along the Wolffian duct (Sainio et al., 1997). Following the initial out-pocketing of the UB the expression of *Ret* decreases in the Wolffian duct and becomes limited to the distal tips of the UB branches (Fig. 8). *Gfra1* seems to be co-expressed with *Ret*. The process of branching morphogenesis of the UB causes *Gdnf* expression to be restricted to the peripheral undifferentiated mesenchyme cells that surround the branch tips (Poteryaev et al., 1999; Trupp et al., 1999; Popsueva et al., 2003).

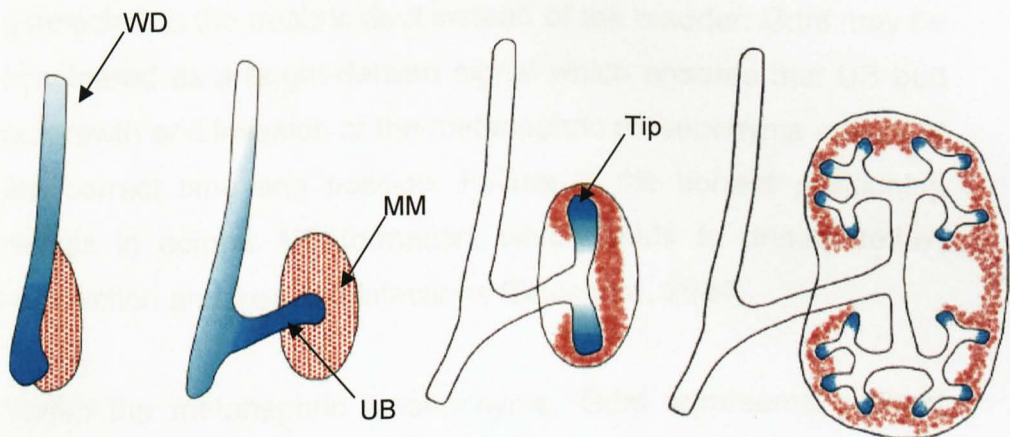


Figure 8. Representation of *Gdnf* (red) and *Ret* and *Gfra1* (blue) expression during kidney development. The figure shows that *Ret* and *Gfra1* expression become restricted to the ureteric bud tips as the process of branching proceeds. *Gdnf* is expressed within the metanephric mesenchyme and becomes limited to the peripheral undifferentiated cells adjacent to the tips of the UB branches. WD: Wolffian duct; MM: metanephric mesenchyme; UB: ureteric bud (Modified from Costantini and Shakya, 2006).

Lack of *Gdnf* expression, *Ret*, or *Gfra1* in mutant mice results in the absence of ureteric bud outgrowth, ranging from blind ending ureters, to tiny and disorganized kidney rudiments, to renal agenesis (Costantini and Shakya, 2006). Conversely, local application of *Gdnf* induces the formation of multiple, ectopic ureteric buds from different locations of the Wolffian duct (Maeshima et al., 2007). *Gdnf* expression is induced by several transcription factors, such as *Pax2*, *Eya1*, *Six1*, and the *Hox11* paralogous group, and is repressed by *Foxc1* and *Bmp4*. The negative regulatory factors seem to be involved in restricting the domain of *Gdnf* expression to the more posterior metanephric region: deletion of one of these genes leads to the formation of multiple ureteric buds and ectopic ureters, which remain connected to the nephric duct instead of the bladder. *Gdnf* may be considered as a target-derived signal which ensures that UB bud outgrowth and invasion of the metanephric mesenchyme occurs at the correct time and position. Failure in the correct positioning results in ectopic UB formation, which leads to urinary reflux, obstruction and frequent infections (Bouchard, 2004).

Within the metanephric mesenchyme, *Gdnf* represents a direct target of the paired-box transcription factor, *Pax2*. The *Pax2* gene plays a crucial role for specification of the nephric lineage, as it is expressed within the intermediate mesoderm from the 6th somite stage (Dressler, 2009). In the metanephros, *Pax2* is expressed both in the MM and UB tips, where it is required for mesenchymal-to-epithelial transition (MET) of the nephron precursors. At the onset of nephrogenesis *Pax2* is expressed in the comma and S-shaped body and, as the kidney develops, the expression becomes restricted to the epithelial cells of the proximal and distal tubules (Dressler, 2009). In the adult kidney, *Pax2* is mainly

expressed in the collecting duct cells (Cai et al., 2005). The competence of the intermediate mesoderm to form the kidney depends on the presence of Pax2: in fact, it has been shown that in *Pax2*^{-/-} mouse embryos, pronephros and mesonephros formation occurs normally, whereas the metanephros and genital tract never develop (Torres et al., 1995). Pax2 induces the expression of *Gdnf* through interactions with at least one high-affinity binding site within the *Gdnf* promoter. It has been demonstrated that *Pax2*^{-/-} embryos have little to no *Gdnf* expression. In these mutants the metanephric mesenchyme is unable to respond to inductive signals *in vitro* (Brophy et al., 2001). These findings agree with those observed by Torres and colleagues reported above, in which in null mutant embryos, the ureteric buds do not form, thus resulting in renal agenesis (Torres et al., 1995). In humans the loss of one *PAX2* allele (*PAX2*^{+/-}) leads to renal hypoplasia, vesicoureteric reflux and optic nerve colobomas (Dressler, 2009). Pax2 plays an important role in regulating the expression of *Ret* by binding to its promoter, as demonstrated by Clarke and colleagues: *Pax2*^{+/-} mice have reduced levels of *Ret* expression at early stages of kidney development (Clarke et al., 2006). This evidence might help to understand why many developing tissues are very sensitive to *Pax2* gene dosage. Pepicelli and colleagues (Pepicelli et al., 1997) have demonstrated that the *Gdnf/Ret* signalling pathway regulates the expression of *Ret* itself. Thus in these tissues the effect of *Pax2* gene dosage may be amplified because of its ability to regulate both the expression levels of *Gdnf* and its receptor *Ret*.

The *odd skipped-related* gene *Osr1*, a homolog of the *Drosophila odd skipped* (*Odd*), represents the earliest marker expressed in the intermediate mesoderm, and in mouse the expression begins

at E7.5 (James et al., 2006, Mugford et al., 2008). *Osr1* plays a crucial role in establishing the metanephric mesenchyme and regulating the differentiation of kidney precursor cells during kidney development. James and colleagues demonstrated that the expression of *Osr1* is only present in undifferentiated cells within the nephric duct, mesonephric mesenchyme and metanephric mesenchyme, then it is gradually downregulated in cells that form pre-tubular aggregates, comma and S-shaped body. Targeted mutagenesis has revealed that *Osr1* is required for MM formation, as homozygous null embryos examined at E11.5 lacked both UB and MM condensation. In addition, several genes required for normal kidney development, such as *Pax2*, *Eya1*, *Six2*, *Sall1* and *Gdnf* were not expressed in the absence of *Osr1* (James et al., 2006). The downregulation of *Osr1* seems to be required for the differentiation of kidney precursors into epithelial structures, as the ectopic expression of *Osr1* inhibited tubule formation. These results suggested that *Osr1* is necessary for the formation and maintenance of kidney precursor cells and for their differentiation into epithelial structures (James et al., 2006). A more recent study provided evidence that *Osr1*⁺ cells are the precursors of a wide spectrum of cells of the developing kidney. Using a temporal fate mapping strategy, Mugford and collaborators showed that cap mesenchyme, epithelial structures of the nephron, ureteric epithelium of the collecting duct, interstitial mesenchyme progenitors, pericytes, mesangium, vasculature and the kidney capsule arise from a common *Osr1*⁺ progenitor cell population that are present in the embryo between E7.5 and E11.5 (Mugford et al., 2008). Since *Osr1* is expressed in the mesoderm before its subdivision into intermediate and paraxial mesoderm (Guillaume et al., 2009), it might be possible that different tissues of the nephron derive from different locations in the early embryo. Using

a fate mapping technique, Guillaume and colleagues demonstrated that in the chick embryo, *Osr1*⁺ progenitor cells present in the paraxial mesoderm give rise to myofibroblasts, vascular smooth muscle, pericytes and mesangial cells of the developing kidney. This study strongly suggests that nephron epithelia derive from intermediate mesoderm, whereas renal stromal cells arise from paraxial mesoderm (Guillaume et al., 2009). Altogether these findings provided further evidence for a role of *Osr1* in establishing the nephron progenitor population before the onset of nephrogenesis.

Another important gene in nephrogenesis is *Eya1*, a homolog of *Drosophila eye absent (eya)*. In mouse, deletion of *Eya1* expression results in renal agenesis (Xu et al., 1999). In humans haploinsufficiency of *EYA1* leads to Branchio-Oto-Renal syndrome characterized by branchial, otic and renal disorders (Kumar et al., 1998). In mouse, *Eya1* is expressed in the intermediate mesoderm at E8.5 next to the presumptive pronephric and mesonephric blastema, and becomes gradually restricted to the metanephric mesenchyme (Sajithlal et al., 2005). Some evidence suggests that *Eya1* might play a critical role in the initial selection of metanephric cell fate in the intermediate mesoderm, since in *Eya1*^{-/-} mouse embryos the blastema do not form. Therefore, the *Eya1* protein may be involved in controlling the gene expression program of metanephric development. Furthermore, *Eya1* positively regulates the expression of *Gdnf*, although this control also requires other elements such as *Pax2* and members of the Six protein family, which in turn appear to be regulated by *Eya1* (Sajithlal et al., 2005).

The *Six1* gene is homologous to *Drosophila sine oculis (so)*. In mouse *Six1* is expressed in the metanephric mesenchyme at E10.5, and in the induced mesenchyme at E11.5 around the ureteric buds. Furthermore, the expression of *Six1* becomes restricted to a subpopulation of collecting duct epithelial cells from E17.5 to birth (P0) (Xu et al., 2003). *Six1* has an important role during early kidney development, since it seems to be required for ureteric bud invasion into the metanephric mesenchyme (Kobayashi et al., 2007). *Six1*^{-/-} mouse embryos lack kidneys because of failure in metanephric induction (Xu et al., 2003). Expression of *Six1* gene is required for the expression of other genes involved in kidney development, such as *Pax2*, *Sall1* and *Six2* in the mesenchyme at E10.5-11.5. In addition *Six1* inactivation is required to reduce the expression domains of *Bmp7*, *Wt1*, and *Gdnf* within the metanephric mesenchyme. However, *Six1* does not appear to regulate the expression of *Eya1*, thus suggesting that *Eya1* may function upstream of *Six1* in the regulatory hierarchy. *Pax2* expression in the metanephric mesenchyme is both *Eya1* and *Six1* dependent. Therefore, in mammals there may be a *Eya1-Six1-Pax2* regulatory hierarchy that controls early kidney development, as proposed by Xu and colleagues (Xu et al., 2003).

The *Six2* gene has been recognised as a key player of metanephros development. While heterozygous mouse embryos do not show any apparent abnormality, inactivation of both *Six2* alleles results in ectopic differentiation of the metanephric mesenchyme, depletion of progenitor cells within the MM and lethality soon after birth. The expression of *Six2* is detectable as early as E10.0 within the metanephric blastema and it is maintained throughout the development of the excretory system

(Self et al., 2006); in adult, *Six2* is not expressed (Humphreys et al., 2008). At the onset of nephrogenesis, *Six2* is expressed in the cap mesenchyme, a domain of the uninduced MM adjacent to the tips of the UB (Self et al. 2006). Kobayashi and colleagues demonstrated that *Six2*⁺ cells represent a population of self-renewing renal progenitor cells that give rise to all cell types present in the body of the mature nephron (Kobayashi et al., 2008). These findings strongly suggest that *Six2* is involved in maintaining a pool of renal progenitor cells during nephrogenesis.

It has been shown that the fibroblast growth factor receptors, *Fgfr1* and *Fgfr2*, play an important role in metanephric mesenchyme formation. Deletion of either *Fgfr1* or *Fgfr2* in mutant mice results in normal-appearing kidney. However, ablation of both receptors results in renal aplasia, thus suggesting that there is a degree of functional redundancy between *Fgfr1* and *Fgfr2* in kidney development (Poladia et al., 2006).

The *Hox11* paralogous genes have been recognized as important regulators of kidney development: they are expressed in the metanephric mesenchyme at E10.5 and in the metanephric mesenchyme stromal cells at E11.0 (Boyle and de Caestecker, 2006). The paralogous genes display functional redundancy: therefore partial loss-of-function of the paralogous group results in hypomorphic phenotypes. For example, in mouse neither *Hoxa11* nor *Hoxd11* single mutants display any altered phenotype. Conversely, *Hoxa11/Hoxd11* double mutants show variably penetrant kidney hypoplasia: in these animals ureteric bud outgrowth occurs normally at E11.5, but by E13.5 kidney abnormalities appear (Wellik et al., 2002). Moreover in *Hoxa11/Hoxc11/Hoxd11* triple mutant mouse embryos induction of

the metanephric mesenchyme is completely absent: there is no ureteric bud outgrowth and neither *Gdnf* nor *Six2* are expressed. Conversely, *Pax2*, *Wt1*, and *Eya1* expression is unperturbed. These findings suggest that *Hox11* paralogous genes are required for the formation of the metanephric mesenchyme (Wellik et al., 2002).

The *Sall1* (*Sal-like 1*) gene is the mammalian homologue of the *Drosophila* gene *sal*. In mouse, *Sall1* is expressed in the nephrogenic primordium at E10.5, and in the metanephric mesenchyme surrounding the ureteric bud at E11.5. Also, at E14.5 *Sall1* is expressed in the comma-shaped body, S-shaped body, renal tubule and podocytes. *Sall1* plays an important role in kidney development: *Sall1* knockout mice die within 24 hours following birth because of renal agenesis or severe renal dysgenesis. In particular, it has been shown that in *Sall1*^{-/-} mouse embryos the metanephric mesenchyme forms but the ureteric bud fails to invade the mesenchyme. This evidence suggests that *Sall1* is important for the correct ureteric bud outgrowth and invasion of the metanephric mesenchyme (Nishinakamura, 2003). In humans heterozygous mutations of *SALL1* lead to Townes-Brocks syndrome, an autosomal dominant disease with some different features such as kidney and heart abnormalities, dysplastic ears, preaxial polydactyly and imperforate anus (Nishinakamura and Takasato, 2005).

The *Lhx1* gene plays an important role during kidney development. In mouse *Lhx1* expression appears in the intermediate mesoderm, then in the nephric duct and ureteric bud. The expression is also present in some metanephric mesenchyme-derived structures such as pretubular aggregates,

comma and S-shaped body (Kobayashi et al., 2005). *Lhx1* seems to regulate urogenital development, as rare *Lhx1* deficient mice, delivered stillborn, lack both kidneys and reproductive tract structures (Kobayashi et al., 2005). As mentioned previously, the competence of the intermediate mesoderm depends on the correct expression of the *Pax2* gene. In *Lhx1* deficient embryos the expression of *Pax2* is considerably reduced between E8.5 – E9.5: this evidence has suggested that one of the possible roles of *Lhx1* is to control the differentiation of the intermediate mesoderm (Tsang et al., 2000). Pedersen and colleagues investigated the role of *Lhx1* by using a *Pax2-cre* conditional *Lhx1* knockout transgenic mouse line. In this line, *Lhx1* gene ablation occurs when *Pax2* is expressed. This study demonstrated that in the absence of *Lhx1*, mice displayed renal hypoplasia and hydronephrosis. Additionally, the nephric duct was impaired, the ureteric bud was smaller than normal and the branching process was reduced. These results indicate that *Lhx1* is required for nephric duct extension and ureteric bud outgrowth (Pedersen et al., 2005).

Wnt4, a member of the *Wnt* gene family, is expressed in aggregating mesenchymal cells, and is maintained in the comma-shaped body before becoming down-regulated in the S-shaped body (Stark et al., 1994). *Wnt4* has a critical role in kidney development. *Wnt4* knockout mice die within 24 hours after birth due to small agenic kidneys. In these animals primary condensation of mesenchymal cells around the ureteric bud tips occurs but the mesenchyme remains undifferentiated, lacking pretubular cell aggregates and epithelial tubules. *Wnt4* plays a crucial role in the epithelial differentiation of the metanephric mesenchyme. Kisper and colleagues demonstrated that the

isolated mouse metanephric mesenchyme undergoes tubulogenesis following co-culture in transfilter culture with a layer of NIH3T3 cells expressing *Wnt4* (Kispert et al., 1998). The canonical Wnt pathway and cytosolic β -catenin act as key players in the induction of the metanephric mesenchyme (see section 4.1 for details) (Kuure et al., 2007; Park et al., 2007; Schmidt-Ott and Barasch, 2008). It has been suggested that following activation by *Wnt9b*, a Wnt factor secreted by the UB, *Wnt4* triggers tubulogenesis in the metanephric mesenchyme by activating the canonical Wnt pathway (Park et al., 2007; Schmidt-Ott and Barasch, 2008).

Figure 9 shows a suggested molecular cascade for the induction of the metanephric mesenchyme.

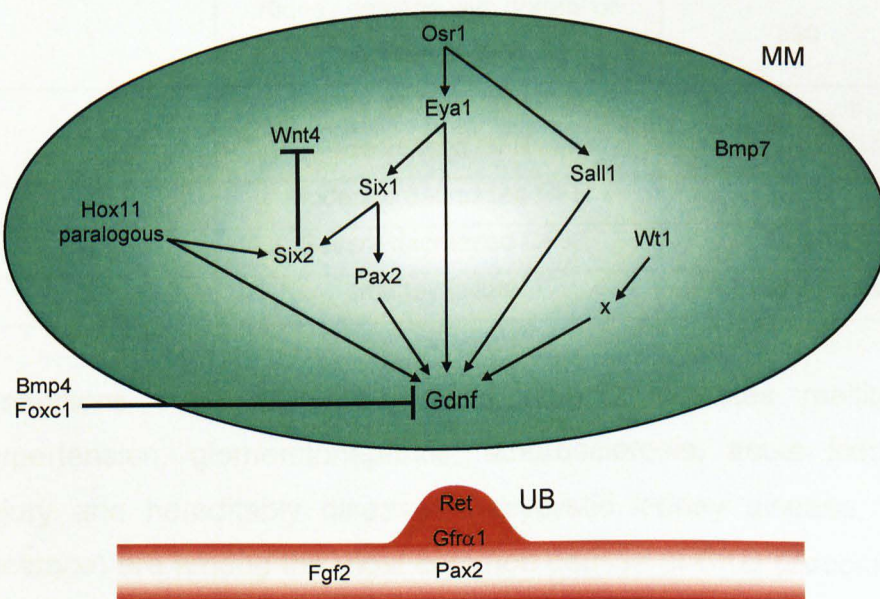


Figure 9. Proposed molecular cascade for metanephric mesenchyme induction. MM: metanephric mesenchyme; UB: ureteric bud. (Modified from Bouchard et al., 2004).

1.2 Chronic kidney disease and end-stage renal disease

Chronic kidney disease (CKD) has been recognised as a major public health problem and its incidence is increasing worldwide (Zoccali et al., 2009; James et al., 2010). CKD has been defined as a condition in which structural or functional abnormalities of the kidneys last for more than three months. CKD is usually detected through the measurement of the glomerular filtration rate (GFR) and it is classified into 5 stages of increasing severity (Table 1).

Table 1. Classification of CKD into 5 stages of increasing severity. Physiological GFR: 90-120 mL/min per 1.73 m² (Source: National Kidney Foundation) (Modified from Zoccali et al., 2009).

Stage	Description	GFR (mL/min per 1.73 m ²)
1	Kidney damage with normal or increased GFR	≥90
2	Kidney damage with mild decreased GFR	60-89
3	Moderate decreased GFR	30-59
4	Severe decreased GFR	15-29
5	Kidney failure	<15 or dialysis

Conditions such as type 1 and type 2 diabetes mellitus, hypertension, glomerulonephritis, atherosclerosis, acute kidney injury and hereditably diseases (polycystic kidney disease, for instance) are among the most common causes of CKD (Zoccali et al., 2009; James et al., 2010; Schiffli, 2010). It has also been demonstrated that patients with neoplasia and chronic infectious diseases, namely hepatitis and HIV, display an increased risk of developing CKD, because of the exposure to nephrotoxic drugs, such as antiretroviral drugs, protease inhibitor and the anticancer

agent cisplatin (Morigi et al., 2004; Zoccali et al., 2009; Kalyesubula and Perazella, 2010). Although data regarding CKD are still very scarce and far from being conclusive, it has been reported that 10% of adult Americans develop CKD and it is believed that Europe and Australia display a similar prevalence of CKD among the adult population. Estimations have revealed that the prevalence of stage 3-5 CKD, which represents the stage with the highest risk for patients to progress toward renal failure, appears to be similar across European countries and more frequent in females than males (Zoccali et al., 2009). There are two main clinical problems secondary to chronic kidney disease: firstly, CKD might progress to end-stage renal disease (ESRD); secondly, patients with CKD present an increased risk to develop cardiovascular complications. Besides these clinical aspects, CKD has also a huge economical impact on society. The renin-angiotensin-aldosterone system (RAAS) plays a pivotal role in promoting ESRD progression in patients with chronic kidney injury by acting through the protein angiotensin II (Ang II) (Aros and Remuzzi, 2002). Ang II promotes ESRD progression as it increases intraglomerular pressure and stimulates the secretion of aldosterone, which induces inflammation and fibrosis (Macconi et al., 2006). Current therapies aimed at preventing ESRD involve the use of angiotensin-converting enzyme inhibitors (ACE-Is) and Ang II receptor blockers (ARBs) (Macconi et al., 2006; James et al., 2010). Although these therapies are capable of significantly delaying the onset of ESRD, they still present several problems: while some patients are unable to respond to ACE-I/ARBs treatment, others cannot continue the therapy because of iatrogenic complications (James et al., 2010; Murray et al., 2010). It is therefore evident that the failure of these treatments likely leads to end-stage renal disease. ESRD is a condition in which

kidneys are no longer functional and renal replacement therapies are required. ESRD is certainly a worldwide health problem and, despite the general improvement of medical treatments, its incidence is constantly increasing (Knauf and Aronson, 2009). Zoccali and colleagues reported that in Europe, the prevalence of renal replacement therapies for ESRD increased from 480 to 807 patients per million population between 1992 and 2005. This surge was in particular due to a catastrophic raise (+130%) in the number of patients older than 65 years old with ESRD (Zoccali et al., 2009). The United States present one of the highest incidence rate of ESRD in the world, which was estimated in approximately 400 patients per million population in 2009 (Knauf and Aronson, 2009). Furthermore, it has also been forecasted that the prevalence of ESRD population in the United States will reach approximately 800,000 patients by 2020 (Fig. 10) (United States Renal Data System, USRDS; <http://www.usrds.org>).

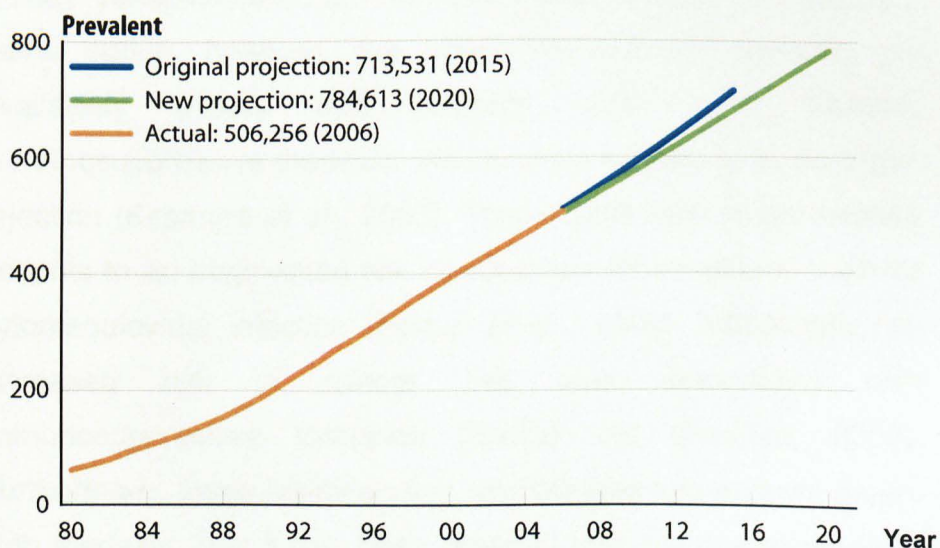


Figure 10. Projection of prevalence of ESRD using data available through 2000 (original projection) and data available through 2006 (new projection). Actual: 2006. Data are expressed in number of patients (in thousands). (Downloaded from USRDS, <http://www.usrds.org>).

This increment will also be accompanied by an escalation in the costs for the overall health care system: it is estimated that the actual cost to treat ESRD is approximately \$50.000 per patient per year, which raises to approximately \$100.000 per patient per year when co-morbidities are present (Knauf and Aronson, 2009). The general improvement in quality of life and medical care, especially in developed countries, has resulted in an extension in life expectancy. This aspect, along with the growing incidence of diabetes, has contributed to the worldwide rise in the prevalence of ESRD (James et al., 2010). At present, dialysis and kidney transplantation are the only renal replacement therapies available, and although they are able to extend life expectancy, these approaches still present several problems. In fact, dialysis cannot fully compensate kidney function, and furthermore, it exposes patients to an increased risk of infections, and requires dramatic lifestyle changes (Kitamura et al., 2005; <http://www.kidney.org.uk>). Kidney transplantation, on the other hand, certainly represents a better option; however, the organ demand still exceeds the availability (Knauf and Aronson, 2009). In addition, immunosuppressive therapies are required in order to avoid organ rejection (Kitamura et al., 2005). These treatments might expose patients to an augmented risk of opportunistic infections, such as cytomegalovirus infection (Fortun et al., 2010); additionally, an increased risk of cancer has been associated with immunosuppressive therapies (Dantal and Souillou, 2005). Furthermore, these life-extending technologies still present a very high mortality rate: it has been reported that the overall mortality rate five years after renal replacement therapies is approximately 52% of all patients, and that dialysis entails a mortality rate approximately five time higher than kidney transplantation (Zoccali et al., 2009). These figures point out that a strategy to replenish

damaged kidney tissues to prevent kidney failure in patients with renal disease is strongly required. Given that stem cells are able to undergo self-renewal and are capable of maintaining organ integrity and functionality by differentiating into specialized cells, an attractive approach is represented by a stem cell-based therapy. In fact, the possibility to differentiate a given stem cell population into a particular renal cell type will make these cells a potential therapeutic tool for the replacement of damaged kidney tissues.

1.3 Stem cells

1.3.1 Stem cells in development and homeostasis

Stem cells are defined as special kinds of cells that have the unique capacity of undergoing self-renewal, often throughout the lifespan of the organism. Moreover, under certain conditions, stem cells are able to differentiate into specialized cells (Fig. 11) (Weissman, 2000).

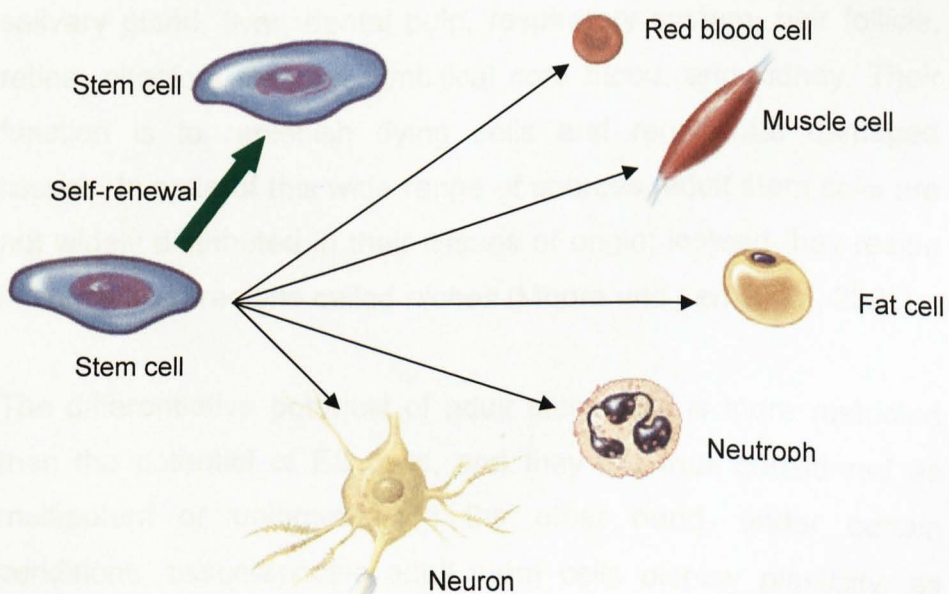


Figure 11. Representation of stem cell self-renewal and differentiation into different specialized cell types (Modified form Kirschstein and Skirboll, 2001).

The differentiation potential of stem cells is defined by the *potency*. Given that the zygote is the only totipotent cells, as they give rise to extra-embryonic tissues as well as all cells present in the adult body, stem cells are usually classified as pluripotent, multipotent and unipotent.

There are two principal categories of stem cells: the embryonic stem (ES) cells and the adult, or somatic, stem cells. ES cells are derived from the inner cell mass of the blastocyst and were isolated for the first time in 1981 by two independent research groups (Evans and Kaufman, 1981; Martin, 1981). ES cells are considered pluripotent stem cells because they are capable of giving rise to all derivatives of the three embryonic germ layers: the endoderm the mesoderm and the ectoderm.

Adult stem cells are undifferentiated cells found in many different sources, such as blood, bone marrow, brain, fat, mammary gland, salivary gland, liver, dental pulp, respiratory system, hair follicle, retina, olfactory mucosa, umbilical cord blood, and kidney. Their function is to replenish dying cells and regenerate damaged tissues. In spite of this wide range of sources, adult stem cells are not widely distributed in their tissues of origin; instead they reside in specialized regions called *niches* (Moore and Lemishka, 2006).

The differentiative potential of adult stem cells is more restricted than the potential of ES cells, and they are thus considered as multipotent or unipotent. On the other hand, under certain conditions, tissue-specific adult stem cells display *plasticity*, as

they seem to be able to generate specialized cells that derive from other germ layers (Galli et al., 2003). Plasticity seems to be accomplished by a mechanism of transdifferentiation, by which tissue-specific stem cells of one lineage can convert into stem cells of an entirely distinct lineage. However, due to a poor experimental reproducibility, the hypothesis that adult stem cells are able to transdifferentiate by activating a dormant differentiation program to generate cells of distinct lineages has been highly controversial (Wagers and Weissman, 2004). In the attempt to explain the apparent plasticity of adult stem cells, at least three distinct mechanisms might be taken into account. First, plasticity might be the result of a mechanism of de-differentiation of a given multipotent stem cell into a pluripotent stem cell, followed by re-differentiation into a cell type of a different lineage. In addition, it has been proposed that there might be rare adult pluripotent stem cells among many adult multipotent stem cells which might be accountable for the generation of cells of distinct lineages. Furthermore, contributions to plasticity might also arise through a mechanism of cell-cell fusion between differentiated cells, a process that occurs normally in adult animals (Wagers and Weissman, 2004). A more recent study has indeed criticised transdifferentiation of adult stem cells. Using an *in vitro* culture system, Rose and colleagues demonstrated that following co-culture with embryonic cardiomyocytes, bone marrow-derived mesenchymal stem cells (MSC) were able to express cardiac-specific genes, however they did not generate either action potentials or ionic currents, thus indicating that these cardiomyocyte-like cells were not functional (Rose et al., 2008).

The origin of adult stem cells has been under intense debate. In a recent review, it has been suggested that the multipotent adult

stem cells may represent a remnant of pluripotent progenitor cells left over during embryo development. The neural crest seems to give rise to some adult multipotent stem cells, as in the embryo it contains many stem cells before migration. As they migrate during embryo development, the number and degree of multipotency of neural crest cells decrease due to exposure of different factors. Cell tracking studies have suggested that skin-derived precursors (SKP) and bone marrow-derived MSC seem to display a neural crest origin (Slack, 2008). According to this view, tissue-specific stem cells present in the postnatal organism may be derived from the embryonic rudiment through a series of hierarchical processes controlled by specific inducing factors (Slack, 2008).

1.3.2 Stem cells for the treatment of acute renal failure

Acute renal failure (ARF) represents one of the causes of chronic kidney disease (Schiffl, 2010). ARF is a condition characterized by an abrupt decline in kidney function due to an extensive damage of kidney tubules, and normally it is marked by a rise in both blood urea nitrogen (BUN) and serum creatinine levels. Conditions such as ischemic insults, sepsis, hypovolemic states, glomerulonephritis and nephrotoxic agents are the most common causes of ARF (Humphreys et al., 2008; Mr Simon Kenny, personal communication). The kidney has the striking capability to undergo regeneration following ARF. Humphreys and colleagues provided strong evidence that the regenerative process seems to be accomplished by intrinsic, and presumably undamaged, epithelial tubular cells: following injury these cells are capable of undergoing rapid proliferation with the purpose of replenishing damaged kidney tissues (Humphreys et al., 2008). Despite this remarkable ability, in some circumstances the kidney is unable to accomplish

a complete recovery; therefore ARF might lead to chronic kidney injury which, in turn, might progress to end-stage renal disease.

ARF has been widely studied in different mouse and rat injury models and can be induced by ischemia-reperfusion, intramuscular injection of glycerol, subcutaneous injection of cisplatin and intravenous injection of adriamycin (see section 7.1). The folic acid (FA) model of induced nephropathy might be used to study the progression of acute kidney failure toward chronic injury. FA is an essential nutrient in humans (Fang et al., 2005). In rodents, intraperitoneal administration of high dose of FA leads to the rapid accumulation of FA crystals within renal tubules, which causes acute tubular necrosis. Although renal tubules can regenerate within a few days following FA injection, it has been demonstrated that a systemic administration of FA leads to chronic kidney injury, characterized by patchy interstitial fibrosis, tubular atrophy and loss of peritubular capillaries (Long et al., 2008).

The feasibility to control the differentiation process of stem cells toward a specific cell lineage represents an extremely important goal in regenerative medicine. This will create a potential opportunity to treat chronic kidney disease by using stem cell-based strategies, instead of renal replacement therapies such as dialysis or kidney transplantation. In this section the characterization and use of renal and non-renal stem/progenitor cells in different ARF-induced animal models will be described.

1.3.2.1 Stem cells from rodent kidney

Several studies have already suggested the presence of stem/progenitor cells in both rodent and human kidney. One strategy to isolate stem/progenitor cells from adult kidney has

involved a pulse of 5-bromo2-deoxyuridine (BrdU), followed by a long chase period. Oliver and colleagues demonstrated that a population of slow cycling label-retaining cells, detected by BrdU incorporation, resided in the interstitium of the rat and mouse renal papilla. Following isolation and *in vitro* culture, papillary cells showed a pluripotent phenotype as they expressed different epithelial, mesenchymal and neuronal proteins, and were able to give rise to spheres, a characteristic which is common to different types of adult stem cells. In addition, when injected into the sub-capsular space of rat kidney subjected to ischemia-reperfusion injury, a fraction of *in vitro* cultured papillary cells could spread into the renal parenchyma and integrate into renal tubules and the interstitium (Oliver et al., 2004). More recently, by using a transgenic approach this research group was able to demonstrate that under normal conditions, a fraction of the papillary slow cycling label-retaining cells migrate to and proliferate in the upper papilla to provide a supply of cells for kidney homeostasis. Notably, the number of proliferating papillary cells decreased as the animals aged. Both migration and proliferation were strongly increased during acute renal failure induced by ischemia-reperfusion injury. Remarkably, a fraction of the proliferating cells were able to migrate deep in the kidney parenchyma, where they integrated into damaged tubules (Oliver et al., 2009). These findings suggest that rat and mouse papilla contains a population of renal progenitor cells which might be able to replenish damaged tissues following kidney injury.

In contrast to these results, Maeshima and colleagues isolated a population of slowly dividing cells from adult rat kidney proximal and distal tubules. These cells, called label-retaining tubular cells (LRTC), expressed epithelial markers, were capable of

proliferating in response to certain growth factors and were able to form tubule-like structures when cultured in collagen gels. Furthermore, following *ex vivo* transplantation into E15 rat metanephros, the majority of LRTC localized in the interstitium, however some cells could integrate into developing proximal tubules and ureteric bud (Maeshima et al., 2006). In this study LRTC integration into developing glomeruli was not investigated. The discrepancy between this work and the Oliver studies published in 2004 and 2009 may be due to the different age of rats used: in the former work the cells were found in 7-week old rat kidneys (adult), while in the latter the cells were detected in neonatal rats, when nephrogenesis was still ongoing. Thus, the different localization of label-retaining cells may be different at each stage of kidney development.

A population of renal progenitor-like cells was isolated from the S3 segment of the rat kidney proximal tubules. In this study, Kitamura and colleagues demonstrated that these cells could be expanded in culture indefinitely, expressed stem/progenitor cell markers such as *Sca-1*, *c-kit* and *Musashi1*; metanephric mesenchyme-specific markers, such as *Pax2*, *Wt1*, *Gdnf* and *Wnt4*; and the tubular epithelial markers *Aquaporin1* and *Aquaporin2*. This phenotype was maintained when the cells were cultured in the presence of mouse mesenchymal cell supernatant (MCS). When injected under the renal capsule in a rat model of ischemia-reperfusion injury, S3-derived cells could engraft into renal tubules of the cortico-medullary region (Kitamura et al., 2005). Although the data presented in this study suggest that the S3 segment might contain a population of renal progenitor-like cells, several questions about these cells still remain unanswered. Firstly, although Kitamura and colleagues claimed that S3-derived cells acquired a more

differentiated phenotype following MCS withdrawal, the published data is not convincing. Secondly, following cell inoculation into damaged rat kidney, renal function might not have improved, as the level of neither blood urea nitrogen and serum creatinine changed.

Dekel and co-workers used a strategy to isolate stem cells based on the selection of a specific stem/progenitor cell marker. Using this approach, a population of non-tubular Sca-1⁺ Lin⁻ cells, most likely of papillary origin, was isolated from adult mouse kidney (Dekel et al., 2006). Sca-1⁺ Lin⁻ cells showed a stem cell phenotype, as they were clonogenic and capable of differentiating into osteogenic, adipogenic and neural lineages. Microarray analysis confirmed that Sca-1⁺ Lin⁻ cells expressed several genes normally found in different population of stem cells and many genes expressed during the development of the mesoderm lineage. The renoprotective effect of Sca-1⁺ Lin⁻ cells was assessed in a mouse model of acute renal failure, which was induced by ischemia-reperfusion injury. Using this model, Dekel and collaborators demonstrated that Sca-1⁺ Lin⁻ cells, when inoculated into the renal parenchyma through the renal pelvis immediately after the induction of renal damage, were able to engraft mainly into damaged tubules and, to a lesser extent, into glomeruli. These authors also noticed that Sca-1⁺ Lin⁻ cells populated mainly the tubules that were confined to the site of cell inoculation, thus suggesting a reduced capability of the cells to spread over the injured organ. In this study, the improvement of the renal function following cell inoculation was not investigated (Dekel et al., 2006).

A similar approach to identify stem/progenitor cells, mainly of bone marrow origin, has been based on the purification of side population (SP) cells from adult organs. SP cells are identified by the low Hoechst nuclear signal, which is due to the capability of the cells to rapidly exclude the dye from the nucleus. Using this strategy, Challen and colleagues reported that both adult and E15.5 embryonic mouse kidney contained a pool of SP cells which displayed a progenitor phenotype. Embryonic and adult SP cells accounted for 0.10% and 0.14% of the total viable cell population of the kidney, respectively. *In situ* hybridization performed on adult kidneys revealed that the possible *niche* of the SP cells were the proximal tubules. Expression profile analyses revealed that both adult and embryonic SP cells expressed several stem/progenitor cell markers, such as the genes *Pax8*, *CD44* and *CD105*; and the proteins Sca-1 and CD24. However, the study showed that approximately 9% of the cells of the SP was formed by macrophages, thus indicating that the SP represents a heterogeneous population of cells. SP cells were able to differentiate into non-renal cell types, such as osteocytes and adipocytes. When injected into E12.5 mouse kidney rudiments, adult SP integrated into Wt1-positive MM-derived structures and, to a lesser extent, into calbindin-positive UB-derived structures. The ability of SP cells to contribute to kidney recovery was investigated in a mouse model of adriamycin-induced nephropathy. Intravenous injection of adriamycin induces a rapid glomerular injury which causes loss of podocytes, severe proteinuria, accumulation of tubular casts and progressive renal failure. SP cells were injected into the tail vein and into the renal parenchyma shortly after adriamycin injection. Despite the suggested tubular origin of SP cells, Challen and colleagues showed that only a few cells could integrate into tubules, as the

vast majority of them remained in the interstitium around the site of cell inoculation. (Challen et al., 2006). Since renal function did not improve following cell inoculation, these cells might not be able to exert a renoprotective effect.

A multipotent renal progenitor cell (MRPC) population was isolated from the adult rat kidney, following disaggregation of the whole organ into single cells. MRPC, characterized by Gupta and collaborators (Gupta et al., 2006), were karyotypically stable for more than 200 population doublings and were able to undergo virtually unlimited self-renewal. These authors demonstrated that MRPC resided mainly in the proximal tubules at the cortical medullary junction. Similar to other progenitor cell types already discussed, MRPC expressed the embryonic markers *Pax2* and vimentin, the pluripotent marker *Oct4* and the progenitor cell markers CD90 and CD44. MRPC displayed a wide spectrum of multipotency, as they were able to express endothelial, neural and hepatocytic markers when cultured under differentiating culture conditions. In addition, MRPC differentiated into a nephron-like epithelium following incubation with a nephrogenic cocktail, which consisted of FGF2, TGF- β and leukemia inhibitory factor (LIF). The ability of MRPC to differentiate *in vivo* was confirmed by inoculating the cells under the renal capsule of healthy rat: several MRPC could incorporate into renal tubules; however, some cells formed cyst-like structures at the site of injection. Furthermore, similar to the observation of Oliver and colleagues (Oliver et al., 2004), when inoculated in a rat model of ischemia-reperfusion injury, some cells could incorporate into damaged tubules. However, it was also noticed that several MRPC became lodged in glomeruli and formed cellular casts. Amelioration of the renal

function following cell inoculation was not observed (Gupta et al., 2006).

During kidney injury, the tubular compartment is greatly exposed to toxic substances capable of severely damaging tubular cells. It is therefore possible that the renal interstitium might serve as a better *niche* for stem cells than renal tubules, as it might constitute a more protected environment. This hypothesis has been investigated by Lee and colleagues who showed that a population of mouse kidney progenitor cells (MKPC) resided in the interstitium of the medulla and papilla. MKPC were isolated using a transgenic strategy in which the last part of the sequence of *Myh9*, a gene expressed in all interstitial cells and encoding myosin heavy chain IIA, was exchanged with the sequence for GFP. MKPC were capable of undergoing extensive self-renewal, were karyotypically stable and expressed several stem cell and renal progenitor cell markers, such as the genes *Wt1* and *Wnt4* and the proteins Pax2, Oct4, vimentin, α -SMA and CD29. MKPC were able to differentiate into non-renal cell types, such as osteocytes and endothelial cells, however they were not capable of differentiating into the adipogenic lineage. These authors investigated whether MKPC were involved in kidney repair by injecting the cells into the renal parenchyma of a mouse model of ARF induced by ischemia-reperfusion, immediately after the induction of the renal damage. Lee and colleagues showed that MKPC were able to incorporate into renal tubules and generate capillaries containing red blood cells, thus demonstrating that the cells were also capable of connecting with the host mouse vasculature. MKPC could ameliorate renal function, as demonstrated by a reduction in the levels of both blood urea nitrogen (BUN) and serum creatinine. In addition, MKPC were able

to improve renal morphology, reduce the infarct zone of injured kidneys and decrease mortality of ARF-induced mice (Lee et al., 2010). These findings suggest that MKPC represent a multipotent population of renal progenitor cells which might contribute to renal repair after ARF.

Previously in the Murray's laboratory, a population of kidney-derived stem cells (KSC), most likely of papillary origin, had been isolated from 2-6 day old mouse kidney, following enzymatic digestion and disaggregation of the organ into single cells. KSC were clonogenic, could be extensively expanded in culture and expressed the transcription factors *Wt1* and *Pax2*. One of the clonal lines established from the bulk population, named clone H6, showed a limitless proliferative capacity and was able to spontaneously generate renal-like cell types in culture, as they displayed a tubular-like and podocyte-like morphology. Although the H6 clonal line maintained the expression of *Wt1*, these cells no longer expressed *Pax2* (Fuente Mora, 2009).

1.3.2.2 Stem cells from human kidney

A population of resident progenitor cells has been found in human adult kidney. These cells, expressing the stem cell marker CD133⁺, were present in the interstitium of the renal cortex, but not in the glomerulus. CD133⁺ cells expressed several markers of progenitor cells, such as PAX2, CD29, CD44 and CD73, thus suggesting that these cells displayed a progenitor cell-like phenotype. However, CD133⁺ renal progenitor cells displayed a limited self-renewal ability, as the cells lost the expression of CD133 when expanded in culture for more than 9 passages. Cell clones were capable of differentiating *in vitro* into epithelial and endothelial cells; they were also able to spontaneously

differentiate *in vivo* into epithelial tubular structures when subcutaneously injected in matrigel in severe combined immunodeficiency (SCID) mice. However, CD133⁺ renal progenitor cells failed to differentiate into osteocytes and adipocytes. When subcutaneously injected into matrigel in SCID mice, *in vitro* endothelial-differentiated CD133⁺ cells were able to organize into functional vessels connected with the host vasculature. The renoprotective ability of CD133⁺ renal progenitor cells was investigated in a SCID mouse model of glycerol-induced ARF. When intravenously injected at the peak of renal injury, which occurred 3 days after the induction of renal damage, these cells could engraft into both proximal and distal tubules, but rarely into glomeruli. Moreover, a fraction of the engrafted CD133⁺ cells was able to undergo proliferation (Bussolati et al., 2005). Since the renal functionality was not assessed, the capability of CD133⁺ cells to exert a renoprotective effect still has to be determined. Although Bussolati and colleagues did not detect CD133⁺ cells in the glomeruli, using a more sensitive assay Sagrinati and colleagues demonstrated that in the adult human kidney a subset of parietal epithelial cells, resident at the urinary pole of the Bowman's capsule, express the stem cell markers CD24 and CD133. Once isolated, these cells exhibited a high clonogenic efficiency and extensive self-renewal capacity. CD24⁺ CD133⁺ cells displayed an undifferentiated phenotype, as the cells expressed the stem cell genes *Oct4* and *Bmi-1*, whereas they did not express markers of differentiated renal cells. CD24⁺ CD133⁺ cells were also able to differentiate into cells expressing markers of proximal and distal tubules, as well as into non-renal-like cell types, such as osteocytes, adipocytes and neuronal-like cells. Interestingly, neuronal-like cells appeared to be functional, as they displayed ionic currents *in vitro* (Sagrinati et al., 2006). More

recently, Ronconi and co-workers demonstrated that $CD24^+$ $CD133^+$ renal progenitor cells consisted of a heterogeneous population hierarchically distributed within the Bowman's capsule of adult human kidney (Fig. 12). Cells expressing CD24 and CD133, but not podocyte markers, were located at the urinary pole of the Bowman's capsule and could act as bi-potent progenitors as they were able to differentiate into both podocytes and tubular cells. A second population of $CD24^+$ $CD133^+$ renal progenitor cells positive for podocyte markers were found between the urinary pole and vascular pole of the Bowman's capsule. These cells showed a more restricted differentiation ability compared with the cell population present at the urinary pole since they could only generate podocytes, and not tubular cells.

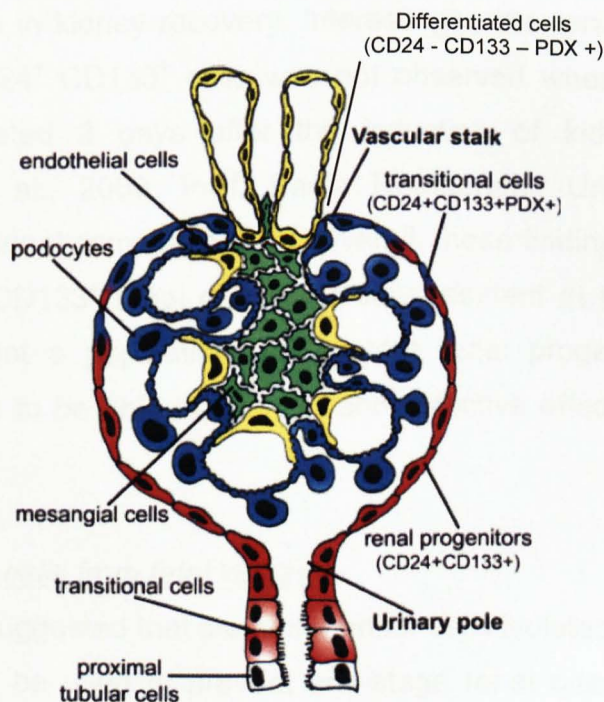


Figure 12. Schematic representation of the Bowman's capsule. The figure shows the hierarchical distribution of $CD24^+$ $CD133^+$ renal progenitor cells within the Bowman's capsule of the adult human kidney (Modified from Romagnani, 2009).

Finally, a third population present at the vascular pole of the Bowman's capsule showed characteristics of terminally differentiated cells: these cells expressed podocyte markers, however they did not express either CD24 or CD133 and failed to generate both podocytes and tubular cells. The renoprotective effect of CD24⁺ CD133⁺ cells was investigated by inoculating the cells into a SCID mouse model of adriamycin-induced nephropathy 1, 4, 9, 18 and 25 days after the induction of renal damage. Following multiple inoculation, only CD24⁺ CD133⁺ cells resident at the urinary pole engrafted into both glomeruli and renal tubules, and were capable of ameliorating renal function. Conversely, CD24⁺ CD133⁺ cells resident between the urinary and vascular pole hardly engrafted into injured kidney and were unable to participate in kidney recovery. Interestingly, the renoprotective effect of CD24⁺ CD133⁺ cells was not observed when the cells were inoculated 3 days after the induction of kidney injury (Ronconi et al., 2009, Prof. Paola Romagnani, University of Firenze, personal communication). Overall, these findings suggest that CD24⁺ CD133⁺ renal progenitor cells resident at the urinary pole represent a population of bi-potent renal progenitor cells which seems to be able to exert a renoprotective effect following kidney injury.

1.3.2.3 Stem cells from fetal kidney

It has been suggested that stem/progenitor cells isolated from fetal kidney might be used to prevent end-stage renal disease. Fetal kidney precursor cells were obtained from E17.5 rat metanephroi, that were enzymatically digested and disaggregated into single cells. Once isolated, a fraction of these cells expressed many stem cell markers, such as Oct4, SSEA-1, c-kit, CD34, CD90 and CD133, thus confirming that the developing metanephros contains

renal progenitor cells (Oliver et al., 2002). The therapeutic effect of fetal kidney progenitor cells was investigated in a rat model of surgically-induced renal failure, which was obtained by removing 5/6 of the total kidney mass (5/6 nephrectomy). Due to nephrectomy, animals developed kidney failure, characterized by severe proteinuria, glomerular hypertrophy and reduced glomerular filtration rate. Fetal kidney precursor cells were transplanted under the kidney capsule of the remaining tissue, five weeks after 5/6 nephrectomy. Six and ten weeks after transplantation, many renal tubules and glomeruli formed within the reconstituted region (Kim et al., 2007). These authors showed that many fetal kidney precursor cells were able to integrate into these renal structures. Furthermore, the cells were able to ameliorate kidney function, reduce mortality and induced a very limited immune response. Conversely, the transplantation of adult kidney cells, isolated from 8-week old rats following the same strategy used to isolate the fetal cells, failed to generate renal tissues and could not improve renal function (Kim et al., 2007). In a subsequent study, these authors showed that the reconstitution of the kidney appeared to be strongly dependent by the gestational age of the fetal kidney precursor cells. When E17.5 cells were transplanted into the omentum of immunocompromised mice, they were able to generate developing glomeruli and renal tubules, whereas E20.5 cells formed very few renal structures. Conversely, E14.5 cells generated glomeruli and renal tubules, however they also differentiated into non-renal tissues, such as cartilage and bone. The formation of non-renal tissues was also observed when E14.5 cells were transplanted under the renal capsule of immunocompromised mice. Besides, the cells were able to generate immature tubules and glomeruli. Compared to omental transplantation, subcapsular transplantation of E17.5 cells

resulted in the formation of more mature glomeruli and tubular structures compared with E14.5 cells; importantly, non-renal tissues did not form. When E20.5 cells were transplanted, only few glomeruli and tubular structures could be observed (Kim et al., 2007). These findings suggest that the transplantation of fetal kidney precursor cells appears to ameliorate renal morphology and function following kidney injury. However, the gestational age of the cells seems to be critical for the correct reconstitution of kidney tissues.

As already described in section 1.3.2.2, the human kidney contains a population of CD24⁺ CD133⁺ renal progenitor cells (Sagrinati et al., 2006) Lazzeri and collaborators demonstrated that CD24⁺ CD133⁺ cells appear in the embryonic human kidney at 8.5-9 weeks of gestation and become progressively restricted to the urinary pole of the Bowman's capsule during nephron development. The cells displayed a progenitor cell phenotype similar with that of their adult counterparts, as they showed clonogenic, self-renewal and multi-differentiation capacity. The ability of CD24⁺ CD133⁺ REC to contribute to renal repair was investigated in a SCID mouse model of ARF induced by glycerol injection. When inoculated intravenously 3 and 4 days after glycerol injection, the cells were able to engraft into renal tubules and differentiate into proximal and distal tubular cells, and collecting duct cells. Very few cells seemed to be able to differentiate into renal endothelial cells. Following CD24⁺ CD133⁺ REC engraftment, renal morphology recovered and renal function displayed an improvement 11 days after the induction of renal damage. Furthermore, when ARF-induced SCID mice were inoculated with the cells a few hours after the induction of renal damage, they displayed a reduced severity of the degree of renal

failure compared with saline-injected mice, thereby suggesting that CD24⁺ CD133⁺ REC might be able to prevent severe ARF. Finally, CD24⁺ CD133⁺ REC did not show any tumorigenic potential (Lazzeri et al., 2007). These results suggest that CD24⁺ CD133⁺ REC might constitute a population of progenitor cells with the ability to prevent and reduce ARF.

Romio and colleagues generated a human metanephric cell line from 10-12 week-old fetal metanephroi that displayed a mesenchymal morphology and was able to express the renal-specific markers WT1, PAX2 and GDNF for more than 20 passages (Romio et al., 2003). In a subsequent study it was shown that metanephroi-derived cells, cultured in serum-free medium, expressed *LIF* and its receptors *LIFR* and *gp130*, however they lost the expression of *PAX2* (Price et al., 2007).

1.3.2.4 Mesenchymal stem cells

The role of mouse bone marrow-derived mesenchymal stem cells (MSC) in renal recovery was investigated by Morigi and collaborators in a mouse model of acute renal failure, induced by subcutaneous injection of cisplatin (Morigi et al., 2004). This group showed that when mice were inoculated with MSC one day after the induction of damage, the cells were able to engraft into damaged kidney tubules, differentiate into tubular epithelial cells, stimulate tubular proliferation and ameliorate renal functions. Similar results were also obtained when a population of MSC immunodepleted of CD45⁺ cells, a marker which identifies hemopoietic precursors, was injected in the same mouse model of ARF. Conversely, the injection of bone marrow-derived hemopoietic stem cells (HSC) did not improve renal recovery (Morigi et al., 2004). Similarly, using a mouse model of glycerol-

induced ARF, Herrera and colleagues provided further evidence for a role of mouse MSC in kidney recovery following acute tubular injury (Herrera et al., 2004). More recently, it was demonstrated that the infusion of human umbilical cord-derived MSC into cisplatin-induced ARF SCID mice could ameliorate renal function and greatly reduce mortality, thereby suggesting that the use of these cells might be of great clinical relevance for the treatment of acute renal failure (Morigi et al., 2010). Interestingly, Fang and colleagues suggested that the contribution of bone marrow-derived cells to tubular repair following acute injury might be very limited. These authors transplanted the whole bone marrow in a lethally irradiated mouse model of folic acid-induced ARF and demonstrated that renal tubular regeneration was largely accomplished by indigenous tubular cells, whereas the transplanted cells played a very marginal role in this process (Fang et al., 2005). The differences between this study and the aforementioned investigations might be due to the use of different cell types, as well as to the use of distinct animal models of kidney injury.

The contribution of mouse MSC to renal recovery following ARF was investigated using an *in vitro* model of acute renal injury, which consisted of cisplatin-treated mouse kidney proximal tubular cells co-cultured with mouse MSC. In this study it was documented that IGF-1, released by MSC, induced a protective effect on proximal tubular cells by stimulating tubular cell proliferation. These results were also confirmed *in vivo* in a mouse model of ARF, induced by cisplatin injection: while MSC could ameliorate both renal function and morphology, IGF-1 gene-silenced MSC showed a more limited protective effect on tubular

injury. Gene silencing did not affect the ability of the cells to engraft into injured kidney (Imberti et al., 2007).

Herrera and collaborators suggested that hyaluronic acid (HA) and its receptor CD44 might play an important role in the homing of MSC into injured kidney. HA is virtually absent in healthy kidney, but it is abundant in tubular basement membrane following acute tubular injury. Bone marrow-derived MSC isolated from *CD44*^{-/-} mice were unable to engraft into glycerol-induced ARF mouse kidneys; conversely, MSC expressing CD44 could integrate into proximal tubules. Cell engraftment was also blocked when *CD44*⁺ MSC were incubated with an anti-CD44 blocking antibody, or with soluble HA before inoculation into ARF-induced mice. In addition, only MSC *CD44*⁺, but not MSC *CD44*⁻, were able to ameliorate renal function and improve renal morphology. These authors also showed that a fraction of cells recovered from the inoculated kidneys expressed epithelial differentiation markers (Herrera et al., 2007). These findings provided evidence for a role of CD44/HA interactions in the recruitment of MSC to injured kidney tissues.

It has been suggested that the renoprotective effect of MSC might be related to the secretion of protective factors in a paracrine manner, rather than being a consequence of cell engraftment and differentiation into renal tubular cells. Togel and colleagues noticed that the injection of MSC into a rat model of ischemia-reperfusion ARF could improve kidney function, even though cell engraftment into the injured kidney was a very rare event. MSC were found mainly inside glomerular capillaries; in addition, these authors also observed that some MSC were entrapped in capillary beds of most organs. Measurement of gene expression levels in

ARF-induced kidneys revealed that MSC infusion could stimulate the expression of the anti-inflammatory cytokine IL-10 and inhibit the expression of the pro-inflammatory cytokines IL-1 β , TNF- α and INF- γ (Togel et al., 2005). Although these results could not be fully confirmed by a semi-quantitative protein level assay, they hinted that in rat the renoprotective effect might be mediated through immunomodulatory mechanisms, rather than cell engraftment. In a subsequent study, these authors documented that MSC released several renoprotective factors, such as VEGF, HGF and IGF-1 that reduced apoptosis in endothelial cells and stimulated cell proliferation (Togel et al., 2007). Altogether, these findings suggest that MSC might mediate a renoprotective effect on injured kidney also through paracrine mechanisms.

More recently, an adult woman with lupus nephritis, an inflammation of the kidney caused by a disease of the immune system, and end-stage renal disease was treated with autologous CD34⁺ hemopoietic stem cells. For reasons that were not quite clear, in this case, the cells were injected directly into the renal parenchyma of both kidneys, instead of being peripherally infused (Nagy and Quaggin, 2010). Following cell injection, the patient's renal failure did not improve and within three months dialysis was required. Furthermore, one kidney developed blood vessels and bone marrow masses at the site of injection, which necessitated nephrectomy. The remaining kidney failed and the patient ultimately died (Thirabanjasak et al., 2010). This case unveils possible and dramatic complications of stem cell-based renal replacement therapies performed with little or no scientific rationale and without investigations carried out in animal models.

1.3.2.5 Human amniotic fluid stem cells

The use of human amniotic fluid stem cells (hAFSC) in renal replacement therapies has recently received great interest. hAFSC can be easily isolated through amniocentesis and propagated *in vitro* for more than 250 population doublings without showing obvious chromosomal rearrangements. These cells express several stem cell markers, such as Oct4, SSEA-4, c-kit, CD29, CD44, CD73, CD90 and CD105, and were able to differentiate into a broad spectrum of lineages, such as osteogenic, endothelial, myogenic, adipogenic, hepatic and neural lineages (De Coppi et al., 2007). The renal protective effect of hAFSC was investigated by Perin and colleagues in immunodeficient mice (*nu/nu* mice) with ARF induced by intramuscular injection of glycerol. These authors documented that following injection into the renal cortex, hAFSC could engraft mostly into damaged tubules and started expressing markers specific of the renal lineage. Moreover, hAFSC reduced the levels of both BUN and creatinine, preserved renal morphology, decreased tubular cell apoptosis and stimulated tubular epithelial cells to undergo proliferation. Furthermore, hAFSC appeared to be able to produce cytokines that could modulate the response of the host immune system to ARF. However, these findings should be considered with circumspection because the mouse model used in this study was partially immunocompromised, as it lacked activated T lymphocytes, but not their precursors. Therefore, the response of the immune system observed in this animal model might differ from the one of an immunocompetent animal model. In addition, Perin and colleagues suggested that the timing of cell inoculation was critical: the renoprotective effect of hAFSC was only observed when the cells were injected contemporaneously with the time of injury, whereas no beneficial effects were achieved when hAFSC

were inoculated at the peak of renal injury, 3 days after glycerol treatment (Perin et al., 2010). Although this study demonstrated that hAFSC could engraft into the kidney, some questions of whether the cells could also engraft into other organs still remain open. The data hinted that following injection into the renal cortex, the cells, transduced with luciferase, spread all over the body of the animal within a few hours, then became localized in the area of the kidney. After 21 days, luciferase signal was still visible around the kidneys, however a rather strong signal could also be detected in the head, which might raise the possibility that hAFSC could also engraft into the brain and differentiate into ectopic tissues.

Hauser and colleagues compared the renoprotective effect of hAFSC with that of human bone marrow-derived mesenchymal stem cells (MSC) in a SCID mouse model of acute renal failure, induced by glycerol injection (Hauser et al., 2010). These authors demonstrated that hAFSC and MSC, intravenously injected at the peak of renal injury, similarly ameliorated renal function. Both cell types engrafted mainly in the interstitium and peritubular capillaries; however, very rare cells integrated into renal tubules. The discrepancies between these results and the findings documented by Perin and colleagues (Perin et al., 2010) might depend on the modality of cell inoculation and on the different mouse strain used. Compared to MSC, hAFSC seemed to be more effective in reducing renal tubular cell apoptosis. On the other hand, MSC were more effective than hAFSC in inducing tubular cells to proliferate. Cytokine assays revealed that hAFSC produced more LIF than MSC; *in vitro* experiments of LIF blockade on tubular epithelial cell proliferation suggested that this factor might account for the biological activity of hAFSC. In conclusion,

these authors proposed that the renoprotective effect of hAFSC might not be greater than of MSC (Hauser et al., 2010).

Despite these studies, summarized in Table 2 and Table 3, as yet a population of renal or non-renal stem/progenitor cells with the potential to give rise to all cell types present in the mature nephron still has to be identified. The isolation of stem/progenitor cells with such ability would therefore be of great clinical relevance for the development of renal replacement therapies aimed at preventing the progression of acute and chronic kidney diseases to end-stage renal disease.

Table 2. Non renal stem cell populations used in animal models of acute renal failure

Cell type	Organism	Niche	Model of acute renal failure	Engraftment	Functional improvement	References
Mesenchymal stem cells (MSC)	Mouse	Bone marrow	Cisplatin-induced ARF mice; Glycerol-induced-ARF mice	Renal tubules	Amelioration of renal function	Herrera et al., 2004; Morigi et al., 2004; Herrera et al., 2007
	Rat		Ischemia-reperfusion-induced ARF rats	Very limited engraftment into glomerular capillaries	Amelioration of renal function likely through paracrine effects	Togel et al., 2005; Togel et al., 2007
	Human	Umbilical cord	Cisplatin-induced ARF SCID mice	Peritubular areas	Amelioration of renal function and morphology, improvement of mice survival	Morigi et al., 2010
Amniotic fluid stem cells (hAFSC)	Human	Amniotic fluid	Glycerol-induced ARF athymic <i>Foxn1^{nu}</i> mice; SCID mice.	Tubules, glomeruli (Perin et al., 2010); Interstitial and peritubular capillaries (Hauser et al., 2010).	Improvement of renal function, morphology; reduction of tubular cell apoptosis, modulate host immune response	Perin et al., 2010 Hauser et al., 2010

Table 3. Renal stem cell populations used in animal models of acute renal failure

Cell type	Organism	Niche	Model of acute renal failure	Engraftment	Functional improvement	References
Multipotent renal progenitor cells (MRPC)	Rat	Proximal tubules at the cortico-medullary junction	Ischemia-reperfusion-induced ARF rats	Engraftment into renal tubules; most of cells formed casts or lodged into glomeruli	No significant improvements were observed	Gupta et al., 2006
Slow-cycling label-retaining cells (LRCs)	Mouse and rat	Interstitialium of the papilla	Ischemia-reperfusion-induced ARF rats	Renal tubules and interstitium	LRCs might generate new cells to replenish damaged kidney tissues following ARF	Oliver et al., 2004; Oliver et al., 2009
Side population (SP) cells	Mouse	Proximal tubules	Adriamycin-induced ARF mice	Most of cells in the interstitium around the site of injection; few cells engrafted into tubules	No significant improvements were observed	Challen et al., 2006

Table 3 (continued). Renal stem cell populations used in animal models of acute renal failure

Cell type	Organism	<i>Niche</i>	Model of acute renal failure	Engraftment	Functional improvement	References
Sca-1+ Lin- cells	Mouse	Interstitialium of the papilla	Ischemia-reperfusion-induced ARF mice	Renal tubules adjacent to the site of cell inoculation	Not investigated	Dekel et al., 2006
Mouse kidney progenitor cells (MKPC)	Mouse	Interstitialium of medulla and papilla	Ischemia-reperfusion-induced ARF SCID mice	MKPC engrafted into renal tubules and capillaries	MKPC ameliorated renal function and morphology, reduced the infarct zone and decreased mortality	Lee et al., 2010
CD133 ⁺ renal progenitor cells	Human	Interstitialium of the renal cortex	Glycerol-induced ARF SCID mice	CD133 ⁺ cells engrafted into proximal and distal tubules and, to a lesser extent, into glomeruli	Not investigated	Bussolati et al., 2005

Table 3 (continued). Renal stem cell populations used in animal models of acute renal failure

Cell type	Organism	Niche	Model of acute renal failure	Engraftment	Functional improvement	References
CD24 ⁺ CD133 ⁺ renal progenitor cells	Human	Urinary pole of the Bowman's capsule	Glycerol- or adriamycin-induced ARF SCID mice. Multiple inoculations	Renal tubules and glomeruli, few cells within the interstitium	Amelioration of both renal function and morphology	Sagrinati et al., 2006; Ronconi et al., 2009
Fetal kidney precursor cells (E17.5)	Rat	Not investigated	5/6 nephrectomy rat	Engraftment into newly formed renal tubules and glomeruli	Amelioration of renal function, generation of renal tissue, reduction of the mortality	Kim et al., 2007
CD24 ⁺ CD133 ⁺ renal embryonic cells (REC)	Human	Present in renal vesicles and S-shaped body at 8.5-9 weeks of gestation	Glycerol-induced ARF SCID mice. Multiple inoculations	Engraftment into renal tubules; REC differentiated into proximal, distal and collecting duct cells	Amelioration of renal function and morphology; prevention of severe ARF	Lazzeri et al., 2007

1.4 Aims of the project

The mammalian kidney develops through a series of extremely complex interactions between two embryonic tissues, the metanephric mesenchyme (MM) and ureteric bud (UB) (Fig. 7) (Saxén, 1987). A domain of the MM adjacent to the tips of the UB, called cap mesenchyme, contains a population of progenitor cells that gives rise to all cell types present in the adult nephron, which represents the functional unit of the kidney (Kobayashi et al., 2008). It is plausible that a fraction of progenitor cells present within the MM remains undifferentiated during nephrogenesis, thereby giving rise to the residential stem/progenitor cells present in the adult kidney. Under physiological conditions these cells might contribute to the normal homeostasis of the kidney; however, following injury kidney stem/progenitor cells might be rapidly recruited to replenish damaged tissues.

The main aim of the present study was to compare the expression profile and nephrogenic potential of the kidney-derived stem cell H6 clonal line, originally derived from postnatal mouse kidney (Fuente Mora, 2009), with those of metanephric mesenchyme cells following *in vitro* culture. A comparable phenotype between the H6 clonal line and *in vitro* cultured MM cells would suggest that H6 cells represented a remnant of the MM that was able to escape differentiation during nephrogenesis. The uninduced MM rapidly undergoes apoptosis when cultured in the absence of either UB or heterologous inducing stimuli (Saxén, 1987; Dudley et al., 1999; Kuure et al., 2007). Since E11.5 mouse MM contains only ~ 15000 cells (Prof. Jamie Davies, University of Edinburgh, personal communication), the first aim of this work was to develop culture

conditions that could support the expansion of the uninduced MM *in vitro* for several days, in order to provide sufficient cell number for subsequent experiments. Then, it became prominent to investigate whether under the culture conditions developed, *in vitro* expanded MM cells could maintain a MM-like phenotype, retain a nephrogenic potential and form developing nephrons in the presence of inducing stimuli.

Having optimized culture conditions that allowed MM cells to undergo *in vitro* expansion for several days and maintain a MM-like phenotype and a nephrogenic potential, in the second part of this study the expression profile of the H6 clonal line was investigated and compared with that of *in vitro* cultured MM cells. If the H6 clonal line derived from the embryonic MM, then it would be able to participate in the formation of nephron-like structures. Therefore, in the subsequent step, the *in vitro* nephrogenic ability of the H6 clonal line was assayed and compared with that of *in vitro* expanded MM cells.

Finally, in the last part of this study, the *in vivo* nephrogenic potential of the H6 clonal line was investigated in a mouse model of acute renal tubular failure, induced by glycerol injection.

CHAPTER 2

2.1 Dissection

Unless otherwise stated, the chemicals, culture media, growth factors and equipments used in the present study were purchased from Sigma-Aldrich (Sigma-Aldrich, Missouri, USA).

2.1.1 Animal husbandry

Female CD1 mice (6-8 week old) were purchased from Charles River UK (Charles River, Margate, UK), whereas 5-8 week old CD1 mice, used for the renal injury studies, were purchased from Charles River Italia (Charles River, Calco, Italy). The animals were housed in a constant temperature room, with 12 hours light – hours dark cycle, and free access to food and water. Animals were killed by asphyxiation with CO₂, which was followed by cervical dislocation. Postnatal CD1 mice (1-3 day old) were killed by decapitation. The present study was conducted in accordance with the Animal (Scientific Procedure) Act and the National Institute of Health Guide for the Care and Use of Laboratory Animals (Italy).

2.1.2 Dissection of organs from adult mice

Kidneys were dissected from adult mice using sterilized stainless steel scissors and forceps. Kidneys were bisected coronally, then disaggregated as described in section 2.7.2, or processed for RNA extraction (see section 2.9.1) or either embedded in paraffin, or frozen in cryo-embedding solution (see section 2.4.7 and section 2.4.8). Small pieces of lung, liver and spleen were dissected from mice and embedded in cryo-embedding solution (see section 2.4.8). In addition, small parts of dissected kidneys were incubated in RNA later solution (Ambion, Texas, USA) at 4°C O/N. The next

day the solution was removed and the specimens were stored at -20°C.

2.1.2.1 Dissection of kidneys from postnatal mice

After being killed (see section 2.1.1), neonatal mouse kidneys were dissected as section 2.1.2 explains and immediately processed for RNA extraction (see section 2.9.1).

2.1.3 Dissection of embryonic kidney rudiments

Pregnant CD1 mice were killed at embryonic day 11.5 (E11.5) and E13.5 by asphyxiation with CO₂ and cervical dislocation. Embryos were removed from uterine horns using Dumont forceps, size 4 (Dumont, Swiss) and placed in MEM. Embryos were dissected under a Nikon SMZ1000 zoom stereomicroscope (Nikon Instruments Inc, New York, USA), decapitated using a 23 gauge hypodermic needle (Becton Dickinson, New Jersey, USA), then the caudal parts were separated from the rostral parts, and placed in fresh MEM. The gender of E13.5 embryos was determined on the basis of the morphology of the embryonic gonads. The caudal parts were placed on their dorsal side and sagittally cut in two halves using 27 gauge hypodermic needles (Becton Dickinson). Kidney rudiments were found adjacent to the hind limbs, at the end of the nephric ducts. Finally the rudiments were carefully isolated from the caudal part of the embryos using 27 gauge hypodermic needles and kept in ice-cold MEM.

2.1.4 Dissection of metanephric mesenchyme

Dissected kidney rudiments were incubated in 0.5 mg/ml collagenase type I for 5 mins at 37°C, then the enzyme was inactivated by transferring the samples to pre-warmed DMEM/F12 with 10% (v/v) fetal calf serum (FCS) (PAA, Pasching, Austria).

Using 27 gauge hypodermic needles the metanephric mesenchyme was carefully teased away from the ureteric bud and placed in fresh DMEM/F12 with 10% FCS. The samples were carefully observed in order to ensure that the dissected metanephric mesenchyme did not contain any part of the ureteric bud.

2.1.5 Dissection of spinal cord

The dissection of embryonic spinal cord was carried out in MEM. Embryos at E11.5 were first decapitated as section 2.1.3 explains, then the developing viscera were removed using Dumont forceps, size 4. The spinal cord was isolated by carefully teasing away the surrounding tissue. The spinal cord was kept in MM medium (see media recipes, page 95) either at 37°C and 5% CO₂, or at 4°C for up to 24 hours.

2.2 Tissue culture

In this study all cells were cultured in a humidified cell incubator (Sanyo Electric Co. Ltd, Osaka, Japan; Thermo Fisher Scientific Inc., Massachusetts, USA) at 37°C and 5% CO₂.

2.2.1 Culture of the kidney-derived H6 and E5 clonal lines

The H6 and E5 clonal lines were originally derived by Dr Cristina Fuente Mora from a population of kidney-derived stem cells (KSC), isolated from 2-6 day old CD1 mice (Fuente Mora, 2009). Briefly, postnatal kidneys were dissected, cut into pieces smaller than 1mm and incubated in 1mg/ml collagenase type I and 0.1mg/ml DNase I for 1h at 37 °C. The cell suspension was passed twice through 21 and 23 gauge needles, finally through a

30 μ m pre-separation filter. The cells were cultured in KSC medium (see media recipes, page 95) and cloned by limiting dilution in a 96-well plate (Nunc) (Fuente Mora, 2009). The clonal lines were routinely cultured in KSC medium on uncoated tissue culture dishes. Medium was changed every 3 days. Cells were passaged at confluence by removing the medium and washing the cells in pre-warmed phosphate buffered saline (PBS) without CaCl₂ and MgCl₂. The cells were incubated in a mixture of trypsin/EDTA in PBS without CaCl₂ and MgCl₂ (final concentration: 0.05% (w/v) trypsin/0.02% (v/v) EDTA) for approximately 1 min at 37°C and 5% CO₂. The trypsin solution was inactivated by adding an equal volume of pre-warmed KSC medium, then the cells were centrifuged at 400 g for 3 mins and the pellet resuspended in pre-warmed KSC medium. The cells were counted in a Neubauer haemocytometer (Hausser Scientific, Pennsylvania, USA), and seeded at a density of 8000 cells/cm².

2.2.2 Freezing of the kidney-derived H6 and E5 clonal lines

The H6 and E5 clonal lines were washed once in PBS without CaCl₂ and MgCl₂ and trypsinized as described in the previous section. After centrifugation the cells were resuspended in 500 μ l of Recovery™ Cell Culture Freezing medium (Invitrogen, California, USA) then the samples were transferred into cryogenic vials (Corning, Amsterdam, Holland). The samples were left at -80°C overnight (O/N) inside a Cryo 1°C Freezing Container (Nalgene, Roskilde, Denmark) containing 250 ml of isopropanol and finally stored in liquid nitrogen.

2.2.3 Thawing of the kidney-derived H6 and E5 clonal lines

The H6 and E5 clonal lines were quickly thawed by immersing the cryovial into a pre-warmed water bath. Thawed cells were transferred into a 15 ml tube (Greiner Bio One, Gloucester, UK) containing 9 ml of pre-warmed KSC medium and centrifuged at 400 g for 3 mins. The pellet was resuspended in KSC medium and the cells were cultured as explained in section 2.2.1.

2.2.4 Culture of metanephric mesenchyme

Each isolated metanephric mesenchyme was plated into 35 mm plastic tissue culture dishes (Nunc, Roskilde, Denmark) in MM medium either in the presence or absence of growth factors. In order to optimize the effect of paracrine/autocrine factors on cell growth, samples were cultured inside a silicon tissue chamber (chamber diameter 20 mm) placed into the tissue culture dish (Greiner Bio One). Samples were cultured in a total volume of 600 μ l of culture medium. Metanephric mesenchyme cells were cultured up to 4 days and medium was changed every 2 days.

Metanephric mesenchyme cells were subcultured at day 4 of culture following the procedure described in section 2.2.1. However, the trypsin was used at a final concentration of 0.01% (w/v) trypsin/0.005% (v/v). After removing the supernatant, the cells were resuspended and plated in a fresh tissue culture dish.

2.2.5 Co-culture of metanephric mesenchyme and spinal cord

Freshly isolated metanephric mesenchyme and embryonic spinal cord (SC) were isolated from E11.5 embryos as reported in section 2.1.4 and section 2.1.5. The SC was cut transversely every two somites. Three pieces of SC were placed on a 1.2 μ m nucleopore membrane filter (Millipore, Massachusetts, USA) which

was previously placed upon a stainless steel grid inside a tissue culture dish containing the culture medium, as shown in Figure 13. A second membrane filter was then deposited upon the pieces of SC. Three freshly isolated metanephric mesenchyme were pooled and placed on a new piece of membrane filter, then the samples were transferred on top of the second membrane filter, taking care to place the metanephric mesenchyme just upon the SC (Fig. 13).

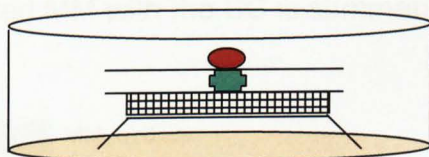


Figure 13. Schematic representation of transfilter culture. The spinal cord (green) is placed between two 1.2 μm nucleopore membrane filters on a stainless steel grid. The metanephric mesenchyme (red) is placed on the upper surface of the third membrane. Specimens are cultured in a tissue culture dish. Culture medium wets the grid surface.

This method allowed the metanephric mesenchyme and spinal cord to establish contacts through cellular processes. The samples were cultured in MM medium. The culture medium wet the grid by capillarity and was changed after 2 days. The samples were co-cultured for 3 days, and then fixed and immunostained (see section 2.4.4 and section 2.8.2 for details).

This induction assay was also performed using MM that had been cultured for 24, 48, and 72 hours. For the 24 hours induction assay, the metanephric mesenchyme was cultured on the membrane filter in MM medium for 24 hours. Three pieces of spinal cord (kept at 4°C, see section 2.1.5 for details) were placed in contact with the metanephric mesenchyme. The samples were co-cultured for 3 days; the culture medium was replaced after 2

days. For the 48 hours and 72 hours induction assay, the metanephric mesenchyme was cultured on membrane filter in MM medium, supplemented with 25 ng/ml BMP7 and 100 ng/ml FGF2 for either 48 hours, or 72 hours. The SC was dissected from E11.5 embryos the same day of the experiments. Three pieces of SC were placed in contact with the metanephric mesenchyme, then the samples were co-cultured for 3 days. The medium was changed every two days. The strategy followed to induce freshly isolated and cultured MM with the SC is summarized in Figure 14.

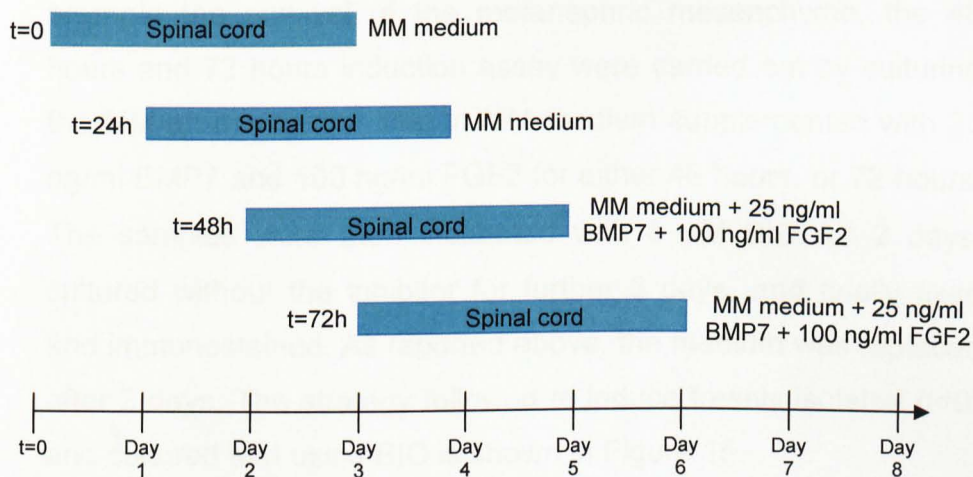


Figure 14. Strategy adopted to induce freshly isolated (t=0) MM and MM following 24h, 48h and 72 hours of culture by stimulation with spinal cord.

2.2.6 Culture of metanephric mesenchyme in the presence of GSK-3 inhibitor IX

Freshly isolated metanephric mesenchyme was dissected as described in section 2.1.4. The induction was carried out by placing three metanephric mesenchymes on 1.2 μm nucleopore membrane filter, and culturing them in MM medium supplemented with 50 ng/ml FGF2, and 5 μM GSK-3 inhibitor IX (BIO) (Calbiochem, Darmstadt, Germany) for 48 hours. The inhibitor was

then removed and the samples were cultured for further 3 days. The culture medium was replaced after 2 days. Finally the samples were fixed and immunostained as described in section 2.4.4 and section 2.8.2. For the 24 hours induction assay, three metanephric mesenchyme were cultured on membrane filter in MM medium supplemented with 50 ng/ml FGF2 for 1 day, afterwards 5 μ M BIO was added to the culture medium. The specimens were cultured in the presence of BIO for 48 hours, then the inhibitor was removed and the samples were cultured for further 3 days, replacing the medium after 2 days. In order to promote the survival of the metanephric mesenchyme, the 48 hours and 72 hours induction assay were carried out by culturing the MM on membrane filter in MM medium supplemented with 25 ng/ml BMP7 and 100 ng/ml FGF2 for either 48 hours, or 72 hours. The samples were then incubated with 5 μ M BIO for 2 days, cultured without the inhibitor for further 3 days, and finally fixed and immunostained. As reported above, the medium was replaced after 2 days. The strategy followed to induce freshly isolated ($t=0$) and cultured MM using BIO is shown in Figure 15.

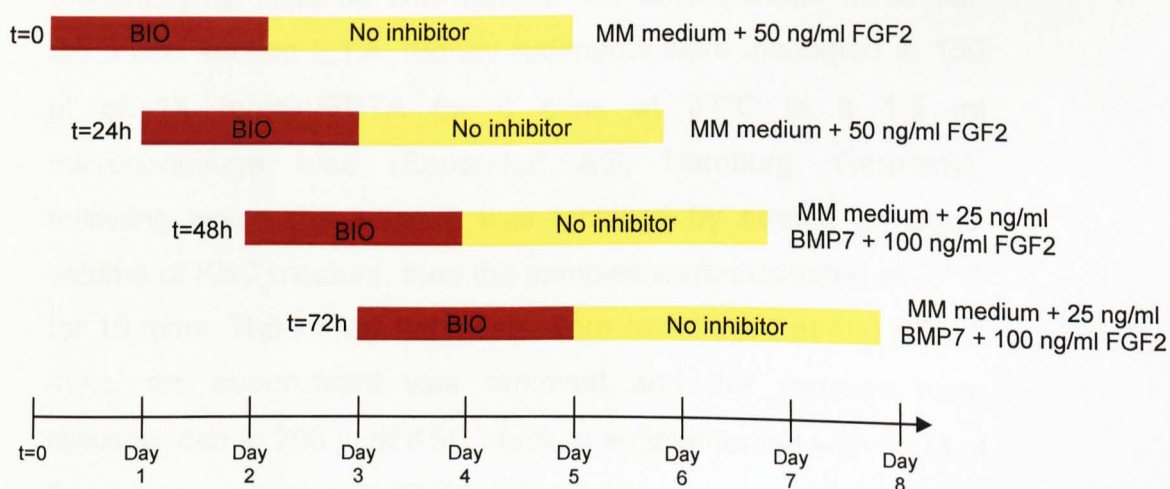


Figure 15. Strategy followed to induce freshly isolated (t=0) MM and MM following 24h, 48h and 72 hours of culture by stimulation with BIO.

2.2.7 Culture of kidney rudiments

E11.5 kidney rudiments were dissected as explained in section 2.1.3. The rudiments were cultured in KSC medium, supplemented with 1X penicillin/streptomycin (PS) on 1.2 μ m nucleopore membrane filter in transfilter culture for up to 6 days. The medium was changed every 2 days.

2.2.8 Culture of kidney rudiment chimeras

The chimera formation assay, which has been described by Unbekandt and Davies (Unbekandt and Davies, 2010) was carried out by recombining freshly isolated metanephric mesenchyme, cultured metanephric mesenchyme and the H6 clonal line with E11.5 kidney rudiments.

2.2.8.1 Culture of metanephric mesenchyme with embryonic kidney rudiments

Dissection of E11.5 kidney rudiments and E11.5 metanephric mesenchyme isolation was carried out as explained in section 2.1.3 and section 2.1.4. Kidney rudiments were incubated in 150 μ l of 1X trypsin/EDTA for 6 mins at 37°C in a 1.5 ml microcentrifuge tube (Eppendorf AG, Hamburg, Germany), following which the enzyme was inhibited by adding an equal volume of KSC medium, then the samples were incubated at 37°C for 10 mins. The kidney rudiments were centrifuged at 400 g for 3 mins, the supernatant was removed and the samples were resuspended in 200 μ l of KSC medium supplemented with 5 μ M of Rho-kinase inhibitor Y-27632 (Calbiochem) and disaggregated into single cells by gentle pipetting and counted. After isolation, the

metanephric mesenchyme was disaggregated into single cells by gentle pipetting, then the cells were counted. The labelled cells (see section 2.3.2 for details) were then mixed with kidney rudiment cells in a ratio of 1:3 (one part of labelled metanephric mesenchyme cells to three parts of kidney rudiment cells). The total number of cells forming each pellet was 8×10^4 . The cell suspension was centrifuged at 400 g for 3 mins. The pellet was collected with a pipette and transferred to a $1.2 \mu\text{m}$ nucleopore membrane filter in transfilter culture. The samples were cultured in MM medium supplemented with 25 ng/ml BMP7, 100 ng/ml FGF2 and $5 \mu\text{M}$ Rho-kinase inhibitor Y-27632 for one day; afterwards the inhibitor was removed and the specimens were cultured for further two days.

The recombination assay was also carried out by recombining 4-days cultured metanephric mesenchyme with E11.5 reaggregated kidney rudiments. Kidney rudiments were isolated and disaggregated into single cells. Metanephric mesenchyme cells were cultured for 4 days as explained in section 2.2.4, then were trypsinized and counted. Labeled metanephric mesenchyme cells were mixed with kidney rudiment cells in a ratio of 1:3. The cell suspension was centrifuged at 400 g for 3 mins, then the pellet was transferred to a membrane filter and cultured in MM medium supplemented with 25 ng/ml BMP7, 100 ng/ml FGF2, $5 \mu\text{M}$ BIO and $5 \mu\text{M}$ Rho-kinase inhibitor Y-27632 for one day. The Rho-kinase inhibitor was removed, whereas BIO was kept in the culture medium for an additional day, then samples were cultured for a further two days.

The strategy adopted to carry out this assay is summarized in Figure 16.

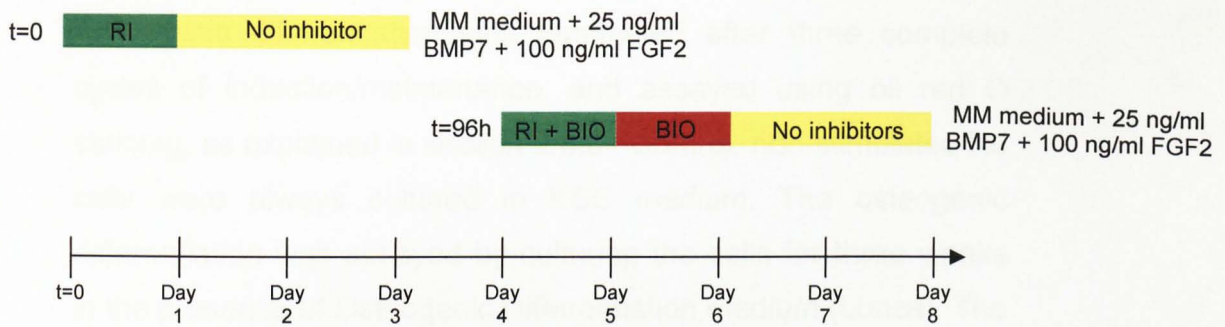


Figure 16. Chimera formation assay protocol. The figure shows a schematic representation of the strategy adopted to carry out the chimera formation assay by recombining either freshly isolated MM (t=0), or 96h cultured MM with E11.5 reaggregated kidney rudiments. RI: Rho-kinase inhibitor Y-27632.

2.2.8.2 Culture of the H6 clonal line with embryonic kidney rudiments

H6 cells and H6 EGFP⁺ cells (see section 2.3.1) were recombined with E11.5 embryonic kidney rudiments following the procedure described in section 2.2.8.1. When required, H6 cells were labeled as described in section 2.3.2. The chimera was cultured in KSC medium supplemented with 1X PS and 5 μ M Rho-kinase inhibitor Y-27632 for one day, then the inhibitor was withdrawn and the pellet cultured for further two days. The culture period was extended up to 7 days when the functional organic anion transport assay (OAT) was carried out (details are explained in section 2.5.3).

2.2.9 In vitro differentiation of the H6 clonal line

The adipogenic, osteogenic and endothelial differentiation ability of H6 cells was assessed. For the adipogenic differentiation the cells were cultured for three days in the presence of Adipogenic Induction medium (Lonza, Basel, Switzerland), followed by three

days in the presence of Adipogenic maintenance medium (Lonza). Adipogenic differentiation was terminated after three complete cycles of induction/maintenance, and assayed using oil red O staining, as explained in section 2.8.3. Control, non-stimulated H6 cells were always cultured in KSC medium. The osteogenic differentiation was assayed by culturing the cells for three weeks in the presence of Osteogenic Differentiation medium (Lonza). The medium was completely replaced every three days. Control, non-stimulated cells were cultured in the presence of KSC medium. Adipogenic and osteogenic stimulations were carried out following manufacturer's instructions (Lonza).

For the endothelial differentiation, the cells were cultured for three weeks in the presence of Endothelial Basal Medium (EBM) (Lonza), supplemented with 10 ng/ml of Vascular Endothelial Growth Factor. The medium was completely replaced every three days. Control, non-stimulated cells were cultured in the presence of KSC medium. The ability of the H6 clonal line to undergo endothelial differentiation was assayed by cytofluorimetric analysis for the expression of the endothelial markers CD31 and CD105, and by immunofluorescence staining for von Willebrand factor as explained in section 2.7.1 and section 2.8.1, respectively.

2.2.10 Cell expansion assay

The expansion of MM and H6 cells was assayed by inoculating 2.5×10^3 cells ($n=6$; $n=5$ for MM cells cultured at passage 2) in a 96-well plate (Nunc) and using a Cell Counting Kit-8. On the day of the experiment the cells were incubated for 4 hours at 37°C and 5% CO₂ with 100 µl of cellular dehydrogenase substrate provided by the manufacturer. Absorbance measurements were taken with a SpectraMax plus microplate reader (Molecular Devices, California, USA) at 24 hours intervals until 96 hours of culture.

Population doubling (PD) time was calculated as previously described (Widera et al. 2009), using the algorithm provided by <http://www.doubling-time.com>.

2.3 Cell labelling

2.3.1 Lentiviral transduction to generate EGFP⁺ H6 cells

In order to permanently label the H6 clonal line, it was decided to transfect the cells with a pHR-SFFV-GFP lentiviral derived vector, constitutively expressing enhanced green fluorescent protein (EGFP), under the control of spleen forming foci virus (SFFV) promoter. Lentiviral supernatant, containing complete transfecting EGFP-expressing vector, was kindly prepared and provided by Mr. Sokratis Theocharatos (University of Liverpool). The diagram of the lentiviral vector is illustrated in Figure 17.

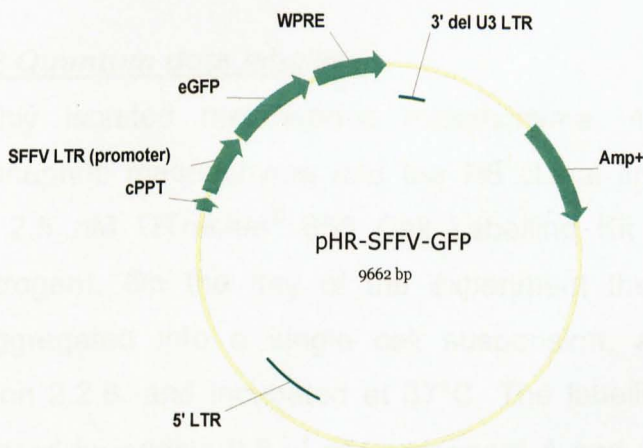


Figure 17. Diagram of the EGFP-expressing vector used to transfect the H6 clonal line. EGFP constitutive expression is controlled by SFFV promoter. The vector carries an ampicillin-resistance marker (Amp⁺), a Woodchuck Posttranscriptional Regulatory Element (WPRE) which increases EGFP expression, and a central Polypurine Tract (cPPT) element which increases the copy number of the lentivirus integrating into the host genome.

The lentivirus supernatant was collected from confluent HEK-293T cells cultured in T175 flasks (Nunc), aliquoted in volumes of 220 μ l and immediately stored at -80°C (Mr. Sokratis Theocharatos, personal communication). On the day of transfection H6 cells were trypsinized and seeded into a fresh tissue culture dish as described in section 2.2.1, then 110 μ l of lentivirus supernatant was added to the culture medium. The cells were incubated with the supernatant for 6 hours in order to allow the cells to adhere to the dish, then the medium was completely replaced with fresh KSC medium. The presence of H6 EGFP-expressing cells (H6 EGFP⁺ cells) was verified by observing the cells under a Leica DMIL fluorescent microscope (Leica, Heidelberg, Germany). The percentage of labelled cells was determined by cytofluorimetric analysis (see section 2.7.1). H6 EGFP⁺ cells were routinely subcultured as described in section 2.2.1 and the expression of EGFP was periodically checked.

2.3.2 Quantum dots labelling

Freshly isolated metanephric mesenchyme, 4 days cultured metanephric mesenchyme and the H6 clonal line were labelled with 2.5 nM QTracker[®] 655 Cell Labelling Kit (quantum dots) (Invitrogen). On the day of the experiment the samples were disaggregated into a single cell suspension, as discussed in section 2.2.8, and incubated at 37°C. The labelling solution was prepared by adding 0.5 μ l of Component A and an equal volume of Component B (both provided with the labelling kit) to a 1.5 ml microcentrifuge tube. After 5 mins of incubation at room temperature, 200 μ l of KSC medium was added to the tube and the labelling solution was immediately vortexed at maximum speed for 30 sec. A total volume of 200 μ l of single cell

suspension, equivalent to $2.5-5.0 \times 10^5$ cells, was then added to the labelling solution and incubated at 37°C for 45 mins. The cells were washed three times in KSC medium by centrifugation at 400 g for 3 mins, and were then resuspended and mixed with unlabelled kidney rudiments cells as described in section 2.2.8.

2.4 Fixation and preparation of tissue sections

2.4.1 Fixation of cultured cells

Metanephric mesenchyme cells and the H6 clonal line were fixed by removing the culture medium and incubating the cells with 4% (w/v) paraformaldehyde (PFA) in PBS for 5 mins at RT. The samples were washed twice in 1X PBS, then processed for immunostaining (see section 2.8.1).

2.4.2 Fixation of cultured cells for osteogenic and adipogenic differentiation assays

In vitro osteogenic and adipogenic differentiation assays were carried out as explained in section 2.2.9. H6 cells were washed twice in PBS without CaCl_2 and MgCl_2 , then were incubated in 10% (v/v) PFA at room temperature for 10 mins before starting the alizarin red S staining (see section 2.8.3). The incubation time was extended to 30 mins before staining the cells with oil red O (details are explained in section 2.8.3).

2.4.3 Fixation of cultured cells for megalin functionality assay

After incubation with fluorescent bovine serum albumin (BSA) (see section 2.5.1 for details) the clonal lines H6 and E5 were incubated with 2% (w/v) PFA in PBS for 2 mins at room

temperature. The samples were washed twice in PBS and either immediately observed under a fluorescent microscope (see section 2.5.1), or processed for immunofluorescence staining, as described in section 2.8.1.

2.4.4 Fixation of samples cultured on membrane filter

The culture medium was removed and the samples were incubated in -20°C pre-cooled methanol for 7 mins at RT. During this step the membrane filters were left on the metal grids. The samples were rinsed once in 1X PBS, then immunostained as described in section 2.8.2.

2.4.4.1 Fixation of chimeras containing H6 EGFP⁺ cells

In order to maintain the signal of EGFP, in this work it was elected to fix kidney rudiments chimeras containing H6 EGFP⁺ cells (see section 2.2.8.2) in 4% (w/v) PFA rather than in methanol. The culture medium was aspirated, then the samples were incubated in 4% PFA for 10 mins at RT. The specimens were washed twice in 1X PBS and processed for the immunostaining as reported in section 2.8.2.

2.4.5 Fixation of kidneys for paraffin-embedded sections

Kidneys were dissected as indicated in section 2.1.2 and bisected coronally. The specimens were immediately placed in 10% PFA and incubated O/N at room temperature. The kidneys were then embedded in paraffin as described in section 2.4.7.

2.4.6 Fixation of frozen organ sections

Adult mouse organs were frozen and sections were prepared as described in section 2.4.8. The sections were left to dry at RT for 5 mins, then were incubated in 70% (v/v) methanol for 10 mins at

RT. The sections were washed three times in 1X PBS, and processed for immunostaining as described in section 2.8.7.

2.4.7 Preparation of paraffin-embedded kidney sections

Adult mouse kidneys were dissected as reported in section 2.1.2. The organs were cut in two halves and incubated in 10% PFA O/N at room temperature. The next day the samples were placed inside biopsy cassettes (Bio Optica, Milano, Italy) and embedded in paraffin through a series of automatically controlled steps using a STP 120 Spin Tissue Processor (Microm International GmbH, Walldorf, Germany). In detail, the samples were dehydrated by incubation in 70% (v/v) ethanol for 1 hour at room temperature, followed by 3 passages in 95% (v/v) ethanol and 3 passages in absolute ethanol, 1 hour each passage. The organs were passaged in 3 changes of xylene, 1 hour each passage, then immersed in 3 changes of liquid paraffin (Bio Optica) at 60°C, 1 hour each passage, and finally incubated for 1 hour at 60°C in liquid paraffin under vacuum. The embedding process was completed by letting the paraffin solidify on a refrigerated plate (Bio Optica). Coronal sections of paraffin-embedded kidney were cut at 4 µm thickness with a Leica microtome RM2125RT (Leica). The sections were stretched out in distilled water at 42 °C, placed on SuperFrost microscope slides (Thermo Fisher Scientific Inc.) and left to dry for 30 mins at 59°C using a Hybaid Shake 'n' Stack Hybridization Oven (Thermo Fisher Scientific Inc.). Paraffin-embedded kidney sections were prepared by Ms Federica Antico (University of Turin, Italy).

2.4.8 Preparation of adult organs frozen sections

Adult organs were dissected from mice as reported in section 2.1.2. Kidneys were coronally cut in two halves. The organs were washed in 1X PBS, then placed in a Peel-A-Way® embedding mould (Polysciences Europe GmbH, Eppelheim, Germany) and completely covered with Tissue-Tek® O.C.T™ Compound (Sakura Finetek, California, USA). The samples were quickly frozen in 2-methylbutane previously refrigerated to -80°C and left there O/N. Sections of frozen organs were cut at 7 µm thickness with a cryostat (HM505N, Microm International, Walldorf, Germany) and C35 Feather microtome blades (VWR, Lutterworth, UK). The frozen sections were placed on twin frost microscope subbed slides (see section 2.4.9) (76×26×0.8 mm, VWR), and stored at -20°C.

2.4.9 Preparation of microscope subbed slides

Twin frost microscope slides were immersed in absolute ethanol (University of Liverpool solvents service) for 15 mins at room temperature, then washed 5 times in distilled water. The slides were soaked in a solution of 0.5% (w/v) gelatine type A from porcine skin and 0.05% (w/v) of CrKSO₄ in distilled water for 25 sec at room temperature, then left to dry in a dust-free environment at room temperature for 2 days.

2.5 Proximal tubule cell functionality assay

2.5.1 Megalin functionality assay

For the megalin functionality assay (Zhai et al., 2000), 5 x 10⁴ H6 or E5 cells were seeded into 8-well chambers (Nunc) and left to

grow to confluence in KSC medium. The cells were washed three times in PBS without CaCl_2 and MgCl_2 , then were cultured for 24 hours in KSC medium without FCS. The clonal lines were incubated with 40 $\mu\text{g/ml}$ of BSA Alexafluor[®] 594 conjugated (Invitrogen) in sterile PBS with CaCl_2 and MgCl_2 for 1 hour at 37°C. After removing the solution the cells were washed once in sterile PBS with CaCl_2 and MgCl_2 , nuclei were stained with 1 $\mu\text{g/ml}$ Hoechst 33342, then the cells were fixed (see section 2.4.3) and either observed under a Leica DM2500 fluorescent microscope (Leica), or processed for immunofluorescence staining as described in section 2.8.1.

2.5.2 Competitive inhibition of BSA uptake

The H6 clonal line was cultured in 8-well chambers and incubated in KSC medium without FCS as described in section 2.5.1. The samples were incubated with 20 $\mu\text{g/ml}$ of BSA Alexafluor[®] 594 conjugated, either alone or in the presence of either 500 ng/ml of recombinant mouse receptor-associated protein (RAP, also named LRPAP) (R&D System, Minnesota, USA), or 4 mg/ml unlabeled BSA for 15 mins at 37°C. After the incubation the samples were washed once in PBS and immediately fixed (see section 2.4.3).

2.5.3 Organic anion transport functionality assay

The following samples were assessed for the organic anion transport functionality assay (OAT) (Rosines et al., 2007):

- E11.5 intact kidney rudiments;
- E11.5 reaggregated kidney rudiments;
- Chimeras formed by recombining Quantum dots-labelled H6 cells with E11.5 reaggregated kidney rudiments.

All samples were cultured for a period of 4-7 days on 1.2 μm nucleopore membrane filter in transfilter culture as described in section 2.2.7 and section 2.2.8.2. On the day of the experiment the samples were washed twice in PBS, then transferred into a 1.5 ml tube and incubated in a solution of 1 μM 6-carboxyfluorescein (6-CF), 20 $\mu\text{g/ml}$ rhodamine-conjugated peanut agglutinin (PNA) lectin (Vector Laboratories, California, USA) and either in the presence or absence of the OAT inhibitor 4 mM probenecid, in PBS with 0.1 mM CaCl_2 and 1 mM MgCl_2 for 1 hour at room temperature in the dark. The samples were washed three times in cold PBS with CaCl_2 and MgCl_2 , the specimens incubated in the presence of the OAT inhibitor were further rinsed in a solution of 8 mM probenecid in PBS with CaCl_2 and MgCl_2 for 5 mins at room temperature. The nuclei were stained by incubating the samples in a solution of 1 $\mu\text{g/ml}$ Hoechst 33342 (Invitrogen) in PBS with CaCl_2 and MgCl_2 for 15 mins at room temperature. The samples were mounted with 80% (v/v) glycerol in water and immediately observed under a Leica AOBs SP2 confocal microscope.

2.6 Renal injury model

2.6.1 Animal husbandry

The renal injury studies were carried out in the laboratory of renal and vascular pathophysiology at the University of Turin (Italy), using 5 to 8 week old male CD1 mice. The animals were housed and killed as explained in section 2.1.1.

2.6.2 Induction of renal injury

For this study a mouse model of acute renal tubular injury (ARF-induced mice) was used. Mice were weighed before being used (healthy animals), after the induction of the damage and after being killed. On the day of the experiment the animals were anaesthetized with 30 μ l of a solution of 12.70 mg/ml Zoletil[®] (Virbac, Carros, France) and 1.58 mg/ml Rompun[®] (Bayer, Leverkusen, Germany) in sterile PBS, which was intramuscularly injected into one hind limb by using a hypodermic syringe (BD). The acute renal damage was then induced by intramuscular injection of 9 ml/kg/body weight of 50% (v/v) sterile glycerol in sterile water, half of the dose injected into each hind limb. The presence of renal injury was assessed by measuring the levels of both blood urea nitrogen (BUN) and serum creatinine (see section 2.6.4 for details).

2.6.3 H6 EGFP⁺ cell inoculation

On the day of the experiment H6 EGFP⁺ cells were trypsinized and counted as reported in section 2.2.1. For the purpose of these experiments it was elected to inoculate 8×10^5 cells, resuspended in 150 μ l of sterile PBS, into the tail vein of AFR-induced mice using a hypodermic syringe, three days after the induction of the renal damage. Control mice were damaged as explained in the previous section, then injected with 150 μ l of sterile PBS into the tail vein. Mice were inoculated with H6 EGFP⁺ cells or PBS by Dr Cristina Grange (University of Turin, Italy). In order to evaluate tubular cell proliferation of damaged kidney, both ARF-mice and control animals were intraperitoneally injected with 300 μ l of 1 mg/ml 5-bromo-2-deoxyuridine (BrdU) in sterile PBS, 48 and 24 hours before the animals were killed, using a hypodermic syringe.

In addition, the animals were intraperitoneally injected with 250 μ l of heparin (5000 U/ml) (B Braun Melsungen AG, Melsungen, Germany) a few minutes before being killed. Mice were killed 5, 8, and 12 days after glycerol injection (2, 5 and 9 days after cell inoculation, respectively), and their organs were processed as described in section 2.1.2.

2.6.4 Determination of blood urea nitrogen and serum creatinine levels

For the measurement of plasma creatinine and blood urea nitrogen (BUN), 300-600 μ l of blood samples were collected from the thoracic cavity after cutting the heart of ARF-induced mice immediately after the animals were killed. The basal levels of both BUN and plasma creatinine were assessed in healthy mice (n=6). The samples were centrifuged at 700 g for 5 mins, then the serum was collected. The levels of plasma creatinine and BUN were assayed using QuantiChrom™ Creatinine Assay Kit (DICT-500) and Quantichrom™ Urea Assay Kit (DIUR-500), respectively (BioAssay System, California, USA), following manufacturer's instructions. BUN and plasma creatinine measurements were taken at 490 nm using a Bio-Rad 680 microplate reader (Bio-Rad, California, USA).

2.6.5 Proliferative activity of kidney tubular cells

ARF-induced mice were injected with 300 μ l of 5-bromo-2-deoxyuridine (BrdU) as explained in section 2.6.3. Kidneys were dissected from ARF-induced mice as explained in section 2.1.2 and paraffin-embedded kidney sections, prepared as previously reported (see section 2.4.7), were stained for BrdU and PCNA (details are explained in section 2.8.6). The proliferative ability of

ARF-induced mouse kidney tubular cells was evaluated 2, 5 and 9 days following cell (or PBS) injection by counting the number of either BrdU-positive or PCNA-positive tubular cells in 10 randomly chosen microscope fields of the renal cortex, observed at 400X magnification with a Leica DMIL inverted microscope.

2.6.6 Tumorigenic assay

In order to evaluate the tumorigenic propensity of H6 EGFP⁺ cells *in vivo*, 2×10^6 cells, resuspended in 300 μ l of sterile PBS, were subcutaneously inoculated in healthy mice (n=5), 10^6 cells at each flank. The mice were regularly monitored over a period of 6 weeks for the formation of tumour masses nearby the inoculation spots; finally they were killed and carefully examined for the presence of tumours.

2.7 Flow cytometry

2.7.1 Flow cytometry on cultured cells

For the cytofluorimetric analysis, H6 cells and H6 EGFP⁺ cells were detached from tissue culture dishes by incubation with a non-enzymatic cell dissociation solution (Cell Dissociation Solution Non-enzymatic 1X) for 15 mins at 37°C. The cell suspension was diluted in KSC medium, then the cells were centrifuged, resuspended in 1X PBS with 0.1% (w/v) BSA and counted. For the purpose of this assay it was elected to stain no less than 10^5 cells, resuspended in 100 μ l of 1X PBS with 0.1% w/v BSA, for each marker. The cells were incubated with the primary antibodies (BD Pharmingen) (primary antibodies used in flow cytometry analyses are listed in Table 4), diluted in 100 μ l of 1X PBS with 0.1% BSA,

for 30 mins at 4°C, then the cells were washed once in 100 µl of 1X PBS with 0.1% BSA by centrifugation at 200 g for 5 mins. When a secondary antibody was required (see Table 4 for details), the cells were incubated with a secondary PE-conjugated goat anti-rat antibody (Caltag, Buckingham, UK), diluted 1:200 in 100 µl of 1X PBS with 0.1% w/v BSA, for 30 minutes at 4° C. The samples were washed once in 1X PBS with 0.1% w/v BSA, finally resuspended in 200 µl of the same buffer. A negative control, where only the secondary antibody was added, as well as a tube containing non-labelled cells, were always prepared. A total number of 10⁴ cells were analysed with a FACSCalibur flow cytometer (BD). The analysis was carried out by Dr Stefania Bruno (University of Turin, Italy) using CellQuest software (Becton Dickinson).

2.7.2 Flow cytometry on ARF-induced disaggregated kidneys

Cell-inoculated and PBS-injected kidneys were dissected from ARF-induced mice as described in section 2.1.2. The organs were washed twice in sterile PBS without CaCl₂ and MgCl₂, then they were transferred into a 10 cm Petri dish (Corning) containing 10 ml of RPMI. The specimens were minced using a sterile blade, then the mixture was filtered through a cell strainer with 40 µm nylon mesh (Becton Dickinson, New Jersey, USA). A 1 ml sterile syringe plunger (BD) was used to allow the mixture to pass through the meshes. The filtrate was centrifuged at 200 g for 5 mins, the pellet was resuspended in 5 ml of PBS and the cell suspension was analysed by flow cytometry.

2.8 Immuno- and histological staining

2.8.1 Immunofluorescence staining of cultured cells

Cultured cells were fixed as reported in section 2.4.1 and section 2.4.3. Using a Pap Pen (Daido Sangyo Co. Ltd., Higashicho, Japan), a hydrophobic ring was drawn to delineate the area to be stained, and afterwards the samples were incubated for 45 mins at room temperature in blocking solution comprising 10% (v/v) serum (depending upon the host in which the secondary antibody was raised in) and 0.1% (v/v) Triton X-100 in PBS. The primary antibody solution, which contained either one or two antibodies in 1% (v/v) serum and 0.1% (v/v) Triton X-100 in PBS, was applied to the cells and left O/N at 4°C in a humidified chamber. Before adding the secondary antibody solution, the cells were washed in PBS three times at room temperature. The cells were then incubated with the secondary antibody in 1% serum and 0.1% Triton X-100 in PBS for 90 mins at room temperature in the humidified chamber in the dark. The blocking, primary and secondary antibody solutions were centrifuged at 13400 g for 5 mins at room temperature in a Microcentaur centrifuge (Sanyo) prior to use. After removing the secondary antibody solution, the samples were washed three times in PBS at room temperature, and afterwards the cells were incubated with DAPI (4',6-diamidino-2-phenylindole, dihydrochloride) (Invitrogen) 1:100,000 in PBS for 5 mins at room temperature in order to visualize the nuclei. The specimens were mounted in Dako fluorescent mounting medium (Dako, Copenhagen, Denmark) and observed under a Leica DM2500 fluorescent microscope (Leica). Each staining included a negative control, in which the primary

antibody was omitted. Antibody concentrations and suppliers are listed in Table 5 and Table 6.

2.8.2 Immunofluorescence staining of samples cultured on membrane filter

Samples cultured on membrane filter were fixed as described in section 2.4.4. The membranes were then placed inside a 1.5 ml microcentrifuge tube and rinsed in PBS for 5 mins at room temperature. The entire immunostaining procedure was carried out inside 1.5 ml microcentrifuge tubes following the protocol described in the previous section. To mount the specimens, the membrane filters were placed on twin frost microscope slides. Particular care was taken to place the side of the membrane with the sample upwards. In some occasions the samples were observed under a Leica AOBSP2 confocal microscope (Leica). As reported in the previous section, each staining included a negative control in which the primary antibody was omitted.

2.8.3 Evaluation of differentiation assays

The adipogenic differentiation was evaluated by performing oil red O staining. A stock solution of 300 mg of oil red O in 100 ml of 99% (v/v) isopropanol was prepared, then 3 parts of the stock solution were mixed with 2 parts of distilled water to make a working solution, which was completely filtered through a Whatman filter paper. The cells were fixed as described in section 2.4.2. The fixative was removed and the cells were washed twice with distilled water, then 2 ml of 60% (v/v) isopropanol was added to the samples and left for 5 mins. The isopropanol was removed and the cells were incubated with 2 ml of oil red O working solution for 5 mins at room temperature, and afterwards the cells were rinsed with distilled water until the water rinsed off clear. Nuclei

were stained by adding 2 ml of 1 mg/ml haematoxylin in 95% (v/v) ethanol to the samples for 1 min at room temperature. The cultures were washed with distilled water until it rinsed off clear, and observed under a Leica DMIL inverted microscope.

The presence of osteocytes was determined by staining the cells for alizarin red S. A working solution of 1 g of alizarin red S in 50 ml of distilled water, pH 4.1 – 4.3 was prepared. The cells were fixed as explained in section 2.4.2, then were rinsed once with distilled water. The cultures were incubated with the solution of alizarin red S for 2 mins at room temperature, then they were rinsed with distilled water until the water rinsed off clear. The staining was observed under a Leica DMIL inverted microscope.

The endothelial differentiation was evaluated by cytofluorimetric analysis for the presence of the cell surface markers CD31 and CD105 (see section 2.7.1) and by immunofluorescence staining for the expression of von Willebrand factor (see section 2.8.1).

2.8.4 Deparaffinization of paraffin-embedded kidney section

Paraffin embedded kidney sections were soaked in two changes of xylene for 5 mins each, then transferred into absolute ethanol for 10 mins. The slides were re-hydrated by sequential immersion in 95%, 70%, 50%, 30% (v/v) ethanol in distilled water, 5 mins each step, then immersed in distilled water for further 5 mins, and finally rinsed in PBS. All steps were carried out at room temperature.

2.8.5 Haematoxylin and eosin staining

Paraffin was removed as explained in the previous section, then kidney sections were immersed in haematoxylin for 6 mins and

washed in a bowl of tap water. The samples were briefly dipped in a solution of 70% (v/v) ethanol and 0.3% (v/v) concentrated HCl in water, then rinsed in running tap water. The slides were placed in a solution of 1 mg/ml of eosin in 95% (v/v) ethanol for 2 mins, then de-hydrated by dipping them in two changes of 70% (v/v) ethanol, followed by immersion in 90% (v/v) and 100% (v/v) ethanol. The slides were soaked in HistoChoice® Clearing Agent for 3 mins, mounted with Histomount Mounting Solution (Invitrogen) and observed under a Leica DMIL inverted microscope.

2.8.6 Immunohistochemistry of paraffin embedded kidney sections

Kidney sections were deparaffinised as described in section 2.8.4, then endogenous peroxidases were blocked by incubating the samples in a solution of 6% (v/v) H₂O₂ in distilled water for 8 mins at room temperature. The reaction was stopped by transferring the slides under running tap water for 2 mins. The antigen retrieval method was performed in a water bath by boiling the samples in citrate buffer (10 mM Citric acid, 0.05% (v/v) Tween 20), pH 6.0, for 20 mins at 98°C. The samples were left to cool in PBS for 10 mins, then were washed in PBS with 0.25% (v/v) Triton X-100 for 10 mins at room temperature. The specimens were washed three times with PBS, then a hydrophobic ring was drawn with a hydrophobic pen to delineate the area to be stained (Dako). The samples were incubated for 45 mins at room temperature in PBS with 2% (w/v) bovine serum albumin (BSA), then the primary antibody, diluted in PBS with 0.1% (w/v) BSA, was applied to the sections either for 1 hour at room temperature or O/N at 4°C in a humidified chamber. The samples were washed twice in PBS with 0.1% (v/v) Tween 20, then the secondary antibody, diluted in PBS with 0.1% (w/v) BSA, was applied to the samples for 1 hour at

room temperature. Both the primary and secondary antibody solutions were centrifuged at 13400 g for 5 mins prior to use. The samples were washed twice in PBS with 0.1% (v/v) Tween 20, and afterwards the staining was developed by incubating the sections with 3,3'-diaminobenzidine (DAB) (Dako) for 3 mins at room temperature. Nuclei were stained by soaking the specimens in haematoxylin for 3 mins at room temperature, then the sections were washed under running tap water, mounted with glycerol and observed under a Leica DMIL inverter microscope. A negative control, in which the primary antibody was omitted, was always prepared. Primary and secondary antibodies are listed in Table 5 and Table 6.

2.8.7 Immunohistochemistry of frozen lung, spleen and liver section

Lung, spleen and liver were fixed as explained in section 2.4.6. Endogenous peroxidases were blocked by incubation in a solution of 0.3% (v/v) H₂O₂ in water for 10 mins at room temperature, then the reaction was stopped by placing the slides under running tap water for 2 mins. The samples were washed three times in PBS, permeabilized in 0.1% (v/v) Triton X-100 in PBS for 10 mins at room temperature, then rinsed in PBS and washed three times before incubating them for 45 mins at room temperature in PBS with 2% (w/v) BSA. The sections were incubated with anti-GFP antibody diluted in PBS with 0.1% BSA for 2 hours at RT. The specimens were washed three times in PBS, then the secondary antibody, diluted in PBS with 0.1% BSA, was applied to the sections for 1 hour at room temperature. The samples were washed three times in PBS, then the staining was developed as section 2.8.6 reports.

2.9 Molecular biology

2.9.1 RNA extraction

RNA was extracted from cultured cells, postnatal or adult kidneys using a phenol:chloroform extraction and ethanol precipitation protocol. Cultured cells were first incubated in trypsin and a pellet was made as reported in section 2.2.1. The supernatant was then removed and 1 ml of TRIzol[®] Reagent (Invitrogen) was added to the pellet. After lysing the cells by gently pipetting, the mixture was transferred to a 1.5 ml microcentrifuge tube and 200 μ l of chloroform (approximately 20% of TRIzol[®] reagent volume) were added. The samples were mixed by inverting the tube several times, then centrifuged at 12000 g for 15 mins at 4°C. The upper aqueous phase, containing RNA, was transferred to a fresh 1.5 ml tube containing 1 μ g/ μ l of glycogen (Boehringer Mannheim GmbH, Mannheim, Germany) and 500 μ l of isopropanol were added. The samples were then incubated at – 20°C O/N in order to improve the RNA yield. The next day the mixtures were centrifuged at 12000 g for 10 minutes at 4°C. At the end of this step a pellet of RNA was visible. The supernatant was discarded and the pellet was washed by briefly vortexing in 75% (v/v) ethanol in nuclease-free water, then was settled by centrifugation at 4400 g for 5 mins at 4°C. The ethanol was removed and the pellet was left to air-dry for a few minutes. Finally the pellet was resuspended in 20 μ l of nuclease-free water and RNA concentration was assayed with a NanoDrop[™] 1000 spectrophotometer (Thermo Fisher Scientific Inc.). RNA overall quality was also assayed by gel electrophoresis (see section 2.9.7). Postnatal and adult kidneys were dissected as explained in section 2.1.2 and section 2.1.2.1, then minced in small pieces. Using a cordless motor and pellet pestles, the

postnatal tissue was homogenised in 1 ml of TRIzol[®] Reagent, whereas the adult tissue was homogenised in 4 ml of TRIzol[®] Reagent, then 1 ml aliquots were prepared. The RNA extraction was carried out as reported above.

2.9.2 DNA extraction

Genomic DNA was isolated from H6 cells, H6 EGFP⁺ cells and E13.5 male and female embryos (see section 2.1.3) with Qiagen Genomic-tip 20/G kit (Qiagen, Crawley, UK), following the manufacturer's instructions. The DNA was resuspended in 100 μ l of 1X TE buffer (see recipes list, page 95) and either immediately used as template for the PCR reaction, or stored at -20°C. The DNA concentration was assayed with a NanoDrop[™] 1000 spectrophotometer.

2.9.3 DNase treatment

The DNase treatment was performed as follows: 8 μ l of RNA was incubated with 1 μ l of RQ1 DNase buffer and 1 μ l (1 U/ μ l) of DNase (both from Promega, Wisconsin, USA) at 37°C for 30 mins. The reaction was inactivated by adding 1 μ l of Stop buffer (Promega) and incubating the sample at 60°C for 15 mins.

2.9.4 cDNA synthesis

For cDNA synthesis, 11 μ l of 200 ng/ μ l DNase-treated RNA was incubated with 1 μ l of 100 ng/ μ l random examers (Abgene, Epsom, UK) and 1 μ l of 10 mM dNTPs mix (Bioline Ltd., London, UK) at 65°C for 5 mins. The samples were chilled on ice for at least one minute, then 4 μ l of 5X First Strand buffer, 1 μ l of 100 mM dithiothreitol (DTT), and 1 μ l of 200 U/ μ l Superscript III[™] reverse transcriptase (all from Invitrogen) were added to the

mixtures. The samples were incubated at 25°C for 5 mins, followed by 60 mins at 50°C, and finally heated at 70°C for 15 mins, to inactivate the reaction. The cDNA was either immediately used as template for the PCR reaction, or stored at – 20°C.

2.9.5 Oligonucleotide primers

All primers used in this study were purchased from. The primer sequences, listed in Table 7, were either previously described in the literature, or designed in-house using the open source Perl Primer software. In the latter case the PCR products were sequenced by the University of Dundee Sequencing Service (<http://www.dnaseq.co.uk/>) to confirm specificity. All primers were diluted in 1X TE buffer and used at a final concentration of 200 nM.

2.9.6 PCR reaction

The reaction mix consisted of 2.5 µl 10X NH₄ Buffer, 0.5 µl of 50 mM MgCl₂, 0.5 µl of 10 mM dNTPs mix, 0.5 µl cDNA, 0.5 µl of 5U/µl Taq DNA polymerase (all from Bioline), 0.5 µl of 10 µM of forward and reverse primers, and 19.5 µl of nuclease-free water to reach a total volume of 25 µl. The PCR was then performed as follows: an initial denaturation step at 94°C for 5 mins, followed by 40 cycles of 94°C for 5 sec, 62°C for 30 sec, 72°C for 30 sec, followed by a final extension at 72°C for 7 mins.

Genomic DNA was amplified by preparing a reaction mix as above. For this reaction a total amount of 500 ng/ml of DNA was used as template. The PCR was performed as follow: 95°C for 5 mins, followed by 40 cycles of 95°C for 5 sec, 62°C for 1 min and

72°C for 1 min. The reaction ended with a final extension at 72°C for 7 mins.

2.9.7 Gel electrophoresis

RNA overall quality was assayed by gel electrophoresis in 50 ml of 1.5% (w/v) agarose gel (Bioline) in 1X TAE buffer (see recipes list, page 95) containing 0.5 µg/ml of ethidium bromide solution. In detail 1 µl of RNA was added to 1 µl of loading buffer (Bioline), then the samples were run at 120V for 20 minutes.

PCR products were detected in 150 ml of 2.5% (w/v) agarose gel in 1X TAE buffer, containing 0.5 µg/ml ethidium bromide. Two µl of loading buffer were added, then a total volume of 12 µl was loaded onto the gel and the samples were run at 180V for 20 mins. Gels were visualized with a Chemi Imager 4400 UV transilluminator (Alpha Innotech Corporation, San Leandro, CA, USA).

2.10 Statistical analysis

One way analysis of variance (ANOVA) and Student's t-test were performed on samples with equal variance. Data were analysed with SigmaPlot 11.0 (Systat Software Inc., London, UK). Differences were considered statistically relevant when $P < 0.05$.

Table 4. List of primary antibodies used for cytofluorimetric analysis.

Antibody	Concentration	Host	Isotype	Supplier
CD24	1:50	Rat	IgG	BD Pharmingen
CD29	1:50			
CD31	1:50			
CD34	1:50			
CD44	1:50			
CD45	1:50			
CD73	1:50			
CD90 PE-conjugated	1:20			
CD105	1:50			
CD117	1:50			
Sca-1 PE-conjugated	1:200			

Table 5. List of primary antibodies used for immunostaining.

Antibody	Host	Isotype	Concentration	Supplier
Calbindin	Mouse	Monoclonal IgG1	1:200	Abcam
Laminin	Rabbit	Polyclonal IgG	1:500	Sigma- Aldrich
Megalyn	Mouse	Monoclonal IgG1	1:200	Acris
Musashi	Rabbit	Polyclonal IgG	1:200	Chemicon Int.
Pax2	Rabbit	Polyclonal IgG	1:200	Covance
Synaptopodin	Mouse	Monoclonal IgG1	1:1	Fitzgerald
Wt1	Mouse	Monoclonal IgG1	1:500	Upstate
Vwf	Rabbit	Polyclonal IgG	1:1000	Sigma- Aldrich
GFP	Rabbit	IgG	1:800	Abcam
PCNA	Mouse	IgG1	1:500	Sigma- Aldrich
BrdU	Mouse	IgG1	1:25	Dako

Table 6. List of secondary antibodies used for immunostaining.

Antibody	Host	Isotype	Fluorochrome or Conjugation	Concentration	Supplier
Anti-mouse	Goat	IgG1	488nm	1:500	Invitrogen
Anti-rabbit	Chicken	IgG	594nm	1:500	Invitrogen
Anti-rabbit	Goat	IgG	350nm	1:400	Invitrogen
Anti-rabbit	Goat	IgG	HRP	1:300	Pierce
Anti-mouse	Goat	IgG1			
Anti-mouse	Goat	IgG		1:500	Abcam

Table 7. Primer sequences and amplicons size.

Gene	Sequence	bp
<i>Aqp1</i>	5'-CGGGCTGTCATGTACATCATCGCCCA-3' 5'-CCAATGAACGGCCCCACCCAGAAA-3'	381
<i>Bax</i>	5'-ATGCGTCCACCAAGAAGCTGA-3' 5'-AGCAATCATCCTCTGCAGCTCC-3'	86
<i>Bcl2</i>	5'-CCGGGAGAACAGGGTATGATAA-3' 5'-CCCCTCGTAGCCCCTCTG-3'	81
<i>Des</i>	5'-CTCAAGGCCAAACTACAGGA-3' 5'-CAGAATCGAATCCCTCAACG-3'	133
<i>Gdnf</i>	5'-GAAGTTATGGGATGTCGTGG-3' 5'-GGATAATCTTCAGGCATATTGGAG-3'	170
<i>Hoxb7</i>	5'-TTCCCCGAACAACTTCTT-3' 5'-CGGAGAGGTTCTGCTCAAAG-3'	217
<i>Krt8</i>	5'-AGGAGCTTATGAACGTCAAG-3' 5'-CCCATAGGATGAACTCAGTC-3'	161
<i>Lhx1</i>	5'-CAACATGCGTGTTATCCAGG-3' 5'-CTTGCGGGAAGAAGTCGTAG-3'	239
<i>Lrp2</i>	5'-CCTTGCCAAACCCTCTGAAAAT-3' 5'-CACAAGGTTTGCGGTGTCTTTA-3'	562
<i>Msi1</i>	5'-CGAGCTCGACTCCAAAACAAT-3' 5'-GGCTTTCTTGCATTCCACCA-3'	304
<i>Msi2</i>	5'-GTCTGCGAACACAGTAGTGGAA-3' 5'-GTAGCCTCTGCCATAGGTTGC-3'	340

Table 7 (continued). Primer sequences and amplicons size.

Gene	Sequence	bp
<i>Nphs1</i>	5'-CCCCAACATCGACTTCACTT-3' 5'-GGCAGGACATCCATGTAGAG-3'	372
<i>Nphs2</i>	5'-GAAAGGAAGAGCATTGCCCAAG-3' 5'-TGTGGACAGCGACTGAAGAGTGTG-3'	288
<i>Osr1</i>	5'-GCAGCGACCCTCACAGAC-3' 5'-GCCATTCACTGCCTGAAGGA-3'	169
<i>p16^{INK4a}</i>	5'-ATGATGATGGGCAACGT-3' 5'-CAAATATCGCACGATGTCT-3'	237
<i>Pax2</i>	5'-ACATCTGGTCTGGACTTTAAGAG-3' 5'-GATAGGAAGGACGCTAAAGAC-3'	158
<i>Podxl</i>	5'-AATTACCAGCTAAACTGTGAACCT-3' 5'-ACGAGTTTCTCTTTCTCATCCA-3'	115
<i>Ret</i>	5'-GCGTCAGGGAGATGGTAAAG-3' 5'-CATCAGGGAAACAGTTGCAG-3'	217
<i>Sall1</i>	5'-GCACATGGGAGGCCAGATCC-3' 5'-GGAAGCGTCCGCTGACTTGG-3'	181
<i>Sry</i>	5'-TGGGACTGGTGACAATTGTC-3' 5'-GAGTACAGGTGTGCAGCTCT-3'	402
<i>Synpo</i>	5'-GCCAGGGACCAGCCAGATA-3' 5'-AGGAGCCCAGGCCTTCTCT-3'	73
<i>Tjp1</i>	5'-CTCATAGTTCAACACAGCCT-3' 5'-TCATCTTCATCTTCTTCCACAG-3'	148
<i>Vegf</i>	5'-GAGATAGAGTACATCTTCAAGCC-3' 5'-TTTCTTTGGTCTGCATTAC-3'	201
<i>Vim</i>	5'-TCTTGACCTTGAACGGAAAGTG-3' 5'-CACATCGATCTGGACATGCT-3'	124
<i>Wt1</i>	5'-CCAGTGTA AAACTTGT CAGCGA-3' 5'-TGGGATGCTGGACTGTCT-3'	234
<i>β-actin</i>	5'-CGTTGACATCCGTA AAGACC-3' 5'-CAGGAGGAGCAATGATCTTGA-3'	143

2.11 Media recipes

2.11.1 KSC medium

- DMEM High glucose (Sigma-Aldrich, Cat. D6546).
- 10% (v/v) FCS (PAA, Cat. A15-108).
- 2 mM L-glutamine (Sigma-Aldrich, Cat. G7513).
- No antibiotics.

2.11.2 MM medium

- DMEM/F12 (Sigma-Aldrich, Cat. D6421).
- 10% FCS
- 2 mM L-glutamine
- 1X insulin/transferrin/selenium (Sigma-Aldrich, Cat. I3146).
- 20 ng/ml dexamethasone (Sigma-Aldrich, Cat. D4902).
- 1X penicillin/streptomycin (Sigma-Aldrich, Cat. P4333).

2.12 Buffer recipes

2.12.1 Phosphate buffered saline (PBS), 1X

- 6 mM, Na₂HPO₄ (Sigma-Aldrich)
- 2 mM KCl (Sigma-Aldrich)
- 0.137 M NaCl (Sigma-Aldrich)

pH adjusted to 7.4 with 1N HCl

2.12.2 Tris EDTA (TE) buffer, 10X

- 10mM Tris-Cl, pH 7.5
- 1mM EDTA

pH adjusted to 8.0 with 1N NaOH

2.12.3 Tris-acetate EDTA (TAE) buffer, 10X

- 48.4 g Tris Base (Sigma-Aldrich)
- 20 ml 0.5 M EDTA (Sigma-Aldrich)
- 11.42 ml glacial acetic acid (Sigma-Aldrich)

pH adjusted to 8.0 with 1N NaOH

2.12.4 Gel loading buffer, 6X

- 25 mg bromophenol blue (Sigma-Aldrich)
- 10 ml of distilled H₂O (Sigma-Aldrich)
- 3 ml glycerol (Sigma-Aldrich)

CHAPTER 3

Development of culture conditions and characterization of mouse metanephric mesenchyme cells

3.1 Introduction

As mentioned in section 1.1.2.3, in mice the functional kidney, the metanephros, starts developing at the embryonic (E) day 10.5 as the ureteric bud (UB) outgrows from the collecting duct and invades the metanephric mesenchyme (MM), a population of mesenchymal cells which give rise to all cell types present in the mature nephron (Kobayashi et al., 2008). At E11.5 the mesenchyme adjacent to the tips of the UB, called the cap mesenchyme, undergoes a mesenchymal-to-epithelial transition (MET), which leads to the formation of the renal vesicle, the epithelial precursor of the nephron. The renal vesicles further develop into the comma- and S-shaped bodies, then differentiate into the renal tubules and glomeruli. Cell interactions between the induced MM and the tips of the UB ultimately lead to the branched network of the urine collecting system (Saxén, 1987).

Since the adult nephron contains more than 26 terminally differentiated cell types (Sagrinati et al., 2006), it might be conceivable that within the uninduced MM there might be a population of *progenitor* cells committed to generate all cell types present in the mature nephron. It is also plausible that some of these *progenitor* cells may remain undifferentiated in the postnatal and adult kidney, thus forming a pool of cells that participates in kidney repair processes after injury. If such *progenitor* cells are present, their isolation and characterization would be of great

interest due to their potential application in renal replacement therapies.

The presence of stem cells in mouse kidney has already been suggested by different research groups. Oliver and colleagues demonstrated that a population of low cycling label-retaining cells, detected by 5-bromo-2-deoxyuridine (BrdU) incorporation, resided in rat and mouse renal papilla. These cells seem to be involved in maintaining the normal homeostasis of the kidney; besides, following renal injury, they might provide a supply of cells able to replenish damaged kidney tissues (Oliver et al., 2004; Oliver et al., 2009).

Humphreys and colleagues (Humphreys et al., 2008) have provided strong evidence that in adult mice intrinsic tubular epithelial cells participate in tubular regeneration after injury. Using a genetic fate-mapping technique which allowed heritable labelling of all metanephric mesenchyme-derived epithelial cells, they showed that after ischemia-reperfusion injury tubular regeneration was accomplished by intrinsic tubular epithelial cells that were able to survive the renal damage. These findings, however, do not rule out the possibility that other cell types, such as renal interstitial cells or bone marrow-derived cells may also play a role in kidney repair, essentially by stimulating tubular epithelial cells to start proliferating via paracrine factors.

In a recently published paper, Lee and colleagues demonstrated that in mice the interstitium of the medulla and papilla contains a population of clonogenic and self-renewing mouse kidney progenitor cells (MKPC) that were able to ameliorate renal function and reduce mortality following injection in a mouse model of acute renal failure, induced by ischemia-reperfusion (Lee et al., 2010).

Despite these and other studies (see section 1.3.2), although it has been established that progenitor cells within the MM of the embryonic kidney can generate all cell types in the nephron (Kobayashi et al., 2008), it still remains to be seen if stem/progenitor cells in the adult kidney have the potential to generate all cell types present in the mature nephron.

The present study aimed to compare the expression profile and nephrogenic potential of the kidney-derived stem cell H6 clonal line, derived from postnatal mouse kidney, with that of MM cells isolated from E11.5 embryos. The rationale of this work was that H6 cells might derive from the metanephric mesenchyme, and therefore might retain the ability to generate different renal cell types. Since the metanephric mesenchyme isolated from E11.5 mouse kidney rudiment contains approximately 15000 cells (Prof. Jamie Davis, University of Edinburgh, personal communication), at first it became paramount to develop culture conditions that could support the expansion of MM cells *in vitro* for several passages.

Previous studies have shown that the uninduced MM, isolated from E11.5 mouse embryo, quickly undergoes apoptosis when cultured in the absence of heterologous inducing stimuli, such as lithium chloride (Saxén, 1987), a synthetic GSK-3 inhibitor (Kuure et al., 2007), or when co-cultured with embryonic spinal cord (Saxén, 1987; Dudley et al., 1999). It has been shown, though, that the presence of two growth factors, BMP7 and FGF2, could promote the survival of MM up to 48 hours in culture, and maintain their ability to undergo tubulogenesis when cultured in transfilter culture with embryonic spinal cord (Dudley et al., 1999).

Alternatively, MM cells can be expanded in culture indefinitely by retroviral transfection of SV40 large T antigen, which transforms the cells into an immortalized cell population (Oliver et al., 2002).

This approach, however, may raise the question of whether the phenotype of MM cells might be altered following retroviral immortalization.

In the absence of exogenous inducers as of yet it has not been possible to expand MM cells *in vitro* for more than 48 hours following isolation. This suggests that the survival of the MM might depend either upon the contact with the UB, or by the presence of other factors, yet not identified, expressed in the UB.

This chapter will present how culture conditions were developed that could support long-term expansion of MM cells isolated from E11.5 mouse embryos. Cell growth assay was carried out in order to determine the extent of MM population expansion following *in vitro* culture. Immunofluorescence staining for Wt1 and Pax2, and RT-PCR analysis for several MM-specific genes were performed in order to investigate whether MM cells maintained a MM-like phenotype following *in vitro* culture.

The expression of Wt1 is initially detected within the intermediate mesoderm. Following the invasion of the ureteric bud into the metanephric mesenchyme Wt1 is expressed within the condensed mesenchyme, comma and S-shaped body. In neonatal and adult kidney Wt1 expression becomes restricted to podocytes (Donovan et al 1999; Dressler, 2006). In the embryonic kidney, Pax2 is expressed in the ureteric bud and at a low level in the uninduced metanephric mesenchyme. The expression of Pax2 increases following induction and becomes localized in the comma shaped body and later in the distal portion of the S-shaped body (Torban et al., 2006; Dressler, 2009). In adult kidney, Pax2 is expressed in the epithelium of the collecting duct and in many cells within the renal papilla (Cai et al., 2005).

3.2 Results

3.2.1 Establishing culture conditions that promote in vitro metanephric mesenchyme cell growth

In an attempt to optimize culture conditions that could prolong the survival of subcultured metanephric mesenchyme cells beyond 4 days of culture, it was decided to culture the cells in the presence of a medium composed of an equal volume of MM medium, supplemented with growth factors (see section 3.2.2 for details), and KSC conditioned medium harvested from the KSC H6 clonal line. The reason for growing MM cells in a conditioned medium collected from a different cell population was that the H6 clonal line showed several features of stem cells and was able to undergo limitless expansion. It was hypothesized that growth factor(s) released by H6 cells in the culture medium could promote both the survival and expansion of subcultured MM cells. Since neither the survival, nor the expansion of MM cells at passage 2 improved in the presence of KSC conditioned medium, this strategy was not pursued (data not shown).

3.2.1.1 Effect of BMP7 and FGF2 on MM cell growth

Since it has been shown that the presence of both BMP7 and FGF2 could enhance the survival of metanephric mesenchyme cells in culture (Dudley et al., 1999) it was elected to culture the cells in MM medium (see recipes list, page 95) in the presence or absence of 50 ng/ml BMP7 +/- 100 ng/ml FGF2 to investigate if these factors could promote MM cell growth. In addition, in order to facilitate analysis, it was decided to culture MM cells on uncoated tissue culture dishes instead of using nucleopore membrane filter, which had been the only substrate used for MM

cell culture (Dudley et al., 1999). To optimise the effect of paracrine/autocrine factors on cell growth, the MM cells were cultured inside a small silicon ring, which enabled the volume of culture medium to be reduced to 600 μ l.



Figure 18. E11.5 embryonic kidney rudiment. The ureteric bud and the surrounding metanephric mesenchyme are indicated by the dotted line and asterisk, respectively.



Figure 19. Metanephric mesenchyme (MM) and ureteric bud (UB) after separation.

Kidney rudiments were isolated from E11.5 embryos (Fig. 18) and the MM was dissected from the ureteric bud (Fig. 19) and cultured in the presence or absence of BMP7 +/- FGF2. MM colonies were imaged every 24 hours to determine the effect of the growth factors on colony expansion and morphology.

The results indicated that in the absence of growth factors MM colonies showed limited expansion: the colony size barely increased throughout 96 hours of culture and cells formed a monolayer colony at the end of the period studied (Fig. 20, top panel). Similar results were observed when MM cells were cultured in the presence of BMP7 only (Fig. 20, central panel).

Under the conditions assayed MM cells displayed a mesenchymal morphology: the cells appeared to be randomly oriented with irregular shape and were elongated. The presence of both factors in the medium stimulated MM colony expansion: pictures taken at different time-points showed that the colony size increased throughout 96 hours of culture. Additionally, at the centre of the colony cells formed a multilayer instead of a monolayer as previously observed. However at the edge of the colony the cells maintained their typical mesenchymal morphology (Fig. 20, bottom panel). It was observed that in the presence of both BMP7 and FGF2 MM cells were able to undergo expansion up to 144 hours in culture (data not shown). However it was noticed that after 5 days in culture the cells started forming a thick multilayer, and it was no longer possible to evaluate their morphology.

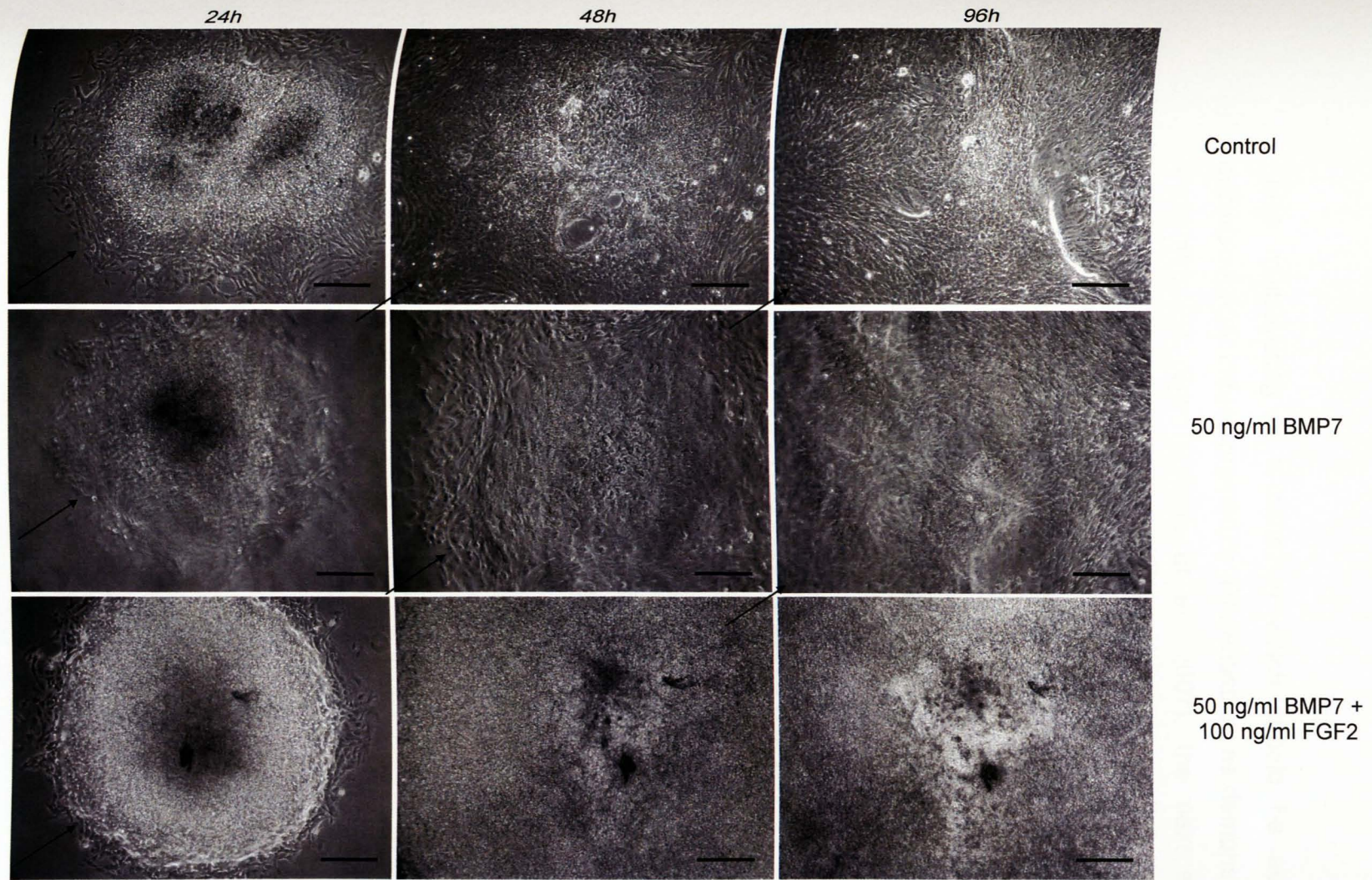


Figure 20. MM cells cultured for 24, 48 and 96 hours in control medium and in the presence of 50 ng/ml BMP7 and 50ng/ml BMP7 + 100ng/ml FGF2. Arrows indicate the edge of the colonies: it can be noticed that in the presence of both BMP7 and FGF2 the edge of the colony cannot be seen as result of colony expansion. Scale bar: 200 μ m

Since multilayering is a condition which should be avoided because it may induce premature differentiation, as demonstrated in human ES cells (Sullivan et al., 2007), the next set of experiments aimed to modify the MM culture conditions in order to promote monolayer, rather than multilayer growth. The modifications included changing the concentration of serum (section 3.2.1.2) and BMP7 (section 3.2.1.3).

3.2.1.2 Effect of serum concentration on MM cell growth

In order to investigate the effect of serum concentration on MM cell growth and morphology, explants were cultured in the presence of BMP7 and FGF2 either in serum-free MM medium, or in MM medium supplemented with low (2%) or high (10%) concentrations of serum for 4 days. MM colonies were imaged every 24 hours to determine the effect of serum concentration on colony expansion and morphology (data not shown).

Table 8. Effect of serum concentration on MM cell growth

No Serum	2% FCS	10% FCS
No growth	Limited colony expansion	Marked colony expansion

The results, summarized in Table 8, demonstrated that in medium supplemented with 0 and 2% FCS, MM cells displayed an absence of growth, or limited expansion, respectively. Therefore, it was concluded that high concentrations of serum are optimal for promoting MM colony expansion, and in subsequent experiments, MM medium was supplemented with 10% FCS.

3.2.1.3 Effect of BMP7 concentration on MM colony growth and morphology

It has been suggested that in addition to promoting MM cell survival, BMP7 also plays a role in inducing mesenchymal-to-epithelial transition (MET) (Zeisberg M et al., 2005; Buijs et al., 2007), and can promote the survival of the mesenchyme in the absence of the ureteric bud (Dudley et al., 1999). Therefore to investigate if MM multilayering was due to the high concentration of BMP7 in the culture medium, MM was dissected as described previously and cultured in MM medium supplemented with 100 ng/ml FGF2 and either 0, 25 or 50 ng/ml BMP7.

The results showed that in the absence of BMP7 cells formed a uniform monolayer and there was no evidence of multilayering (Fig. 21, left panel). The presence of 25 ng/ml of BMP7 seemed to promote the formation of a thin multilayer at the centre of the colony (Fig. 21, central panel); however this multilayering effect was much more pronounced in the presence of 50 ng/ml BMP7 (Fig. 21, right panel). MM cells maintained their typical mesenchymal morphology under all conditions assayed. However, due to the thick multilayer that formed in the presence of 50 ng/ml BMP7, the morphology of the cells at the centre of the colony was difficult to assess.

Taken together, the above results show that the optimal culture medium for mouse MM cells isolated from E11.5 embryos is MM medium (see recipes list, page 95) supplemented with 25 ng/ml of BMP7 and 100 ng/ml of FGF2.

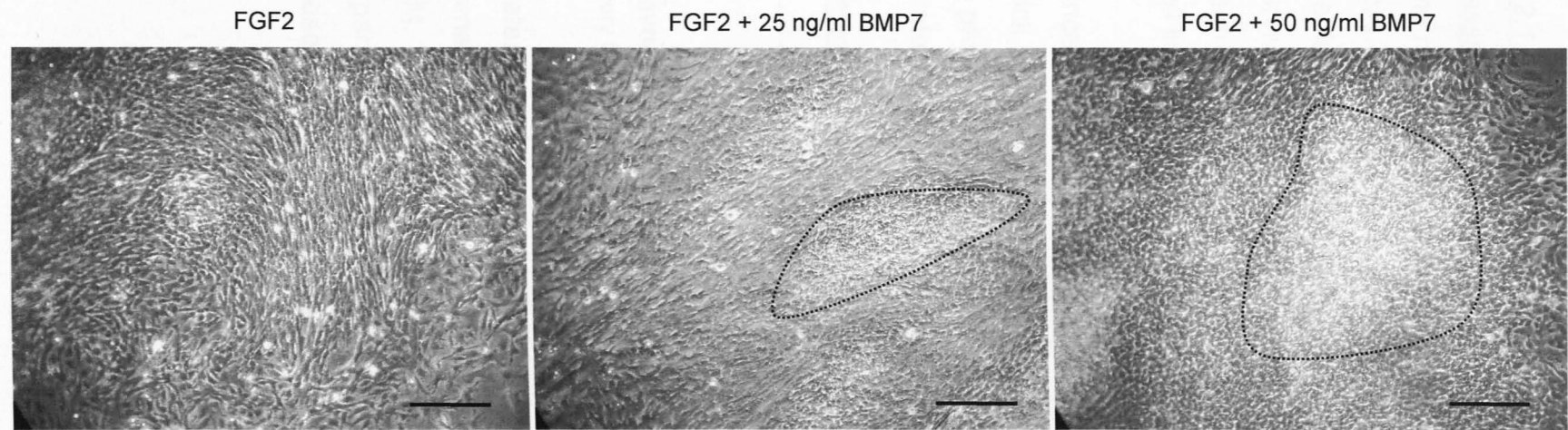


Figure 21. MM cells cultured for 96 hours in the presence of FGF2 only (left), FGF2 + 25ng/ml BMP7 (centre), and FGF2 + 50ng/ml BMP7 (right). Dotted lines evidence the presence of multilayer. Scale bar: 200 μ m.

3.2.1.4 Determining the number of times that MM cells can be passaged under optimal culture conditions

The next objective was to determine the number of times that MM cells could be passaged when cultured in the optimal culture medium described above. As already mentioned, due to the short survival of MM cells in culture, until now these cells have only been maintained in the long term by generating an immortalized cell line (Oliver et al., 2002).

Since it was observed that MM cells started organizing into a quite thick multilayer when cultured longer than 4 days, it was decided to passage the cells after 96 hours of culture. Figure 22 shows the strategy followed to subculture MM cells.

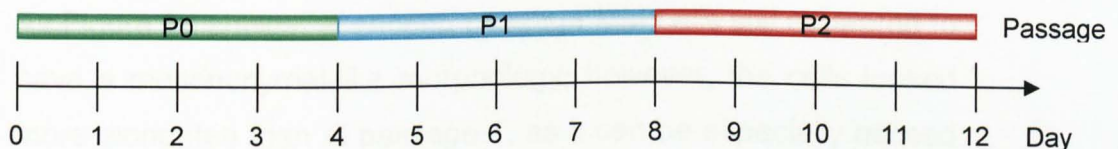


Figure 22. Strategy followed to subculture MM cells. The cells were passaged every four days and cultured for up to 2 passages and 12 days.

Metanephric mesenchyme cells were initially subcultured in the same culture medium that was used to expand freshly isolated MM. The results showed that MM cells at passage 1 were able to organize into a fairly uniform monolayer and maintain their typical mesenchymal-like morphology (Fig. 23).

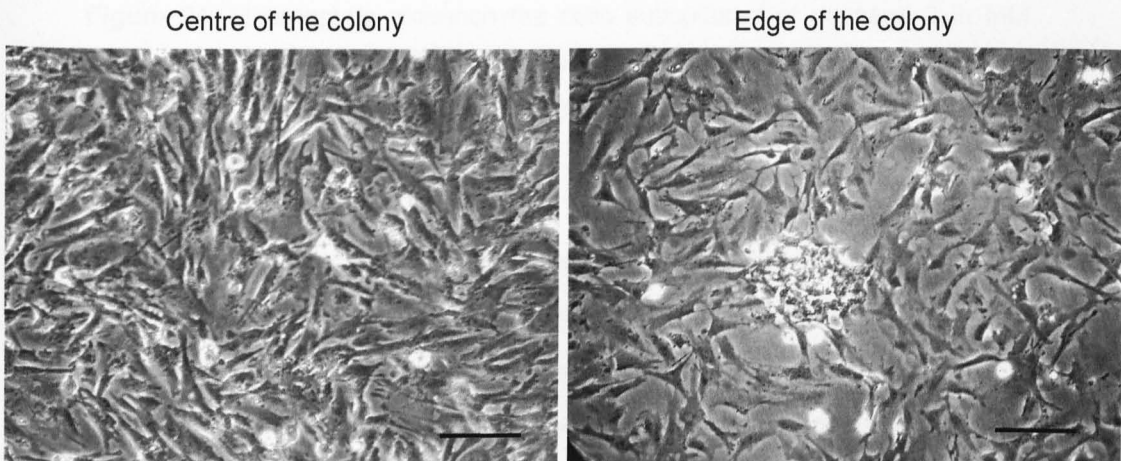


Figure 23. Metanephric mesenchyme cells subcultured at passage 1 in MM medium supplemented with 25 ng/ml BMP7 and 100 ng/ml FGF2. Left and right sides of the panel show pictures taken at the centre and edge of the colony, respectively. Scale bar: 100 μ m.

As Figure 24 shows, at second passage MM cells still appeared to have a mesenchymal-like morphology; however, the cells looked more elongated than at passage 1, as it can be especially noticed at the edge of the colony (Fig. 24, right side). Under these conditions, at passage 2 the colony never expanded and MM cells could not survive for more than 4 days (12 days after MM isolation, see Fig. 22).

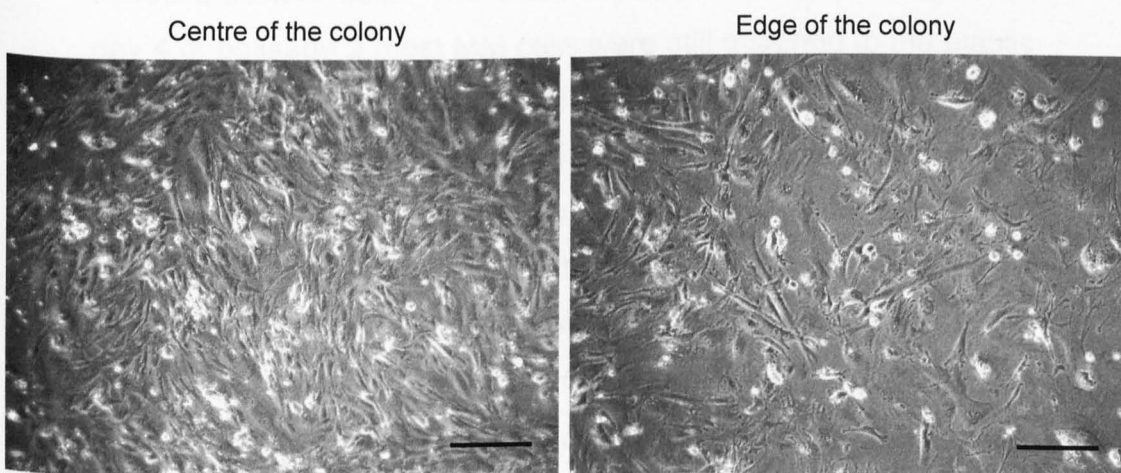


Figure 24. Metanephric mesenchyme cells subcultured at passage 2 in MM medium supplemented with 25 ng/ml BMP7 and 100 ng/ml FGF2. Centre and edge of the colony are shown on the left and right side of the panel, respectively. Scale bar: 100 μm .

In an attempt of trying to enhance *in vitro* growth of cultured MM cells, it was decided to supplement the MM medium with 100 ng/ml stem cell factor (SCF). This growth factor is involved in the survival, proliferation and migration of different stem/progenitor cell types, such as hemopoietic stem cells, mast cells, neural progenitor cells and cortical stem cells (Ueda et al., 2002). As shown by Schmidt-Ott and co-workers, in the developing kidney SCF is expressed in the ureteric bud and its receptor, c-kit, is expressed in E11.5 metanephric mesenchyme both at the entry point of the ureteric bud, and in a multilayer of cells that surrounds the entire rudiment (Schmidt-Ott et al., 2006). It has been shown that SCF is able to accelerate the growth of the developing kidney *in vitro*, by expanding the population of embryonic interstitial cells (Schmidt-Ott et al., 2006). Since the culture conditions to support the expansion of P0 MM cells were considered optimized for the purposes of the present study, it was decided to add SCF only to subcultured MM cells. The initial results looked promising, as at day 4 of passage 2 most MM cells were still attached to the plastic of the dish and appeared healthy; however, the colony did not undergo further expansion. At passage 3, no further population expansion was observed and, as can be seen in Figure 25, the morphology of the cells had notably changed, as the cells had acquired a myofibroblasts-like morphology. In future immunostaining for α -smooth muscle actin, a myofibroblasts marker, might be carried out on long term-cultured MM cells in order to shed light on this assumption. Since MM cells could be

expanded up to passage 1, whereas after passage 2 the cells were able to survive for a few days only, in this work it was elected to investigate the expression profile of MM cells cultured up to passage 2 (12 days following initial isolation).

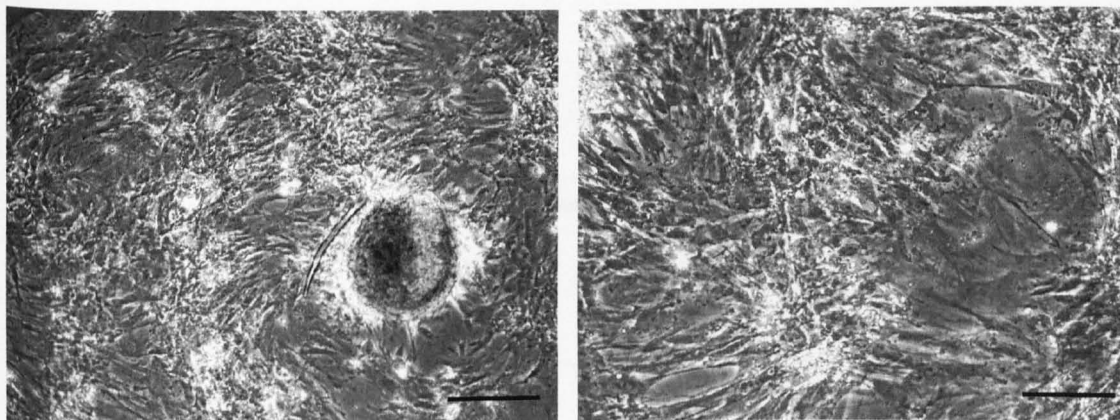


Figure 25. MM cells cultured at passage 3 in MM medium supplemented with 25 ng/ml BMP7, 100 ng/ml FGF2 and 100 ng/ml SCF. It can be observed that MM cells no longer displayed a mesenchymal-like morphology. Scale bar: 100 μm .

3.2.2 Determining the extent of MM population expansion

For the purpose of this work it was important to demonstrate that the culture conditions developed could support not only the survival but also the proliferation of MM cells in culture. To determine the extent of MM population expansion over a 12 day period (2 passages), MM growth was assayed using a colorimetric reaction based on the activity of cellular dehydrogenases. Measurements were taken every 24 hours following initial plating of dissected MM (passage 0 (P0)) (n=6) or following trypsinization/replating, (P1 and P2) (n=6 for P1 MM cells; n=5 for P2 MM cells) for a 96 hour period. Cell expansion was determined in terms of increments of absorbance values. The absorbance values are reported in Table 9 through Table 11, and the growth curves are shown in Figure 26.

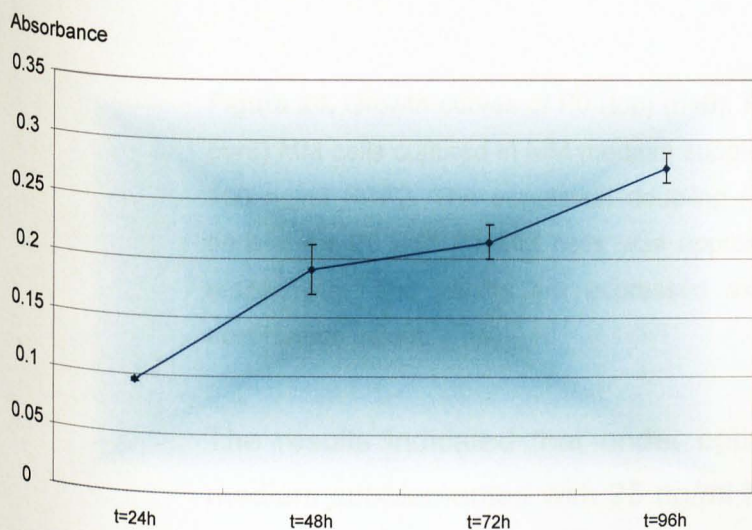


Table 9. Expansion of P0 MM cells

P0	t=24h	t=48h	t=72h	t=96h
Mean	0.095	0.190	0.214	0.276
SD	0.001	0.021	0.014	0.012

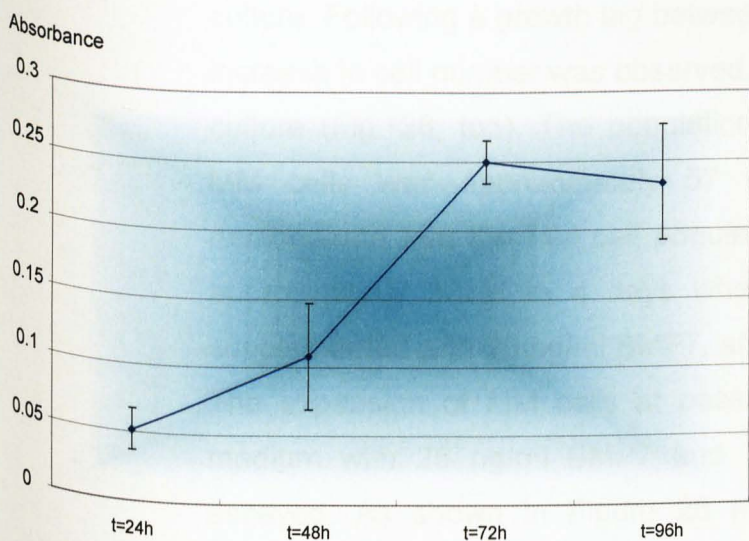


Table 10. Expansion of P1 MM cells

P1	t=24h	t=48h	t=72h	t=96h
Mean	0.051	0.108	0.250	0.234
SD	0.014	0.039	0.015	0.041

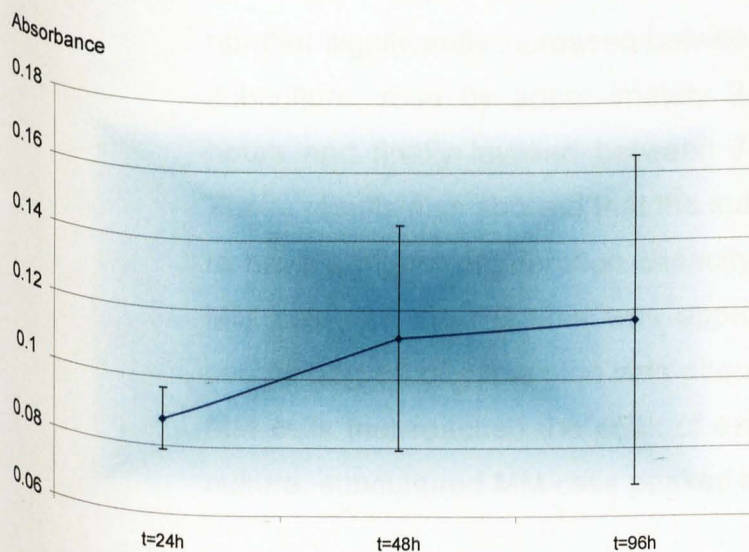


Table 11. Expansion of P2 MM cells

P2	t=24h	t=48h	t=96h
Mean	0.087	0.111	0.117
SD	0.009	0.032	0.047

Figure 26. Growth curves of P0 (top) (n=6), P1 (centre) (n=6) and P2 (bottom) (n=5) MM cells cultured in MM medium supplemented with 25 ng/ml BMP7 and 100 ng/ml FGF2. The population doubling (PD) time (see section 2.2.10 for details) for P0 and P1 MM cells was approximately 57 hours and 39 hours, respectively. The results are expressed as mean \pm standard deviation of absorbance values.

The results indicated that under optimal culture conditions (MM medium supplemented with 25 ng/ml BMP7 and 100 ng/ml FGF2) the population of MM cells doubled between 24 and 48 hours of culture. Following a growth lag between 48 and 72 hours, a further increase in cell number was observed between 72 and 96 hours of culture (Fig. 26, top). The population doubling (PD) time for P0 MM cells was approximately 57 hours. Overall the results demonstrate that the MM cell population was able to expand by approximately 3-fold in 4 days when cultured in MM medium supplemented with 25 ng/ml BMP7, and 100 ng/ml FGF2.

The expansion of MM cells at passage 1 (P1) cultured in MM medium with 25 ng/ml BMP7 and 100 ng/ml FGF2 was then assayed. As shown in Figure 26 (centre), the cells were still capable of expansion throughout 96 hours of culture (8 days following initial isolation). The results demonstrated that the cell number significantly increased between the first and second day of subculture, rose by approximately 2.5-fold between 48 and 72 hours and finally levelled between 72 and 96 hours of culture. These results also showed that the subculture of MM cells seemed to have a higher proliferation capacity than the primary culture of MM cells, as the PD time was approximately 37 hours and the overall degree of expansion was about 5-fold. However, unlike P0 MM cells that reached the peak of expansion at the fourth day of culture, subcultured MM cells peaked after 72 hours of culture.

When subcultured at passage 2 (P2) MM cells were no longer able to undergo further expansion, as results show in Figure 26 (bottom).

The results of the proliferation assay showed that MM cells cultured in MM medium with 25 ng/ml BMP7 and 100 ng/ml FGF2 expanded by approximately 15-fold in 7 days of culture. Altogether, the results obtained represent a considerable achievement as they demonstrate for the first time that a non-immortalized MM cell line, cultured in the presence of BMP7 and FGF2 can undergo expansion up to the third day of culture at passage 1 (7 days following initial isolation). Moreover, these conditions allowed the cells to maintain a mesenchymal-like morphology up to passage 1 and 8 days in culture.

3.2.3 Expression of Wt1 and Pax2 in MM cells following in vitro culture

The previous experiments showed that MM cells could be expanded by approximately 15-fold following 7 days of culture. Moreover, during this time, the cells maintained a mesenchymal-like morphology. To investigate whether MM cells continued to express the MM-specific markers Wt1 (Donovan et al., 1999; Dressler, 2006) and Pax2 (Dressler, 2009) following several days of *in vitro* culture, immunostaining was performed at 24 hour intervals following initial MM isolation.

The results showed that almost all freshly isolated MM cells were Wt1 positive, and many of them were also Pax2 positive. Since both Wt1 and Pax2 are transcription factors, the staining is localized in the nuclei (Fig. 27). It was found that the expression of Wt1 was maintained throughout 96 hours of culture in the vast

majority of MM cells (Fig. 27 through Fig. 31). The expression of Pax2 was still present in MM cells cultured for 24 hours; however, unlike Wt1, it disappeared after 48 hours in culture (Fig. 27 through Fig. 29). Control staining, where the primary antibodies were omitted, did not display any fluorescence (Fig. 33).

In order to determine if Wt1 expression was maintained following extended culture, immunostaining was performed on MM cells subcultured at passage 1 and passage 2. The results, shown in Figure 32 indicates that P1 MM cells still expressed Wt1, although it seemed that several cells had lost the expression of this transcription factor, as only about half of them displayed a positive immunostaining (Fig. 32, top panel, arrows). The expression of Wt1 was still detectable in MM cells at P2, but became restricted to a limited number of cells compared with P1 (Fig. 32, bottom panel, arrows).

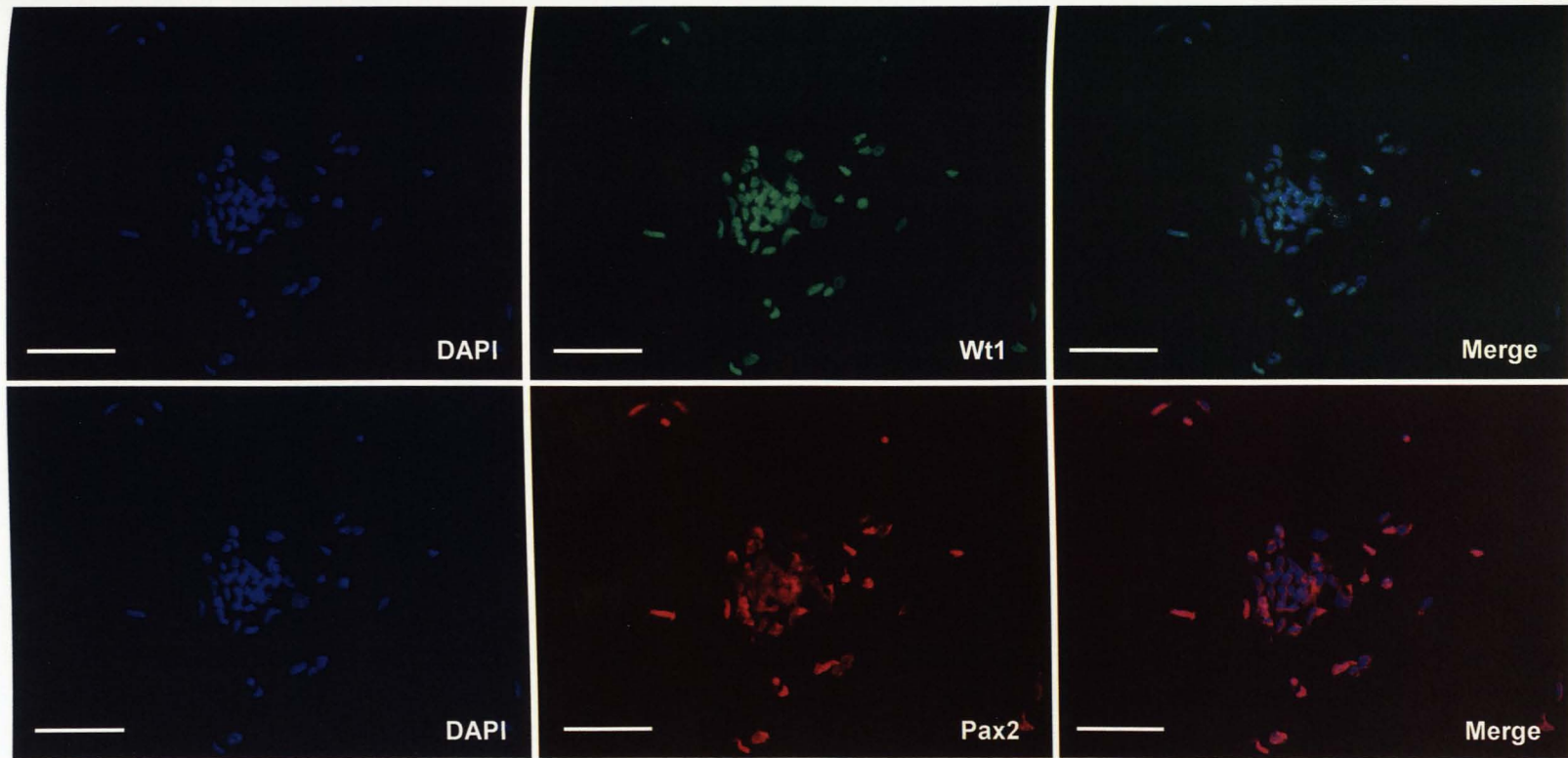


Figure 27. Freshly isolated MM cells cultured in MM medium supplemented with 25 ng/ml BMP7 and 100 ng/ml FGF2 stained for Wt1 (green) and Pax2 (red). Nuclei are stained for DAPI (blue). Scale bar: 100 μ m.

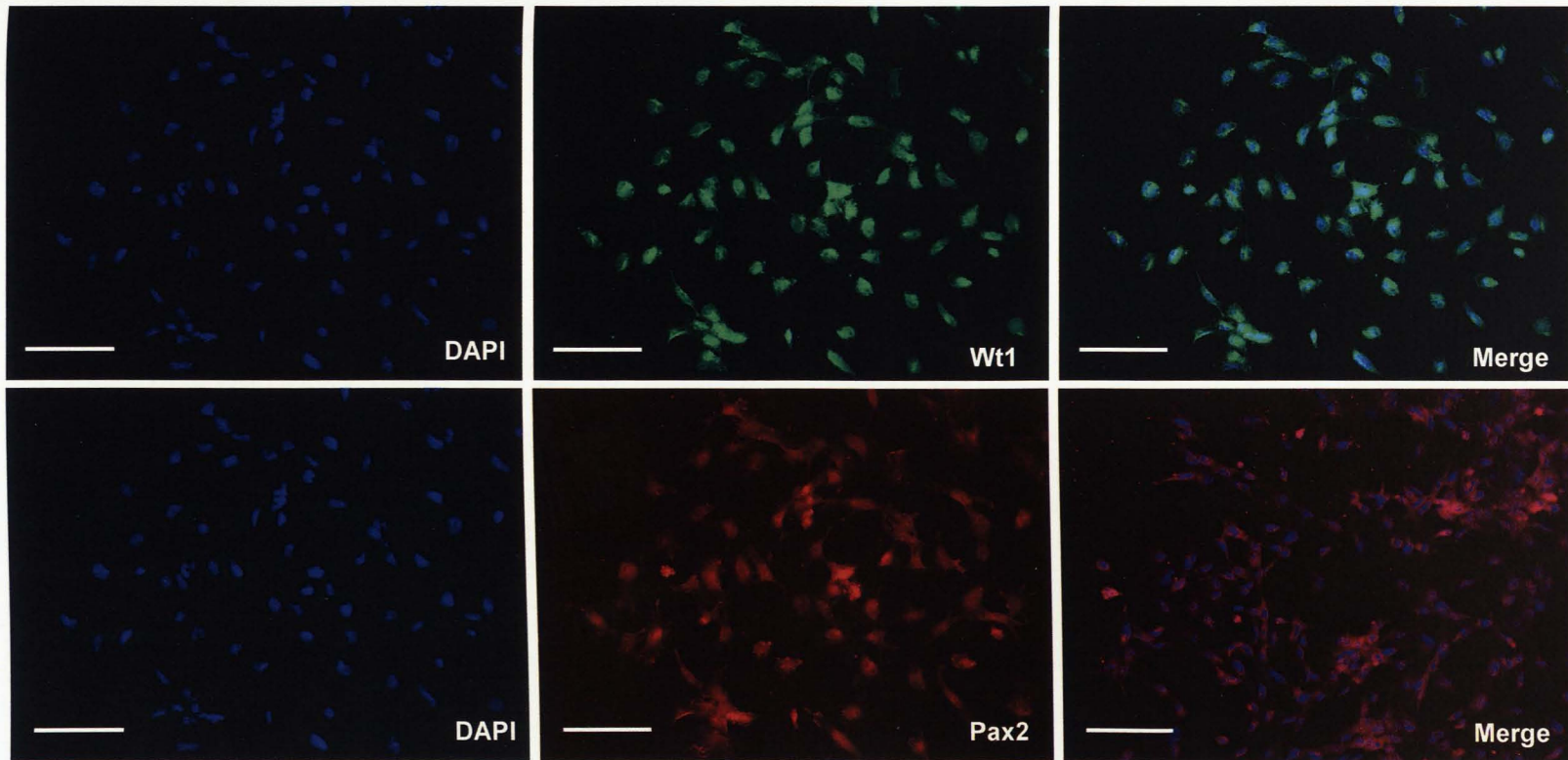


Figure 28. MM cells cultured for 24 hours in MM medium supplemented with 25 ng/ml BMP7 and 100 ng/ml FGF2 stained for Wt1 (green) and Pax2 (red). Nuclei are stained with DAPI (blue). Scale bar: 100 μ m.

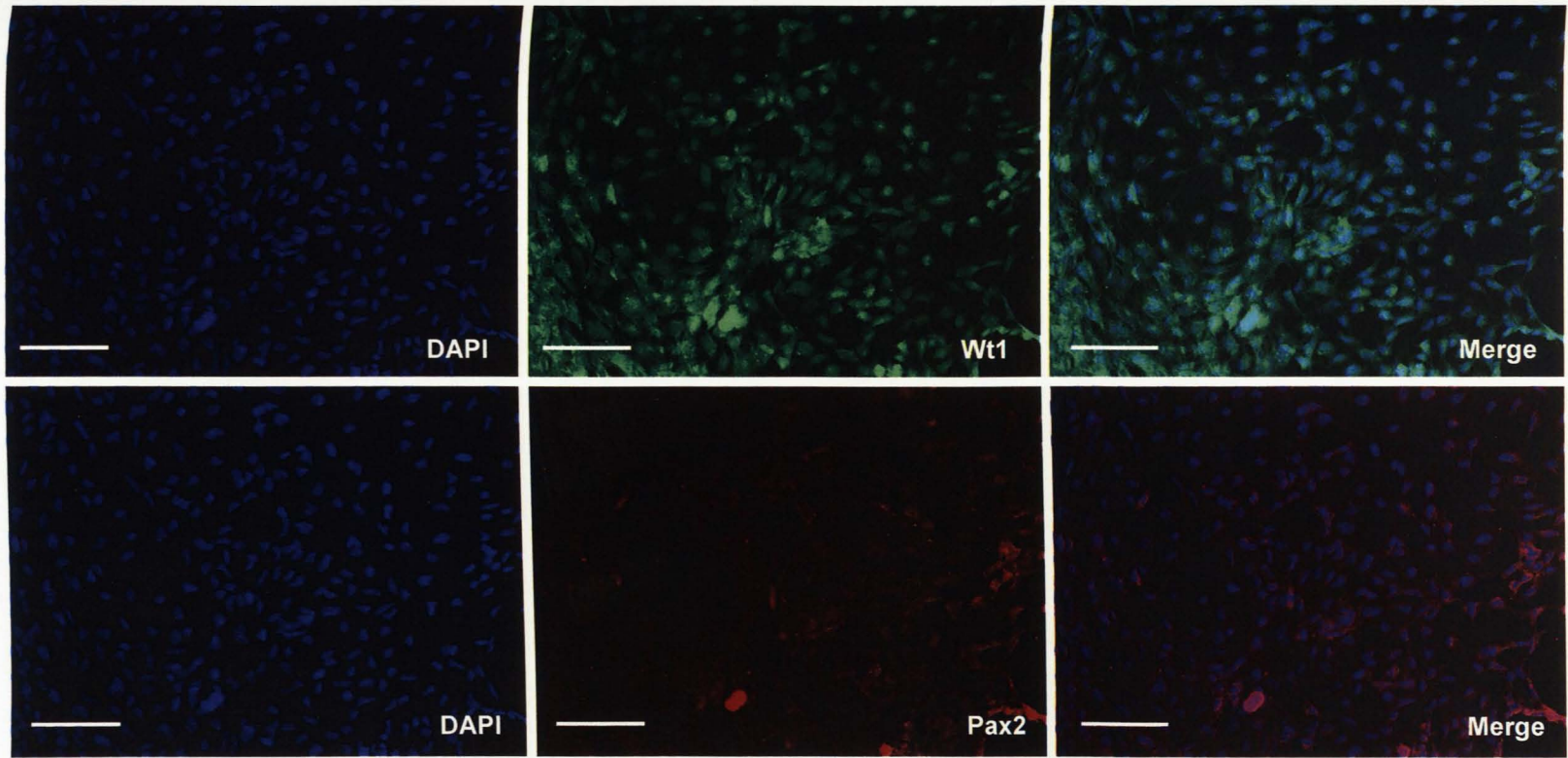


Figure 29. MM cells cultured for 48 hours in MM medium supplemented with 25 ng/ml BMP7 and 100 ng/ml FGF2 stained for Wt1 (green) and Pax2 (red). Nuclei are stained with DAPI (blue). Scale bar: 100 μ m.

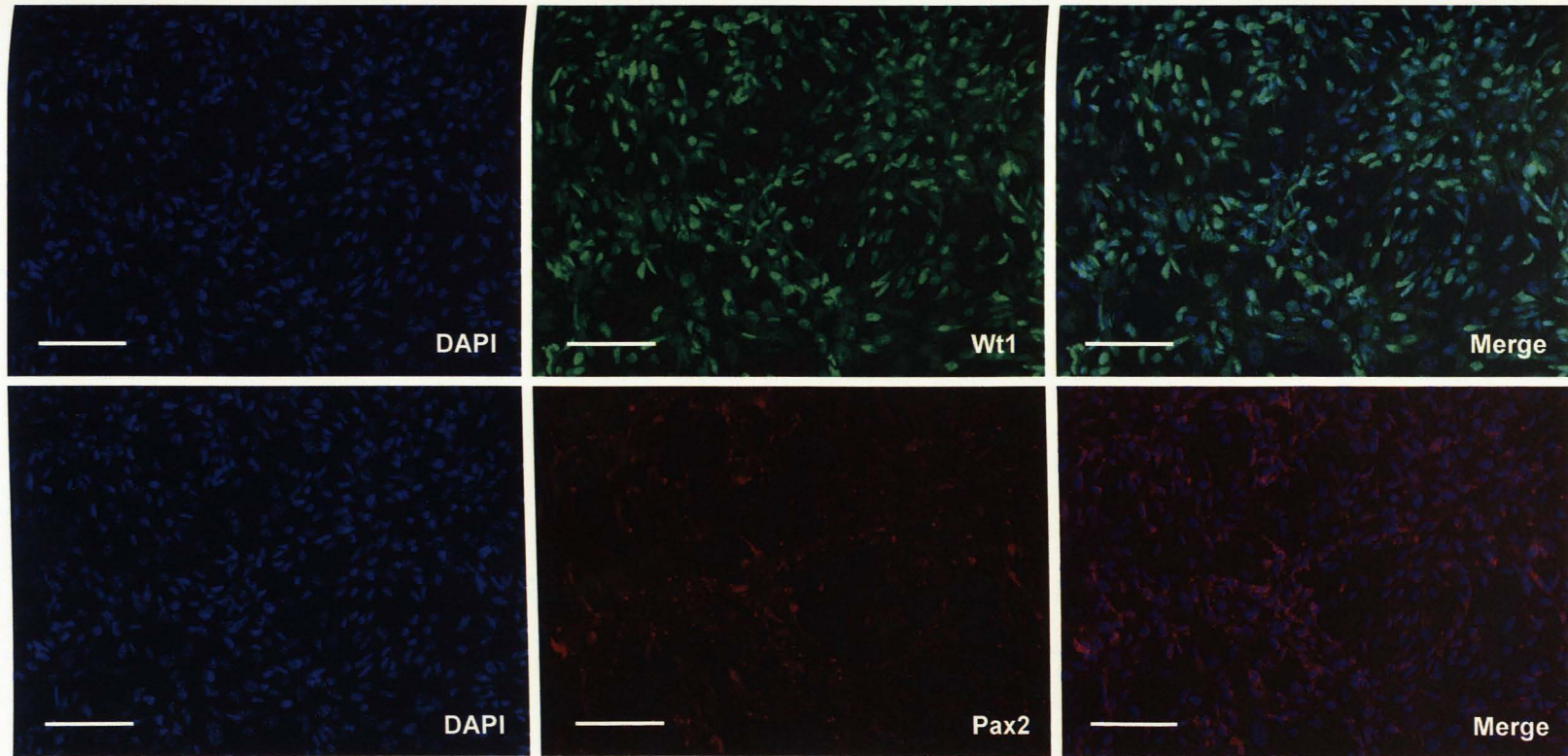


Figure 30. MM cells cultured for 72 hours in MM medium supplemented with 25 ng/ml BMP7 and 100 ng/ml FGF2 stained for Wt1 (green) and Pax2 (red). Nuclei are stained with DAPI (blue). Scale bar: 100 μ m.

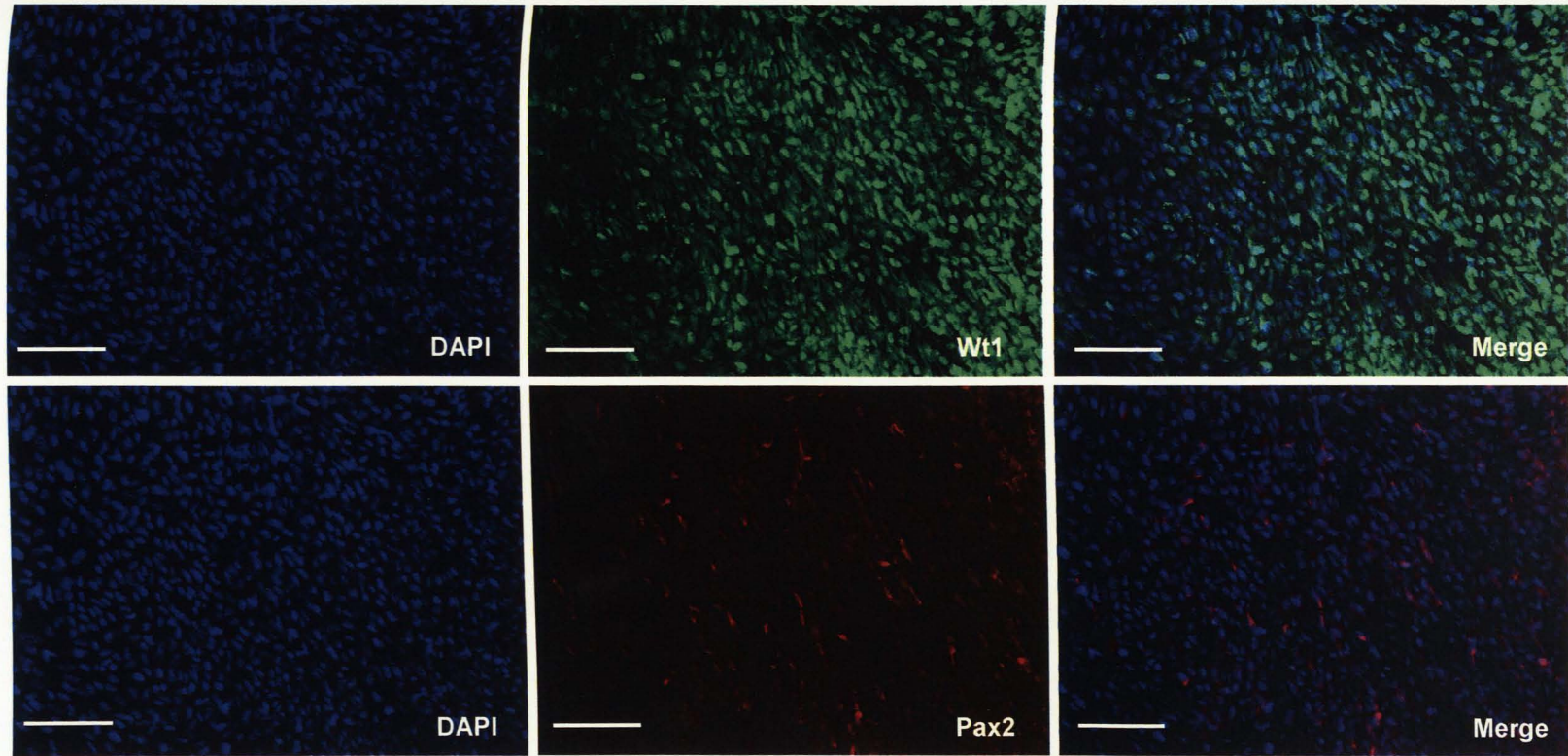


Figure 31. MM cells cultured for 96 hours in MM medium supplemented with 25 ng/ml BMP7 and 100 ng/ml FGF2 stained for Wt1 (green) and Pax2 (red). Nuclei are stained with DAPI (blue). Scale bar: 100 μ m.

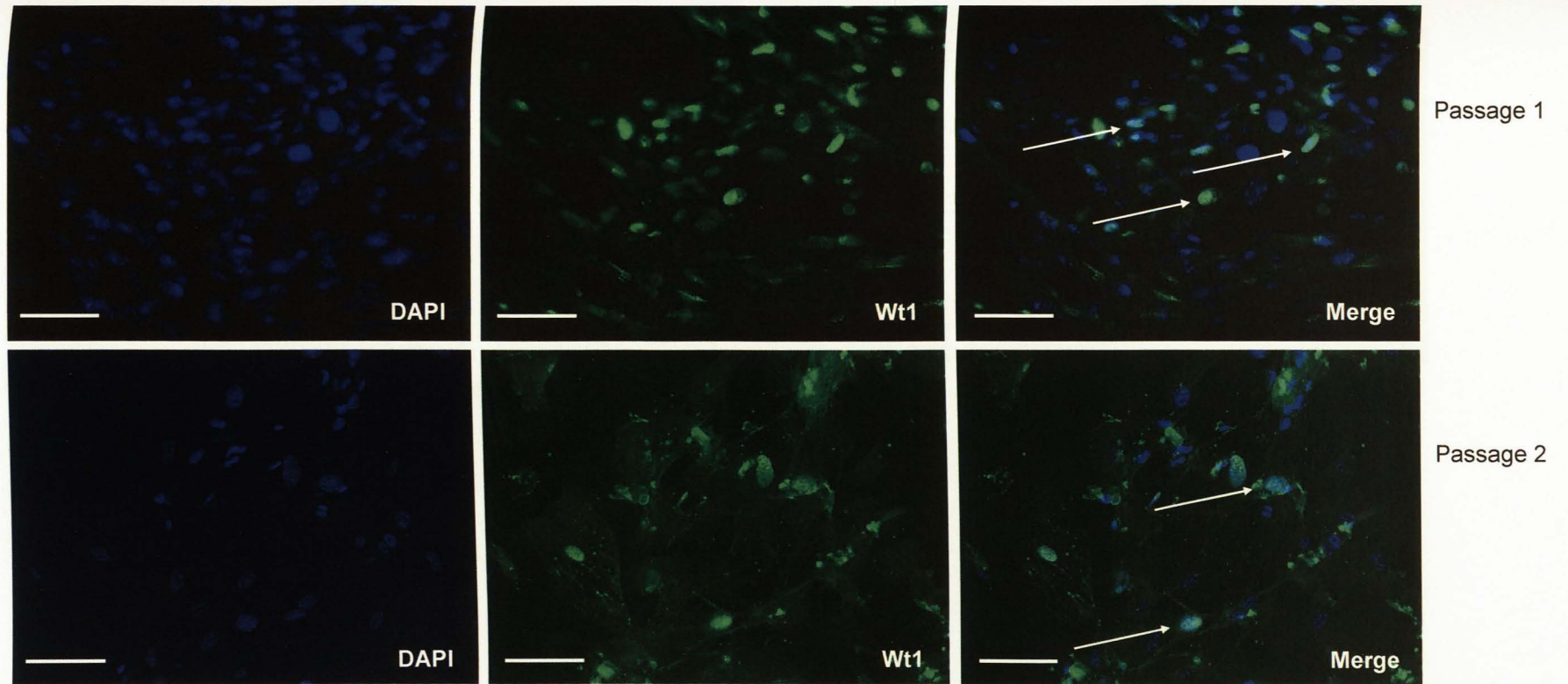


Figure 32. Immunofluorescence staining of MM cells cultured at passage 1 (top) and passage 2 (bottom) for Wt1 (green). The cells were cultured in MM medium supplemented 25 ng/ml BMP7 and 100 ng/ml FGF2. Nuclei are stained with DAPI (blue). Arrows indicate Wt1-positive cells. Scale bar: 100 μ m.



Figure 33. Negative controls for the immunostaining. Scale bar: 100 μ m.

3.2.4 Gene expression profiling of MM cells following *in vitro* culture

In order to investigate the gene expression profile of MM cells following *in vitro* culture, RT-PCR analysis was performed to compare the expression of key MM-specific genes in freshly isolated MM cells with that of cultured cells. Table 12 shows the list of genes selected for the expression analysis. Primer sequences are shown in Table 7, page 93. This list of genes comprises specific markers for metanephric mesenchyme, such as *Wt1*, *Pax2*, *Sall1*, *Osr1* and *Gdnf*. It is expected that most of these genes are expressed in the MM cell population following *in vitro* culture. If most of these genes are not expressed, it would indicate that the cells are not able to maintain a MM-like phenotype following *in vitro* expansion.

Table 12. List of markers selected for the RT-PCR analysis.

<u>Gene</u>	<u>Specificity</u>
<i>Wt1, Sall1, Osr1, Gdnf</i>	Metanephric mesenchyme
<i>Ret, Hoxb7</i>	Ureteric bud
<i>Pax2</i>	Metanephric mesenchyme, Ureteric bud
<i>Lhx1</i>	Nephric duct, Ureteric bud, MM- derived structures
<i>Vim</i>	Mesenchymal cells
<i>Tjp1</i>	Epithelial cells
<i>Msi1, Msi2</i>	Stem/progenitor cells
<i>Bax, Bcl2</i>	Apoptosis
<i>p16^{INK4a}</i>	Senescence

The genes *Ret* and *Hoxb7* are ureteric bud markers: they were selected in order to verify that the metanephric mesenchyme does not contain UB cells. The expression of *Lhx1* is detectable in the intermediate mesoderm, then in the nephric duct, ureteric bud and some MM-derived structures such as comma and S-shaped body (Kobayashi et al., 2005). *Vimentin* (*Vim*) is a mesenchymal marker that was included in order to verify that MM cells maintain a mesenchymal-like phenotype following *in vitro* culture. Conversely, the epithelial marker *Tight junction protein* (*Tjp1*) was selected in order to detect the presence of epithelial cells in explants, and to assay whether the MM cell population undergoes mesenchymal to epithelial transition following *in vitro* culture. *Musashi1* (*Msi1*) and *Musashi2* (*Msi2*) are markers for multipotency expressed in neural stem and progenitor cells (Sugiyama-Nakagiri et al., 2006), and in renal progenitor-like cells (Kitamura et al., 2005). These markers were chosen to determine whether freshly isolated MM show a progenitor cell-like phenotype, and whether their expression can be maintained following *in vitro* culture. The expression of genes involved in apoptosis and senescence was also investigated, namely the pro-apoptotic gene *Bax*, the anti-apoptotic gene *Bcl2* and the senescence marker *p16^{INK4a}* (Kim et al., 2008). These markers were selected in order to investigate if the failure of MM cells to be propagated in long term culture was due to the cells undergoing apoptosis or senescence. In this study *β -actin* (*β -act*) represented the reference gene and it was chosen in order to verify that the PCR reaction worked appropriately.

RT-PCR was performed on freshly isolated MM and MM cells cultured for 24 hours, 48 hours, 72 hours and 96 hours in MM medium always supplemented with 25 ng/ml BMP7 and 100 ng/ml FGF2. The results showed that freshly isolated MM expressed all

of the MM-specific genes assayed, i.e. *Wt1*, *Pax2*, *Osr1*, *Sall1* and *Gdnf*. In addition the cells expressed *Vim*, thus demonstrating that they showed a mesenchymal phenotype (Fig. 34). Moreover, the expression of both *Msi1* and *Msi2* was detected, thus suggesting the presence of progenitor-like cells within the population of freshly isolated MM cells. It is interesting to point out that the cells expressed both the pro-apoptotic marker *Bax* and the anti-apoptotic marker *Bcl2*, whereas the senescence marker $p16^{INK4a}$ was not found. Surprisingly, it was found that the epithelial marker *Tjp1* and the ureteric bud markers *Ret* and *Hoxb7* were expressed by the freshly isolated MM (Fig. 34). Although particular care was taken to separate the MM from the ureteric bud, it cannot be ruled out that a small number of UB cells remained attached to the MM after dissection. Following 96 hours in culture the expression profile of cultured MM was almost unchanged, except that *Pax2* was no longer expressed following 48 hours of culture (Fig. 34). This result is in agreement with the immunofluorescence staining, which shows that the presence of *Pax2* protein was lost following 2 days of culture (Fig. 27 through Fig. 29). The results presented here indicate that all MM-specific markers are expressed by MM cells following 96 hours of culture, thus indicating that under the culture conditions developed MM cells were able to maintain a MM-like phenotype. In addition, the presence of both *Msi1* and *Msi2* suggests that MM cells might retain a progenitor cell-like phenotype (Fig. 34). It was also observed that under these culture conditions the pro-apoptotic stimulus of *Bax* seemed to be counterbalanced by the expression of the anti-apoptotic gene *Bcl2*. Moreover, the senescence marker $p16^{INK4a}$ was never detected in MM cells throughout 4 days of culture (Fig. 34).

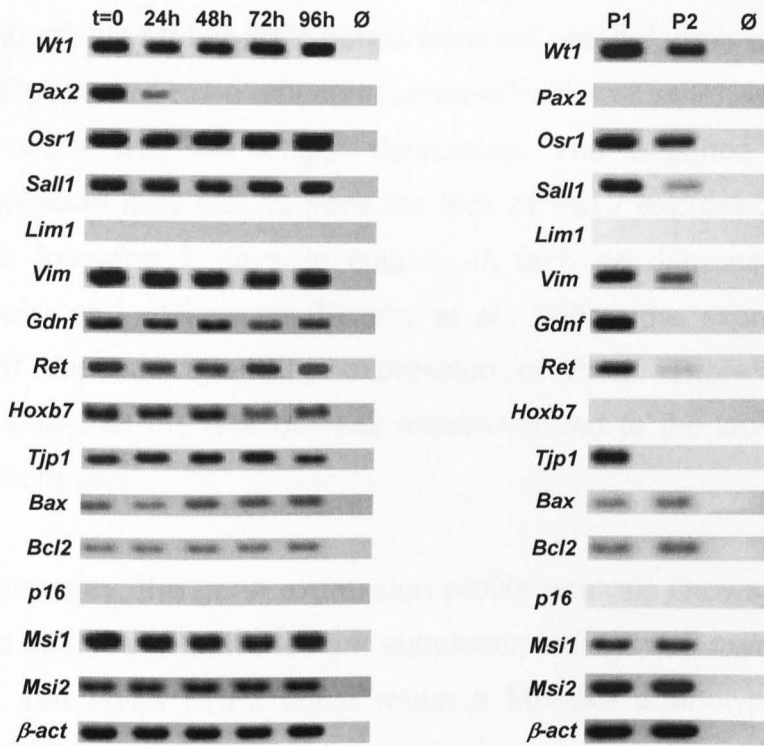


Figure 34. Expression profile of freshly isolated and cultured MM cells. Left: RT-PCR performed on freshly isolated MM (t=0) and MM cells following 24, 48, 72, and 96 hours of culture. Right: RT-PCR performed on MM cells at passage 1 (P1) and passage 2 (P2). MM cells were always cultured in MM medium containing 25 ng/ml BMP7 and 100 ng/ml FGF2. *p16*: *p16^{INK4a}*, *β-act*: reference gene; Ø: No template. MM cells cultured up to 96 hours: *Wt1*, *Pax2*, *Osr1*, *Sall1*, *Lim1*, *Vim*, *Gdnf*, *Ret*, *Tjp1*, *Bax*, *Bcl-2*, *p16* and *β-act* n≥2; *Msi1*, *Msi2* and *Hoxb7* n=1. P1 and P2 MM cells: all genes except *β-act* n=1; *β-act* n=2.

In order to investigate the expression profile of long-term cultured MM cells, RT-PCR analysis was performed on cells cultured at P1 and P2. The results show that at P1 the expression profile of MM cells appeared to be very similar to that of 4-days cultured MM cells. The results also suggest that even at P1 MM cells retained a progenitor cell-like phenotype, as both *Msi1* and *Msi2* were still clearly detectable (Fig. 34). The expression profile changed when MM cells were cultured at P2. As it can be seen in Figure 34,

although the MM-specific genes were still present, their expression levels seemed to be reduced compared with that at P1. Notably, at P2 *Gdnf* was no longer detectable. The absence of *Gdnf* expression may result from the lack of *Pax2* expression in MM cells following 2 days in culture. In fact, as demonstrated by Brophy and colleagues (Brophy et al., 2001), the expression of *Gdnf* depends upon the expression of *Pax2*. Therefore, it is possible that the lack of *Pax2* expression led to the lack of *Gdnf* transcription.

In summary, the gene expression profile analysis shows that MM cells cultured in MM medium supplemented with 25 ng/ml BMP7 and 100 ng/ml FGF2 could retain a MM-like phenotype and a progenitor cell-like phenotype following several days of *in vitro* culture, as they expressed the metanephric mesenchyme markers *Wt1*, *Osr1* and *Sall1*, the mesenchymal marker *Vim* and the progenitor cells markers *Msi1* and *Msi2*. The expression of several MM markers was still detectable at P1 and, in part, at P2. In addition, the presence of *Msi1* and *Msi2* suggests that MM cells might also maintain a progenitor cells-like phenotype following 12 days of culture.

3.3 Discussion

In this chapter it was shown that metanephric mesenchyme cells cultured in MM medium supplemented with 25 ng/ml BMP7 and 100 ng/ml FGF2 could undergo expansion by approximately 15-fold and maintained a MM-like phenotype after 7 days of culture,

as evidenced by the presence of several MM-specific markers, such as *Wt1*, *Osr1*, *Sall1*, *Gdnf* and *Vim*.

Cell growth assays showed that the population doubling (PD) time for freshly propagated (P0) MM cells was about 57 hours. Interestingly, P1 MM cells displayed a shorter PD time, which was approximately 37 hours. However, under the conditions developed, MM cells were no longer able to undergo further expansion beyond the third day of culture at P1 (7 days after initial isolation). It is plausible that the culture conditions developed were appropriate for the expansion of MM cell population in the short term, but were not ideal to support cell expansion beyond 7 days of culture. Adult stem or progenitor cells usually reside in specialized regions, called *niches* that represent sheltering microenvironments that allow the cells to undergo self-renewal and protect them from premature differentiation (Moore and Lemischka, 2006). Given that the metanephric mesenchyme represents a population of progenitor cells (Oliver et al., 2002) committed to generate all cell types present in the adult nephron, it is plausible that the culture conditions developed simply did not provide a suitable *niche* for the long term culture of MM cells.

Immunostaining and RT-PCR assays suggested that the phenotype of MM cells changed when the cells were cultured for 4 days at P2 (12 days following initial isolation), as a downregulation in the expression of key MM-specific markers, namely *Wt1*, *Osr1*, *Sall1*, and *Vim* was observed in P2 MM cells compared with P1 MM cells. Furthermore, P2 MM cells lost the expression of the MM-specific gene *Gdnf*. As previously observed, the expression of *Pax2*, another key MM marker, was lost after 24 hour of culture. Xu and colleagues proposed the existence of an *Eya1-Six1-Pax2*

hierarchy that is involved in mammalian kidney development (Xu et al., 2003). The lack of expression of Pax2 observed in this study might be due to a downregulation of either Eya1 or Six1, or both genes, in cultured MM cells that in turn determined the loss of Pax2 expression. Therefore, in order to provide evidence to support this hypothesis, in future it would be important to investigate the expression of both Eya1 and Six1 in freshly isolated MM and MM cells following *in vitro* culture.

These results appear to indicate that under the culture conditions developed, apart from no longer expressing Pax2, MM cells were able to maintain a MM-like phenotype for 7 days of culture. The incapacity of MM cells to undergo expansion at P2 might be due to the inability of the cells to maintain a MM-like phenotype when cultured beyond P1.

The inability of MM cells to undergo long term growth may also be due to a downregulation of the MM-specific gene *Sall1*, which occurs at passage 2. The expression of *Sall1* is required for normal kidney development. Nishinakamura and Takasato observed that in E11.5 *Sall1*-null embryos the metanephric mesenchyme develops, but the ureteric bud fails to invade the metanephric blastema, resulting in kidney agenesis or severe dysgenesis in the progeny (Nishinakamura and Takasato, 2005). The gene expression profile shows that *Sall1* appeared to be downregulated in MM cells at passage 2 compared with freshly propagated MM cells and MM cells at passage 1. The downregulation of *Sall1* may represent another factor that determined the failure of MM cells to undergo further expansion after one passage and 7 days of culture.

Finally, RT-PCR showed that the UB markers *Ret* and *Hoxb7* and the epithelial marker *Tjp1* were present in both freshly isolated and cultured MM cells. Although particular care was taken to isolate the intact UB from the MM, it might still be possible that a small number of UB cells remained inside a diligently cleaned MM after completing the dissection procedure. These UB cells might therefore be accountable for the presence of *Ret*, *Hoxb7* and *Tjp1* transcripts detected in freshly isolated and cultured MM cells. However, it is believed that the presence of few UB cells within the MM did not stimulate MM cells to undergo induction, as the expression of *Pax2*, which is expected to increase following induction, was never detected following 2 days in culture. The use of *Hoxb7-GFP* transgenic mouse (Bush et al., 2006) would represent an ideal solution to avoid the presence of UB fragments inside the dissected metanephric mesenchyme.

CHAPTER 4

Investigating the nephrogenic potential of mouse metanephric mesenchyme

4.1 Introduction

In chapter 3 it was shown that metanephric mesenchyme (MM) cells, isolated from E11.5 mouse embryos, could be expanded in culture by approximately 15-fold in 7 days when cultured on tissue culture plastic dishes in MM medium supplemented with 25 ng/ml BMP7 and 100 ng/ml FGF2. In addition, MM cells were able to maintain a metanephric mesenchyme-like phenotype during this period, as demonstrated by the expression of several MM-specific markers, such as *Wt1*, *Osr1*, *Sall1*, *Gdnf* and *Vim*.

In the second part of this work it became important to investigate whether the culture conditions developed allowed MM cells to retain the ability to undergo induction and form nephron-like developing structures in the presence of heterologous inducing stimuli.

The natural inducer of the MM in the developing embryo is the ureteric bud (UB). As illustrated in section 1.1.2.3, in the developing metanephros each tip of the UB stimulates the surrounding MM to undergo mesenchymal-to-epithelial transition and form pretubular aggregates, a process which leads to the establishment of a functional nephron (Saxén, 1987; Kuure et al., 2007).

During the last sixty years several studies have shown that the freshly isolated, uninduced metanephric mesenchyme can undergo tubulogenesis when recombined in transfilter culture with

embryonic tissues. In a pioneering experiment Grobstein demonstrated that E11.0 isolated MM could undergo tubulogenesis when cultured in transfilter culture with the ureteric bud or a heterologous inducer such as the embryonic spinal cord (SC) (Grobstein, 1953; Grobstein, 1955). Since then, due to its larger size SC has become the most commonly used inducer of the metanephric mesenchyme in experimental tubulogenesis. In the presence of SC pretubular aggregates containing polarized cells become visible as early as the second day of culture within the induced MM. As later described by Saxén, these aggregates can further develop into renal vesicles, which give rise to tubular epithelial structures (Saxén, 1987). However, following induction with SC the tubulogenesis usually arrests at the comma-shaped body stage, and very few regular S-shaped bodies are able to form (Saxén, 1987). This limitation has been in part overcome by Dudley and co-workers: these authors demonstrated that in the presence of BMP7 and FGF2, SC-induced MM was able to give rise to more developed renal tubules and form primitive glomeruli (Dudley et al., 1999).

In the original Grobstein's assay the mesenchyme and the inducer were separated by a Millipore filter placed upon a metal grid (Grobstein, 1953). Millipore filters were later replaced by Nucleopore membrane filters, characterized by a more uniform pore size (Wartiovaara et al., 1972). In this system, it has been established that induction is dependent upon cell-cell contact between the SC and MM cells, rather than paracrine factor. In fact, it was demonstrated that tubulogenesis did not take place when membrane filter with pore size of 0.1 μm or less were used, as cell-cell contacts could not be established between the MM and its

inducer (Wartiovaara et al., 1974; Saxén et al., 1976, Saxén, 1987).

Davies and Garrod provided evidence that lithium chloride elicited an inductive effect on mouse metanephric mesenchyme. When incubated with 15 mM LiCl the uninduced MM was able to begin nephrogenesis; however, these authors noticed that LiCl exerted a weaker inductive effect than spinal cord, as the nephrogenic process stalled at the comma-shaped body stage (Davies and Garrod, 1995).

Several studies have suggested that members of the Wnt family of secreted glycoproteins play a mayor role in the induction of the MM. Herzlinger and colleagues demonstrated that freshly isolated MM can undergo induction when cultured in the presence of a layer of NIH3T3 cells expressing Wnt1. This gene is not present in the kidney but it is normally expressed in the dorsal spinal cord (Herzlinger et al., 1994). Further evidence about the involvement of Wnt signaling in the induction of the metanephric mesenchyme was reported in a study published by Kispert and colleagues. This group showed that the isolated metanephric mesenchyme undergoes tubulogenesis when cultured in transfilter culture on a layer of cells stably expressing Wnt4, a factor which is present in pretubular mesenchyme cells. They also showed that Wnt4 signal could be replaced by other Wnt factors, namely Wnt3a, Wnt7a and Wnt7b, all of which are expressed in the spinal cord (Kispert et al., 1998).

Although Wartiovaara (Wartiovara et al., 1974) and Saxén (Saxén et al., 1976) demonstrated that soluble factors released from the inducer could not initiate tubulogenesis in mouse MM, Barasch

and co-workers demonstrated that transient exposure to leukemia inhibitory factor (LIF), released by the UB, can trigger nephrogenesis in isolated E13.0 rat mesenchyme. The induced tissue was able to undergo mesenchymal-to-epithelial transition, develop renal tubules with the appearance of comma and S-shaped body, and give rise to primitive glomeruli (Barasch et al., 1999).

Several reports have indicated that the canonical Wnt pathway and cytosolic β -catenin play a central role in the induction of the metanephric mesenchyme. In the absence of Wnt signaling cytosolic β -catenin is continuously phosphorylated at its N-terminal domain by glycogen synthase kinase-3 β (GSK-3 β), then ubiquitinated and targeted for proteasomal degradation. When, on the other hand, Wnt signaling is present it activates the FZD/LRP/DLV (Dishevelled) complex which inhibits the β -catenin degradation complex (Schmidt-Ott and Barasch, 2008). As result β -catenin accumulates in the cytoplasm, then translocates to the nucleus where it activates transcription factors of the TCF/Lef family involved in nephron formation (Fig. 359 (Kuure et al., 2007; Park et al., 2007; Schmidt-Ott et al., 2007). These studies have suggested that renal tubulogenesis is triggered by Wnt9b, a glycoprotein secreted by the UB. Wnt9b activates *Wnt4* which is expressed in metanephric mesenchyme and pretubular aggregates of the metanephric mesenchyme following induction (Park et al., 2007; Schmidt-Ott and Barasch, 2008).

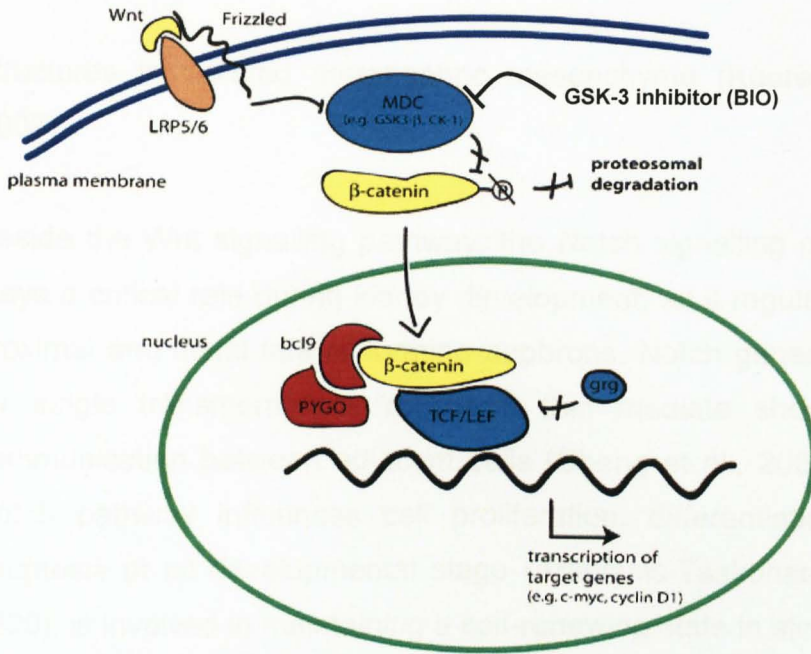


Figure 35. Schematic representation of the canonical Wnt signaling pathway. In the absence of Wnt signaling the cytosolic β -catenin is phosphorylated by GSK-3 β and targeted for proteasomal degradation. In the presence of Wnt signaling cytosolic β -catenin accumulates within the cytoplasm, then translocated to the nucleus where activates *TCF/Lef* family of transcription factors involved in nephron formation (Kuure et al., 2007). GSK-3 β can be inactivated using a synthetic GSK-3 inhibitor (BIO) (Adapted from Mikesch et al., 2007).

It has been suggested that both Wnt9b and Wnt4 act through cytosolic β -catenin, as genetic stabilization of β -catenin led to mesenchymal induction in *Wnt9b*^{-/-} and *Wnt4*^{-/-} mouse embryo (Park et al., 2007). More recently Kuure and co-workers provided further evidence for a role of the downstream effectors of Wnt signaling in the induction of the metanephric mesenchyme. These authors illustrated that it is possible to induce tubulogenesis in isolated metanephric mesenchyme by transient inactivation of GSK-3 β using a synthetic GSK-3 inhibitor (BIO) (Fig. 35). In addition it was shown that genetic stabilization of β -catenin leads to the spontaneous formation of developing nephron-like

structures in isolated metanephric mesenchyme (Kuure et al., 2007).

Beside the Wnt signalling pathway, the Notch signalling pathway plays a critical role during kidney development, as it regulates the proximal and distal fate of forming nephrons. Notch genes codify for single transmembrane receptors that mediate short-range communication between adjacent cells (Cheng et al., 2007). The Notch pathway influences cell proliferation, differentiation and apoptosis at all developmental stage (Artavanis-Tsakonas et al., 1999), is involved in maintaining a self-renewing state in stem cells isolated from different sources and in adult mice is involved in tissue maintenance and repair (Challen et al., 2006). Following the binding with its ligand, the Notch receptor undergoes two proteolytic cleavages that release the intracellular domain of Notch (NICD). The intracellular domain, which represents the active form of the Notch receptor, translocates to the nucleus where it binds with the protein RBP-J κ and activates the transcription of its target genes (Cheng et al., 2007; Piggott et al., 2011). Kobayashi and colleagues provided evidence that the Notch pathway plays an important role in the proximodistal patterning of the S-shaped body, as it determines the formation of proximal tubules, capillaries and glomerular podocytes (Kobayashi et al., 2005). It has been shown that in *Notch2* null heterozygous mice the glomerular and proximal segments of the nephron do not form, whereas the more distal part and the collecting duct could develop normally (Cheng et al., 2007). More recently, Fujimura and colleagues provided new insights into the role of Notch2 in the specification of the proximal fate of developing nephrons. Using a transgenic strategy in which *Notch2* was activated in *Six2*-positive nephron progenitors of the MM, these authors demonstrated that

the over-expression of *Notch2* caused *Six2*-positive nephron progenitor cell depletion, ectopic expression of *Wnt4* and premature tubular formation. On the basis of their results, Fujimura and co-workers suggested the existence of a positive feedback loop between *Notch2* and *Wnt4* in which the former regulator, once activated, induced the expression of *Wnt4* which in turn accelerates tubular differentiation of nephron precursors and inhibits their reversion to the undifferentiated condition (Fujimura et al., 2010).

The first part of this chapter will investigate the ability of *in vitro* cultured MM to become induced and undergo tubulogenesis following stimulation with embryonic spinal cord (SC) and a GSK-3 inhibitor (BIO) in transfilter culture. The induction process was assessed by immunostaining for *Wt1*, *Pax2*, calbindin and laminin. The expression of *Wt1* is expected to increase dramatically after mesenchymal condensation and induction, particularly in the developing podocytes within the nascent glomeruli (Donovan et al., 1999). Laminin is also a useful indicator for the induction because following mesenchymal condensation MM cells deposit a basement membrane at their basal surface, which can be detected by laminin immunostaining. Calbindin is a marker for ureteric bud and distal convoluted tubules, and is expected to be expressed within the induced MM due to the presence of developing distal segments of the nephrons (Georgas et al., 2008). *Pax2* expression is low in uninduced MM, but the expression level increases following MM induction (Torban et al., 2006).

One of the crucial points of this work was to investigate whether MM cells could maintain a nephrogenic potential following *in vitro* culture and participate in the formation of kidney structures.

Unbekandt and Davies developed a protocol in which disaggregated embryonic kidney rudiments formed organotypic renal structures following reaggregation and culture in transfilter culture. These authors showed that the reaggregated tissues could develop nephron-like structures and distal tubules that displayed both normal morphology and expression of characteristic markers (Unbekandt and Davies, 2010). Since the method easily allows the formation of chimeras by simply mixing reaggregated kidney rudiments with a given cell population, in this study it was elected to adopt this protocol to investigate the *in vitro* nephrogenic potential of MM cells. If MM cells retained a nephrogenic potential, then it would be expected that they would be able to participate in nephrogenesis.

In the present study the nephrogenic potential of MM cells following 4 days of *in vitro* culture was explored by recombination with E11.5 reaggregated kidney rudiments; furthermore, the ability of cultured MM cells to integrate into nephron-like developing structures was compared with that of freshly isolated MM, as the latter population would represent a positive control for the integration.

In order to track MM cells within the chimera, it was decided to label these cells with quantum dots (QD). QD are highly fluorescent nanocrystals that are greatly resistant to photobleaching (Solanki, 2008). The uptake of QD does not involve an enzymatic mechanism, as the internalization occurs through a targeting peptide that covers the surface of the nanocrystals. Once internalized, QD appear to be localized inside cytoplasmic vesicles (Rosen et al., 2007). According to the manufacturer (Invitrogen) and Rosen and colleagues (Rosen et

al., 2007), QD can be inherited by daughter cells for several generations. It has also been demonstrated that QD do not affect cell proliferation, viability and differentiation capacities. Besides, it was shown that, following internalization, QD are not transferred to adjacent cells (Rosen et al., 2007; Invitrogen). Rosen and colleagues demonstrated that QD could be used to track individual human mesenchymal stem cells (hMSC) for up to 8 weeks following implantation into canine ventricles. These authors also demonstrated that QD were not uptaken by canine cells following hMSC lysis (Rosen et al., 2007). Due to their properties and the ease and rapid labelling protocol, in this Thesis it was decided to use QD to label freshly isolated and cultured MM cells with the aim of tracking them within the chimera.

Immunostaining for Wt1 and laminin will be used to identify developing nephron-like structures. Pax2 was chosen to mark the induced metanephric mesenchyme and to assess whether MM cells could express this transcription factor following chimera formation.

4.2 Results

4.2.1 Investigating the ability of cultured MM cells to undergo induction using Grobstein's assay

In order to investigate whether MM cells following *in vitro* culture retain their ability to undergo induction, MM cultured for 24 hours, 48 hours and 72 hours under the conditions previously described (see section 3.2.1) were assessed for their ability to undergo induction using Grobstein's assay.

During the dissection procedure particular care was taken to tease away the intact UB from the MM. In addition, before starting the stimulation with the inducer, the MM was carefully examined in order to make sure that no UB fragments were still present within the mesenchyme. The results showed that after 72 hours of co-culture with the spinal cord, freshly isolated metanephric mesenchyme had undergone induction, as the staining for Wt1 revealed that developing glomeruli were present (Fig. 36, plain arrow). Furthermore, the staining for laminin showed the presence of basement membranes (Fig. 36, dotted arrow), confirming that the induction had taken place, as basement membranes were deposited on developing epithelial structures. The staining also showed the presence of calbindin, which suggested that distal convolute tubules had started forming (Fig. 36, blue arrow). The staining for Pax2 had a poor quality (Fig. 36 and Fig. 37), most likely because these images were not taken with a confocal microscope. Therefore, the expression of Pax2 within the induced MM will have to be further investigated.

The MM cultured without inducer did not express any of the markers assayed (Fig. 39).

Metanephric mesenchyme cultured for 24, 48 and 72 hours was then stimulated with spinal cord to undergo induction. Cultured MM cells retained the potential to undergo complete induction after 24 hours of culture: several developing glomeruli had started forming, extracellular laminin was present, and some renal tubules had started developing (Fig. 37).

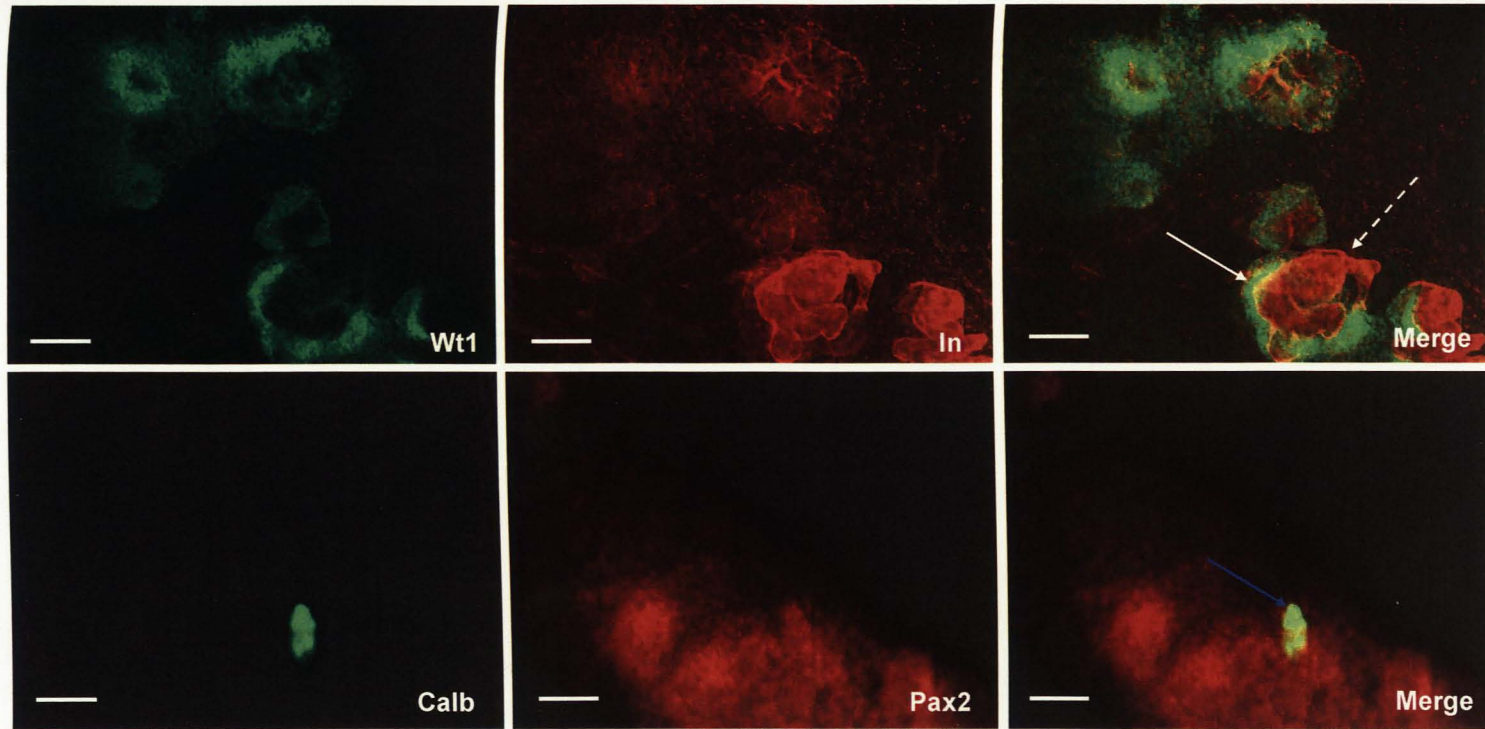


Figure 36. Induction of freshly isolated metanephric mesenchyme (MM) with embryonic spinal cord (SC). Metanephric mesenchyme was stained for Wt1, laminin, calbindin and Pax2. After 72 hours of stimulation with SC freshly isolated MM presented some immature glomeruli (plain arrow), basement membranes (dotted arrow) and started developing renal tubules (blue arrow). Scale bar: 100 μ m.

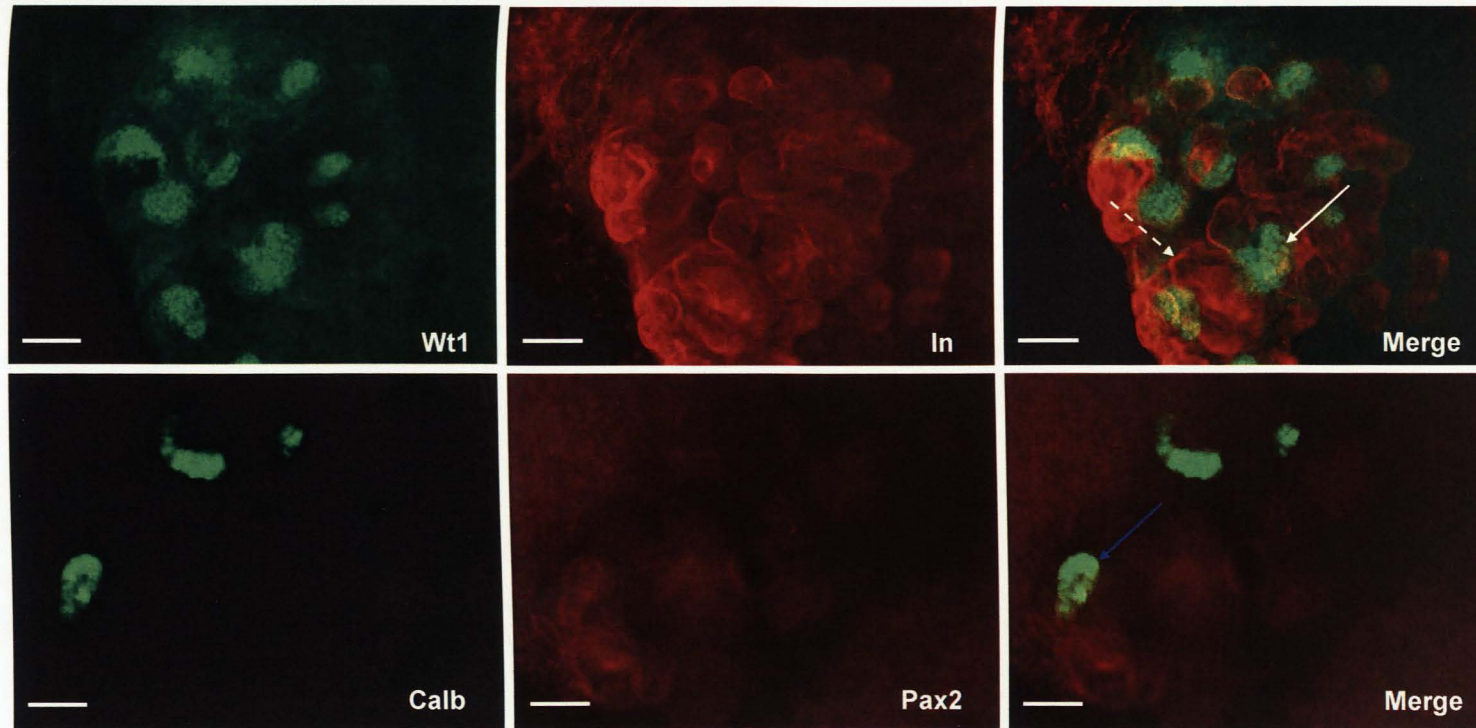


Figure 37. Induction of 24 hours cultured metanephric mesenchyme (MM) with embryonic spinal cord (SC). Following 72 hours of stimulation with SC, 24 hours cultured MM developed immature glomeruli (plain arrow), presented basement membranes (dotted arrow) and started forming renal tubules (blue arrow). Scale bar: 100 μ m.

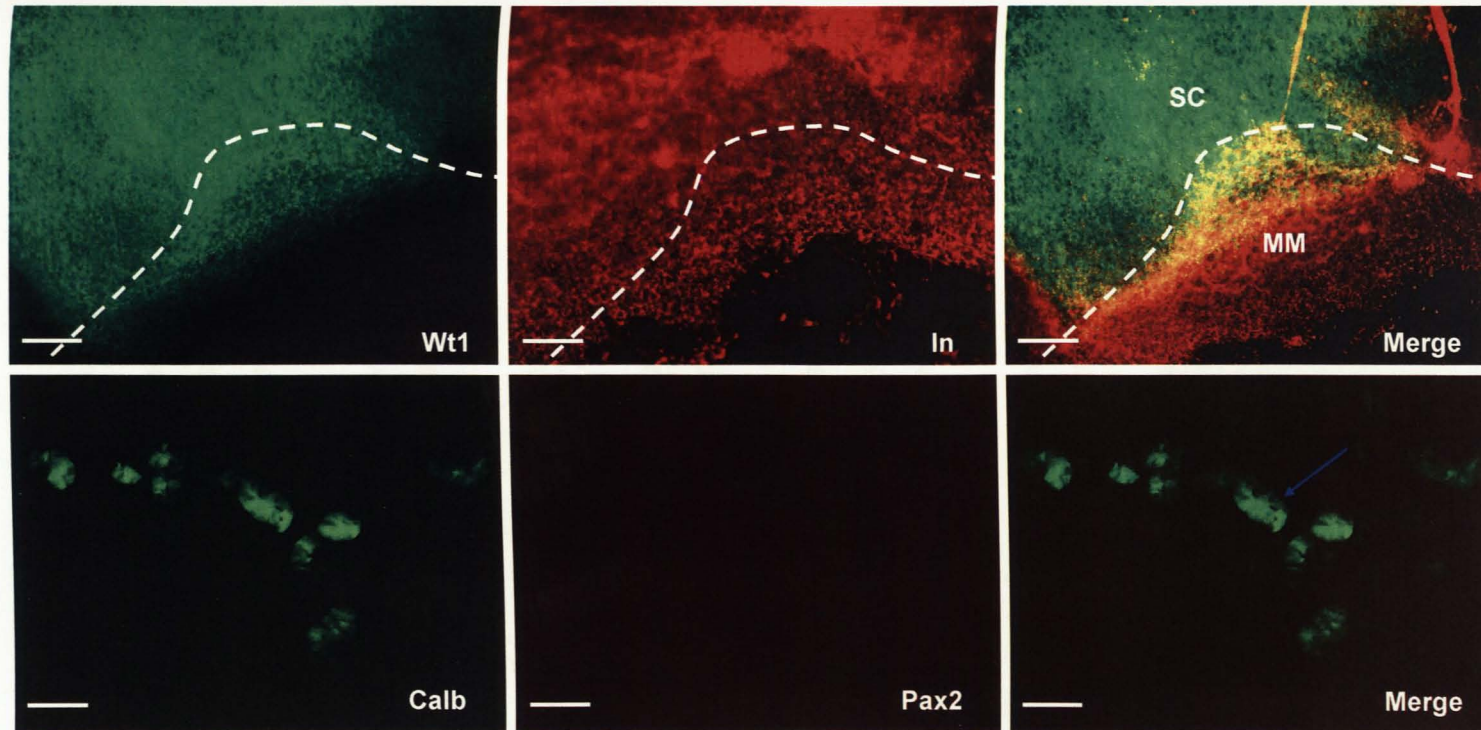


Figure 38. Induction of 48 hours cultured metanephric mesenchyme (MM) with embryonic spinal cord (SC). Following 48 hours in culture, MM cells partially lost the ability to be induced by the spinal cord as neither primitive glomeruli, nor basement membranes were found. However, calbindin staining revealed the presence of developing nephron distal segments (blue arrow). Dotted line separates the MM from the SC. Scale bar: 100 μ m.

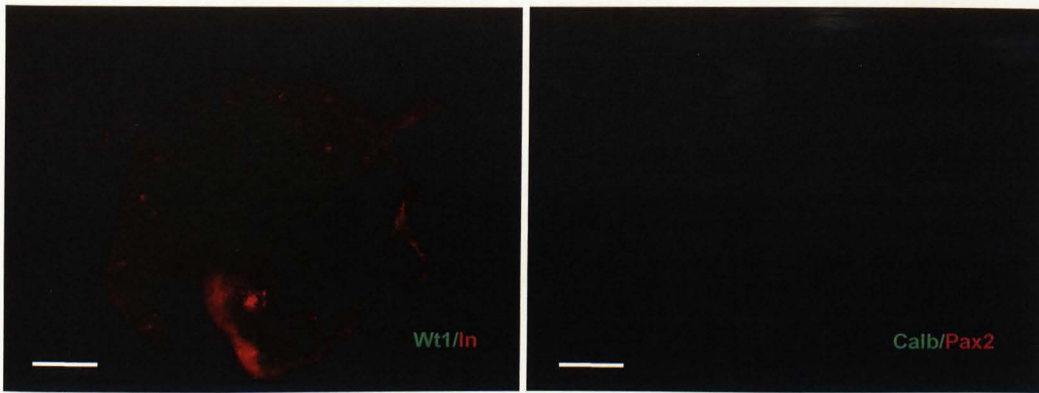


Figure 39. Freshly isolated metanephric mesenchyme cultured without spinal cord did not undergo induction (Control). Scale bar: 100 μ m.

After 48 hours of culture the MM was hardly visible and it became no longer possible to place the SC underneath it. It was then decided to stimulate 48 hours and 72 hours MM by juxtaposing the spinal cord directly to the mesenchyme. The results showed that after 48 hours of culture the mesenchyme seemed to partially lose the ability to respond to spinal cord stimulation, as just a few structures positive for calbindin were found (Fig. 38, blue arrow), but neither developing glomeruli, nor the basement membrane formed (Fig. 38). After 72 hours of culture the mesenchyme completely lost the ability to undergo induction, as none of the markers assayed were found (data not shown).

MM cells cultured for 24, 48 and 72 hours in the absence of spinal cord behaved similarly to freshly isolated MM (Fig. 39) and neither underwent induction nor expressed markers for ureteric bud cells (data not shown).

4.2.2 Investigating the ability of cultured MM cells to undergo induction following BIO incubation

As introduced in section 4.1, several works have provided evidence that Wnt signaling and the canonical pathway are involved in MM induction (Herzlinger, 1994; Kispert et al., 1998; Kuure et al., 2007; Park et al., 2007). Because Pax2 activates the expression of *Wnt4* both *in vitro* and *in vivo*, as demonstrated by Torban and colleagues (Torban et al., 2006), it was hypothesized that MM cells failed to undergo induction following 72 hours of culture because of the lack of Pax2 expression, which occurred after 2 days of culture (see section 3.2.3 and section 3.2.4).

One of the downstream targets of Wnt signaling in the canonical pathway is represented by the cytosolic β -catenin, which activates *Tcf1/Lef1* family of transcription factors that are involved in the tubulogenesis of the metanephric mesenchyme (Kuure et al., 2007, Schmidt-Ott and Barasch, 2008). In order to bypass the lack of Pax2 expression and mimic the presence of Wnt signaling, it was decided to transiently incubate cultured MM cells with a synthetic GSK-3 inhibitor (BIO). The rationale for incubating MM cells with BIO was that if the lack of induction was due to the absence of Pax2 expression, which in turn was required for Wnt signaling, then the specific inhibition of GSK-3 β would restore the canonical pathway and allow the metanephric mesenchyme to undergo induction (Fig. 35).

MM cells cultured up to 72 hours in MM medium supplemented with 25 ng/ml BMP7 and 100 ng/ml FGF2 were transiently incubated with 5 μ M BIO, then the inhibitor was withdrawn and the sample subcultured for a further three days (see section 2.2.6 for

details). The strategy adopted to stimulate MM cells with BIO is shown in Figure 15 (chapter 2). Freshly isolated MM was used as a positive control for the induction. In accordance with Kuure and co-workers, the culture medium was supplemented with 50 ng/ml FGF2 (Kuure et al., 2007). The presence of induction was assessed by immunofluorescence staining for Wt1, laminin, Pax2 and calbindin.

The results showed that in the transient presence of BIO freshly isolated MM had undergone induction, as two early aggregates positive for Wt1 and laminin had started forming (Fig. 40, plain arrow and dotted arrow, respectively). Moreover, the mesenchyme had started developing several distal convolute tubules (Fig. 40, blue arrow). Control samples cultured without the inhibitor did not present any sign of induction (Fig. 43). In addition, many cells within the uninduced mesenchyme were able to retain Wt1 expression, as Figure 43 shows. Metanephric mesenchyme cells cultured for 24 and 48 hours were able to undergo induction following BIO incubation (Fig. 41 and Fig. 42, respectively). Additionally, it was noticed that BIO exerted a stronger effect than spinal cord on metanephric mesenchyme cultured longer than 24 hours: it was observed that several glomeruli and distal convoluted tubules had started developing, and basement membrane had started depositing. Indeed, the staining for Pax2 was not quite convincing (Fig. 40 through Fig. 42), therefore the use of a confocal microscope would help to determine whether Pax2 was expressed within the metanephric mesenchyme following BIO incubation. Control samples did not present any sign of tubulogenesis (data not shown). The results demonstrated that 72 hours cultured MM cells failed to undergo induction, as none of the markers assayed were expressed (data not shown).

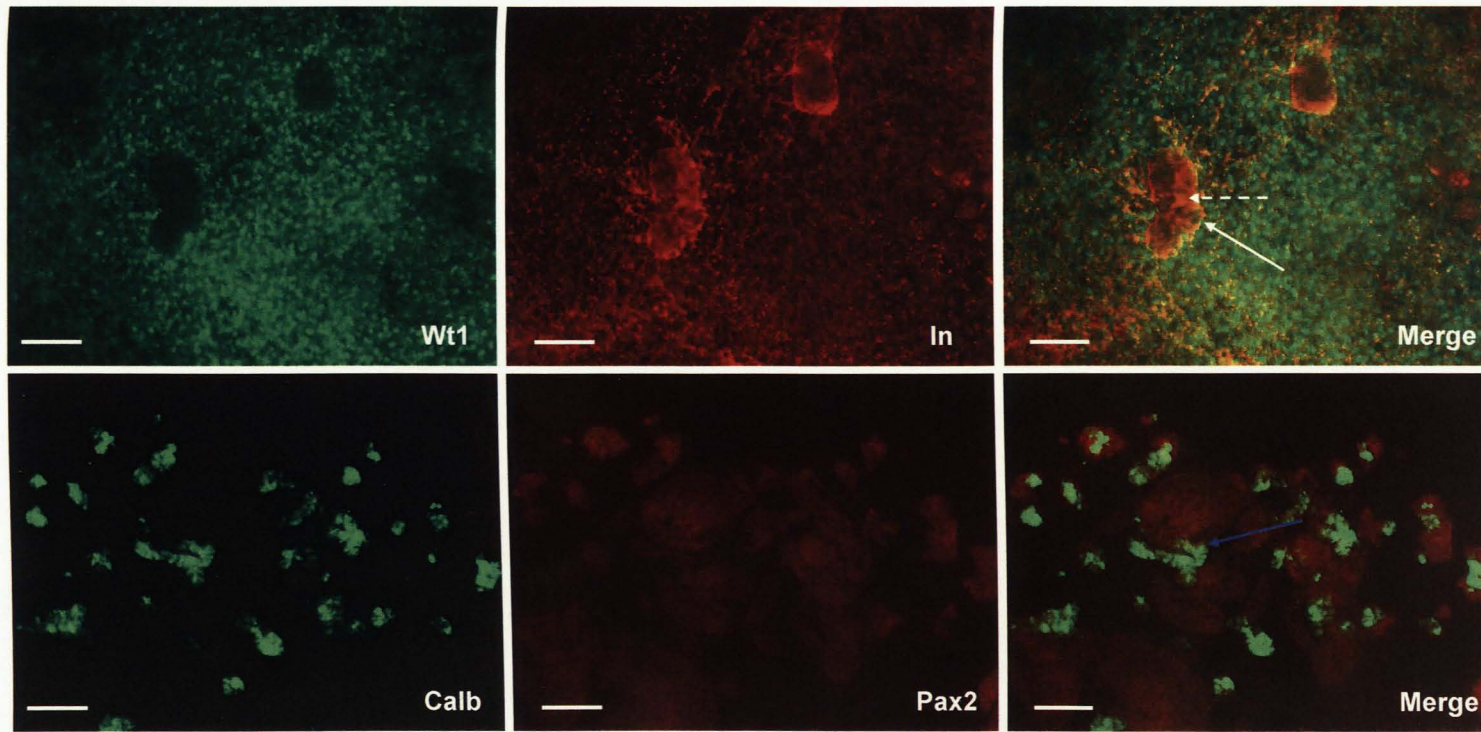


Figure 40. Induction of freshly isolated metanephric mesenchyme with 5 μ M BIO. Metanephric mesenchyme was stained for Wt1, laminin, calbindin and Pax2. The induction had taken place, as evidenced by the presence of early condensed mesenchyme (plain arrow), basement membranes (dotted arrow) and developing renal tubules (blue arrow). Scale bar: 100 μ m.

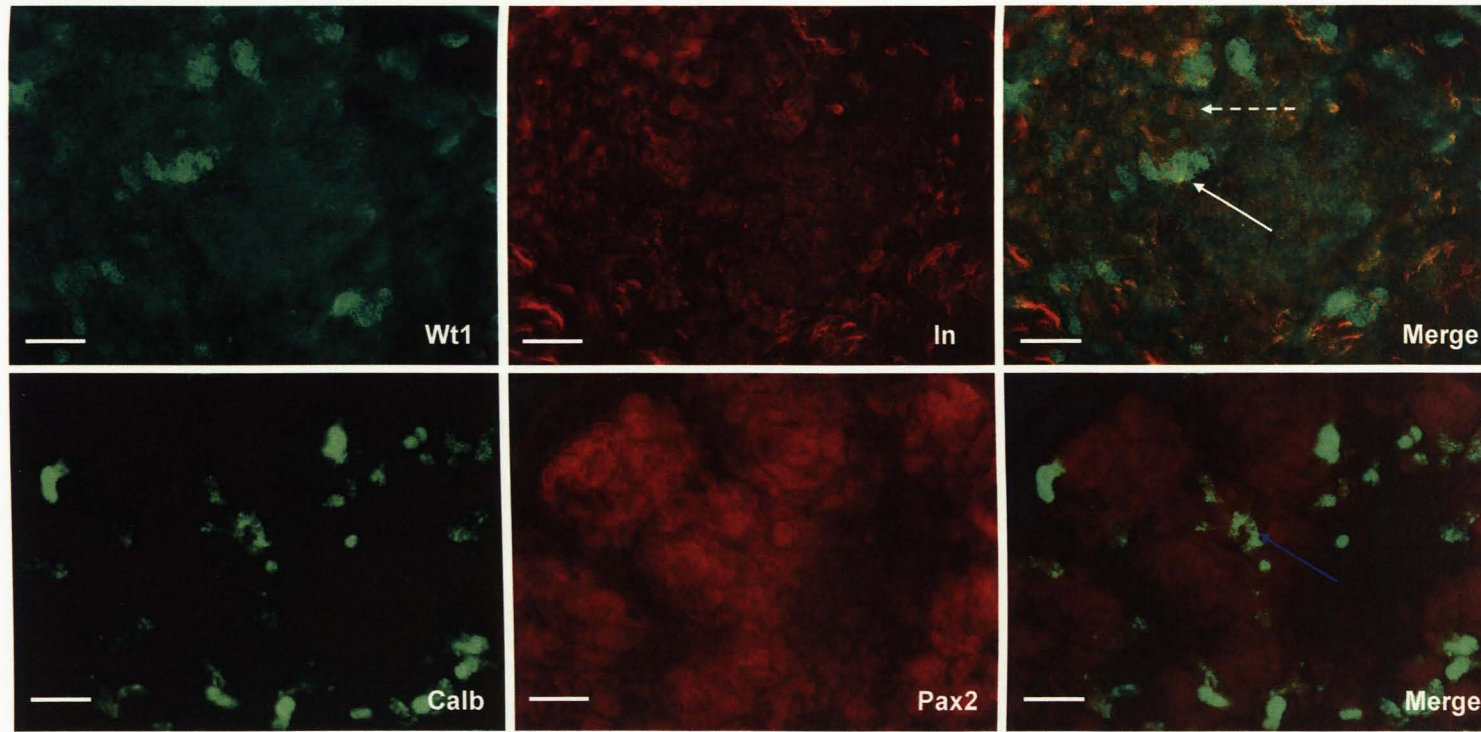


Figure 41. Induction of 24 hours cultured metanephric mesenchyme with 5 μ M BIO. Following 24 hours in culture, the MM was able to undergo induction and form primitive glomeruli (plain arrow) and basement membranes (dotted arrow), and started developing renal tubules (blue arrow). Scale bar: 100 μ m.

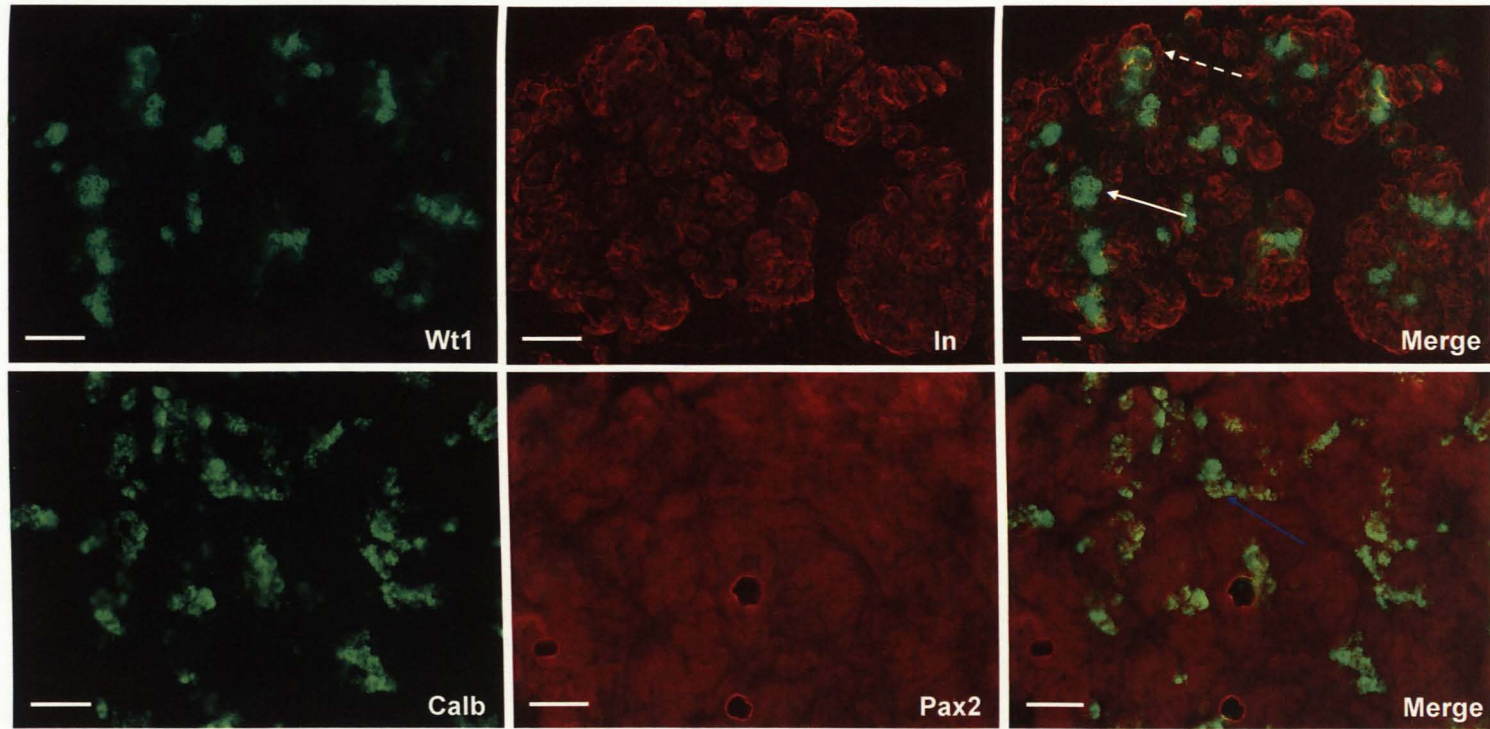


Figure 42. Induction of 48 hours cultured metanephric mesenchyme with 5 μM BIO. Following 48 hours in culture, the MM could undergo complete induction, as shown by the presence of immature glomeruli (plain arrow), basement membranes (dotted arrow), and developing renal tubules (blue arrow). Scale bar: 100 μm .

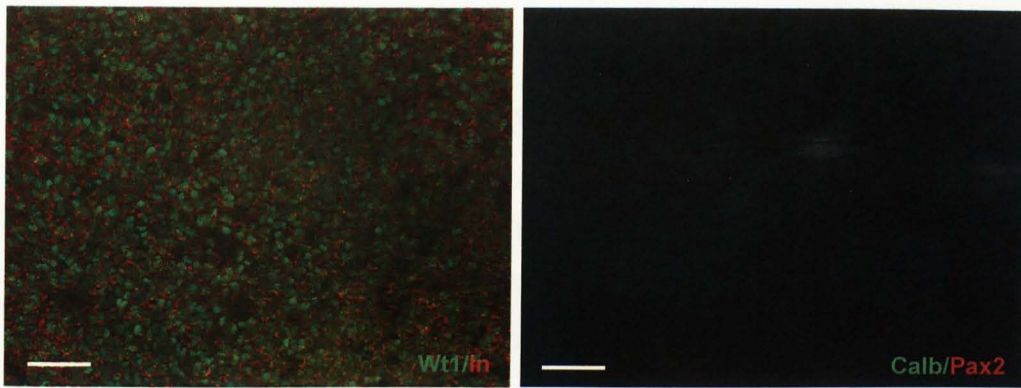


Figure 43. Freshly isolated metanephric mesenchyme cultured in the absence of BIO (Control) did not undergo induction. Scale bar: 100 μ m.

In order to investigate if MM cells could undergo tubulogenesis when cultured for more than 48 hours, it was decided to incubate 60 hours cultured MM cells with BIO. The results indicated that MM cells seemed to lose the ability to become induced when cultured longer than 2 days, as the specimens did not express any of the markers assayed (data not shown).

In summary, the results showed that MM cultured up to 48 hours in transfilter culture in MM medium supplemented with 25 ng/ml BMP7 and 100 ng/ml FGF2 was able to undergo induction and form developing nephrons and renal tubules following transient incubation with 5 μ M BIO. The induction was confirmed by the presence of developing glomeruli, expressing Wt1, and the formation of renal tubules, positive for calbindin. In addition, the samples had started depositing basement membranes around developing epithelial structures (Fig. 40 through Fig. 42). SC is capable of inducing tubulogenesis in MM cultured up to 48 hours; however, it appears to exert a weaker inductive effect than BIO, as 48 hours cultured MM stimulated with SC had started forming the distal part of the nephrons but no developing glomeruli were present (Fig. 38).

4.2.3 Investigating the *in vitro* nephrogenic potential of MM cells

In the previous section it was shown that metanephric mesenchyme cultured up to 48 hours retains the ability to undergo induction and forms nascent glomeruli and renal tubules following transient incubation with the glycogen synthase kinase-3 inhibitor BIO. Furthermore, it was observed that the proportion of distal tubules to nascent glomeruli appeared greater following induction with BIO compared to spinal cord (Fig. 40 through Fig. 42). However, the mesenchyme seemed to lose the ability to undergo induction when cultured longer than 48 hours in transfilter culture.

In the present study it was also important to elucidate whether MM cells could maintain the capability to participate in nephrogenesis following long-term *in vitro* culture. Since MM cells following 96 hours of *in vitro* culture were still able to undergo expansion and retain a MM-like phenotype when cultured on tissue culture dish (see chapter 3), in the present study it was decided to investigate the nephrogenic potential of these cells. As anticipated in section 4.1, the chimera formation assay, recently described by Unbekandt and Davies (Unbekandt and Davies, 2010), was used to investigate the *in vitro* nephrogenic potential of cultured MM cells.

The detailed procedure followed to generate and culture chimeras is explained in section 2.2.8. Briefly, following 4 days of *in vitro* culture MM cells were dissociated into a single cell suspension, labelled with 2.5 nM QTracker[®] 655 Cell Labelling Kit (quantum dots, QD) and mixed with reaggregated E11.5 kidney rudiments in a ratio of 1:3. The specimens were cultured in transfilter culture in MM medium supplemented with 25 ng/ml BMP7 and 100 ng/ml FGF2. In addition, in order to enhance the survival of the

embryonic kidney cells following the disaggregation procedure, the specimens were incubated with Rho-kinase inhibitor Y27632 for 24 hours (Unbekandt and Davies, 2010). After 3 days, the samples were stained for Wt1, Pax2 and laminin. Reaggregated kidney rudiments, without the addition of any exogenous cells, were used as control for the correct development of organotypic renal structures.

Figure 44 shows that following three days of culture E11.5 reaggregated kidney rudiments had started forming organotypic renal structures. Upregulation of Wt1 indicated that the metanephric mesenchyme had started to undergo induction and had given rise to renal vesicles (RV) and comma-shaped bodies (CB) (Fig. 44).

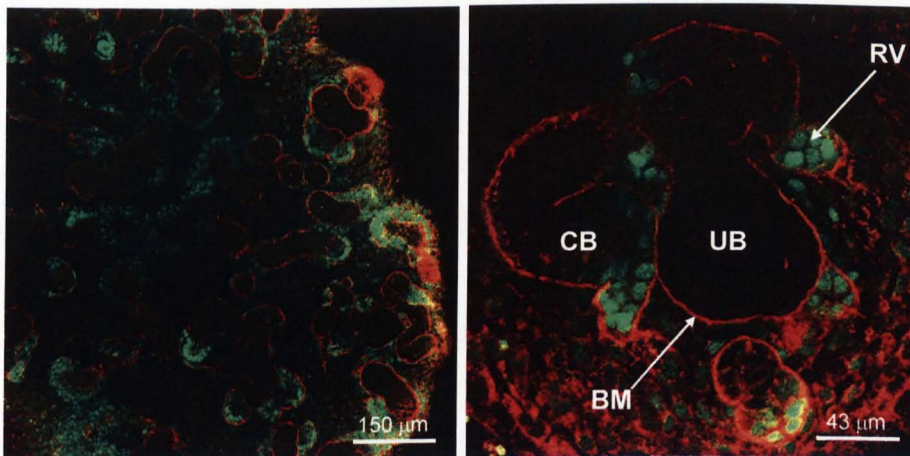


Figure 44. E11.5 reaggregated kidney rudiments could form organotypic renal structures after 3 days of culture. Immunofluorescence staining showed that the samples had started developing renal vesicles (RV) and comma-like shaped bodies (CB) positive for Wt1 (green). Laminin staining (red) showed the presence of basement membranes (BM) around the ureteric bud (UB) and developing nephrons.

The capacity of reaggregated kidney rudiments to give rise to organotypic renal structure was further confirmed by double immunostaining for Wt1 and Pax2.

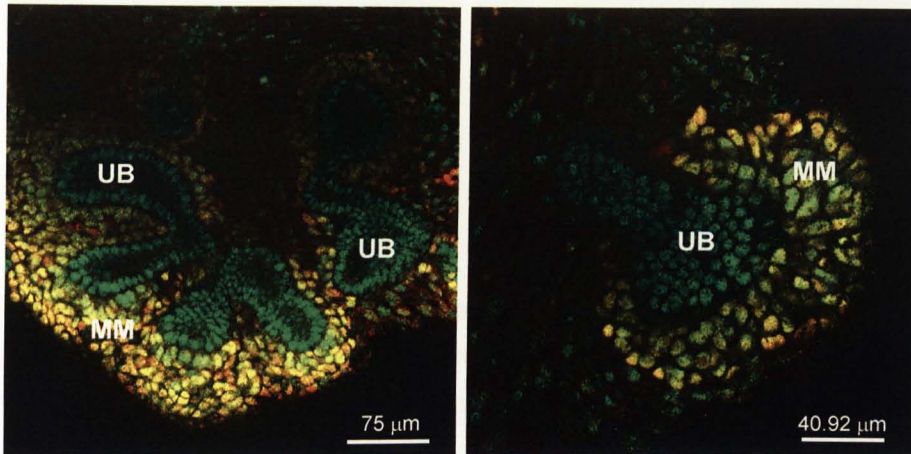


Figure 45. Immunofluorescence staining of E11.5 reaggregated kidney rudiments showed the correct spatial expression of Wt1 (red) and Pax2 (green). The expression of Wt1 could only be detected within the induced MM, whereas Pax2 was present both in the ureteric bud (UB) and the surrounding MM.

The results illustrated that the expected spatial expression of Wt1 and Pax2 took place: Wt1 was expressed within the induced MM (Fig. 45, MM), whereas Pax2 was present both in the ureteric bud (Fig. 45, UB) and the surrounding metanephric mesenchyme.

4.2.3.1 Recombination of freshly isolated MM cells with E11.5 reaggregated kidney rudiments

Freshly isolated metanephric mesenchyme cells, labeled with QD, were recombined with E11.5 reaggregated kidney rudiments (see section 2.2.8.1). The results demonstrated that, as expected, freshly isolated MM cells (Fig. 46, arrows) displayed a nephrogenic potential, as they were able to integrate into Wt1-positive nephron-like developing structures (Fig. 46, ND), but rarely into the ureteric bud (Fig. 46, UB).

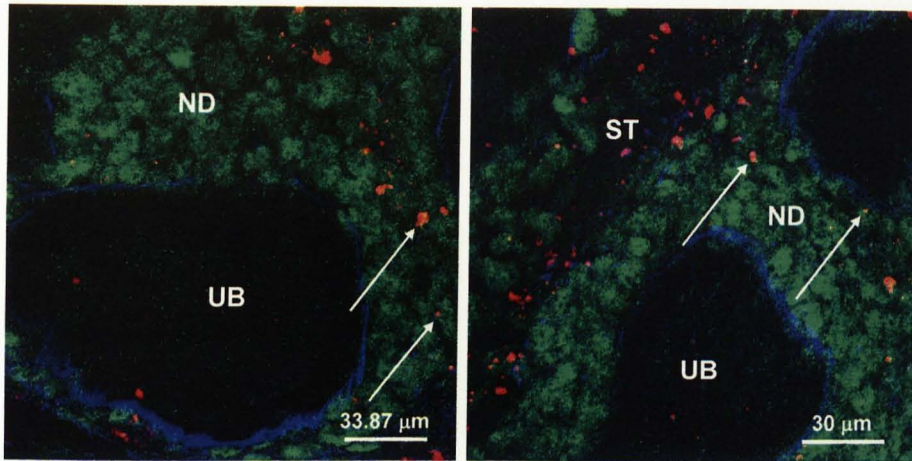


Figure 46. Immunostaining of freshly isolated MM cells labeled with quantum dots (red) and recombined with E11.5 reaggregated kidney rudiments. Freshly isolated MM cells could integrate into nephron-like developing structures (ND) expressing *Wt1* (green), but not into the ureteric bud (UB) surrounded by laminin (blue). ST: stroma.

Some QD-labelled MM cells were also found into the stromal compartment (Fig. 46, ST).

Immunostaining and RT-PCR (see section 3.2.3 and section 3.2.4, respectively) assays demonstrated that MM cells lost the expression of *Pax2* when cultured longer than 24 hours. In this work it was important to investigate whether freshly isolated MM cells could maintain the expression of *Pax2* after recombination with E11.5 reaggregated kidney rudiments. Immunostaining for *Pax2* demonstrated that following recombination with reaggregated kidney rudiments many of the freshly isolated MM cells maintained the expression of *Pax2* (Fig. 47, arrows).

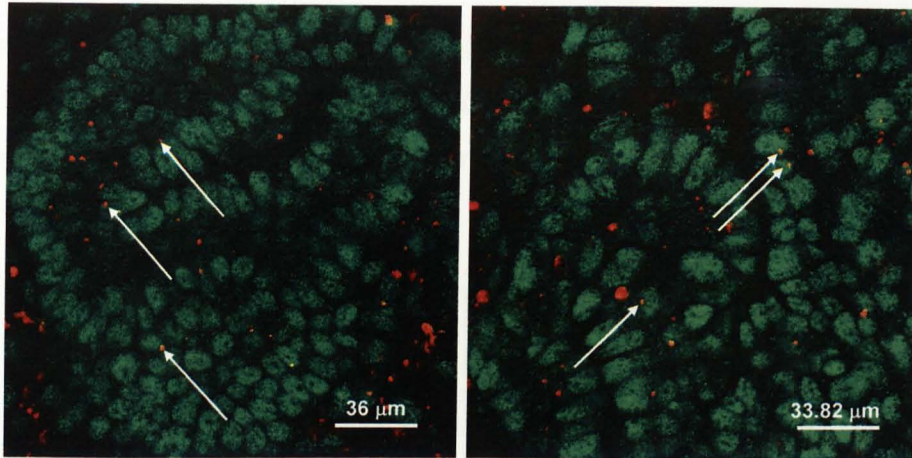


Figure 47. Immunostaining for Pax2 (green) of QD-labelled freshly isolated MM cells (red) recombined with E11.5 reaggregated kidney rudiments. Several freshly isolated MM cells (arrows) could retain the expression of Pax2 after recombination with E11.5 reaggregated kidney rudiments.

4.2.3.2 Recombination of 4 days cultured MM cells with E11.5 reaggregated kidney rudiments

It was assessed whether MM cells cultured for 4 days in MM medium supplemented with 25 ng/ml BMP7 and 100 ng/ml FGF2 could retain a nephrogenic potential and participate in the formation of nephron-like developing structures after recombination with E11.5 reaggregated kidney rudiments. The chimeras were cultured in MM medium in the presence of 5 μ M GSK-3 inhibitor (BIO) for 48 hours and the culture period was extended to 4 days (see section 2.2.8.1 for details). Since BIO is able to activate the canonical Wnt signalling pathway (Kuure et al., 2007), it was hypothesized that the presence of BIO in the culture medium could stimulate cultured MM cells to form nephron-like developing structures.

The results demonstrated that the culture conditions developed in section 3.2.1 allowed 96 hours cultured metanephric mesenchyme cells to retain a nephrogenic potential, as the cells (Fig. 48,

arrows) were still capable of integrating into nephron-like developing structures (Fig. 48, ND). In addition, similar to freshly isolated MM, cultured MM cells rarely integrated into the ureteric bud (Fig. 48, UB).

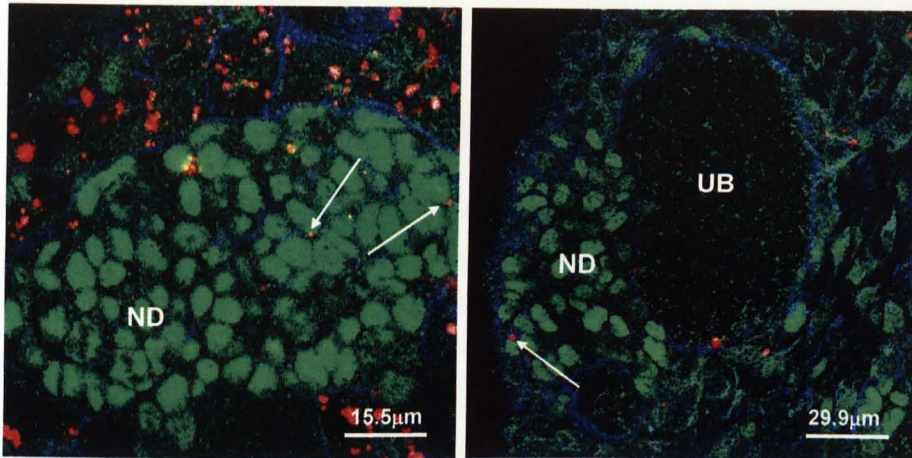


Figure 48. Immunostaining of 4 days cultured MM cells labeled with quantum dots (red) and recombined with E11.5 reaggregated kidney rudiments. Cultured MM cells (arrows) were able to integrate into nephron-like developing structures (ND), but rarely into the ureteric bud (UB). Wt1 (green) identified nephron-like developing structures, laminin surrounded the ureteric bud (blue).

In section 4.2.3.1 it was shown that freshly isolated MM cells could maintain the expression of Pax2 after recombination with reaggregated kidney rudiments. To determine if 4 days cultured MM cells were able to re-express Pax2, the rudiment reaggregation assay was performed. The results demonstrated that the chimera environment could induce the re-expression of Pax2 in cultured MM cells (Fig. 49, arrows).

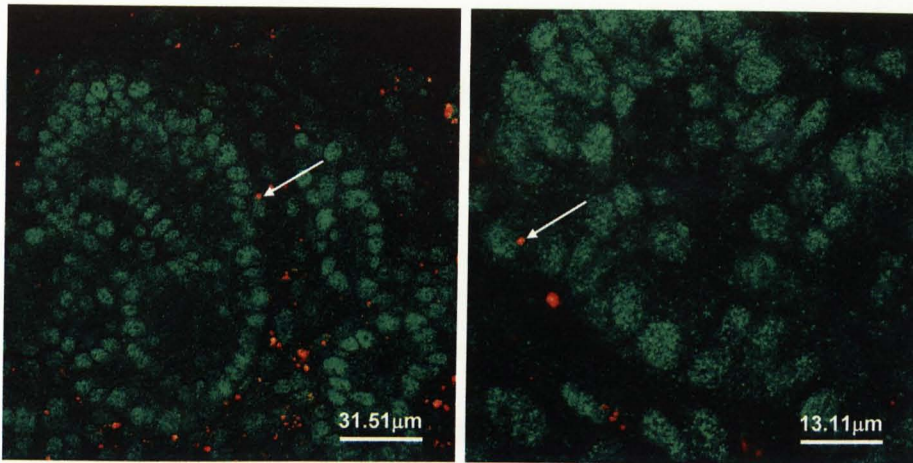


Figure 49. Immunostaining for Pax2 of cultured MM cells, labeled with quantum dots (red), recombined with E11.5 reaggregated kidney rudiments. The panel shows that some cultured MM cells (arrows) were able to re-express Pax2 (green) following recombination with reaggregated kidney rudiments.

4.2.4 Comparing the ability of freshly isolated and cultured MM cells to integrate into developing nephrons

Freshly isolated MM cells and MM cells following 4 days of *in vitro* culture were capable of integrating into nephron-like developing structures but not into the ureteric bud. To determine the percentage of freshly isolated and cultured MM cells that integrated into nephron-like developing structures, the number of cells forming 7 randomly chosen nephron-like developing structures present in one chimera and the number of quantum dots-labeled MM cells present in each structure were quantified.

The results, summarised in Table 13 and Figure 50 illustrate that the percentage of freshly isolated MM cells that integrated into nephron-like developing structures was $13.29\% \pm 0.72\%$ (mean of three independent experiments) and the percentage of cultured MM cells that integrated into developing nephrons was $12.36\% \pm 3.02\%$ (mean of three independent experiments). Student's t-test

revealed that the differences in the integration ability of these two cell populations were not statistically relevant ($P > 0.05$).

Table 13. Integration ability of MM cells. Mean and standard deviation (SD) of the percentages of freshly isolated ($n=3$) and cultured ($n=3$) MM cells, labeled with quantum dots, integrated into nephron-like developing structures.

	Freshly isolated MM cells	4-days cultured MM cells
Mean \pm SD	13.29% \pm 0.72%	12.36% \pm 3.02%

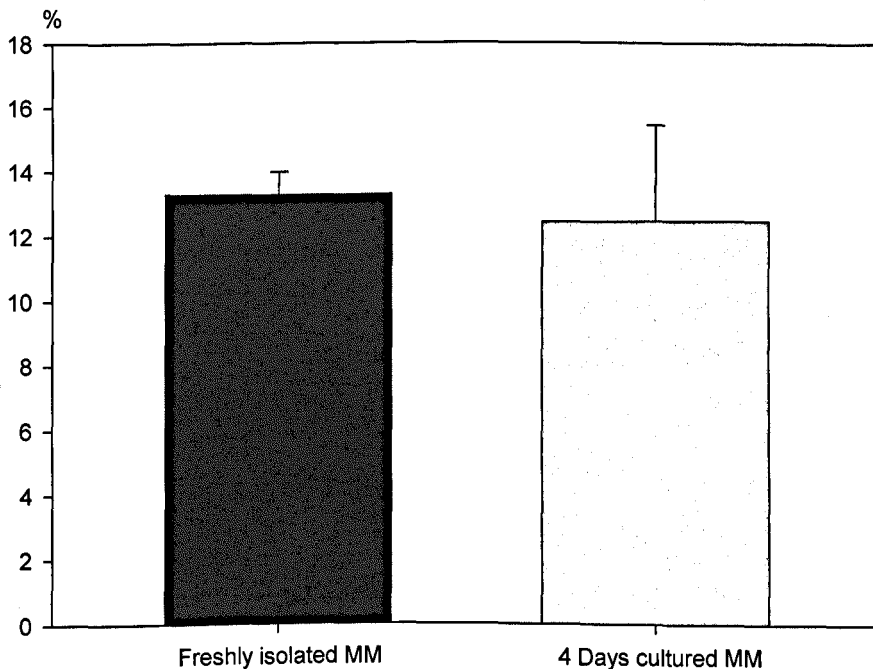


Figure 50. Percentage of freshly isolated ($n=3$) and cultured ($n=3$) MM cells, labeled with quantum dots, integrated into nephron-like developing structures. Results demonstrated that the two cell populations showed a comparable ability of integration (Student's t-test: $P > 0.05$). Error bars indicate standard deviations of the means.

In summary, the chimera formation assay demonstrated that both freshly isolated and cultured MM cells maintained a nephrogenic potential and were able to integrate into nephron-like developing structures following recombination with E11.5 reaggregated kidney

rudiments. The integrated cells expressed the MM-specific marker *Wt1* and, importantly, could maintain or re-activate the expression of *Pax2*. Moreover, freshly isolated MM and cultured MM cells could integrate into nephron-like developing structures at a comparable ratio (Student's t-test, $P > 0.05$).

4.3 Discussion

In this chapter it was shown that MM cultured up to 48 hours in MM medium supplemented with 25 ng/ml BMP7 and 100 ng/ml FGF2 in transfilter culture maintained the ability to undergo induction and form developing glomeruli and renal tubules when transiently incubated with a GSK-3 inhibitor (BIO). The embryonic spinal cord (SC) could initiate tubulogenesis in 48 hours cultured MM; however, it appeared to exert a weaker inductive effect than BIO.

The nephrogenic potential of freshly isolated and cultured MM cells was investigated using the chimera formation assay, which consisted of recombining MM cells, labeled with quantum dots, with E11.5 disaggregated kidney rudiments (Unbekandt and Davies, 2010). The reaggregated tissues developed organotypic renal structures displaying normal morphologies and the expression of characteristic renal markers. The results demonstrated that both freshly isolated and cultured MM cells retained a nephrogenic potential, as they were capable of integrating at a comparable ratio into nephron-like developing structures, but not into the ureteric bud. Importantly, following

chimera formation, exogenous MM cells located within the developing nephrons could re-express Pax2.

In this work it was hypothesized that the inability of MM cells to undergo induction when cultured for more than 2 days in transfilter culture was due to the lack of Pax2 expression, which occurred after 48 hours of culture. During mouse kidney development Pax2 might act upstream of Wnt4 (Dressler, 2002). Moreover, Pax2 activates the expression of *Wnt4* both *in vitro* and *in vivo*. It is recognised that Wnt4 plays a crucial role in metanephric mesenchyme induction by activating the canonical Wnt/ β -catenin signaling pathway (Kispert et al., 1998; Kuure et al., 2007; Park et al., 2007; Schmidt-Ott and Barasch, 2008). In this work it was decided to incubate cultured MM cells with BIO in order to mimic the presence of Wnt signaling, therefore restoring the canonical pathway and inducing tubulogenesis. The results showed that the response of the mesenchyme to BIO stimulation was only marginally better than the one following stimulation with spinal cord: following 48 hours of *in vitro* culture, MM could form developing glomeruli and renal tubules when incubated with BIO, whereas following co-culture with SC the mesenchyme failed to form developing glomeruli, although it was able to form a few structures that resembled the distal developing segments of the nephron. MM cultured longer than 2 days was not able to start tubulogenesis either following BIO incubation or co-culture with SC (data not shown). These results suggested that the presence of a Wnt4-like signal might not be sufficient to trigger tubulogenesis in MM cultured longer than 48 hours, and that other factors are likely required to induce nephrogenesis. The inability of MM cells to undergo tubulogenesis when cultured longer than 2 days may be also due to the nucleopore membrane filter, which most likely does

not represent the ideal surface to culture the mesenchyme. In fact, it was noticed that after 48 hours of culture on the membrane filter the specimens were hardly visible, which suggests that a considerable amount of cells had detached from the filter or died.

During kidney development, under normal circumstances, the proximal parts of the nephrons appear first, whereas the distal segments form later (Dorup and Maunsbach, 1982). Saxén demonstrated that MM stimulated with spinal cord for less than 24 hours gave rise to the distal parts of the nephron without forming the proximal segments, whereas a longer incubation led to the formation of both proximal and distal segments (Saxén, 1987). In this work it was found that following stimulation with spinal cord, MM cultured for 48 hours failed to form glomerular-like structures, as evidenced by the lack of Wt1 expression and the absence of basement membrane deposition. However, calbindin staining revealed that distal segments of developing nephrons had started forming. Although a previous study showed that MM cultured for 48 hours in transfilter culture in the presence of both BMP7 and FGF2 formed developing renal tubules and early glomeruli following stimulation with spinal cord (Dudley et al., 1999), in my work it was not possible to replicate these results.

The results showed that following transient incubation with BIO freshly isolated and *in vitro* cultured metanephric mesenchyme could develop more calbindin-positive renal tubules compared with MM stimulated with SC. The presence of developing distal segments of the nephrons in MM following BIO incubation is in agreement with the findings reported by Kuure and co-workers. These authors demonstrated that following transient BIO incubation the mesenchyme was able to form developing proximal

and distal tubules stained for Lotus tetragonolobus (LTA) lectin and Tamm-Horsfall glycoprotein, respectively. In addition, developing glomeruli expressing the podocyte marker podocin were found (Kuure et al., 2007). As discussed in section 4.2, due to poor quality images, further immunostaining analysis performed with a confocal microscope might be required in order to ascertain whether Pax2 became expressed within the MM following SC or BIO stimulation.

Beside being a marker for distal convolute tubules (Georgas et al., 2008), calbindin is also a marker for ureteric bud epithelial cells (Unbekandt and Davies, 2010). Although meticulous care was always taken to separate the MM from the UB, and although the non-stimulated samples never expressed calbindin, thus indicating that a good isolation procedure was carried out, it cannot be completely ruled out that the calbindin-positive staining present within the induced MM might be due to the presence of ureteric bud-derived structures. However, another explanation might be taken into account. When the metanephric mesenchyme is stimulated by the spinal cord to undergo tubulogenesis in transfilter culture, it appears to contribute for up to 3% to the formation of the developing renal collecting system (Qiao et al., 1995). Nevertheless, the possibility that the calbindin-positive structures I observed within the induced MM were of ureteric bud origin might be excluded, as a more recent *in vivo* cell-fate analysis documented the absence of MM cell recruitment for the formation of the ureteric epithelium (Kobayashi et al., 2008).

As explained in section 4.1, the proximal and distal fate of the nephrons is regulated by the Notch signalling pathway (Cheng et al., 2007). It has also been demonstrated that Notch signaling

requires direct cell-cell contact (Jeffries and Capobianco, 2000). On the basis of the results presented in my work, I speculate that following BIO stimulation the absence of direct cell-cell contact between the mesenchyme and its inducer led to a downregulation of Notch signaling which promoted the formation of more distal renal tubules and partially inhibited the development of glomeruli and proximal segments of the nephron. This speculation might be tested by determining the level of the activated form of Notch2 receptor in freshly isolated MM by western blotting, using an antibody specific for the intracellular form of this receptor. The expression level will then be compared with the levels of intracellular Notch2 receptor in BIO-incubated and SC-stimulated MM.

The chimera formation assay revealed that MM cells cultured for 4 days retained a nephrogenic potential and could integrate into developing nephrons at a comparable ratio with freshly isolated MM. Freshly isolated and cultured MM cells were rarely found into the ureteric bud. This evidence is consistent with the fact that during development the metanephric mesenchyme gives rise to all cell types present in the adult nephron, but none of the ureteric bud-derived structures (Kobayashi et al., 2008). Importantly, following recombination with E11.5 reagggregated kidney rudiments both freshly isolated and cultured MM cells were able to express Pax2 for several days, whereas the expression of this transcription factor was lost in MM cells cultured for more than 24 hours, as illustrated in section 3.2.3 and section 3.2.4. These findings suggest that ureteric bud-derived factors might be required to induce the expression of Pax2 in the mesenchyme.

It might be worth taking into account that the results presented in this section might be influenced by events of cell-cell fusion that occurred between MM cells and kidney rudiment cells. Cell-cell fusion is a process which occurs normally in vertebrate. For instance, fusion between the sperm and egg marks the very first event in mammalian development. Besides, cell-cell fusion between myoblasts generates multinucleated skeletal myofibers. The mechanism of cell-cell fusion is also involved in patophysiological conditions, such as the formation of granulomatous tissue in response to inflammation (Wagers and Weissman, 2004). Several works have documented the occurrence of cell-cell fusion *in vitro* involving stem/progenitor cells. Bone marrow-derived cells and progenitor cells of the central nervous system can spontaneously fuse *in vitro* with embryonic stem cells (Terada et al., 2002; Ying et al., 2002). Using a Cre/loxP transgenic strategy, Alvarez-Dolado and colleagues demonstrated that these two cell populations fuse spontaneously *in vitro*. Additionally, following bone marrow transplantation, these authors documented that bone marrow-derived cells were able to fuse *in vivo* with hepatocytes, Purkinje neurons in the brain, and cardiomyocytes (Alvarez-Dolado et al., 2003). More recently, it was demonstrated that mouse or rat neural stem cells (NSC), cultured in monolayer or as neurospheres, can undergo spontaneous fusion at a frequency of approximately 0.2%. However, it was also documented that fused cells were not able to divide, could not be propagated in culture and died soon after the fusion event (Jessberger et al., 2007). If cell-cell fusion arose between MM cells and kidney rudiment cells within the chimera, I would expect that some cells of the former cell population ended up labelled with QD due to the fusion of their cytoplasm with that of MM cells. Although I cannot rule out the occurrence of cell-cell

fusion within the chimera, even among a very small number of cells, in this Thesis there are no data that could support or oppose the existence of cell-cell fusion events.

The chimera formation assay also showed that several freshly isolated and cultured MM cells remained in the stroma. The stroma of the developing kidney neither contains ureteric bud structures, nor gives rise to developing nephrons. However, an increasing amount of evidence suggests that the stroma may play an important role during nephrogenesis. For instance, in the developing mouse kidney, *Foxd1* positive stromal cells appear in the nephrogenic zone as the ureteric bud invades the metanephric mesenchyme (Cullen-McEwen et al., 2005). Hatini and colleagues demonstrated that *Foxd1* null embryos exhibit ectopic mesenchymal condensates, reduced ureteric bud branching and inhibited mesenchymal-to-epithelial (MET) transition (Hatini et al., 1996). These findings suggest that stromal cells expressing *Foxd1* are essential for MET and appropriate kidney development.

Using a transgenic strategy to fate map *Wnt4*-expressing cells in the developing mouse metanephros, Shan and colleagues demonstrated that the first presumptive nephrons of the developing kidney appeared to be only vestigial as they degenerated shortly after formation; the tissue derived from these vestigial nephrons accumulated within the stromal compartment (Shan et al., 2010). It might be hypothesized that quantum dots-labeled MM cells present in the stromal domain of the chimera may be a remnant of the early developing nephrons that underwent degeneration and accumulated within the stroma. These cells may still play a role in the correct development of renal structures. However, it is also possible that some QD-labelled MM cells present within the stroma did not participate in the formation

of developing nephrons because, during the formation of the chimera, they were not close enough to the developing ureteric bud to become induced and undergo nephrogenesis.

CHAPTER 5

Characterization of the kidney-derived stem cell H6 clonal line

5.1 Introduction

Recent studies from several groups have suggested the presence of stem/progenitor cells in adult kidney. As already explained in section 1.3.2.1, these cells have been found in different *niches* of the rodent kidney, such as the interstitium of the papilla (Oliver et al., 2004; Dekel et al., 2006; Oliver et al., 2009), the interstitium of both medulla and papilla (Lee et al., 2010) and in proximal tubules (Challen et al., 2006; Gupta et al., 2006). In addition, renal stem/progenitor cells have been isolated from the renal cortex (Bussolati et al., 2005) and the Bowman's capsule (Sagrinati et al., 2006; Ronconi et al., 2009) of adult human kidney (see section 1.3.2.2).

Despite these and other studies (see section 1.3.2), the ability of a single kidney stem/progenitor cell population to generate all cell types present in the mature nephron still remains to be seen.

The length of nephrogenesis varies among different mammalian species. While in human and sheep nephron formation is completed during intrauterine life, in rodents such as in mouse and rat, nephrogenesis continues until postnatal day (P) 7 and P10, respectively (Dickinson et al., 2005). It has also been demonstrated that at birth each mouse kidney contains approximately 70% of the 11000 glomeruli present in the adult kidney (Cebrian et al., 2004). These studies strongly suggest that the postnatal mouse kidney may contain a considerable number of stem/progenitor cells that under normal circumstances are

committed to give rise to the complete endowment of nephrons present in the adult organ. Some of these cells may remain in an undifferentiated state as the animal ages, thus giving rise to adult stem/progenitor cell populations that can be found in the mature kidney. It is conceivable that if such progenitor cells exist, they may be isolated from postnatal mouse kidney in greater numbers than from the adult organ. This makes the postnatal mouse kidney an attractive organ where stem/progenitor cell populations may be found.

One of the main aims of this work was to compare the expression profile and the nephrogenic potential of *in vitro* expanded metanephric mesenchyme cells with that of a clonal line of kidney-derived stem cells (KSC). As already stated in section 1.3.2.1, KSC were isolated from postnatal mouse kidney by Dr Cristina Fuente Mora (University of Liverpool). One of the crucial properties of stem cells is clonogenicity, which represents the ability of a single cell to form a colony of identical cells that then gives rise to a range of differentiated phenotypes of the tissue in which it resides. It was demonstrated that a clonal line derived from the KSC population, named clone H6 and expressing the renal marker *Wt1*, displayed features of stem cells, as it showed limitless proliferative capacity and could spontaneously generate renal-like cell types in culture (Fuente Mora, 2009).

In this work it was hypothesized that the H6 clonal line might represent a MM-like stem cell population resident in the postnatal mouse kidney. In order to investigate this assumption, the expression of key metanephric mesenchyme-specific genes was explored in H6 cells and their expression profile compared with those of freshly isolated MM and MM cells following *in vitro*

culture. The presence of surface markers for stem cells was investigated in the H6 cell population by flow cytometry. In addition, it was important to explore whether H6 cells were able to generate renal cells in culture, such as podocytes and proximal tubule cells. Podocytes (or glomerular visceral epithelial cells) are highly specialized, quiescent cells present in the Bowman's capsule of the glomerulus with the task of filtering the blood. Podocytes are polarized, often binucleated cells characterized by a voluminous cell body, an arborized morphology and foot processes that form a size barrier and charge barrier to proteins, secrete VEGF and maintain the glomerular loop shape (Shankland, 2006; Shankland et al., 2007). Since mature podocytes are post-mitotic cells, these cells can only be propagated in culture by generating immortalized cell lines which have showed high proliferative capacity when cultured under permissive conditions (Mundel et al., 1997). Podocytes are of critical importance in the development of kidney diseases: it is known that podocyte depletion secondary to infection, genetic, immune and toxic mechanisms can result in glomerulonephritis, which can lead to end-stage renal disease (ESRD), a condition in which kidneys are no longer functional and dialysis or transplantation are required (Ronconi et al., 2009; Murray et al., 2010). Kidney proximal tubules are of great importance for the normal homeostasis of the body, as they mediate the reabsorption of water and many solutes present in the glomerular ultrafiltrate (Christensen and Gburek, 2004, Kobayashi et al., 2005); besides, proximal tubules play a pivotal role in the secretion of a wide spectrum of molecules, including drugs, pollutants and potentially toxic metabolites from the circulation into the lumen of proximal tubules (Masereeuw et al., 1999). Many conditions, such as ischemic injury, sepsis and hypovolemic states due to

haemorrhage, blood volume depletion and burns, can lead to acute renal tubular failure (ARF), a condition characterized by renal tubular damage and an abrupt decline in renal function (Mr. Simon Kenny, personal communication; Perin et al., 2010). Although data available are still controversial, in some circumstances ARF might lead to chronic kidney disease and renal failure (Schiffl, 2010).

To explore whether the H6 clonal line generated podocyte-like and proximal tubule-like cells in culture, RT-PCR analysis for podocyte and proximal tubule markers and immunofluorescence staining for Wt1, synaptopodin and megalin were carried out. As previously explained, Wt1 expression is present in the MM; in adult kidney, the expression of Wt1 is restricted to podocytes (Donovan et al 1999; Dressler, 2006). Synaptopodin is an actin-associated protein which represents a key marker for podocytes, as *in vivo* it is expressed in post-mitotic, terminally differentiated podocytes (Shankland et al., 2007). Megalin is a marker for kidney proximal tubule cells. During kidney development the expression of megalin is detected in the mesonephros, renal vesicles and ureteric bud, and later in the S-shaped body. In adult kidney, the expression of megalin is restricted to the apical surface of proximal tubules and in part is found within the glomerulus (Christensen and Birn, 2001). Since a previous study has shown that the H6 clonal line neither expressed distal tubule nor collecting duct genes (Fuente Mora, 2009), in this study the ability of H6 cells to generate these renal cell types was not explored. Furthermore, to determine if the H6 clonal line was similar to other kidney-derived stem cell populations and displayed multipotency, the ability of H6 cells to differentiate into non-renal cell types, such as osteocytes, adipocytes and endothelial cells was investigated. Finally, the

growth rate of the H6 cell population was determined and compared with that of MM cells.

5.2 Results

5.2.1 Ability of H6 cells to form renal-like cell types in vitro

5.2.1.1 Morphology of the H6 clonal line

The H6 clonal line was cultured in KSC medium on plastic tissue culture dishes and subcultured as explained in section 2.2.1.

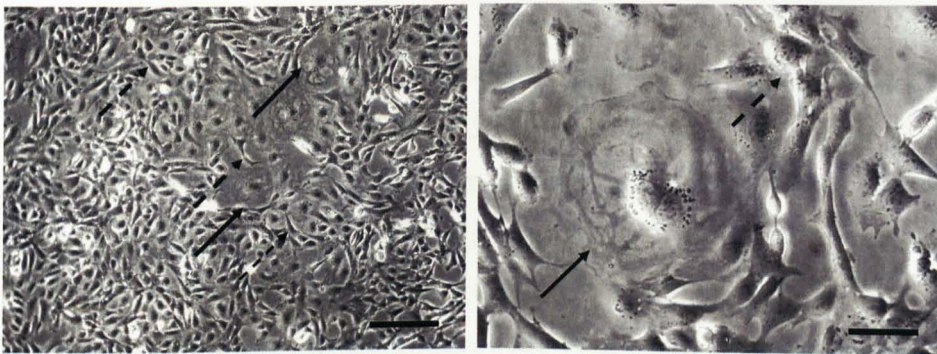


Figure 51. Phase contrast micrographs of H6 cells. The H6 clonal line could spontaneously form mesenchymal-like cells (dotted arrows), podocyte-like cells (arrows) and epithelial-like cells (data not shown) when cultured in KSC medium on plastic tissue culture dishes. Scale bar: 200 μm (left); 50 μm (right).

The H6 clonal line was able to spontaneously form three distinct cell types: podocyte-like cells (Fig. 51, arrows) mesenchymal-like cells (Fig. 51, dotted arrows) and epithelial-like cells (Fuente Mora, 2009 and data not shown). Mesenchymal-like cells represented the most abundant cell types: these cells were randomly oriented and displayed a spindle-shape morphology. Epithelial-like cells displayed a cobblestone-like morphology and were organized in small, sparse clusters. Podocyte-like cells constituted the most

interesting cell type. These cells were characterized by an arborized morphology and a large cytoplasmic-to-nuclear volume ratio. In addition, podocyte like cells were often binucleated (Fig 51, arrows). It was observed that the H6 clonal line could maintain the ability to originate podocyte-like cells, mesenchymal-like cells and epithelial-like cells after repeated subcultivation and several freezing/thawing cycles (data not shown).

5.2.1.2 Renal cell-specific gene expression in the H6 clonal line

In this work it was hypothesized that the H6 clonal line could represent a MM-like cell population present in the postnatal mouse kidney. In order to investigate this assumption the renal cell-specific gene expression profile of the H6 cells was compared with those of freshly isolated MM and MM cells following 4 days of *in vitro* culture by RT-PCR. The markers included in this analysis were as follow: *Wt1*, *Pax2*, *Osr1*, *Sall1*, *Lim1*, *Gdnf*, *Ret*, *Hoxb7* and *Vim* (see section 3.2.4 for details). In addition, since the H6 clonal line appeared to spontaneously generate renal-like cells in culture, the expression of markers normally expressed by differentiated cells of the adult kidney was also investigated. The list of markers analysed is shown in Table 14. The genes *nephrin* (*Nphs1*), *podocin* (*Nphs2*) and *synaptopodin* (*Synpo*) were selected as they are markers for podocytes (Shankland et al., 2007). The markers *aquaporin1* (*Aqp1*) and *megalyn* (*Lrp2*) were selected as they identify proximal tubule cells (Gburek et al., 2003; Georgas et al., 2008). In addition, it was decided to check for the expression of *vascular endothelial growth factor A* (*Vegfa*) and *desmin* (*Des*). In the kidney *Vegfa* is normally expressed in glomerular podocytes, distal tubules and collecting ducts (Liu et al., 2007), whereas the mesangial marker *Des* is present in the extraglomerular and glomerular mesangium (Georgas et al.,

2008). The sequence of β -actin was amplified in order to verify that the PCR reaction worked appropriately. Freshly isolated MM was used as positive control for the expression of *Wt1*, *Pax2*, *Osr1*, *Sall1*, *Vim*, *Gdnf*, *Bax* and *Bcl2*. Postnatal or adult kidneys were used as positive controls for the expression of the remaining genes assayed (data not shown).

Table 14. List of markers selected for the RT-PCR analysis.

<u>Gene</u>	<u>Structure</u>
<i>Wt1, Sall1, Osr1, Gdnf</i>	Metanephric mesenchyme
<i>Ret, Hoxb7</i>	Ureteric bud
<i>Pax2</i>	Metanephric mesenchyme, Ureteric bud tips
<i>Lhx1</i>	Nephric duct, Ureteric bud, MM- derived structures.
<i>Vim</i>	Mesenchymal cells
<i>cytokeratin 8, tight junction protein 1</i>	Epithelial cells
<i>vascular endothelial growth factor A</i>	Endothelial cells
<i>nephrin, podocin, podocalyxin- like</i>	Podocyte
<i>synaptopodin</i>	Fully differentiated podocyte
<i>desmin</i>	Mesangial cells
<i>Aquaporin 1, megalin</i>	Proximal tubules
<i>Musashi1, Musashi2</i>	Stem/Progenitor cells
<i>Bax, Bcl2</i>	Apoptosis
<i>p16INK^{4a}</i>	Senescence

The results showed that the H6 clonal line expressed several markers found in freshly isolated and cultured MM cells, such as the MM-specific markers *Wt1*, *Ors1*, *Vim* and *Gdnf*, the progenitor cell markers *Msi1* and *Msi2*, the epithelial markers *Tjp1* and *Hoxb7*, and the pro- and anti- apoptotic markers *Bax* and *Bcl2*. Like cultured MM cells, the H6 cells did not express either *Pax2* or *p16^{INK4a}* (Fig. 52).

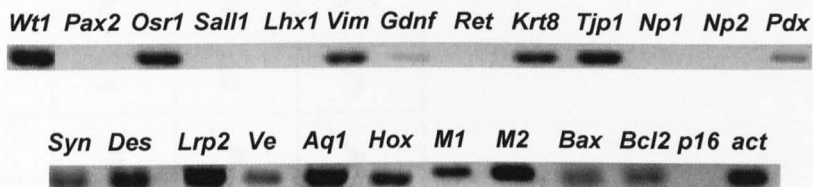


Figure 52. Gene expression profile of the H6 clonal line cultured in KSC medium. *Np1*: *nephrin*; *Np2*: *podocin*; *Pdx*: *podocalyxin-like*; *Syn*: *synaptopodin*; *Ve*: *vascular endothelial growth factor A*; *Aq1*: *Aquaporin1*; *Hox*; *Hoxb7*; *M1*: *Musashi1*; *M2*: *Musashi2*; *p16*: *p16^{INK4a}*; *act*: β -act. β -actin: reference gene. For *Bax*, *Bcl2*, and *p16*: $n=2$; for the remaining genes: $n \geq 3$.

Additionally, the H6 clonal line expressed several markers for podocytes, such as *Podxl* and *Synpo*; however, the expression of *Nphs1* and *Nphs2* was not found. The gene expression profile also showed that the H6 cells were positive for *Des*, which is expressed in the extraglomerular and glomerular mesangium, and for the proximal tubular cell markers *megalyn* and *Aqp1* (Fig. 52).

The genes expressed in freshly isolated MM, in MM cells following 4 days of *in vitro* culture and those expressed in H6 cells are listed in Table 15.

Table 15. Genes expressed in freshly isolated metanephric mesenchyme (MM), MM cells following 4 days of *in vitro* culture (4d MM) and in the H6 clonal line. The symbol ✓ indicates that the gene is expressed, whereas the symbol ✗ indicates that the gene is not expressed. NT: not tested. *Hox*: *Hoxb7*; *p16*: *p16^{INK4a}*; *M1*: *Musashi1*; *M2*: *Musashi2*; *Np1*: *nephrin*; *Np2*: *podocin*; *Pdx*: *Podocalyxin-like*; *Syn*: *synaptopodin*; *Ve*: *Vegfa*. β -actin was always expressed.

	<i>Wt1</i>	<i>Pax2</i>	<i>Osr1</i>	<i>Sall1</i>	<i>Lhx1</i>	<i>Vim</i>	<i>Gfnf</i>	<i>Ret</i>	<i>Hox</i>	<i>Tjp1</i>	<i>Bax</i>	<i>Bcl2</i>	<i>p16</i>	<i>M1</i>	<i>M2</i>	<i>Krt8</i>	<i>Np1</i>	<i>Np2</i>	<i>Pdx</i>	<i>Syn</i>	<i>Des</i>	<i>Ve</i>	<i>Lrp2</i>	<i>Aqp1</i>
MM	✓	✓	✓	✓	✗	✓	✓	✓	✓	✓	✓	✓	✗	✓	✓	NT	NT	NT	NT	NT	NT	NT	NT	NT
4d MM	✓	✗	✓	✓	✗	✓	✓	✓	✓	✓	✓	✓	✗	✓	✓	NT	NT	NT	NT	NT	NT	NT	NT	NT
H6	✓	✗	✓	✗	✗	✓	✓	✗	✓	✓	✓	✓	✗	✓	✓	✓	✗	✗	✓	✓	✓	✓	✓	✓

5.2.1.3 Cytofluorimetric analysis of the H6 clonal line

The gene expression profile (see section 5.2.1.2) revealed that the H6 clonal line expressed a wide spectrum of markers characteristic of different cell types, such as progenitor cell markers, MM-specific markers, epithelial markers and markers of fully differentiated cells. Flow cytometry was used to investigate the expression of the stem cell markers CD24, CD90, CD117 and Sca-1 (Bussolati et al., 2005; Dekel et al., 2006; Sagrinati et al., 2006). Furthermore, the H6 clonal line was also screened for the expression of the mesenchymal stem cell markers CD29, CD44 and CD73, also found in adult kidney renal progenitor cells (Bussolati et al., 2005; Sagrinati et al., 2006) and the hemopoietic stem cell markers CD34 and CD45 (Bussolati et al., 2005).

The results revealed that the vast majority of H6 cells expressed CD29 and CD44, markers for mesenchymal stem cells and renal progenitor cells, and the hemopoietic gene CD34 (Fig. 53). In addition, it was observed that approximately 30% of the H6 cell population comprised cells expressing the stem cell markers Sca-1 and CD24, and the renal progenitor cell marker CD73, also known as SH3 (Bussolati et al., 2005). Moreover, 19% of the H6 cells presented the surface marker CD45 and approximately 10% were positive for the stem cell marker CD117, also known as c-kit (Bussolati et al., 2005) (Fig. 53). The flow cytometry analysis revealed that the H6 clonal line did not express the stem cell marker CD90 (data not shown).

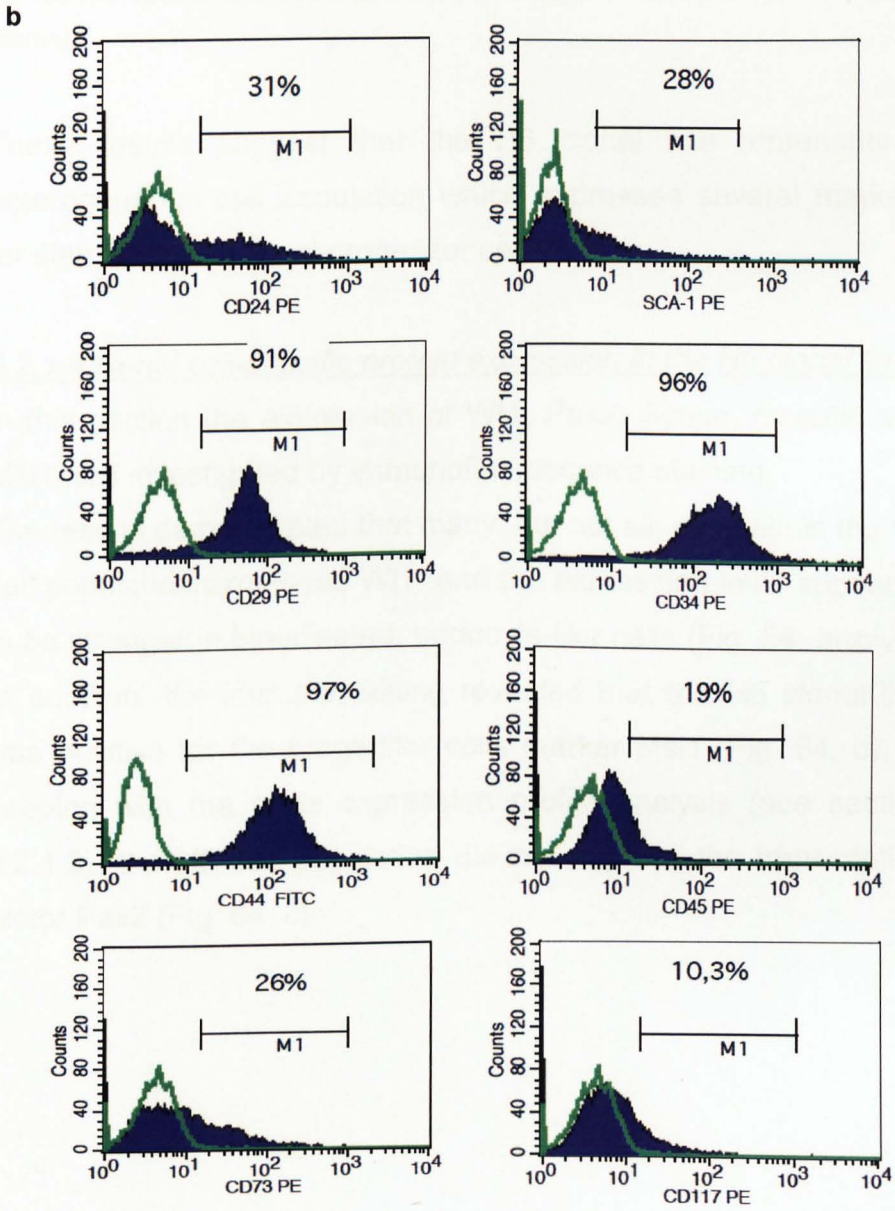
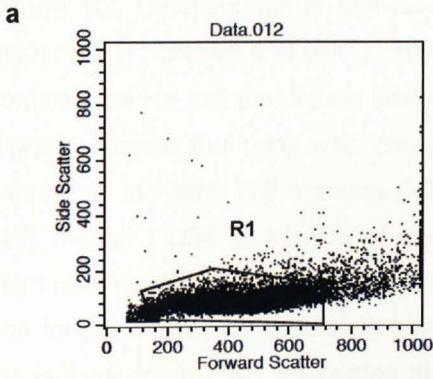


Figure 53. Cytofluorimetric analysis of the H6 clonal line cultured in KSC medium. (a) Forward and side scatters of the H6 cell population. The gate R1 contains the H6 cell population analysed for the presence of surface antigens. Signals outside the gate was considered cell debris. (b) Most of H6 cells expressed the stem cell markers CD29 and CD44, and the hemopoietic stem cells marker CD34. A fraction of the H6 clonal line was also positive for the stem cells markers Sca-1 and CD24, the mesenchymal stem cell marker CD73, and for the marker for circulating hemopoietic cells CD45. Green lines indicate the isotype control. M1 delineates the percentage of cells positive for a given marker.

These results suggest that the H6 clonal line represents a heterogeneous cell population which expresses several markers for stem cells and renal progenitor cells.

5.2.1.4 Renal cell-specific protein expression in the H6 clonal line

In this section the expression of Wt1, Pax2, Synpo, megalin and Msi1 was investigated by immunofluorescence staining.

The results demonstrated that many, but not all, cells within the H6 cell population expressed Wt1, and the expression level appeared to be stronger in binucleated, podocyte-like cells (Fig. 54, arrows). In addition, the immunostaining revealed that the H6 clonal line was positive for the progenitor cells marker Msi1 (Fig. 54, b). In keeping with the gene expression profile analysis (see section 5.2.1.2), the H6 cell population did not express the transcription factor Pax2 (Fig. 54, c).

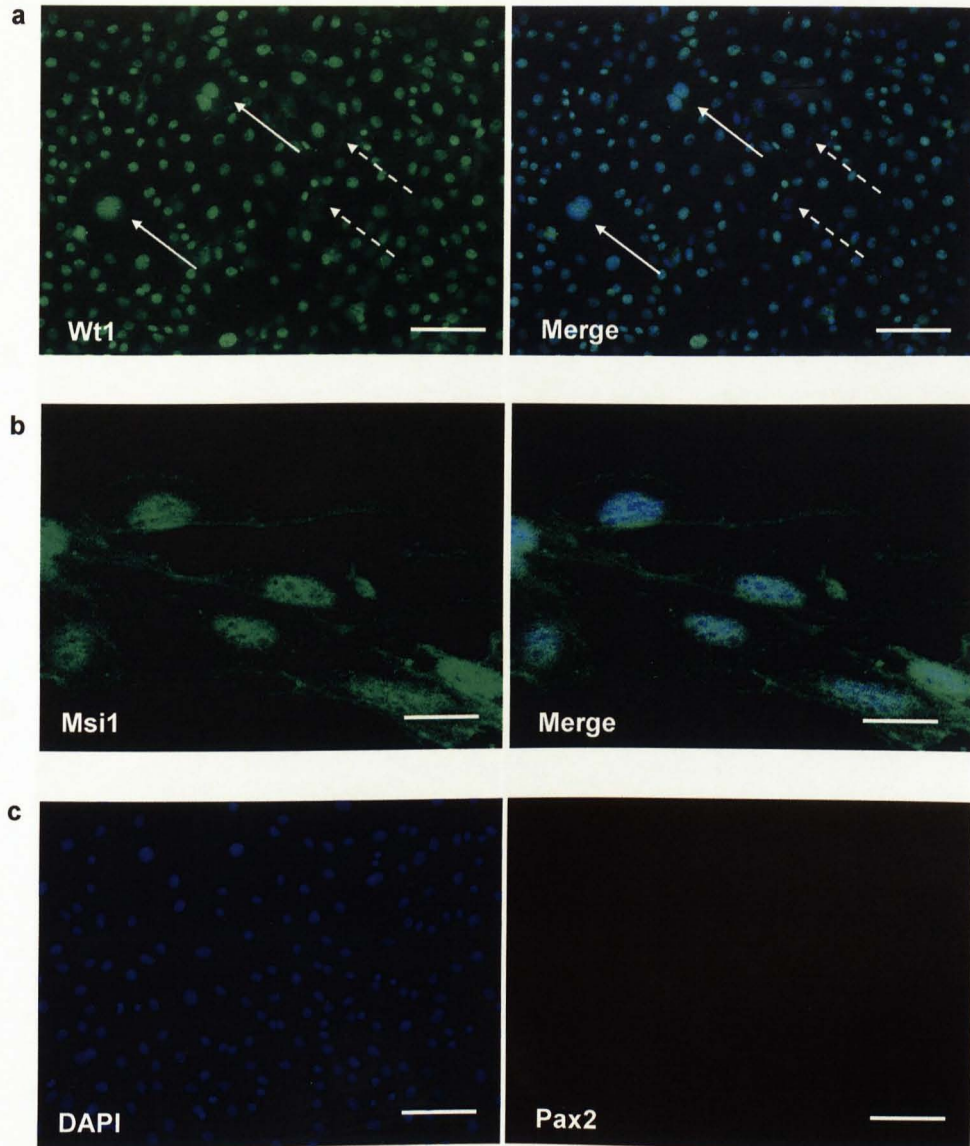


Figure 54. Immunostaining for (a) Wt1 (green), (b) Msi1 (green) and (c) Pax2 (red). Many H6 cells were positive for Wt1 and Msi1, whereas the expression of Pax2 was not detected. Nuclei were stained with DAPI (blue). Micrographs of Msi1 staining were taken with a confocal microscope. Arrows indicate podocyte-like cells. Dotted arrows indicate Wt1-negative cells. Scale bar: 100 μm (a, c); 25 μm (b).

The expression of megalin was found in a subset of H6 cells (Fig. 55, a). In addition, the results showed that only podocyte-like cells expressed synaptopodin. The staining was mainly localized in the cell membrane and within the cytoplasm around the nucleus (Fig. 55, b arrows).

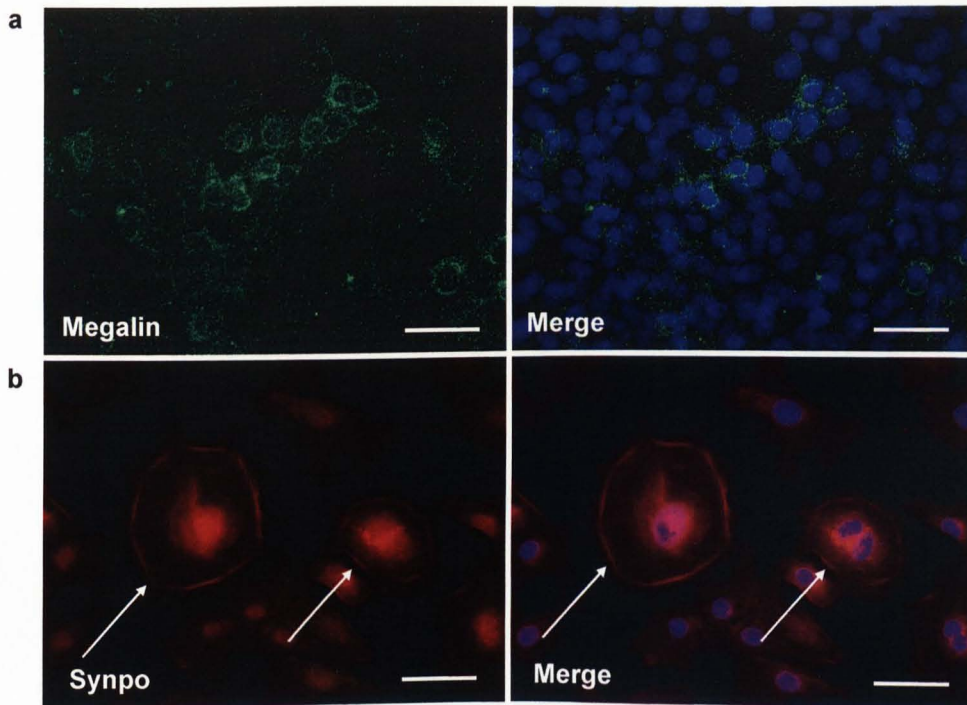


Figure 55. Immunostaining for megalin and synaptopodin. (a) A fraction of H6 cells expressed megalin (green). (b) Synaptopodin (red) was present in podocyte-like cells only (arrows). Nuclei were stained with DAPI (blue). Scale bar: 100 μm (a), 50 μm (b).

5.2.2 Evaluating the ability of H6 cells to differentiate into non-renal cell types

Other stem cell types derived from adult human kidney have been shown to have similar properties to mesenchymal stem cells, such as the ability to undergo differentiation toward osteogenic, adipogenic and endothelial lineages (Bussolati et al., 2005; Sagrinati et al., 2006). To see if the H6 clonal line displayed

mesenchymal stem cell-like properties, the capacity of the H6 cells to differentiate into osteocytes, adipocytes and endothelial cells was assayed.

5.2.2.1 Ability of H6 cells to differentiate into osteocytes and adipocytes

The results showed that after 3 weeks of culture in osteogenic differentiation medium the H6 clonal line was able to differentiate into osteocytes, as demonstrated by the presence of calcium deposits stained with alizarin red S (Fig. 56, a).

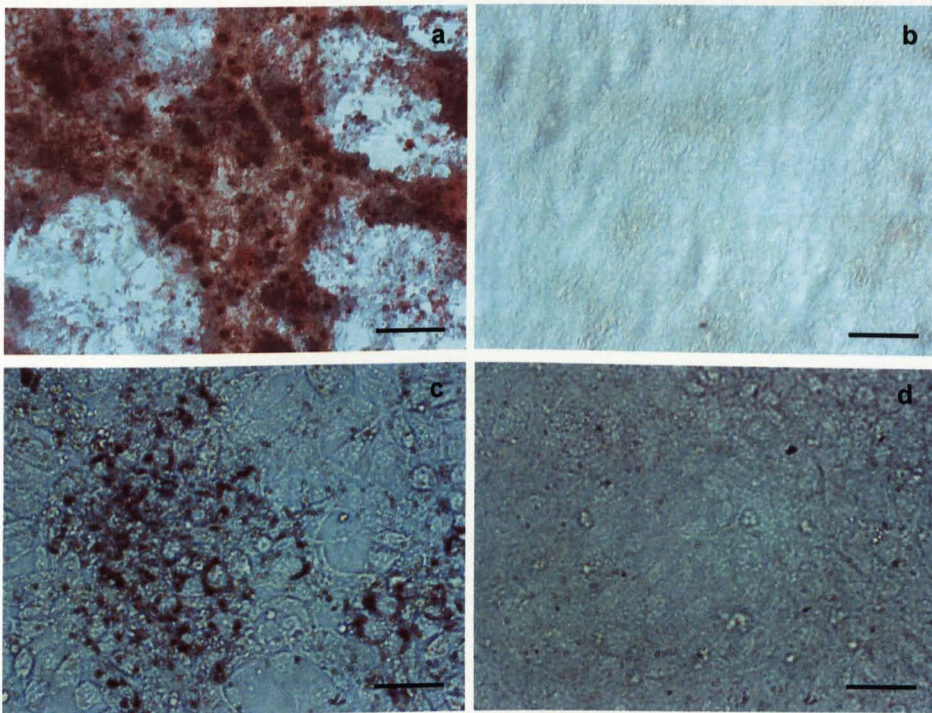


Figure 56. Light micrographs of osteogenic and adipogenic differentiation assays. (a) Calcium deposits stained with alizarin red S demonstrated that the H6 clonal line could differentiate into osteocytes. (b) H6 cells expanded in KSC medium did not differentiate. (c) H6 cells were capable of differentiating into adipocytes, as showed by the presence of lipid droplets stained with oil red O. (d) H6 cells cultured in KSC medium did not show adipogenic differentiation. Scale bar: 50 μm .

H6 cells cultured in KSC medium did not form calcium deposits and were negative for alizarin red S (Fig. 56, b). The presence of lipid droplets, identified by oil red O staining, demonstrated that after 3 complete cycles of induction the H6 clonal line could differentiate into adipocytes (Fig. 56, c). whereas the cells cultured in KSC medium did not differentiate (Fig. 56, d).

5.2.2.2 Ability of H6 cells to differentiate into endothelial cells

The capacity of the H6 clonal line to generate endothelial cells was assayed as described in section 2.2.9. The presence of endothelial cells was assessed by cytofluorimetric analysis for the presence of the endothelial markers CD31, CD105, and by immunostaining for the expression of von Willebrand factor (Vwf) (Bussolati et al., 2005; Sagrinati et al., 2006) (details are explained in section 2.7.1 and section 2.8.1, respectively). These markers were chosen as they had been regularly selected to investigate endothelial differentiation in the laboratory where this part of the work was carried out (University of Turin, Italy).

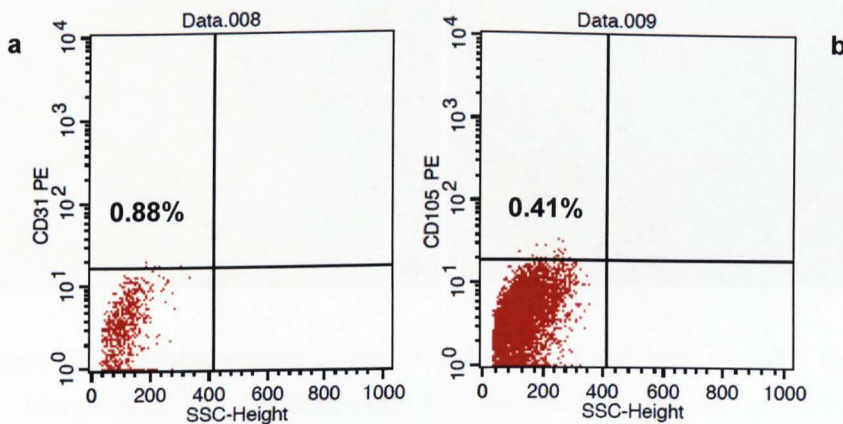


Figure 57. Cytofluorimetric analysis of H6 cells cultured in Endothelial Basal Medium supplemented with 10 ng/ml VEGF. After 3 weeks of culture the cells failed to differentiate into endothelial lineage, as 0.88% of the total cell population expressed CD31 (a) and 0.41% expressed CD105 (b).

Flow cytometry analysis revealed that the H6 clonal line was not able to differentiate into endothelial cells because more than 99% of the cell population did not express either CD31 or CD105 (Fig. 57). Interestingly, the immunostaining revealed that following induction the H6 cells expressed the endothelial marker Vwf and maintained the expression of Wt1 (Fig. 58, a).

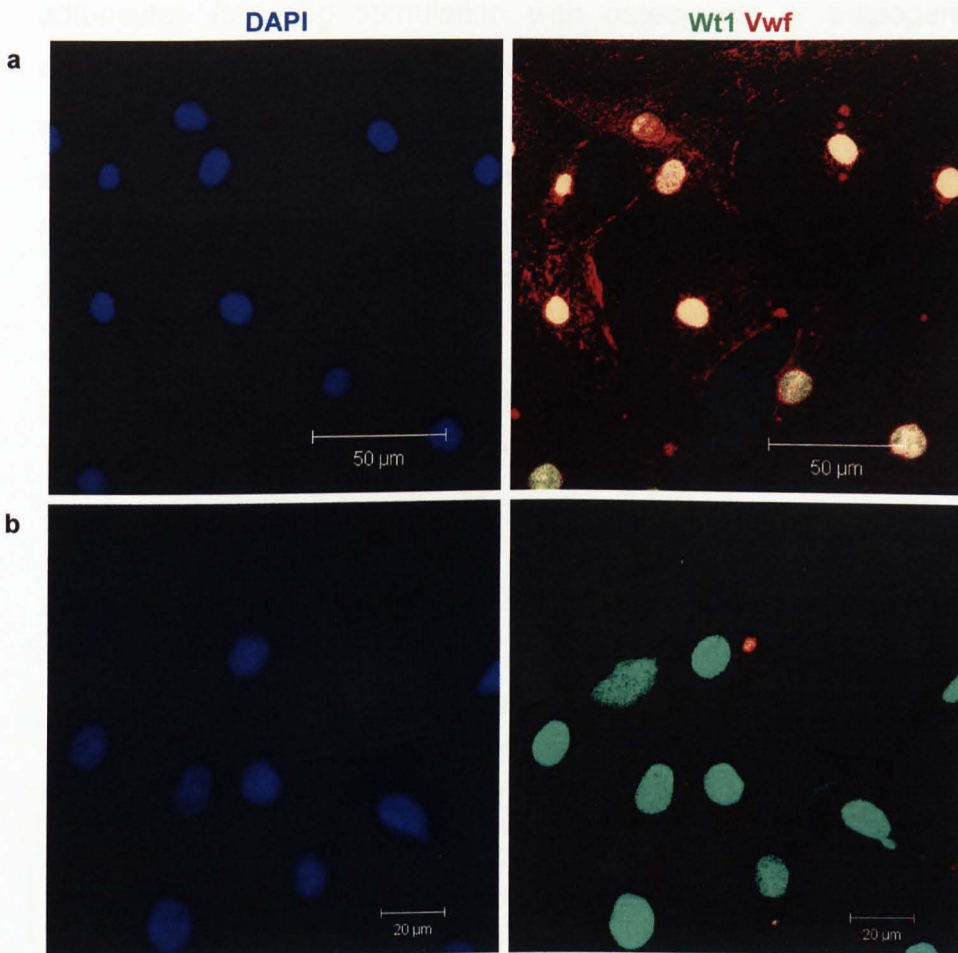


Figure 58. Confocal images of H6 cells stained for Vwf (red) and Wt1 (green). (a) Immunostaining demonstrated that following 3 weeks of culture in Endothelial Basal Medium supplemented with 10 ng/ml VEGF the H6 clonal line expressed both the endothelial marker Vwf and the MM-specific marker Wt1. (b) Control, non-stimulated cells were negative for Vwf but expressed Wt1. Nuclei of stimulated and control H6 cells were stained with DAPI (blue).

H6 cells expanded in KSC medium were positive for Wt1 but did not express Vwf (Fig. 58, b).

These findings suggest that the H6 clonal line could spontaneously generate podocyte-like cells and renal tubular-like cells in culture (Fig. 55) and differentiate into osteocytes or adipocytes following stimulation with osteogenic or adipogenic differentiation medium, respectively (Fig. 56). Although after 3 weeks of culture in the presence of VEGF most of H6 cells expressed the endothelial marker Vwf (Fig. 58), the H6 clonal line failed to differentiate into endothelial lineage as they did not express either CD31 or CD105 (Fig. 57).

5.2.3 Determining the growth rate of the H6 cell population

The growth of the H6 clonal line was assayed using the colorimetric reaction described in section 3.2.2.

Table 16. Expansion of H6 cells. Results are indicated as mean \pm standard deviation of the number of cells.

	t=0	t=24h	t=48h	t=72h
Mean	2500	6757	14343	23514
St. Dev		907	3094	2565

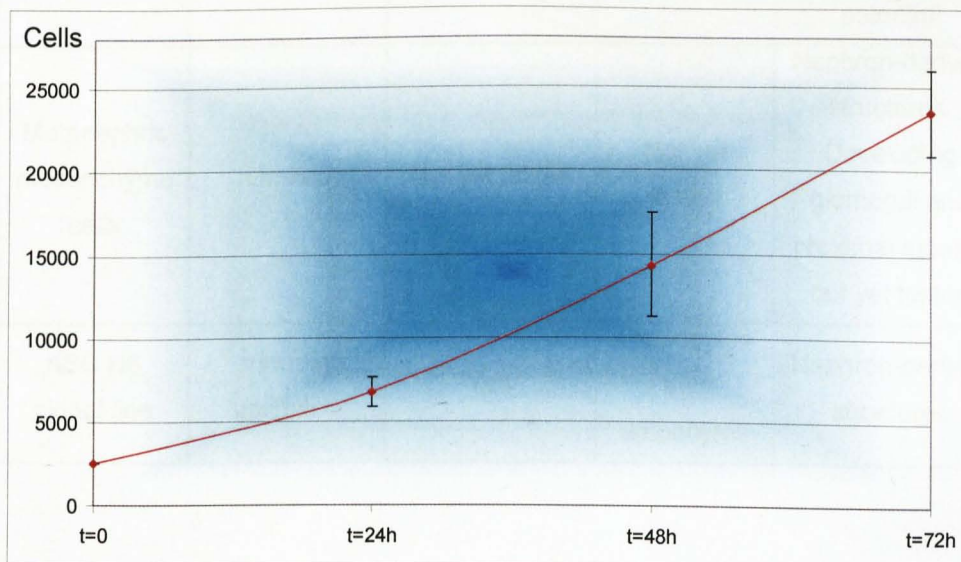


Figure 59. Growth curve of the H6 clonal line, determined with a colorimetric reaction based on the activity of cellular dehydrogenases. The population doubling time was calculated as described in section 2.2.10 and was approximately 25 hours. Error bars indicate standard deviations of cell numbers.

A total number of 2.5×10^3 H6 cells were inoculated into a 96-well plate and absorbance measurements were taken every 24 hours ($n=6$), following initial plating ($t=0$) for a 72 hours period of culture (Fig. 59 and Table 16). The population doubling (PD) time (see section 2.2.10) for the H6 clonal line was approximately 25 hours.

Overall, these results, together with the clonogenic origin of H6 cells and their ability to undergo *in vitro* expansion for indefinite number of passages, suggest that the H6 clonal line display a stem cell phenotype. On the other hand, MM cells appear to be a progenitor cell population, as these cells displayed a limited ability to undergo *in vitro* expansion; besides, their clonogenic capability still has to be proven. Table 17 summarizes the main differences between MM cells and the kidney-derived stem cell H6 clonal line.

Table 17. Principal differences between MM cells and the H6 clonal line.

	Self-renew	Clonogenicity	<i>In vitro</i> multipotency	<i>In vitro</i> nephrogenic potential
Metanephric mesenchyme cells	Limited	Not yet tested	Not yet tested	Nephron-derived structures. Developing glomeruli and proximal tubules not yet tested
KSC H6 clonal line	Virtually unlimited	Yes	Osteocytes and adipocytes	Nephron-derived structures

5.3 Discussion

The H6 clonal line was established from a kidney-derived stem cell population originally isolated from postnatal mouse kidney (Fuente Mora, 2009). The H6 clonal line had a PD time of approximately 25 hours and showed the capacity to spontaneously generate cells with a podocyte-like, mesenchymal-like, and epithelial-like morphology (Fuente Mora, 2009). It was found that H6 cells could also differentiate into non-renal cell types such as osteocytes and adipocytes when stimulated with osteogenic and adipogenic differentiation medium, respectively. Cytofluorimetric analysis demonstrated that the H6 clonal line expressed markers for renal progenitor cells, such as CD29, CD44 and CD73 (Bussolati et al., 2005; Sagrinati et al., 2006). In addition, a fraction of the cell population expressed the stem cell marker Sca-1 and the renal progenitor cell antigen CD24 (Dekel et al., 2006; Sagrinati et al., 2006). It was also found that the H6 clonal line was positive for several MM-specific markers expressed in freshly isolated metanephric mesenchyme and metanephric mesenchyme cells following *in vitro* culture, such as Wt1, Osr1, Gdnf, Vim and Msi1. Furthermore, the H6 clonal line expressed markers commonly found in differentiated cells, such as Aqp1, megalin, synaptopodin and desmin. *Megalin* and *Aqp1* are markers for proximal tubule cells (Gburek et al., 2003; Georgas et al., 2008), whereas *synaptopodin* and *desmin* identify different cell types present in the glomerulus, the former being a marker for post-mitotically differentiated podocytes (Shankland et al., 2007), the latter being expressed by glomerular mesangial cells (Georgas et al., 2008). The presence of transcripts and proteins normally found in differentiated cells strongly supports the presumption that the H6

clonal line is able to spontaneously generate renal-like cells in culture.

As reported in section 5.2.1.1, the H6 clonal line was able to spontaneously give rise to podocyte-like cells that displayed an arborized morphology and a high cytoplasmic-to-nuclear volume ratio. In addition, very often these cells were binucleated. Immunostaining results confirmed that these cells expressed synaptopodin. It was observed that the ability of the H6 cells to generate cells with a podocyte-like morphology could be maintained for an indefinite number of passages and several freeze/thaw cycles. The capacity of a non-immortalized cell line to continue generating podocyte cells in culture may be of great clinical relevance, as it may represent a valuable tool to investigate cell responses to injury and elucidate cell repair mechanisms following damage. Surprisingly, RT-PCR analysis demonstrated that the H6 clonal line did not express the podocyte markers nephrin and podocin. Both nephrin and podocin are key components of the podocyte slit diaphragm, a structure formed by adjacent interdigitating podocyte foot processes that constitutes a size and charge barrier to proteins (Shankland, 2006). It has been shown that conditionally immortalized mouse podocytes express many podocyte proteins normally detected *in vivo* and are capable of forming a slit diaphragm-like structure (Shankland et al., 2007). It is plausible that the culture conditions developed in the present study allowed H6 cells to generate podocyte-like cells that displayed a characteristic podocyte morphology and the expression of the cytoskeleton-associated protein synaptopodin (Garovic et al., 2007); however, when cultured under these conditions, H6 cells neither express nephrin nor podocin and a slit diaphragm-like structure most likely did not form.

RT-PCR analysis revealed that the H6 clonal line expressed markers for proximal tubular cells, such as Aqp1 and megalin. In addition, immunofluorescence staining demonstrated that a subset of the H6 cell population expressed megalin. These findings suggest that the H6 population contains proximal tubule-like cells. The capability of the H6 clonal line to give rise to proximal tubular-like cells will be of great importance and might also have clinical implications in developing therapies to replenish damaged tubular cells. In the next chapter the ability of the H6 clonal line to generate proximal tubular-like cells that show functionality *in vitro* will be further investigated.

A previous study carried out in our laboratory has shown that the H6 clonal line did not generate either renal distal tubular cells or renal collecting duct cells (Fuente Mora, 2009). These findings, together with the results presented in this work, suggest that the differentiation potential of the H6 clonal line seems to be restricted to generate cells present within the initial part of the nephron, such as podocyte-like cells and proximal tubular-like cells, whereas H6 cells seem not to be able to generate distal tubular cells or collecting duct cells. However, another possibility might be taken into account in the attempt to explain the absence of distal tubular markers in the H6 cell population. It has been reported that distal tubular cells, isolated from adult human kidney, lost the expression of distal tubular markers and acquired a more proximal tubular cell phenotype after a few days of *in vitro* culture. On the other hand, proximal tubular cells, isolated from human kidney, were able to maintain their characteristic phenotype during the same period of culture (Baer et al., 1999). It might therefore be possible that H6 cells were able to generate distal tubular-like cells; nevertheless,

these cells might have lost a distal tubular cell-like phenotype and acquired characteristics of proximal tubular-like cells.

The ability to differentiate into different cell types represents an important feature of stem cells. For instance, bone marrow-derived mesenchymal stem cells (MSC) have been extensively used as a model of adult stem cells being able to differentiate into osteocytes and adipocytes (Nagai et al., 2007; Lee et al., 2010). It has been demonstrated that CD24⁺ CD133⁺ renal progenitor cells present in the Bowman's capsule of adult human kidney were able to differentiate toward osteogenic, adipogenic and neuronal lineages (Sagrinati et al., 2006). The ability of renal precursor to give rise to non-renal derivatives has also been illustrated in xenotransplant studies. Dekel and collaborators found that following transplantation under the renal capsule of immunocompromised mice, E20-E25 porcine kidney precursors underwent complete nephrogenesis and formed an organ able to produce urine. In addition, this group noticed that bone tissue, cartilage, myofibroblasts and blood vessels also formed within the grafts, likely because a fraction of embryonic renal precursors had failed to correctly differentiate into the renal lineage (Dekel et al., 2003). More recently, Kim and collaborators transplanted E14.5 rat fetal kidney precursors under the renal capsule of immunocompromised mice. These authors observed that the transplanted cells generated immature glomeruli and renal tubules; however, they also differentiated into non-renal tissues, such as bone and cartilage (see section 1.3.2.3) (Kim et al., 2007). Notably, using a whole-embryo culture system Yokoo and colleagues demonstrated that following injection into the intermediate mesoderm of mouse embryos, human MSC could differentiate into different renal cell types (Yokoo et al., 2005).

The ability of the H6 clonal line to differentiate into osteocytes and adipocytes, two cell types commonly derived from MSC, suggests that H6 cells display a multipotent phenotype and underlines important analogies with other kidney stem/progenitor cell populations (Bussolati et al., 2005; Dekel et al., 2006; Sagrinati et al., 2006). The fact that the H6 clonal line displayed some characteristics of MSC might be explained by considering that the aorta-gonad-mesonephros region where MSC arise (Mendes et al., 2004), like the kidney, originates from the intermediate mesoderm.

My work also showed that the H6 cells could not achieve endothelial differentiation: flow cytometry analysis revealed that the vast majority of the H6 cells did not express the endothelial markers CD31 and CD105 (Bussolati et al., 2005). Interestingly, following 3 weeks of culture in Endothelial Basal Medium (EBM) supplemented with 10 ng/ml VEGF, the cells expressed the endothelial marker von Willebrand factor (Vwf) (Bussolati et al., 2005) and the MM-specific marker Wt1. This gene was also found to be activated in endothelial cells under reduced oxygen supply conditions, such as in rat coronary vasculature following myocardial infarction (Wagner et al., 2003). Conversely, H6 cells expanded in control KSC medium did not express Vwf, but they did maintain the expression of Wt1. It has been shown that CD133⁺ renal progenitor cells isolated from adult human kidney could differentiate into endothelial cells *in vitro* (Bussolati et al., 2005). Since the protocol followed to differentiate H6 cells into endothelial cells was the same of that used to differentiate human CD133⁺ cells, it might be hypothesized that these culture conditions, although they could induce the expression of Vwf, were

not ideal to trigger endothelial differentiation in kidney-derived stem cells isolated from mouse.

One of the most interesting features of the H6 clonal line was that it expressed the same set of metanephric mesenchyme-specific markers already found in freshly isolated metanephric mesenchyme and metanephric mesenchyme cells following *in vitro* culture, such as the MM-specific marker and progenitor cell marker Wt1, the MM-specific genes *Osr1* and *Gdnf*, and the mesenchymal marker *Vim*. In addition, similar to freshly isolated and cultured MM cells, H6 cells expressed the progenitor cells markers *Msi1* and *Msi2*. Like *in vitro* cultured MM cells, the H6 clonal line did not express the MM- and UB-specific marker *Pax2*. Interestingly, the expression of the UB-specific marker *Hoxb7* (Park et al., 2007) was found. This result might be due to the culture conditions developed that determined the expression of *Hoxb7* in H6 cells. Since the expression of the UB-specific marker *Ret* (Osafune et al., 2006) was not detected, it can be concluded that the H6 cell population did not contain UB-derived cells.

Cytofluorimetric analysis revealed that approximately 30% of H6 cells expressed the stem cell marker stem cell antigen-1 (*Sca-1*) which has been previously found to be expressed by a population of non-tubular multipotent progenitor cells isolated from adult mouse kidney (Dekel et al., 2006). Moreover, a similar percentage of the H6 clonal line was positive for the renal progenitor cell markers *CD24* (Sagrinati et al., 2006) and *CD73* (Bussolati et al., 2005). Furthermore it was observed that the H6 clonal line expressed several markers normally found in adult stem cells, such as *CD29*, *CD44* and *CD73*. Of note, Bussolati and colleagues demonstrated that these markers were expressed in

CD133⁺ renal progenitor cells isolated from the interstitium of adult human kidney (Bussolati et al., 2005). The expression of the hemopoietic stem cell marker CD34 (Bussolati et al., 2005) might suggest that the H6 clonal line also displayed characteristics of this stem cell population; however, a hemopoietic stem cell phenotype for the H6 clonal line can most likely be ruled out since H6 cells expressed the podocyte markers desmin and synaptopodin, and the proximal tubule markers Aqp1 and megalin. CD133 has been considered a marker for organ-specific stem cells. However, Shmelkov and colleagues demonstrated that in mouse CD133 is also expressed in many differentiated epithelial cells of adult organs with hollow cavities, such as the kidney, lung, pancreas and liver (Shmelkov et al., 2008). Since CD133 might not represent an appropriate marker for the identification of stem/progenitor cell populations, the expression of CD133 in the H6 cell population was not assayed.

Finally, a cell growth assay demonstrated that the H6 clonal line had a population doubling (PD) time of approximately 25 hours, which was shorter than the PD time of both P0 and P1 MM cells (approximately 57 hours and 37 hours, respectively).

Overall, these findings suggest that a fraction of the H6 clonal line was able to maintain a stem cell phenotype and might therefore represent a remnant of the embryonic metanephric mesenchyme present in the postnatal mouse kidney. The ability to differentiate into osteocytes and adipocytes, together with the ability to express many adult stem cell markers, underline several analogies with CD24⁺ CD133⁺ adult human renal progenitor cells present within the Bowman's capsule. However, the findings also indicate that under the culture conditions developed, a fraction of these cells

might be able to undergo spontaneous differentiation, thus giving rise to more differentiated, renal-like cells found in the H6 cell population.

CHAPTER 6

Investigating the nephrogenic potential of the H6 clonal line *in vitro*

6.1 Introduction

The H6 clonal line was obtained from a population of kidney-derived stem cells, originally isolated from postnatal mouse kidney. In chapter 5 it was presented that the H6 clonal line showed a population doubling time of approximately 25 hours and the ability to give rise to renal-like and non renal cell types in culture (see section 5.2.1 and section 5.2.2). The results demonstrated that H6 cells displayed an expression profile similar to that of MM cells following 4 days of *in vitro* culture, as they expressed MM-specific markers such as *Wt1*, *Osr1*, *Vim* and *Gdnf*. In addition the expression profile analysis revealed that the H6 clonal line was positive for markers for stem/progenitor cells, namely *Msi1*, *Msi2*, *Sca-1*, *CD24*, *CD29* and *CD73*, and for markers normally found in differentiated renal cells, such as *synaptopodin*, *megalyn*, *Aqp1*, *Des* and *Vegfa*.

These findings suggest that the H6 clonal line might derive from metanephric mesenchyme cells that persist in the postnatal mouse kidney and, therefore, might maintain the capability to give rise to different cell types present in the nephron. In addition, the expression of the renal proximal tubular markers, *megalyn* and *Aqp1*, suggested that a subset of the H6 clonal line underwent either partial or complete differentiation in order to give rise to proximal tubular-like cells.

In chapter 4 it was demonstrated that freshly isolated MM and MM cells following 4 days of *in vitro* culture could maintain a

nephrogenic potential, as they were able to participate in the formation of developing nephrons following recombination with E11.5 reaggreated kidney rudiments. One of the crucial point of the present study was to determine whether, similar to freshly isolated and cultured MM cells, the H6 clonal line could participate in the formation of nephron-like derived structures *in vitro*. The *in vitro* nephrogenic potential of the H6 clonal line was investigated by recombination with E11.5 reaggreated kidney rudiments and the ability of H6 cells to integrate into nephron-like developing structures was compared with that of freshly isolated and cultured MM cells. In addition, since H6 cells expressed markers for podocytes and proximal tubules, it was decided to assess whether the cells were also able to participate in the formation of glomeruli and proximal tubules following chimera formation. If the H6 clonal line maintained a nephrogenic potential, then it would be expected to find these cells integrated into developing nephrons, proximal tubules and glomeruli. Furthermore, a similar integration ability for H6 cells and MM cells would underline important similarities between these two cell populations and hint that the H6 clonal line might be a postnatal remnant of the embryonic MM.

If H6 cells were of use for the treatment of renal injury, it would be paramount that these cells display normal functionality and differentiate appropriately. As previously mentioned, the H6 clonal line expressed markers for proximal tubular cells. The renal proximal tubule plays a pivotal role in the reabsorption of water and a wide variety of inorganic and organic molecules present in the glomerular ultrafiltrate (Christensen and Gburek, 2004, Kobayashi et al., 2005) and in the elimination of potentially toxic compounds such as pollutants and metabolic wastes and pollutant metabolites present in the body (Masereeuw et al., 1999). Under

normal circumstances vitamins and proteins present in the blood are filtered through the glomerular filtration barrier, and subsequently, are reabsorbed as they pass through the proximal tubules in order to be metabolized or reused and secreted into the circulatory system. This results in an almost protein-free urine (<20 mg/l) (Nielsen and Christensen, 2010). However, several conditions such as diabetes mellitus, infections, genetic and immune mechanisms, can lead to podocyte depletion (Ronconi et al., 2009) which, by impairing the glomerular filtration capacity, may eventually lead to proteinuria, a condition characterized by the presence of non-physiological levels of proteins in the urine (>200 mg/l). Although the effects of protein-rich ultrafiltrate in the distal segment of the nephron have still to be fully elucidated, it seems that the excess of proteins may induce inflammation and fibrosis, which could eventually lead to renal failure (Nielsen and Christensen, 2010).

A vast variety of molecules present in the ultrafiltrate, such as ions, amino acids, hormones, proteins, enzymes, drugs and toxins, are reabsorbed as a complex with two endocytic receptors, megalin and cubulin, and the cooperating protein amnionless (Nielsen and Christensen, 2010). The reabsorption takes place principally within the S1 segment of the kidney proximal tubules, which represent the portion of the proximal tubule adjacent to the Bowman's capsule (Casarett et al., 2007; Russo et al., 2007; Nielsen and Christensen, 2010). Megalin is a 600 kDa transmembrane protein which belongs to the low density lipoprotein (LDL) receptor family; cubulin is a 460 kDa peripheral cooperating receptor which interacts with megalin before internalization (Fig. 60) (Nielsen and Christensen, 2010).

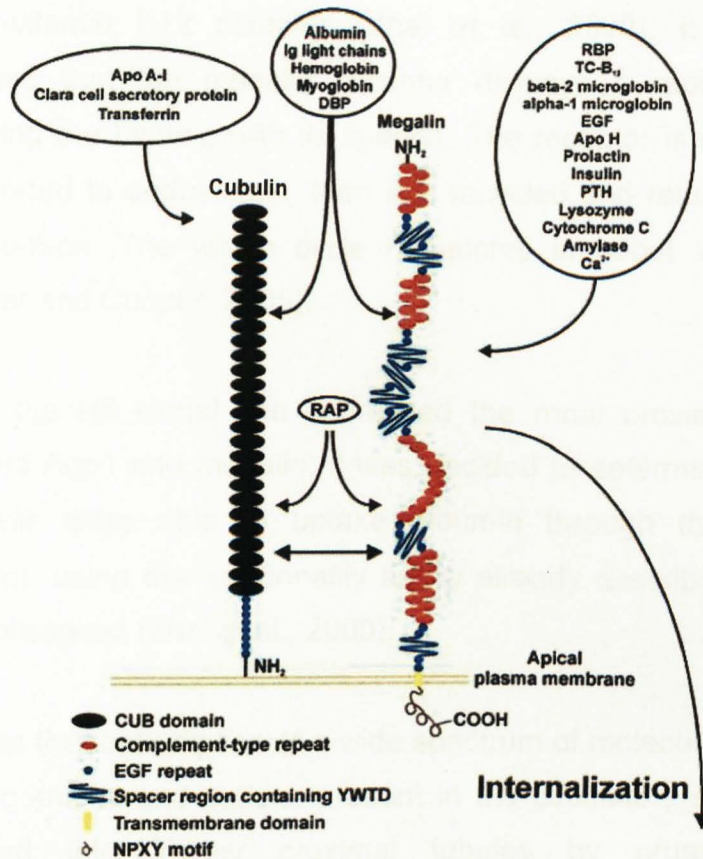


Figure 60. Schematic representation of megalin and cubulin receptors in the apical membrane of kidney proximal tubules. Specific and shared ligands for megalin and cubulin are internalized as a complex with the receptors (Christensen and Gburek, 2004, with permission).

It has been demonstrated that megalin and cubulin mediate the reabsorption of haemoglobin, myoglobin, albumin and receptor-associated protein (RAP) (Zhai et al., 2000; Nielsen and Christensen, 2010). Zhai and colleagues demonstrated that megalin and cubulin are expressed on the apical surface of kidney proximal tubules (Zhai et al., 2000). These authors showed that megalin could mediate the endocytosis of albumin in opossum kidney proximal tubular cells in culture, and that the uptake could be competitively reduced in the presence of either RAP or intrinsic

factor-vitamin B12 complex (Zhai et al., 2000). It has been reported that the megalin receptor displays a rapid turnover following the binding with its ligands. The receptor is internalized and sorted to endosomes, then it is recycled and returned to the cell surface. The whole cycle completes in about 20 minutes (Maurer and Cooper, 2005).

Since the H6 clonal line expressed the renal proximal tubular markers Aqp1 and megalin, it was decided to determine whether H6 cells were able to uptake albumin through the megalin receptor, using the functionality assay already described by Zhai and colleagues (Zhai et al., 2000).

Besides the reabsorption of a wide spectrum of molecules, several organic anions and cations present in the circulatory system are secreted into kidney proximal tubules by organic anion transporters (OATs) and organic cation transporters (OCTs), to be eliminated in the urine. These transporters belong to the Amphiphilic Solute Transporter (*Slc22a*) family of the Major Facilitator Superfamily. Substrates for OATs and OCTs include physiological compounds, such as folate, urate, prostaglandins and neurotransmitters (Sweet et al., 2006); however many potentially toxic xenobiotic agents, namely non-steroidal anti-inflammatory drugs, antibiotics, antivirals, heavy metals, chemotherapeutics and mycotoxins, are also ligands for OATs and OCTs. Since many drugs and toxins are substrates for OATs and OCTs, this family of transporters has become of great pharmacological interest (Sweet, 2005; Sweet et al., 2006).

The expression of OATs is not limited to the kidney, but it has been found in barrier epithelia of different organs and tissues

including liver, placenta, choroid plexus and brain capillaries (Sweet et al., 2005).

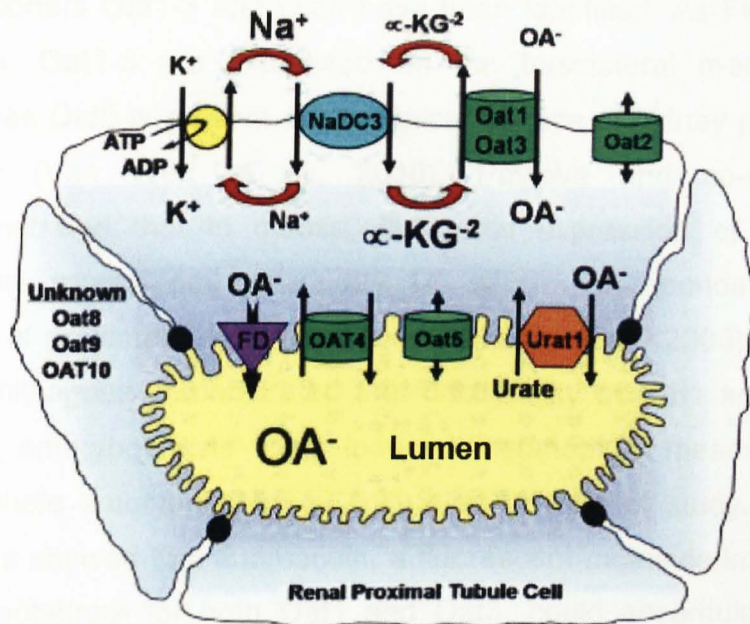


Figure 61. Schematic representation of OAT family members in kidney proximal tubules. Oat1-3 appear on the basolateral membrane, whereas Oat5 and OAT4 (the latter expressed in human) are located on the apical surface of proximal tubular cells (Modified from Van Wert et al., 2010).

In the kidney, OATs are expressed mainly within the S2 segment of kidney proximal tubules, where most of the tubular secretion takes place. These channels are located either on the basolateral or apical membrane of proximal tubules and their disposition reflects their roles in basolateral uptake or apical secretion of anions (Brenner, 2000; Anzai et al., 2005; Sweet et al., 2006; Casarett et al., 2007; Hwang et al., 2010). This pattern implies that organic anion molecules are first uptaken from the blood through basolateral organic anion transporters, and subsequently, are secreted into the lumen of proximal tubules by organic anion transporters located on the apical surface of the tubules (Van Wert et al., 2010).

In human kidneys, five members of the OAT family, OAT1-4 and OAT10, have been found, whereas in mouse kidneys the transporters Oat1-3 and Oat5 have been identified. As Figure 61 shows, Oat1-3 are expressed on the basolateral membrane, whereas Oat5 is present on the apical surface of kidney proximal tubule (Van Wert et al., 2010). Pavlova and co-workers demonstrated that in mouse, the renal expression of Oat1-3 appears around embryonic day 14, which corresponds to the onset of proximal tubule formation (Pavlova et al., 2000). Sweet and colleagues demonstrated the functionality of Oat1 and Oat3 during embryogenesis using induced metanephric mesenchyme and whole embryonic kidney culture as models of study. These authors showed that fluorescein, a fluorescent molecule known to be a substrate for both Oat1 and Oat3, could accumulate into presumptive proximal tubules of rat embryonic kidney and rat MM that had been induced by spinal cord stimulation. In addition, it was shown that the uptake of fluorescein could be completely blocked in the presence of probenecid, an organic anion transporter competitive inhibitor (Sweet, 2005). In a subsequent study this research group demonstrate that MM induced by recombination with ureteric bud showed OAT functionality as evidenced by the fact that the recombined tissue was able to uptake 6-carboxyfluorescein (6-CF), whereas in the presence of probenecid, the uptake was inhibited (Rosines et al., 2007).

The possibility to look at the uptake of fluorescent molecules represents a valuable tool to elucidate the functionality of OATs *in vitro*. In order to provide further evidence that some cells within the H6 cell population showed a renal proximal tubular cell-like phenotype, it was decided to investigate whether the H6 clonal line

was able to uptake 6-carboxyfluorescein (6-CF) via the organic anion transporters, using the chimera formation assay.

If H6 cells were capable of displaying functionality *in vitro*, then it would indicate that the H6 clonal line was able to generate cells with a proximal tubule-like phenotype.

6.2 Results

6.2.1 Investigating the *in vitro* nephrogenic potential of the H6 clonal line

In this work it was hypothesized that the H6 clonal line represented a remnant of the embryonic metanephric mesenchyme present in the postnatal mouse kidney. It became important to elucidate whether the H6 clonal line maintained a nephrogenic ability, i.e. whether the cells were still able to participate in nephron formation. In chapter 4, it was shown that reaggregated kidney rudiments were able to form organotypic renal structures, such as comma and S-shaped body and developing nephrons (see section 4.2.3 and Unbekandt and Davies, 2010). It was also demonstrated that metanephric mesenchyme cells following 4 days of culture could retain a nephrogenic potential since they were capable of integrating into developing nephrons at a comparable ratio with that of freshly isolated MM (see section 4.2.3).

In order to track H6 cells in the chimera, it was decided to label the cells with quantum dots (QD). In addition, in some experiments the cells were transfected with a lentiviral vector constitutively expressing enhanced green fluorescent protein (EGFP). Cell labelling protocols are explained in section 2.3. The chimeras were

cultured for a period of 3-5 days, then the samples were stained for Wt1, laminin, Pax2, megalin and synaptopodin.

Wt1 and laminin were selected as they are useful markers to identify developing nephrons. In section 4.2.3.1 and section 4.2.3.2 it was demonstrated that freshly isolated and cultured MM were able to maintain the expression of Pax2 for several days after being recombined with E11.5 reaggreated kidney rudiments. Since the H6 clonal line did not express Pax2 (see section 5.2.1.2 and section 5.2.1.4), in this section it was decided to investigate whether H6 cells could re-express Pax2 following recombination with reaggreated kidney rudiments. Megalin is a marker for proximal tubules (Gburek et al., 2003), whereas synaptopodin is expressed by podocytes (Shankland et al., 2007). The former marker was selected in order to see whether H6 cells could participate in the formation of developing proximal tubules, the latter one was included to ascertain if the H6 clonal line could also contribute to the formation of presumptive glomeruli.

6.2.1.1 H6 cells expressing enhanced green fluorescent protein

The H6 clonal line was transfected with a lentiviral vector expressing enhanced green fluorescent protein (EGFP) as explained in section 2.3.1. The expression of EGFP reached a plateau level three days after transfection (Mr Sokratis Theocharatos, University of Liverpool, personal communication and data not shown). Figure 62 shows H6 cells expressing EGFP (hereafter referred to as H6 EGFP⁺ cells).

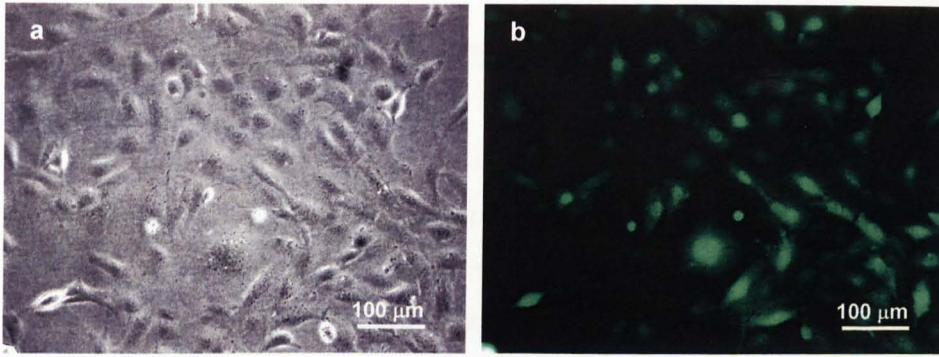


Figure 62. Micrographs of H6 cells transfected with EGFP vector. (b) H6 EGFP⁺ cells (a, phase contrast) expressed enhanced green fluorescent protein within the cytoplasm and the nucleus (green).

The fluorescent signal was localized in the cytoplasm and in the nucleus (Fig. 62). Cytofluorimetric analysis demonstrated that approximately 90% of the transfected H6 cells expressed EGFP (Fig. 63). The percentage of EGFP-expressing cells remained constant for the entire duration of this study (data not shown).

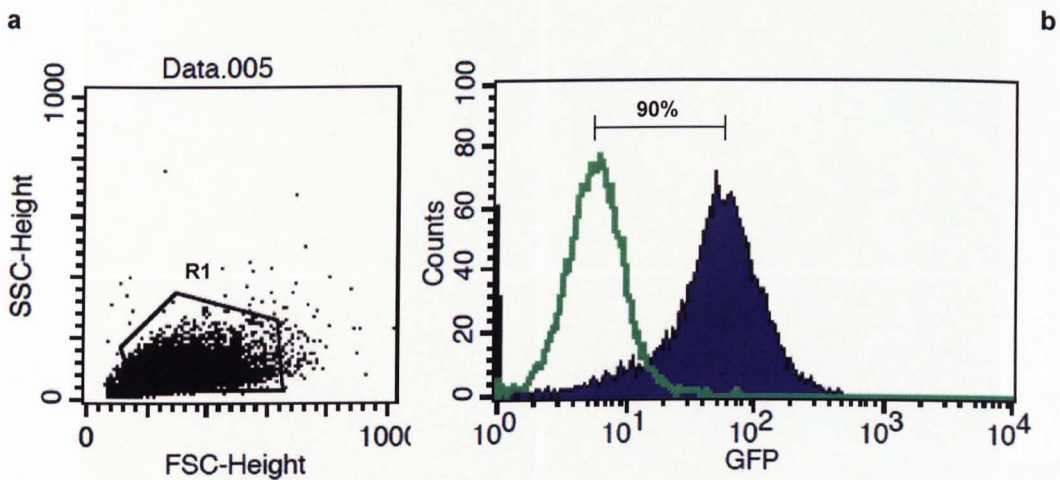


Figure 63. Cytofluorimetric analysis performed on H6 EGFP⁺ cells. (a) Forward and side scatters of H6 EGFP⁺ cells. The gate R1 includes the cells analysed for the expression of EGFP. (b) Approximately 90% of the transfected cells expressed green fluorescent protein (violet). Green line indicates non-transfected H6 cells (control).

6.2.1.2 Recombination of the H6 clonal line with E11.5 reaggregated kidney rudiments

The H6 clonal line, labelled with quantum dots (QD), was recombined with E11.5 reaggregated kidney rudiments. The samples were cultured in KSC medium in the presence of Rho-kinase inhibitor for the first 24 hours of culture (see section 2.2.8.2).

The results demonstrated that similar to freshly isolated and 4 days cultured MM (see section 4.2.3.1 and section 4.2.3.2) the H6 clonal line showed a nephrogenic potential.

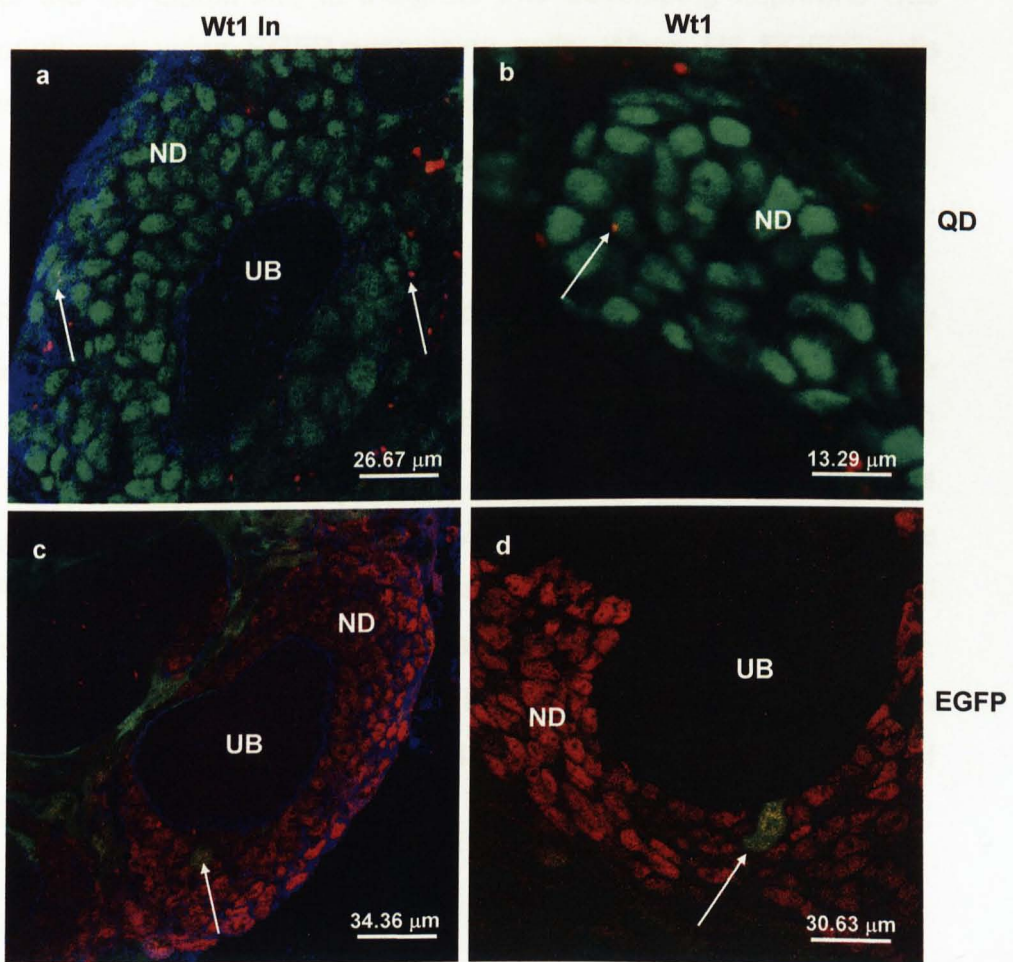


Figure 64. Immunostaining of H6 cells recombined with E11.5 reaggregated kidney rudiments. Panels a and b show that H6 cells, labelled with quantum dots (QD) (red), could integrate into nephron-like developing structures (ND, arrows) expressing Wt1 (green), but not into the ureteric bud (UB). Laminin (blue) surrounded the UB. (c, d) The ability of H6 cells to integrate into developing nephrons was confirmed using H6 EGFP⁺ cells (green). Nephron-like developing structures were stained for Wt1 (red). Arrows indicated integrated H6 EGFP⁺ cells.

Figure 64 shows that the cells integrated into nephron-like developing structures (ND) expressing Wt1 (Fig. 64, a and b arrows), but not into the ureteric bud (UB) (Fig. 64, a). The ability of the H6 clonal line to integrate into developing nephrons was confirmed using EGFP-expressing cells. When H6 EGFP⁺ cells were recombined with reaggregated kidney rudiments, it was found that EGFP⁺ cells could integrate into developing nephrons, but not into the ureteric bud (Fig. 64, c and d, arrows).

Previous findings from this work demonstrated that both freshly isolated MM and MM following 4 days of *in vitro* culture were able to maintain the expression of the transcription factor Pax2 following recombination with E11.5 reaggregated kidney rudiments (details are shown in section 4.2.3.1 and section 4.2.3.2). Since RT-PCR and immunostaining assays revealed that the H6 clonal line did not express Pax2 (see section 5.2.1.2 and section 5.2.1.4, respectively), it was elected to investigate whether the chimera environment could allow H6 cells to activate the expression of Pax2.

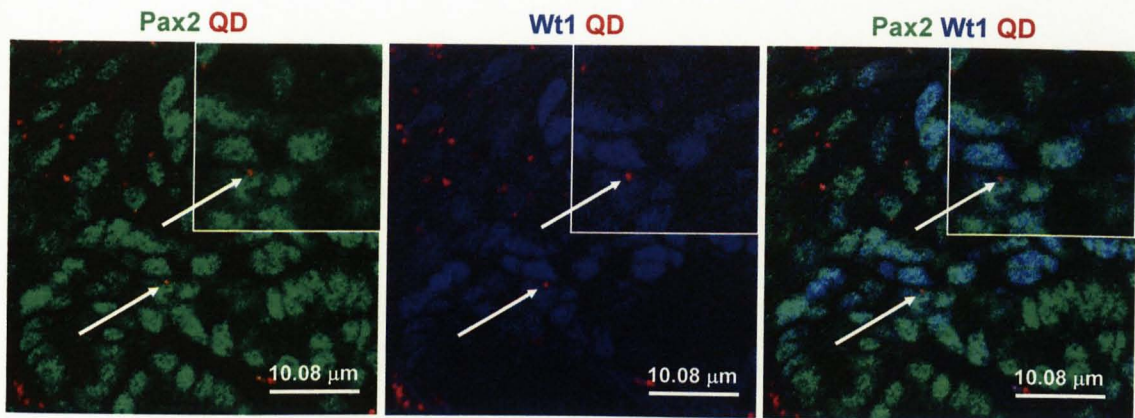


Figure 65. Immunostaining for Pax2 and Wt1. Following recombination with E11.5 reaggregated kidney rudiments, some H6 cells, labelled with QD (red), expressed both Pax2 and Wt1 (arrows). Inlets show higher magnification of H6 cells expressing both pax2 and Wt1.

After culturing the chimera for three days it was found that some QD-labelled H6 cells expressed Pax2. In addition, it was observed that in some cases Pax2-expressing cells were also positive for Wt1, as double immunofluorescence staining revealed (Fig. 65). Notably, no Pax2⁺ Wt1⁻ H6 cells were found (Fig. 65 and data not shown), which provides further evidence that the H6 clonal line was not derived from the ureteric bud.

The H6 clonal line expressed the podocyte marker synaptopodin and the proximal tubular markers Aqp1 and megalin (see section 5.2.1.2 and section 5.2.1.4). It became important to investigate whether H6 cells were able to form developing proximal tubules and presumptive glomeruli following recombination with E11.5 reaggregated kidney rudiments. Following three days of culture the chimera had started forming proximal tubules that showed a correct spatial expression of megalin: Figure 66 shows that megalin staining was found on the apical surface of developing tubules.

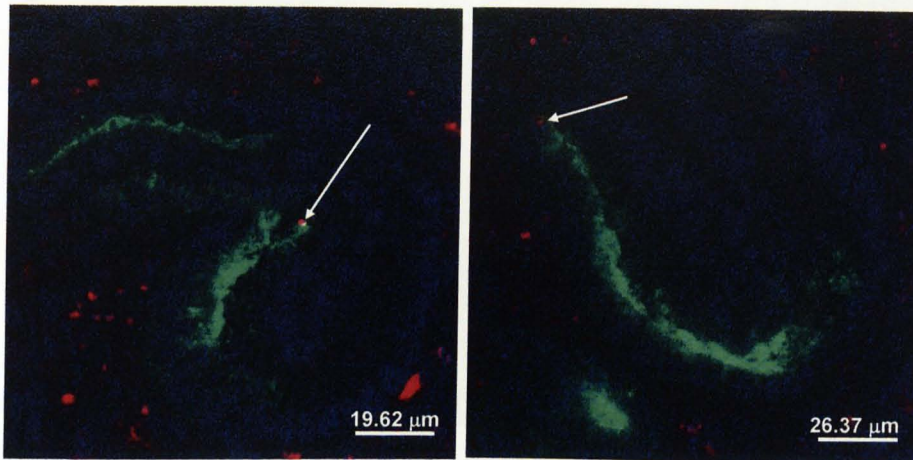


Figure 66. The H6 clonal line could participate to the formation of developing proximal tubules. Following recombination with E11.5 reaggregated kidney rudiments, QD-labelled H6 cells (red) were able to integrate into developing proximal tubules, stained for megalin (green). Arrows indicate QD-labelled megalin-positive H6 cells integrated into developing proximal tubules. Pax2 is in blue.

Quantum dot-labelled H6 cells could participate in the formation of developing proximal tubules: arrows in Figure 66 indicate QD-labelled megalin-positive H6 cells integrated into proximal tubule-like structures.

The ability of the H6 clonal line to form developing glomeruli was investigated. For this assay it was decided to extend the chimera culture period to five days in order to allow the formation of more mature glomeruli. Developing glomeruli were stained for the podocyte marker synaptopodin. The results showed that QD-labelled H6 cells could integrate into glomerular-like developing structures (Fig. 67, a arrow). In addition, the integration ability of the H6 clonal line was confirmed using H6 EGFP⁺ cells: it was possible to observe EGFP-expressing cells integrated into developing glomeruli (Fig. 67, b arrow).

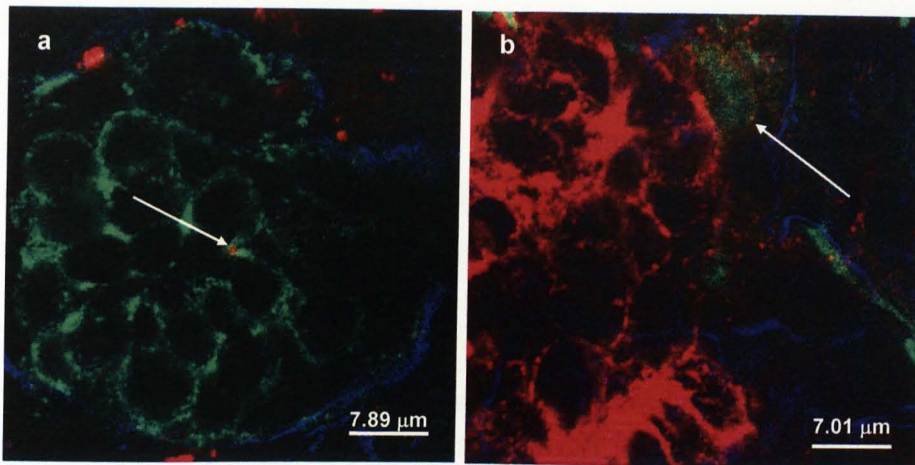


Figure 67. The H6 clonal line could participate in the formation of developing glomeruli. (a) Developing glomeruli expressed synaptopodin (green) and were surrounded by laminin (blue). QD-labelled H6 cells (red) could integrate into developing glomeruli (arrow). (b) H6 EGFP⁺ cells (green, arrow) integrated into glomerular-like developing structures positive for synaptopodin (red). Laminin stained basement membrane (blue).

These findings demonstrated that the H6 clonal line displayed a nephrogenic potential *in vitro* since it was able to integrate, and hence participate in the formation of developing nephrons, proximal tubules and developing glomerular-like structures.

6.2.2 Determining the percentage of H6 cells integrated into nephron-like developing structures

To determine the percentage of H6 cells integrated into developing nephrons it was decided to follow the strategy already adopted to determine the percentage of freshly isolated and cultured MM cells integrated into developing nephrons (see section 4.2.4).

The results, summarized in Table 18 and Figure 68, showed that QD-labelled H6 cells integrated into nephron-like developing structures (n=7) at a ratio of $8.39\% \pm 0.54\%$ (mean of three distinct experiments); freshly isolated and cultured MM cells could

integrate at a ratio of $13.29\% \pm 0.72\%$ and $12.36\% \pm 3.02\%$, respectively (see section 4.2.4). Statistical analysis revealed that the potential of H6 cells to form developing nephrons was lower than that of freshly isolated MM (Student's t-test, $P < 0.05$), however it was not dissimilar with that of cultured MM cells (Student's t-test, $P > 0.05$).

Table 18. Integration ability of freshly isolated MM (fresh MM) (n=3), MM cells following 4 days of *in vitro* culture (4d MM cells) (n=3) and H6 cells (n=3). Results are expressed as mean and standard deviation (SD) of the percentage of QD-labelled freshly isolated MM, cultured MM cells and H6 cells integrated into nephron-like developing structures.

Samples	Fresh MM	4d MM cells	H6 cells
Mean \pm SD	$13.29\% \pm 0.72\%$	$12.36\% \pm 3.02\%$	$8.39\% \pm 0.54\%$

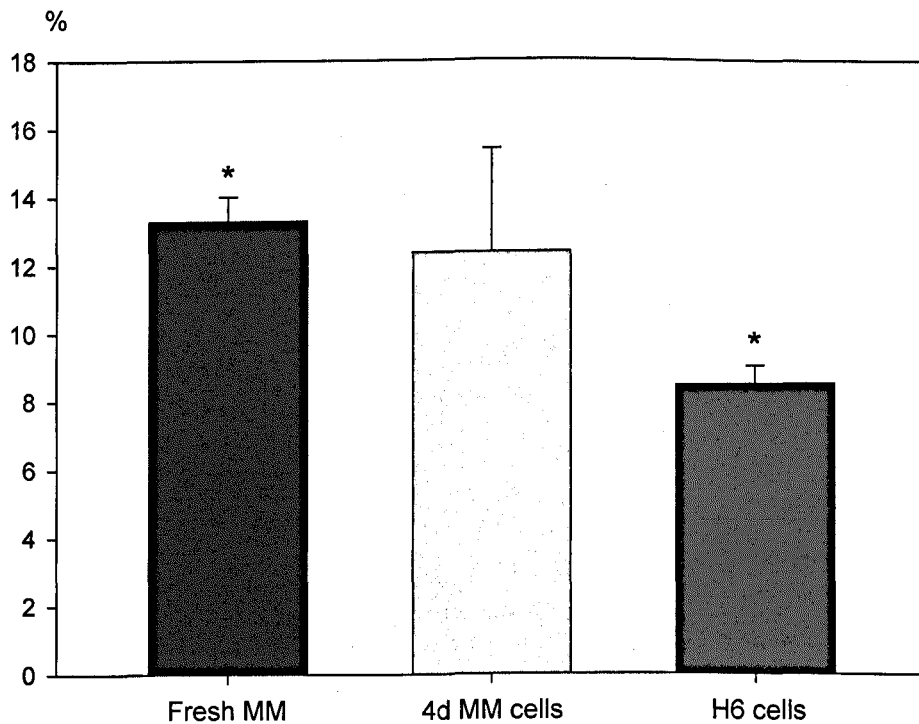


Figure 68. Percentage of freshly isolated MM (n=3), 4 days cultured MM cells (n=3) and H6 cells (n=3) labelled with quantum dots, integrated into nephron-like developing structures. Student's t-test demonstrated that the percentage of integration of H6 cells was smaller than that of freshly isolated MM ($P < 0.05$); nevertheless, cultured MM and H6 cells integrated at a comparable ratio into developing nephrons ($P > 0.05$). Error bars indicate standard deviations of the means. Asterisks indicate differences with statistical relevance.

Overall these findings demonstrated that the H6 clonal line maintained a nephrogenic potential and was able to integrate into nephron-like, proximal tubular-like and glomerular-like developing structures following recombination with E11.5 reaggregated kidney rudiments. Similarly with freshly isolated and 4 days cultured MM cells, H6 cells did not integrate into ureteric bud. In addition, it was found that the ability of the H6 cells to integrate into developing nephrons was comparable with that of cultured MM cells.

6.2.3 Investigating the functionality of the H6 clonal line in vitro

The H6 clonal line expressed markers for proximal tubule cells and could participate in the formation of developing proximal tubules when recombined with E11.5 reaggregated kidney rudiments. It became paramount to determine whether the H6 clonal line were also able to generate proximal tubule-like cells that displayed functionality *in vitro*.

6.2.3.1 The H6 clonal line expressed functional megalin

In this work the ability of H6 cells to uptake albumin *via* the megalin receptor was assessed as described in section 2.5.1. The E5 clonal line, which did not express neither Aqp1 nor megalin (Fuente Mora, 2009), was used as a negative control for FBSA endocytosis.

The results demonstrated that a group of H6 cells showed functionality and was able to uptake FBSA. The punctate staining in the cell cytoplasm indicated that FBSA had been internalized into endocytic vacuoles (Fig. 69, a). The E5 clonal line did not display FBSA endocytosis (Fig. 69, b).

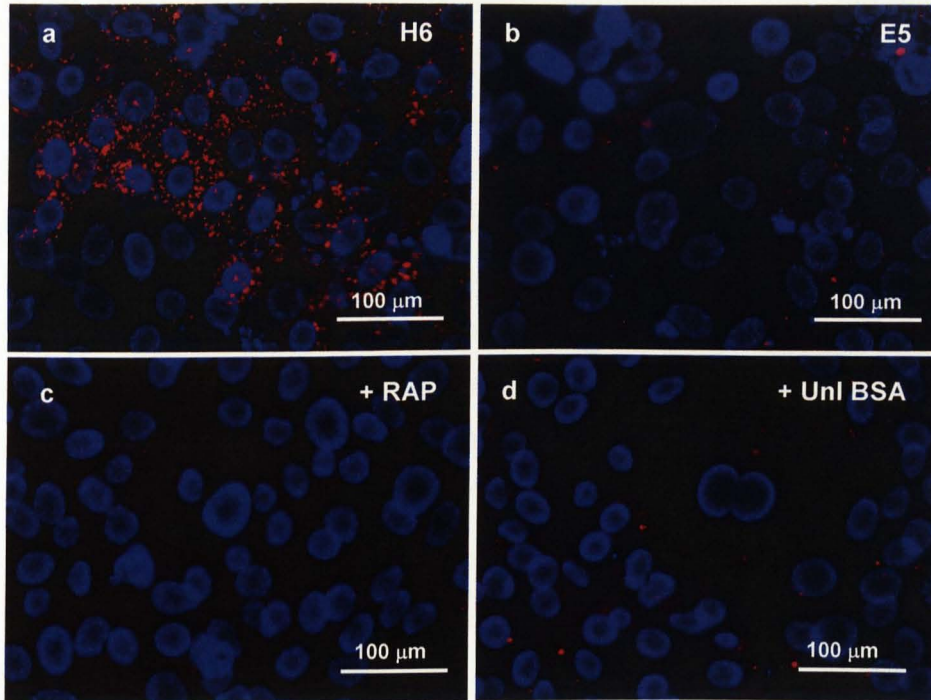


Figure 69. *In vitro* megalin functionality assay. (a) Fluorescent bovine serum albumin (FBSA) (red) uptake was observed in a subset of H6 cells following 1 hour of incubation at 37°C, whereas (b) no uptake was detected in the E5 clonal line. (c) The endocytosis of FBSA was strongly inhibited when H6 cells were incubated with RAP or (d) unlabeled BSA. Nuclei were stained with the vital dye Hoechst 33342 (blue).

The uptake of FBSA in H6 cells was then investigated in the presence of either receptor-associated protein (RAP) or unlabeled bovine serum albumin (BSA), two potential competitors for the uptake of FBSA (Zhai et al., 2000). It was found that in the presence of RAP the endocytosis of FBSA was almost completely

blocked due to a competitive inhibitory effect of RAP for megalin binding (Fig. 69, c). The uptake of FBSA was also greatly reduced when the cells were incubated in the presence of unlabeled BSA (Fig. 69, d).

These findings suggested that a fraction of H6 cell population could mediate the endocytosis of albumin *via* the megalin receptor.

6.2.3.2 Co-localization of megalin with fluorescent BSA

In order to confirm that in H6 cells the endocytosis of albumin occurred through the megalin receptor, it was decided to establish if there was a co-localization of the endocytic uptake of FBSA with megalin. For this purpose, immunostaining for megalin was performed on H6 cells following incubation with FBSA (details are explained in section 2.5.1).

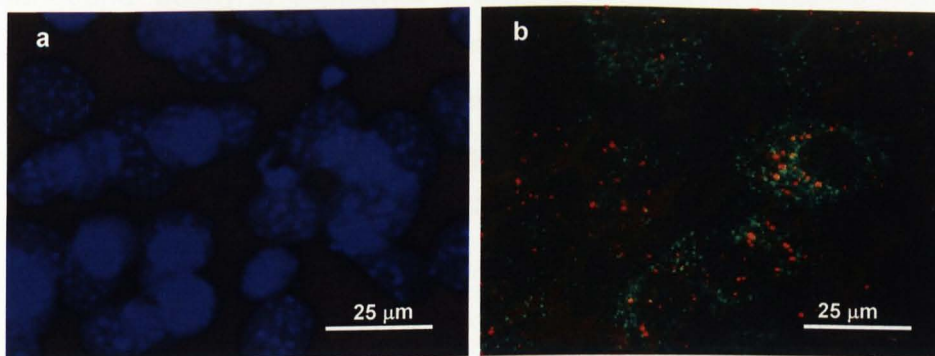


Figure 70. Co-localization of megalin and FBSA. (b) Immunofluorescence staining performed on H6 cells following incubation with FBSA demonstrated a co-localization of FBSA uptake (red) with megalin (green). (a) Nuclei are stained with DAPI.

Figure 70 shows that H6 cells that expressed megalin also presented the punctate staining characteristic of the endocytosis of FBSA. H6 cells that did not express megalin did not display

FBSA uptake (Fig. 70 and data not shown). These results strongly suggest an association between megalin and the uptake of albumin in H6 cells. Overall these findings demonstrated that a subset of the H6 clonal line showed a proximal tubular cell-like phenotype and functionality *in vitro*, as they were able to uptake albumin *via* the megalin receptor. In addition, the endocytosis of albumin could be competitively inhibited in the presence of receptor-associated protein (RAP) or unlabeled bovine serum albumin.

6.2.3.3 Investigating organic anion transporter functionality in the H6 clonal line

The functionality of organic anion transporters (OATs) *in vitro* was initially assessed in E11.5 intact kidney rudiments culture and E11.5 reaggregated kidney rudiments. The protocol for the functional assay is explained in section 2.5.3. The samples were incubated with 6-carboxyfluorescein (6-CF) either in the presence or absence of the competitive inhibitor probenecid. The specimens were also stained with peanut agglutinin (PNA) in order to identify developing epithelial structures (Rosines et al., 2007).

Firstly, the functionality of OATs in E11.5 intact kidney rudiments was assayed by culturing the samples for a period of 4-6 days. The results showed that in E11.5 intact kidney rudiments the organic anion transporters had become active after 4 days of culture, demonstrated by the accumulation of 6-CF into presumptive proximal tubules (Fig. 71, a). After 6 days of culture the uptake of 6-CF into forming proximal tubules was even more pronounced than after 4 days (Fig. 71, c). The presence of probenecid completely inhibited the uptake of 6-CF into presumptive proximal tubules (Fig. 71, b and d).

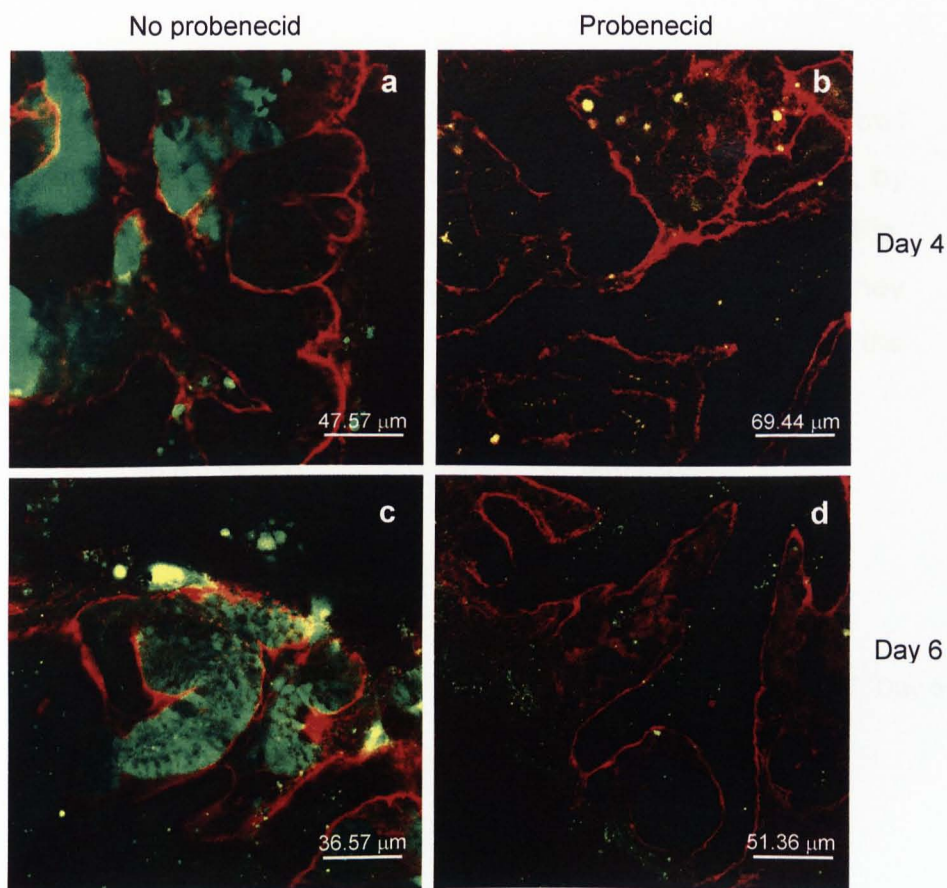


Figure 71. Organic anion transporter (OAT) functionality assay performed on E11.5 intact kidney rudiment. 6-CF (green) had started accumulating into presumptive proximal tubules after 4 days of culture (a), whereas in the presence of probenecid the uptake resulted inhibited (b). Following 6 days of culture the uptake of 6-CF into presumptive proximal tubules through OATs was more pronounced than after 4 days (c). The presence of probenecid blocked 6-CF uptake in specimens cultured for 6 days (d). Developing epithelial structures were stained for peanut agglutinin (PNA) (red).

To investigate whether reaggreated kidney rudiments could form functional proximal-like tubules that were able to uptake 6-CF *via* OATs, E11.5 reaggreated kidney rudiments were incubated with 6-CF following 4-6 days of *in vitro* culture.

It was found that OATs in reaggreated kidney rudiments required a longer culture period to become active compared with intact embryonic kidneys. The specimens were not able to uptake 6-CF after 4 days of culture (data not shown). Figure 72, panel a, shows

that after 5 days of culture a very limited amount of 6-CF (arrow) could be uptaken into presumptive proximal tubules. However, by days, the organic anion transporters had become fully active (Fig. 72, c). As previously observed in intact embryonic kidney rudiments, the uptake of 6-CF was completely blocked in the presence of probenecid (Fig. 72, b and d).

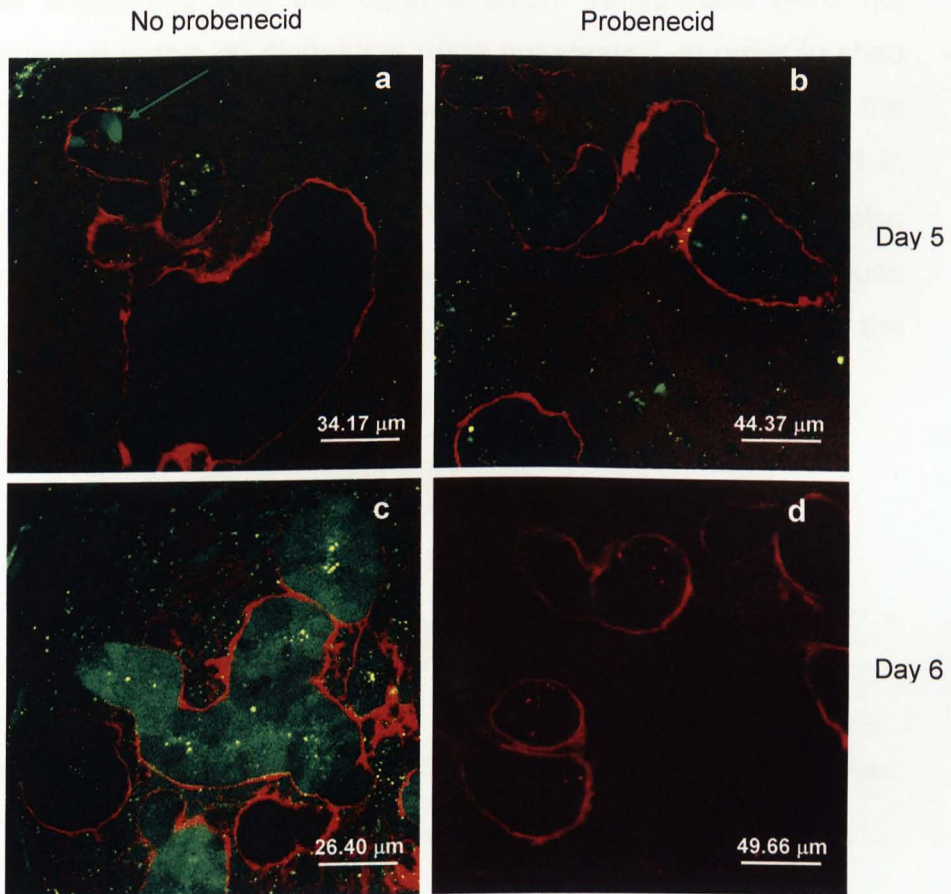


Figure 72. Organic anion transporter (OAT) functionality assay performed on E11.5 reagggregated kidney rudiments. The uptake of 6-CF (green) into developing proximal tubules was very limited after 5 days of culture (a, arrow). Presumptive proximal tubules were able to uptake 6-CF *via* OATs after 6 days of culture (c). In the presence of probenecid 6-CF uptake was completely blocked in reagggregated rudiments after 5 days (b) and 6 days (d) of culture. PNA (red) labeled developing epithelial structures.

6.2.3.4 Investigating the expression of OAT genes in H6 cells

The ability of the H6 clonal line to uptake 6-CF through the organic anion transporters was investigated by recombining H6 cells with E11.5 reaggregated kidney rudiments, using the chimera formation assay (see section 2.2.8.2). The results showed that H6 cells, labelled with quantum dots (QD), did not show 6-CF uptake, thus suggesting that the organic anion transporters were not expressed in the H6 clonal line (data not shown). In order to shed light on this assumption, it was decided to investigate whether the OAT genes *Oat1*, *Oat2*, *Oat3* and *Oat5*, normally expressed in mouse kidney proximal tubules (Van Wert et al., 2010), were also expressed in H6 cells. RNA extracted from postnatal mouse kidney represented the positive control for the presence of the genes examined.

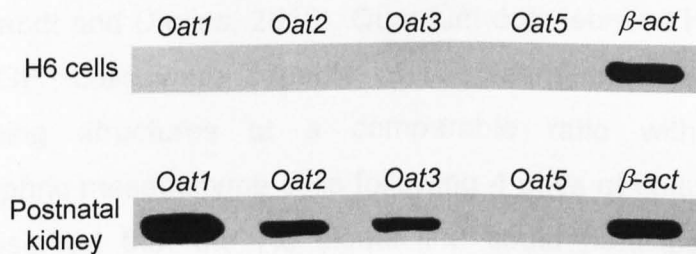


Figure 73. RT-PCR performed on H6 cells and postnatal mouse kidney. β -act: internal control.

The results indicated that none of the OAT genes assayed was expressed in H6 cells. In addition, *Oat5* was not detected in neonatal kidney (Fig. 73).

Overall these results suggest that a fraction of the H6 clonal line displayed a proximal tubular cell-like phenotype as it showed megalin functionality; however, they did not express any of the OAT genes assayed. Since OATs are mainly expressed in the S2

segment of the proximal tubules, whereas megalin is principally expressed in the S1 segment, these findings postulate that the H6 clonal line might be able to give rise to cells present within the first segment of the nephron only.

6.3 Discussion

The H6 clonal line expressed several stem/progenitor cell and MM-specific markers as well as markers for fully differentiated renal cells (see chapter 5 for details). It was therefore hypothesized that the H6 clonal line could contribute to the formation of renal structures. The *in vitro* nephrogenic potential of H6 cells was investigated using the chimera formation assay (Unbekandt and Davies, 2010). Quantum dots-labelled H6 cells or H6 EFGP⁺ cells were capable of integrating into nephron-like developing structures at a comparable ratio with that of metanephric mesenchyme cells following 4 days of culture. It was also observed that the H6 clonal line could participate in the formation of developing proximal tubules as well as developing glomeruli; however, like freshly isolated and cultured MM cells, they did not integrate into the ureteric bud.

Since H6 cells were positive for the proximal tubular markers Aqp1 and megalin, and could participate in the formation of developing proximal tubules, it was hypothesized that a fraction of the H6 cell population might comprise proximal tubular-like cells. A megalin functionality assay demonstrated that the cells were able to uptake fluorescent-conjugated albumin *via* the megalin receptor and that the endocytosis of albumin could be almost completely blocked in the presence of structurally unrelated competitors such as

receptor-associated protein (RAP) or unlabelled albumin. Co-localization of endocytosed albumin with the megalin receptor, determined by immunostaining, confirmed that in H6 cells megalin mediated the uptake of albumin. Although the H6 clonal line displayed a proximal tubular cell-like phenotype, the expression of organic anion transporter (OAT) genes, normally present in kidney proximal tubules, was not detected.

In this work it was hypothesized that the H6 clonal line was a remnant of the embryonic metanephric mesenchyme present in the postnatal mouse kidney. Since all cell types present in the mature nephrons derive from the MM (Kobayashi et al., 2008), it was conceivable that H6 cells retained a nephrogenic potential and were able to participate in the formation of developing nephrons. This assumption was investigated *in vitro* with the chimera formation assay (Unbekandt and Davies, 2010). The results unveiled several analogies between the H6 cell population and MM cells: similarly with MM cells, the H6 clonal line was able to participate in the formation of nephron-like developing structures following recombination with E11.5 reaggregated kidney rudiments. H6 cells were able to integrate into nephron-like developing structures at a ratio of $8.39\% \pm 0.54\%$, which represents a comparable integration capability with that of cultured MM cells. In addition, as with freshly isolated and cultured MM cells, the H6 cells did not integrate into the ureteric bud. However, it was found that the integration ability of the H6 clonal line into developing nephrons was lower than that of freshly isolated MM. This might be due to the fact that, compared with the H6 clonal line, the MM represents a more undifferentiated and homogeneous cell population already committed to generate all cell types present in the nephron. Since the metanephric

mesenchyme does not originate UB-derivatives (Kobayashi et al., 2008; Dressler, 2009; Shah et al., 2009), these results are in agreement with the assumption that the H6 clonal line derived from the nephrogenic mesenchyme. In section 5.2.1.2 and section 5.2.1.4 it was presented that the H6 clonal line did not express the transcription factor Pax2. In my work I was found that, like freshly isolated and cultured MM, some cells within the H6 cell population were able to express Pax2 following recombination with E11.5 reaggregated kidney rudiments. I also showed that the H6 cell population could integrate into developing proximal tubules and developing glomerular-like structures. The ability of the cells to form developing proximal tubules is in accordance with the fact that H6 cells expressed markers for proximal tubules and with the capability of a subset of H6 cells to uptake albumin through the megalin receptor. Moreover, the ability of the cells to integrate into developing glomeruli confirms that some cells within the H6 clonal line displayed a glomerular-like phenotype. This result concords with previous findings from this work showing that H6 cells could give rise spontaneously to cells morphologically similar to podocytes (see section 5.2.1.1), as well as with the fact that H6 cells expressed podocyte-specific markers such as Wt1, synaptopodin and desmin (see section 5.2.1.2 and section 5.2.1.4).

Recently, Siegel and colleagues claimed that a clonal line of human amniotic fluid stem cells (hAFSC) could participate in the formation of renal-like structures following recombination with E11.5 reaggregated kidney rudiments (Siegel et al., 2010). Although the data presented in this study show that cell tracker-labelled hAFSC seemed to be able to integrate into UB structures, the ability of these cells to contribute to the formation of developing nephron-like structures was not entirely convincing.

In this chapter it was also presented that a subset of the H6 clonal line showed functionality, as demonstrated by their ability to uptake fluorescent albumin through the megalin receptor. The punctate staining uniformly distributed within cell cytoplasm indicated that fluorescent albumin had been internalized into endocytic vacuoles. The results also showed that albumin uptake was nearly completely blocked in the presence of either RAP or unlabelled albumin, two structurally unrelated molecules. Similar results were observed by Zhai and co-workers (Zhai et al., 2000). It has been reported that following the binding with its ligands, megalin receptor undergoes a rapid turnover: the receptor is internalized and sorted to endosomes, then it is recycled and returned to the cell surface. The whole cycle completes in about 20 minutes (Maurer and Cooper, 2005). The small amount of fluorescent albumin internalized into H6 cells in the presence of either RAP or unlabelled albumin might be therefore due to the rapid turnover of the megalin receptor.

Kidney proximal tubular cells are characterized by the presence of basolateral and apical organic anion transporters (OATs) that mediate the secretion of a wide spectrum of molecules from the circulatory system into the lumen of proximal tubules (Sweet, 2005; Sweet et al., 2006). The functionality of OATs in embryonic tissues can be assessed *in vitro* by looking at the uptake of the anionic molecule 6-carboxyfluorescein (6-CF) into presumptive proximal tubules. The uptake of 6-CF into developing proximal tubules can be blocked by incubating the tissues with the OATs competitive inhibitor probenecid (Sweet et al., 2006; Rosines et al., 2007). Since the H6 clonal line exhibited features of proximal tubular cells, it was decided to see whether they could uptake 6-CF through OATs. Surprisingly, it was found that none of the OAT

normally present in kidney proximal tubular cells, namely Oat1, Oat2, Oat3 and Oat5, were expressed in the H6 cell population. The expression of OATs in the H6 clonal line could not be induced even in the chimera, as the cells failed to uptake 6-CF following recombination with E11.5 reaggregated kidney rudiments. These results seem to conflict with the proximal tubular cell-like phenotype displayed by a subset of the H6 cell population. However, several studies showed that megalin is mainly expressed in the S1 segment of kidney proximal tubules, which is the subunit responsible for most of the reabsorption of many molecules present in the ultrafiltrate (Casarett et al., 2007; Russo et al., 2007; Nielsen and Christensen, 2010). OATs, on the other hands, are largely localized in the S2 segment of the proximal tubules, which generally mediates proximal tubular secretion (Anzai et al., 2005; Casarett et al., 2007; Hwang et al., 2010). Therefore, these evidences suggest that the H6 clonal line might be capable of giving rise to renal cells normally resident within the first segment of the nephron. It might also be plausible that different factors, such as the procedure followed to isolate the cells or the culture conditions, influenced the expression profile of the H6 cells in such way that the reabsorption machinery represented by megalin (and maybe cubulin) receptor was expressed, whereas the secretion apparatus depicted by organic anion transporters was not present.

Ronconi and colleagues documented that CD24⁺ CD133⁺ human renal progenitor cells, resident at the urinary pole of the Bowman's capsule, acted as bi-potent progenitor cells, as they were capable of generating both tubular-like and podocytes-like cells in culture (Ronconi et al., 2009). The results present in this chapter, together with those showed in chapter 5, unveiled some important

similarities between the H6 clonal line and CD24⁺ CD133⁺ human renal progenitor cells: in fact both cell populations seem to be able to give rise to cells present within the first part of the nephron, namely podocytes and proximal tubular cells.

CHAPTER 7

Investigating the *in vivo* nephrogenic potential of the kidney-derived stem cell H6 clonal line

7.1 Introduction

In chapter 6 it was shown that a subset of the kidney-derived stem cell H6 clonal line was able to differentiate *in vitro* into functional proximal tubular-like cells that could uptake fluorescent albumin through the megalin receptor (see section 6.2.3.1). In addition the chimera formation assay (Unbekandt and Davies, 2010) revealed that the H6 clonal line displayed an *in vitro* nephrogenic potential and was able to integrate into glomerular-like and proximal tubular-like structures, but not into the ureteric bud, following recombination with E11.5 reaggregated kidney rudiments (see section 6.2.1). The ability of the H6 clonal line to integrate into developing nephrons was comparable with that of metanephric mesenchyme cells following 4 days of *in vitro* culture (see section 6.2.2). In the final part of this work the behaviour of the H6 clonal line in an *in vivo* mouse model of induced renal injury has been investigated.

Ischemic insults, sepsis, nephrotoxic agents and hypovolemic states are the most common causes of acute renal failure (ARF), a condition characterized by an abrupt decay in kidney function due to an extensive damage of kidney tubules. In rodents, ARF is normally detected by measuring levels of blood urea nitrogen (BUN) and plasma creatinine, both of which are raised in ARF (Humphreys et al., 2008; Perin et al., 2010).

The kidney has a remarkable capability to recover from acute injury. Recovery appears to be accomplished by endogenous

epithelial cells that rapidly proliferate in response to injury in order to replenish damaged tissues (Humphreys et al., 2008). However, in some circumstances the recovery of the kidney from acute renal failure is inadequate (Schiffl, 2010) and the disease might progress to chronic kidney disease leading to end-stage renal disease (ESRD). Acute renal failure is emerging as a worldwide health problem. The incidence of ARF ranges from 5% of all hospitalized patient to 50% in critical care units (Thadhani et al., 1996; Imberti et al., 2007). It has been reported that approximately 40% of patient affected by ARF fail to completely recover their renal function, with 10% of them requiring renal replacement therapies after 5 years (Sagrinati et al., 2006).

The mouse has become a common model used to study experimental acute renal tubular injury. ARF can be induced in mice as a consequence of an ischemic insult (i.e., ischemic-reperfusion injury) caused by transient occlusion of the renal pedicles (Humphreys et al., 2008). ARF can also be caused by using drugs that target kidney tubules: for instance Morigi and collaborators showed that the antitumor compound cis-diaminedichloroplatinum (cisplatin) can promote ARF following subcutaneous injection in mice (Morigi et al., 2004). Furthermore, kidney tubules undergo extensive damage following intramuscular injection of glycerol: this leads to rhabdomyolysis and the consequent release of myoglobin in the circulation which reaches the kidneys and causes necrosis of tubular epithelial cells. However, this model does not affect glomerular structure (Bussolati et al., 2005; Perin et al., 2010).

Due to the complexity of the kidney, advances in traditional therapeutic treatments have so far been very limited and dialysis

or kidney transplantation still represent the only renal replacement therapies available for patients with ESRD. However, both of these treatments present severe limitations: dialysis cannot fully compensate kidney function, might cause infections and requires significant lifestyle changes (Kitamura et al., 2005; <http://www.kidney.org.uk>); the major drawbacks associated with kidney transplantation are limited organ availability and the requirement for immunosuppressive therapies in order to avoid organ rejection (Kitamura et al., 2005, Knauf and Aronson, 2009).

The use of stem cells as a therapeutic tool might represent an alternative and promising strategy to replenish damaged kidney tissues. Several studies have investigated the ability of different stem cell types to contribute to the amelioration of renal function in mice with acute tubular injury (see section 1.3.2 and Table 2 for more details). Bone marrow-derived mesenchymal stem cells (MSC) have shown to be able to ameliorate renal function in different animal models of ARF (Herrera et al., 2004; Morigi et al., 2004; Herrera et al., 2007). It has also been suggested that the renoprotective effect of MSC might be due to paracrine mechanisms, rather than cell engraftment into damaged tubules (Togel et al., 2005; Imberti et al., 2007).

Stem/progenitor cell populations resident in the adult kidney have also been investigated for their capacity to contribute to the amelioration of kidney damage following acute tubular injury. Bussolati and collaborators demonstrated that CD133⁺ renal progenitor cells isolated from the interstitium of adult human kidney were able to differentiate into non renal lineages, both *in vitro* and *in vivo*. When injected into severe combined immunodeficiency (SCID) mice with glycerol-induced ARF at the

peak of the damage, CD133⁺ cells could engraft into proximal and distal tubules (Bussolati et al., 2005). CD24⁺ CD133⁺ human progenitor cells resident within the Bowman's capsule of adult human kidney were able to improve renal function following acute tubular injury. These cells, inoculated intravenously in SCID mice with glycerol-induced ARF at the peak of renal injury, engrafted mainly inside the tubules and, to a lesser extent, in the interstitium and glomeruli. An appreciable improvement of the renal function compared with saline-injected mice was observed one week after cell inoculation (Sagrinati et al., 2006).

More recently, a population of mouse kidney progenitor cells (MKPC) has proven to have the ability to engraft into renal tubules and capillaries and improve renal function following injection in a mouse model of ischemia-reperfusion-induced acute tubular injury, immediately after the reperfusion (Lee et al., 2010).

The renoprotective ability of human amniotic fluid stem cells (hAFSC) has been investigated in a mouse model of ARF induced by glycerol injection. As discussed in section 1.3.2.5, hAFSC exhibited self-renewal capacity, clonogenic ability, expressed many stem cell markers, and displayed multi-lineage differentiation capability. Following injection into the renal cortex of ARF-induced mice concomitantly with the induction of renal damage, hAFSC were able to engraft into damaged tubules, improve both renal function and morphology, and stimulate tubular cells to undergo proliferation. Interestingly, when the cells were injected into mice at the peak of renal injury, 3 days after glycerol injection, no beneficial effects were observed (De Coppi et al., 2007; Perin et al., 2010). In contrast with these results, Hauser and co-workers demonstrated that hAFSC exerted a renoprotective effect when

inoculated at the peak of renal damage into the tail vein of a SCID mouse model of glycerol-induced ARF (Hauser et al., 2010).

The H6 clonal line might constitute a remnant of the embryonic metanephric mesenchyme present in the postnatal mouse kidney. Renal-specific gene expression profiling showed that the H6 clonal line expressed MM-specific markers and markers normally found in adult kidney (see section 5.2.1.2 and section 5.2.1.4). The H6 clonal line was also shown to have the ability to maintain a nephrogenic potential *in vitro* as it was able to integrate into developing nephrons, glomeruli and proximal tubules following recombination with E11.5 reaggregated kidney rudiments (see section 6.2.1).

In the final part of this work investigations were undertaken to determine whether the nephrogenic potential of the H6 clonal line could also be retained *in vivo*. Since a subset of the H6 clonal line showed a proximal tubular cell-like phenotype (see section 6.2.3), it was decided to explore the *in vivo* nephrogenic ability of the cells using a mouse model of acute renal tubular failure (ARF-induced mice), which was induced by intramuscular injection of glycerol. Enhanced green fluorescent protein (EGFP)-transfected H6 cells (EGFP⁺ H6 cells) were inoculated into the tail vein of ARF-induced mice, at the peak of renal damage, with the purpose to see whether the cells were able to engraft into damaged kidney tubules, ameliorate renal function and stimulate tubular cell proliferation. Previous studies have demonstrated that in mouse the peak of tubular injury, assessed by measuring the levels of blood urea nitrogen (BUN) and serum creatinine, was observed three days after glycerol injection (Zager et al., 2001; Bussolati et al., 2005; Perin et al., 2010; Hauser et al., 2010; Dr. Stefania Bruno, University of Turin, personal communication). Ronconi and

collaborators reported that, following inoculation into the tail vein, some CD24⁺ CD133⁺ adult human renal progenitor cells displayed a non-specific engraftment into the lung of ARF-induced mice (Ronconi et al., 2009). Therefore, a second objective of this work was to determine whether any of the H6 cells colonized non-target organs, such as the lung, spleen or liver, following introduction unto the circulation of ARF-induced mice *via* the tail vein. It was also important to determine whether the H6 clonal line could form tumours when inoculated into mice. This question was answered by subcutaneously inoculating the cells into healthy mice and chasing them for a period of 6 weeks.

7.2 Results

7.2.1 Establishing the acute renal tubular injury model in CD1 mice

As yet, most of rhabdomyolysis-induced acute renal failure studies have been conducted in immunocompromised mice, as the stem/progenitor cell populations investigated have been of human origin (Bussolati et al., 2005; Sagrinati et al., 2006; Lazzeri et al., 2007; Perin et al., 2010). Given that the H6 clonal line originally derived from the out-bred strain CD1, in this work it was elected to use the CD1 mouse strain.

7.2.1.1 Determining the presence of the gene *Sry* in the H6 clonal line

At the beginning of this part of the work it was decided to determine the sex of the H6 clonal line. The reason for this was that if the cells were of male origin, then it would be possible to

detect them in female host tissues using fluorescent *in situ* hybridization (FISH) for the Y chromosome. Sex determination of the H6 clonal line was carried out by searching for the presence of the Y chromosome-specific gene *Sry* (Koopman et al., 1991) by PCR, performed on genomic DNA isolated from H6 and H6 EGFP⁺ cells (see section 2.9.2 and section 2.9.6). Genomic DNA extracted from E13.5 mouse male embryos was used as a positive control for the presence of the *Sry* gene, whereas genomic DNA isolated from E13.5 mouse female embryos DNA was used as a negative control.

The results demonstrated the female origin of the H6 clonal line, as the gene *Sry* was not detected in the genome of H6 cells and H6 EGFP⁺ cells (Fig. 74 and data not shown).

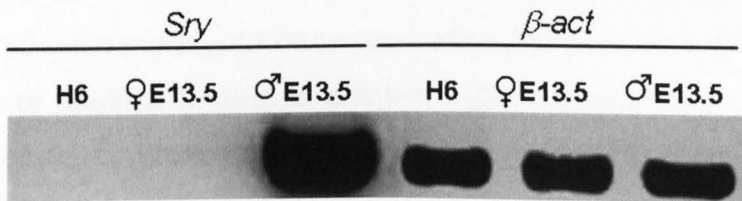


Figure 74. PCR performed on genomic DNA isolated from H6 cells. The PCR demonstrated that the H6 clonal line was of female origin, as the Y chromosome-specific gene *Sry* was not detected. The gene was present in the genome of E13.5 mouse male embryos and absent in the genome of E13.5 mouse female embryos. *β-act*: *b-actin*, reference gene.

It was then decided to use immunohistochemical staining for EGFP to detect H6 EGFP⁺ cells within ARF-induced mouse organs. Male animals were chosen as a previous study conducted on this injury model was carried out with male CD1 mice (Zager et al., 2001).

7.2.1.2 Optimization of glycerol dose in mice

For the purpose of this work it was important to determine the optimal dose of glycerol that would cause acute renal tubular failure in male CD1 mice with minimal mortality. The first attempt was to induce ARF using a dose of 8.5 ml/Kg body weight of glycerol, injected into both hind limbs. The efficacy of this treatment was demonstrated in an earlier study by Zager and colleagues (Zager et al., 2001). Mice were killed at the peak of renal injury, 3 days after glycerol injection. The presence of renal damage was determined by assessing the renal morphology and measuring both BUN and serum creatinine concentration. Basal levels of BUN and creatinine were determined in healthy mice. The results revealed that this dose of glycerol failed to cause ARF in male CD1 mice, as both BUN and creatinine levels of glycerol-injected mice measured three days after injection were similar with those of healthy, untreated animals (data not shown). It was then decided to increase the dose of glycerol to 9 ml/Kg body weight, a condition already investigated by Zager and co-workers (Zager et al., 2008). The results demonstrated that a dose of 9 ml/Kg body weight of glycerol could induce ARF in male CD1 mice. Figure 75 shows the normal morphology of a healthy kidney (a, b) and the typical acute tubular damage caused by intramuscular injection of glycerol (c, d). Compared with healthy organs, ARF-induced mouse kidneys presented extensive tubular damage, brush border disruption, tubular necrosis and protein cast formation (arrows). However, most of glomeruli (G) remained intact.

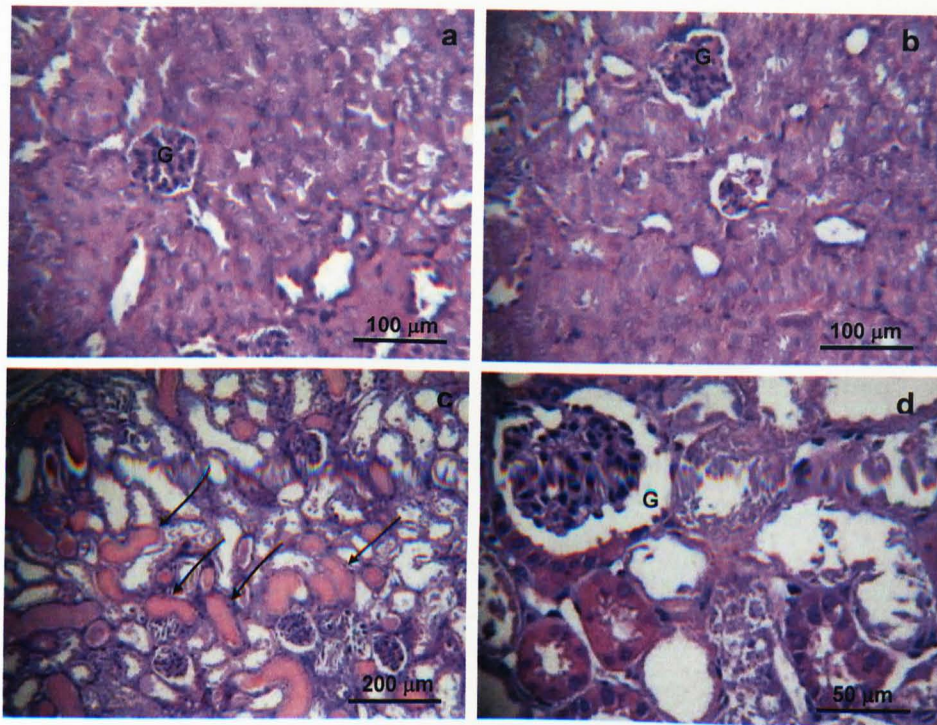


Figure 75. Haematoxylin and eosin staining of paraffin-embedded kidney sections. Control, healthy kidneys presented a normal morphology in which tubules and glomeruli (G) were intact (a, b). Morphological alterations were evident three days after intramuscular injection of 9 ml/Kg body weight of glycerol: renal tubules showed extensive damages with loss of brush border, tubular necrosis and protein cast formation (arrows). Most of glomeruli (G) though, remained intact (c, d).

BUN and creatinine concentration measured in healthy mice ($n=6$) were 23.58 ± 7.03 mg/dL and 0.54 ± 0.10 mg/dL, respectively. BUN concentration was similar with the value of 25-30 mg/dL observed in a previous study (Zager et al., 2001). The levels of these biomarkers significantly increased three days after intramuscular injection of 9 ml/Kg body weight of glycerol: in ARF-induced mice ($n=6$) BUN concentration rose to 90.64 ± 37.24 mg/dL (Student's t-test: $P < 0.05$) whereas creatinine concentration reached 2.12 ± 1.21 mg/dL (Student's t-test $P < 0.05$) (Fig. 76).

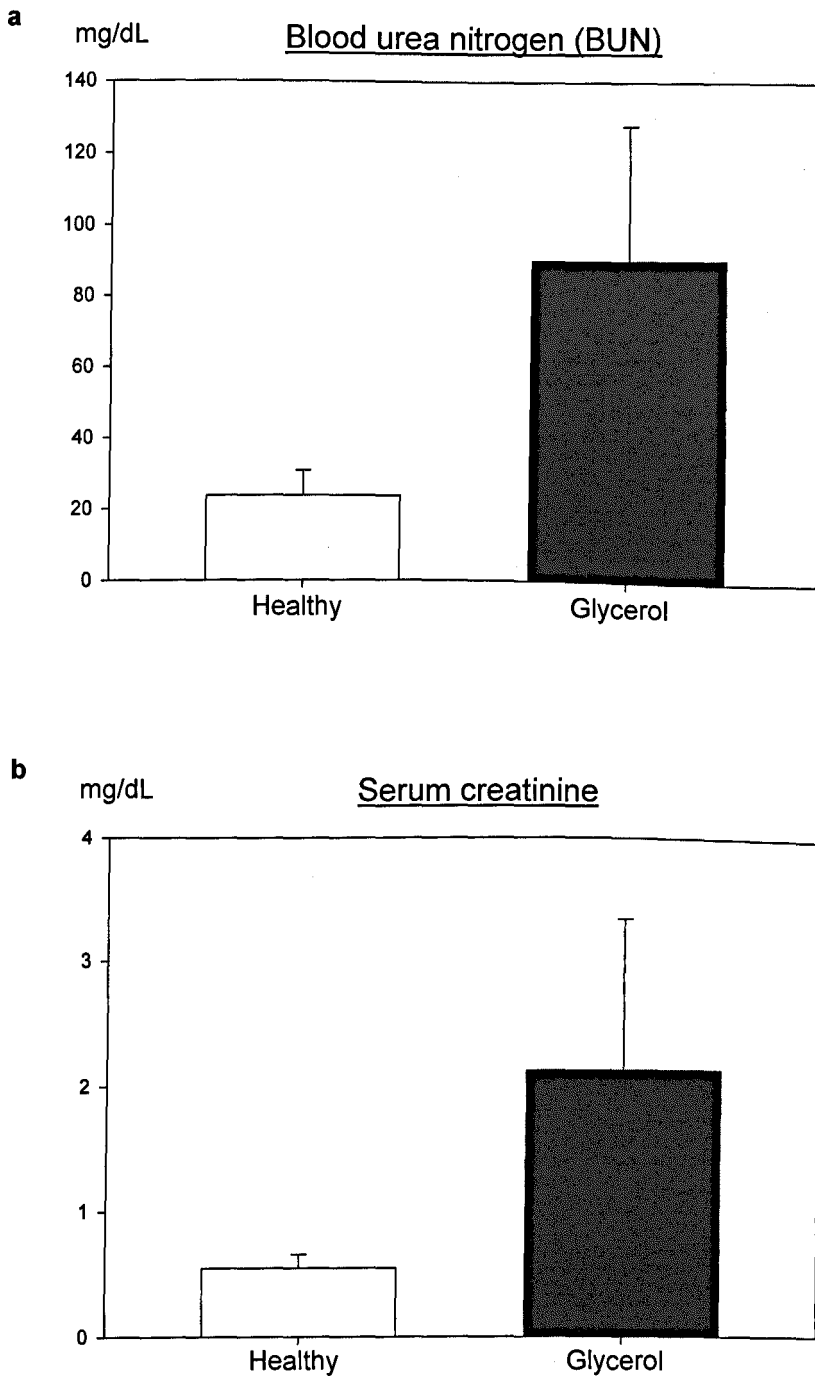


Figure 76. Blood urea nitrogen (BUN) (a) and serum creatinine (b) concentrations measured in healthy mice (n=6) and in ARF-induced mice three days after injection of 9 ml/Kg body weight of glycerol (n=6). Both BUN and creatinine concentrations were significantly higher in ARF-induced mice compared with healthy animals (Student's t-test: $P < 0.05$). Error bars indicate standard deviations of the means.

However, it was observed that a rather high mortality rate accompanied the increased dose of glycerol, as 5 out of 15 ARF-induced mice died within 3 days of the induction of damage. Given that the lower dose of glycerol did not induce ARF, it was decided to continue this study using a dose of glycerol of 9 ml/Kg/body weight.

7.2.2 Investigating the ability of the H6 clonal line to engraft into ARF-induced mouse kidneys

The ability of the H6 clonal line to engraft into kidneys with acute tubular injury was investigated by inoculating 8×10^5 H6 EGFP⁺ cells, resuspended in 150 μ l of PBS, into the tail vein of glycerol-induced ARF mice, three days after the induction of damage. Animals were killed 2, 5 and 9 days after cell inoculation. Since previous studies have documented that the mouse kidney nearly completely recovers from acute injury after 2 weeks from the initial damage (Zager et al., 2001; Perin et al., 2010), in the present study mice were killed 12 days after glycerol injection as the latest time point. Controls comprised mice that were injected with glycerol, then inoculated with 150 μ l of sterile PBS and examined together with H6 EGFP⁺ cell-injected mice (see section 2.6.3). The strategy followed to inoculate the cells into ARF-induced mice is illustrated in Figure 77.

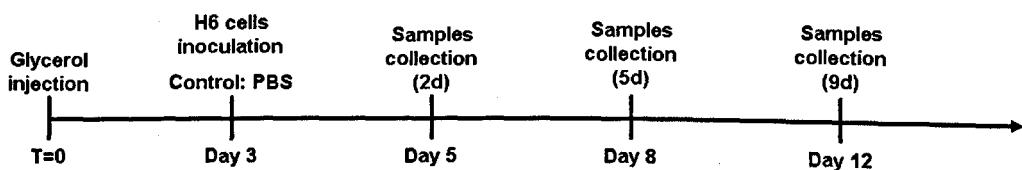


Figure 77. Strategy followed to investigate the ability of the H6 clonal line to engraft into and participate in the recovery of ARF-induced mouse kidneys. H6 EGFP⁺ cells were inoculated into the tail vein of ARF-induced mice three days after intramuscular injection of glycerol into the hind limb muscles. The animals were killed 2, 5 and 9 days following cell inoculation. Control animals were injected with sterile PBS.

The renal damage was evaluated by measuring both BUN and creatinine concentration in ARF-induced mice when they were killed (see section 2.6.4). Since the EGFP signal was never detectable after sample preparation, the first attempt to detect H6 EGFP⁺ cells engrafted into glycerol-induced ARF mouse kidneys was by using immunofluorescence staining for GFP. However, it was observed that damaged kidneys showed a very high level of autofluorescence (data not shown). Therefore, it was decided to detect H6 EGFP⁺ cells by chromogenic immunohistochemistry (see section 2.8.6).

7.2.2.1 Immunohistochemical staining to detect the presence of H6 cells in host kidney

Immunohistochemistry results showed that H6 EGFP⁺ cells (arrows) were able to reach the kidney and could be detected at 2, 5 and 9 days after inoculation into the tail vein of ARF-induced mice (Fig. 78, a-f). Moreover, it was observed that the cells did not engraft either in the interstitium, or inside glomeruli (G) (Fig. 78, a-f and data not shown).

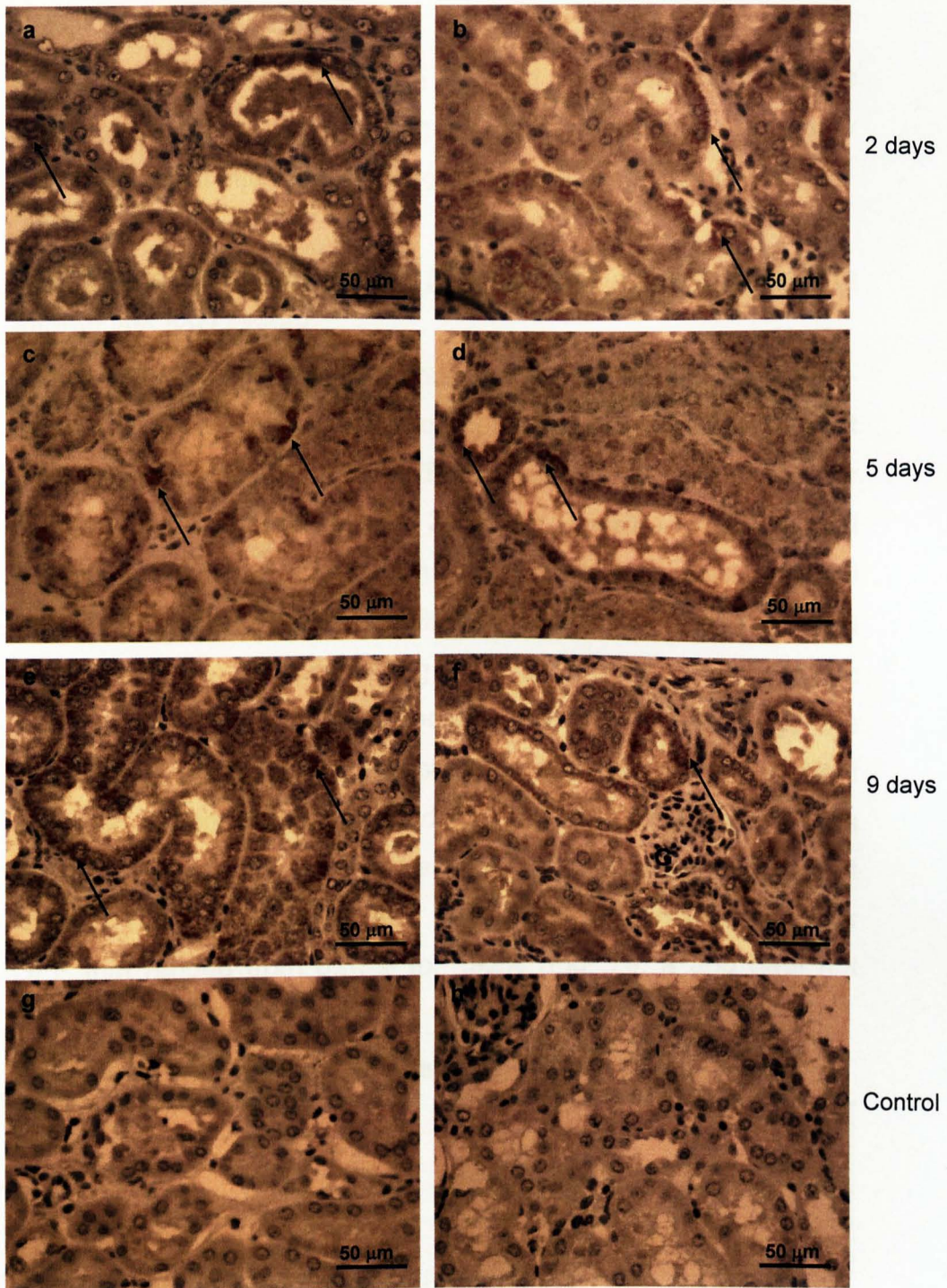


Figure 78. Immunohistochemical staining for EGFP performed on paraffin-embedded kidney sections of ARF-induced mice. The staining demonstrated the presence of H6 EGFP⁺ cells (arrows) engrafted into damaged tubule 2 (a, b), 5 (c, d) and 9 (e, f) days after cell inoculation. No cells were found either in the interstitium or inside glomeruli (G). (g, h) Section of PBS-injected ARF-induced kidneys (Control) did not show any unspecific staining for EGFP.

Sections of kidneys injected with PBS did not show any unspecific EGFP staining (Fig. 78, g and h). Negative control, where primary antibody was omitted, did not show any staining (data not shown).

7.2.2.2 Cytofluorimetric analysis to confirm the ability of H6 cells to engraft into host kidney

In order to confirm the presence of H6 EGFP⁺ cells in ARF-induced mouse kidneys, cytofluorimetric analysis was carried out on single-cell disaggregated ARF-induced kidneys two days after cell inoculation (see section 2.7.2 for details). PBS-injected kidneys were used as control. The results showed a positive signal for GFP that ranged from 0.15% to 3.88% (n=4) (Fig 79, b and data not shown), thus indicating the engraftment of H6 cells into cell-inoculated ARF-induced mouse kidneys. Interestingly, the sample that showed the highest percentage of cell engraftment was also the most damaged kidney, as indicated by blood urea nitrogen (BUN) and serum creatinine concentrations (data not shown). Control samples (n=2) showed an unspecific signal for GFP that ranged from 0.67% to 1.92% (Fig. 79, a and data not shown).

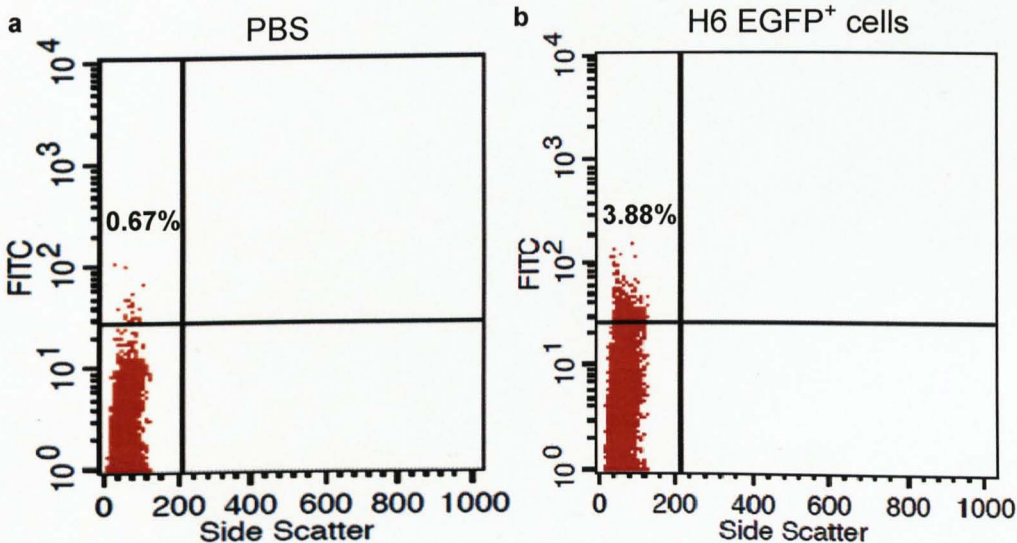


Figure 79. Flow cytometry analysis performed on single-cell disaggregated ARF-induced mouse kidneys. (b) H6 EGFP⁺ cells were present into cell-inoculated kidneys (n=4). The highest percentage of integrated cells was 3.88%. (a) Kidneys injected with PBS (n=2) showed an unspecific EGFP signal.

7.2.3 Investigating the unspecific engraftment of the H6 clonal line

In this work it was important to clarify whether following inoculation into the circulation of ARF-induced mouse, the H6 cells engrafted in other organs than the kidney. In order to check for unspecific cell engraftment, small pieces of lung, spleen and liver of cell-inoculated ARF-induced mice were analysed by immunohistochemistry to detect the presence of EGFP⁺ cells (see section 2.8.7). As control, PBS-injected animals were used. Immunohistochemical staining demonstrated the absence of H6 EGFP⁺ cells within lung, spleen and liver of ARF-induced mice treated with cells (Fig. 80. b, d, f) which indicated that the H6 clonal line was able to engraft only into the kidney. Control tissues did not show any background signal (Fig. 80, a, c, e). Negative controls, where the primary antibody was omitted, did not show any staining (data not shown).

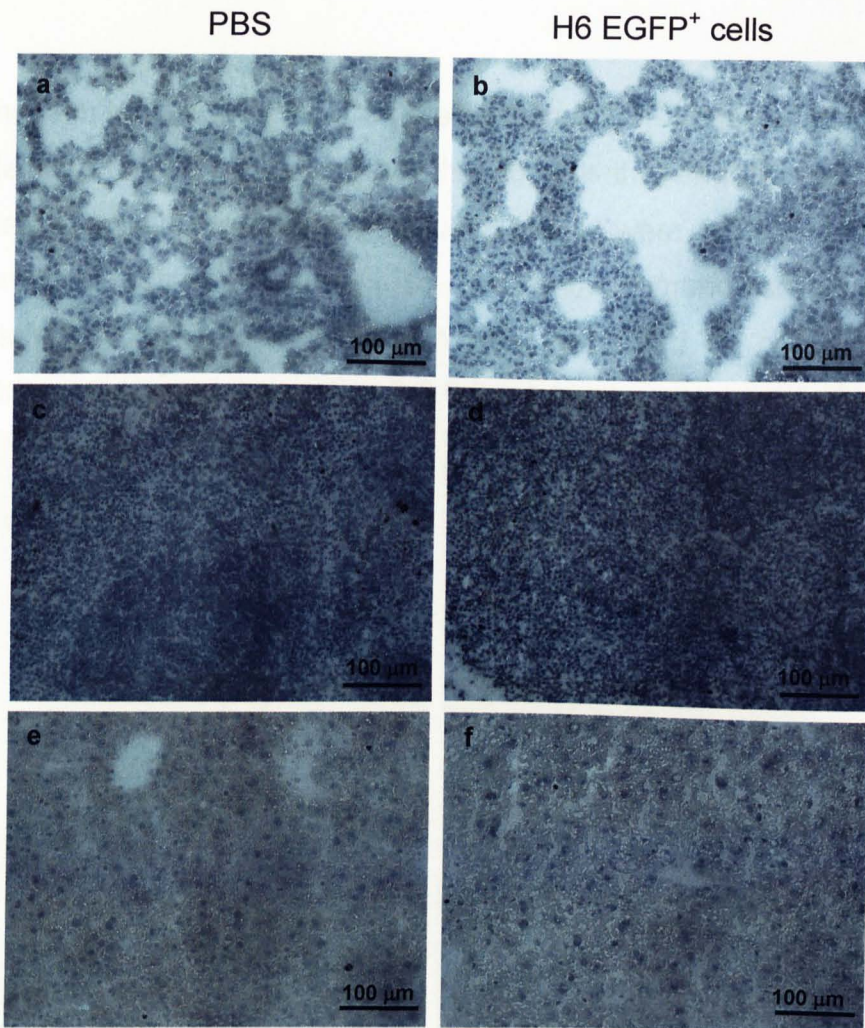


Figure 80. Immunohistochemical staining for EGFP performed on frozen sections of lung (a, b), spleen (c, d) and liver (e, f) of ARF-induced mice. EGFP⁺ cells did not engraft into these organs (b, d, f). Organs dissected from PBS-injected ARF-induced mice (control) did not present unspecific staining for EGFP (a, c, e).

7.2.4 Investigating the ability of the H6 clonal line to differentiate into renal tubular cells

In chapter 5 and chapter 6 it was shown that the H6 clonal line could give rise to proximal tubular-like cells that expressed markers for proximal tubules, such as Aqp1 and megalin (see section 5.2.1.2 and section 5.2.1.4), were able to integrate into developing proximal tubules following recombination with reaggregated kidney rudiments (see section 6.2.1) and showed

megalyn functionality *in vitro* (see section 6.2.3). In this work it was decided to investigate whether the H6 cells that engrafted into the damaged tubules following induced injury, were able to adopt a proximal tubule cell fate. To this end, immunohistochemical staining for EGFP and megalyn was performed on consecutive kidney sections (see section 2.8.6 for details).

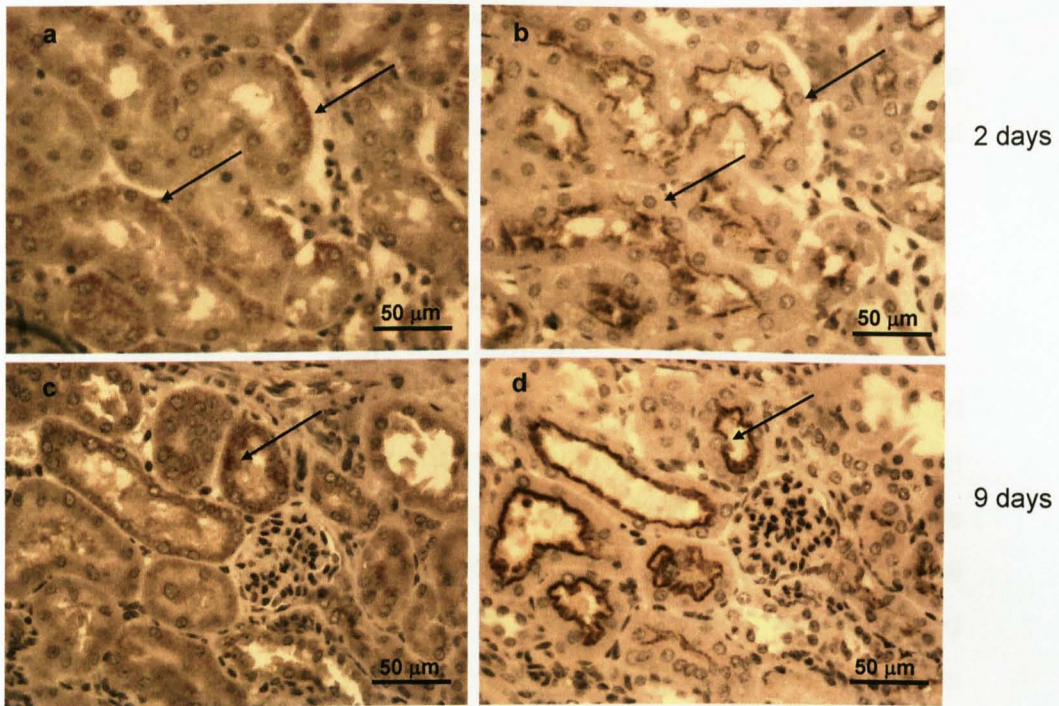


Figure 81. Immunohistochemical staining for EGFP and megalin performed on consecutive paraffin-embedded kidney sections of ARF-induced mice. H6 EGFP⁺ cells (arrows in a and c) were able to engraft into damaged kidney proximal tubules, and appeared to differentiate to form proximal tubule cells, as evidenced by the fact that they expressed megalin at their apical surface (arrows in b and d). Kidneys were dissected 2 and 9 days after cell inoculation.

The results showed that most, if not all, H6 EGFP⁺ cells (arrows in Fig. 81, a and c) that engrafted into proximal tubules expressed megalin, which was localized to the apical surface of the cells (arrows in Fig. 81, b and d). The negative control, in which megalin

antibody was omitted, did not show any positive staining (data not shown).

These findings demonstrated that the H6 EGFP⁺ cells that engrafted into the proximal tubules appeared to have differentiated to proximal tubule cells, as evidenced by the fact that they expressed megalin that was localized to their apical surface. These megalin-positive cells were still detectable up to 9 days (the latest time point tested) after inoculation into the tail vein of glycerol-induced ARF-mice.

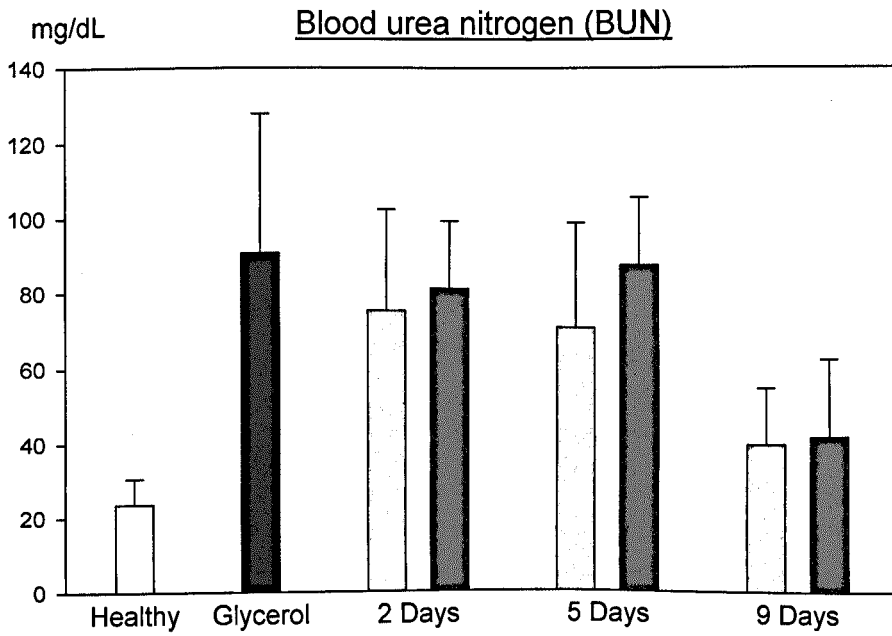
7.2.5 Evaluating the renal function of ARF-induced mice following H6 EGFP⁺ cells inoculation

To determine whether the presence of H6 EGFP⁺ cells could contribute to the improvement of renal physiology of ARF-induced mice, both blood urea nitrogen (BUN) and serum creatinine concentrations were determined 2, 5 and 9 days following cell inoculation (see section 2.6.4); these levels were then compared with those determined in PBS-injected ARF-induced mice. Results are shown in Table 19 and Figure 82.

Table 19. Blood urea nitrogen (BUN) (mg/dL) and serum creatinine concentrations (mg/dL) measured in healthy and ARF-induced mice. The animals were inoculated with 8×10^5 H6 EGFP⁺ cells or injected with 150 μ l of PBS and the levels of BUN and serum creatinine measured after 2 (n=12 for experimental animals, n=8 for control animals), 5 (n=6 for experimental animals, n=3 for control animals) and 9 days (n=3 for both experimental and control animals). Healthy: no renal damage; Glycerol: BUN and serum creatinine were measured 3 days after the induction of renal damage. Results are expressed as mean \pm standard deviation of BUN and serum creatinine concentrations.

	Healthy	Glycerol	2 Days		5 Days		9 Days	
			H6 EGFP ⁺ cells	PBS	H6 EGFP ⁺ cells	PBS	H6 EGFP ⁺ cells	PBS
BUN	23.5 \pm 7.0	90.6 \pm 37.2	75.1 \pm 27.3	81.0 \pm 18.2	71.0 \pm 28.1	87.8 \pm 18.1	40.1 \pm 14.9	41.9 \pm 20.7
Serum creatinine	0.5 \pm 0.1	2.1 \pm 1.2	1.1 \pm 0.4	1.0 \pm 0.4	0.8 \pm 2.4	0.9 \pm 0.3	0.5 \pm 0.1	0.4 \pm 0.1

a



b

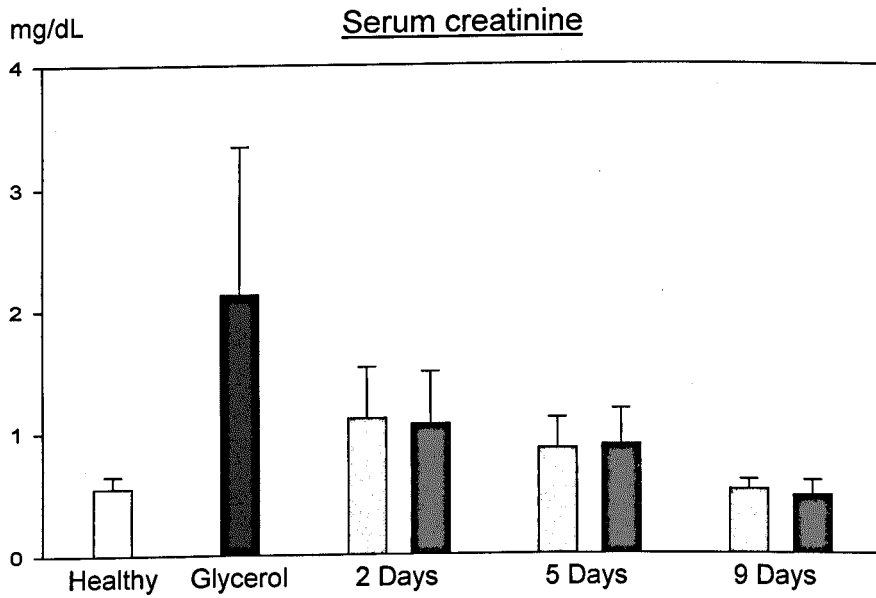


Figure 82. Evaluation of renal function in healthy and ARF-induced mice. Blood urea nitrogen (BUN) (a) and serum creatinine (b) concentrations measured in healthy mice (white bars), in ARF-induced mice three days after glycerol injection (black bars), and in ARF-induced mice that were inoculated with 8×10^5 H6 EGFP⁺ cells (light gray) or injected with PBS (dark gray) after 2, 5 and 9 days. Three days after glycerol injection BUN and creatinine levels were considerably higher in ARF-induced mice than in healthy animals (Student's t-test, $P < 0.05$). The results show that by the 12th day after glycerol injection (i.e. 9 days following stem cell or PBS injection), BUN and serum creatinine levels had almost returned to baseline levels ($n=3$ in each group studied) (ANOVA, $P > 0.05$). The levels of BUN and serum creatinine in animals inoculated with H6 EGFP⁺ cells were not significantly lower than in control animals at all time points studied; i.e. day 2 ($n=12$ for experimental animals, $n=8$ for control animals); day 5 ($n=6$ for experimental animals, $n=3$ for control animals) or day 9 ($n=3$ for both experimental and control animals) (Student's t-test, $P > 0.05$). Error bars indicate the standard deviations of the means.

As shown in section 7.2.1.2, the injection of glycerol significantly raised both BUN and serum creatinine levels compared with healthy animals (Fig. 76). The results, showed in Figure 82, documented that the renal function of glycerol-induced ARF-mice improved throughout the period studied and that ARF-induced mouse kidneys showed a functional recovery 12 days after glycerol injection, as both BUN and creatinine levels were comparable with the concentrations measured in healthy animals (ANOVA, $P > 0.05$). However, it was also observed that at each time point investigated, the presence of H6 EGFP⁺ cells did not lead to an appreciable improvement of the renal function compared with animals injected with PBS (Student's t-test between animal groups, $P > 0.05$).

7.2.6 Determining the proliferative activity of ARF-induced mouse kidney tubular cells

The proliferative activity of ARF-induced mouse kidney tubular cells was evaluated 2, 5 and 9 days after H6 EGFP⁺ cell inoculation or PBS injection by counting the number of either 5-bromo-2-deoxyuridine (BrdU) or PCNA positive cells present in the renal tubules of ten randomly chosen microscope fields of the renal cortex observed at 400 X magnification (see section 2.6.5 for details) (Fig. 83). Both BrdU and PCNA staining results, expressed as number of positive cells, indicated that the proliferative activity of ARF-induced kidney tubular cells progressively decreased throughout the period investigated. Although the results were not significantly different (Student's t-test between animal groups, $P > 0.05$), the numbers of proliferating tubular cells appeared to be higher in H6 EGFP⁺ cell-inoculated mice compared with PBS-injected animals (Fig. 84).

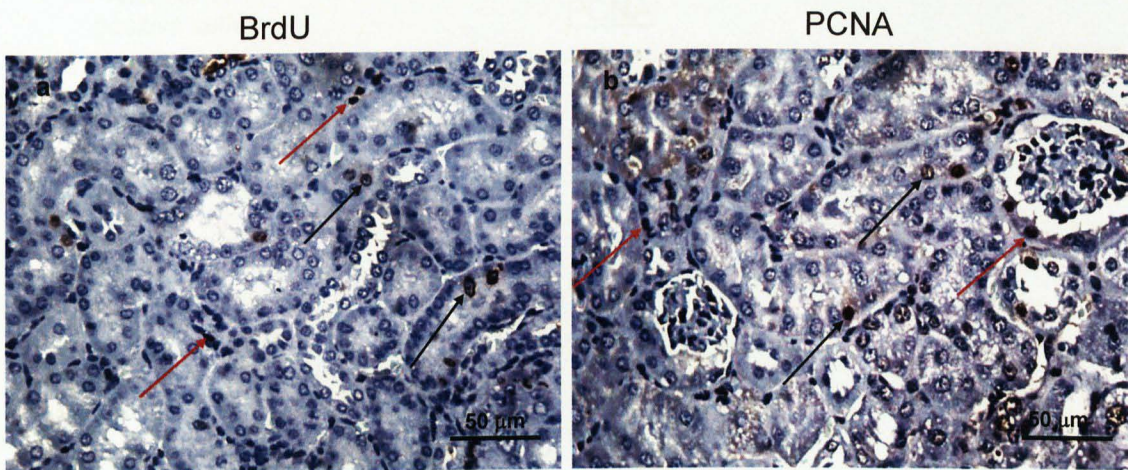


Figure 83. Immunohistochemical staining for BrdU and PCNA performed on paraffin-embedded kidney sections of ARF-induced mice. Black arrows indicate BrdU-positive (a) or PCNA-positive (b) tubular cells. Red arrows point to interstitial or glomerular cells positive for either BrdU (a) or PCNA (b). The figures are representative of an ARF-induced mouse killed 2 days after cell inoculation.

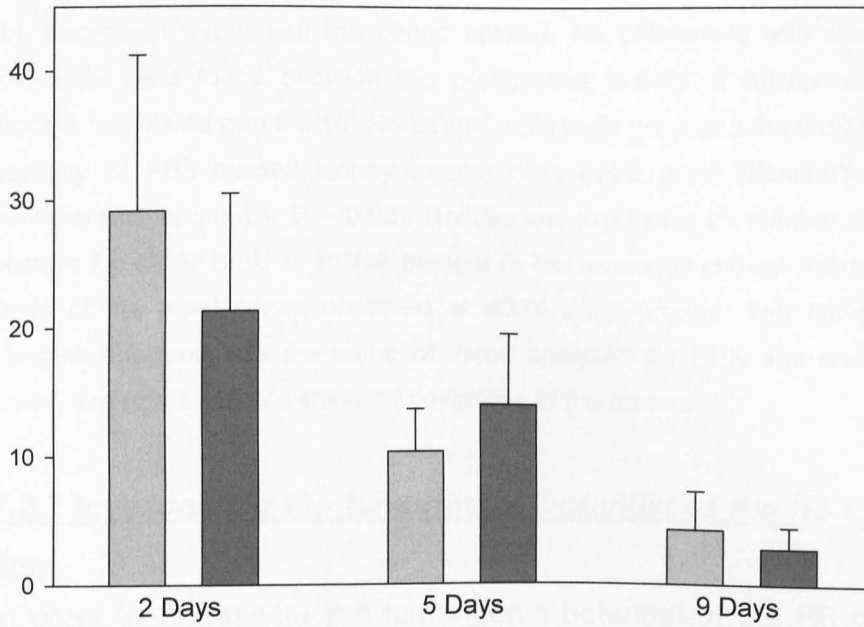
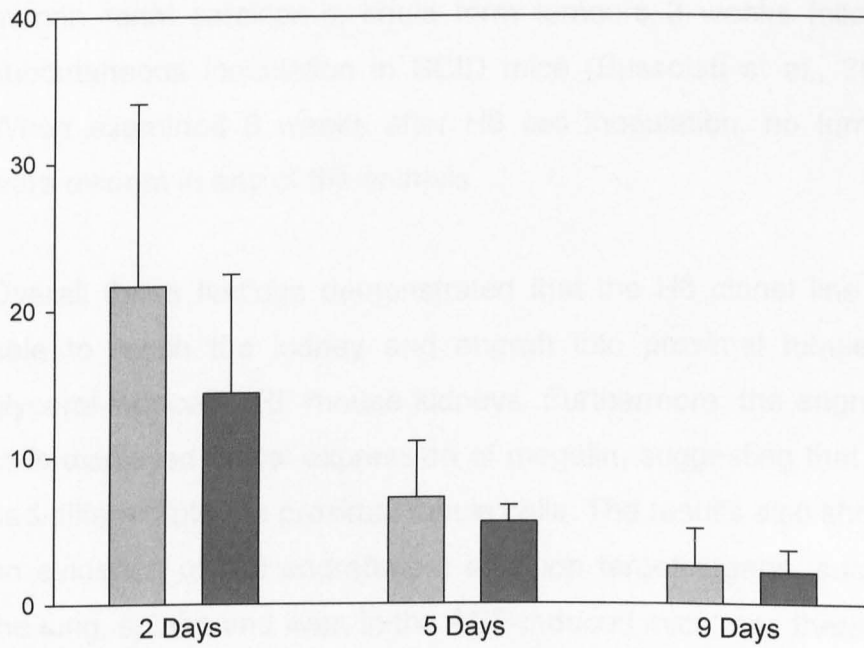
aNumber of
positive cells5-bromo-2-deoxyuridine (BrdU)**b**Number of
positive cellsPCNA

Figure 84. Evaluation of tubular cell proliferation in ARF-induced mice. The proliferative activity of ARF-induced mouse kidney tubular cells, assessed by immunohistochemical staining for 5-bromo-2-deoxyuridine (BrdU) (a) and PCNA (b), decreased throughout the period studied. No differences with statistical relevance were found between the proliferative activity of tubular cells of kidneys inoculated with 8×10^5 H6 EGFP⁺ cells (light grey) and the proliferative capacity of PBS-injected kidney tubular cells (dark grey) (Student's t-test between animal groups, $P > 0.05$). Results are expressed as number of cells positive for either BrdU or PCNA present in ten randomly chosen microscope fields of the renal cortex observed at 400X magnification. The number of samples analysed was the same of those analysed for BUN and creatinine levels. Error bars indicate standard deviations of the means.

7.2.7 Investigating the tumorigenic potential of the H6 clonal line

In order to investigate the tumorigenic potential of the H6 clonal line, in this work it was decided to subcutaneously inoculate 2×10^6 H6 EGFP⁺ cells in healthy mice ($n=5$) (see section 2.6.6). An earlier study demonstrated that a tumorigenic line, derived from human renal carcinoma, could form tumours 3 weeks following subcutaneous inoculation in SCID mice (Bussolati et al., 2008). When examined 6 weeks after H6 cell inoculation, no tumours were evident in any of the animals.

Overall these findings demonstrated that the H6 clonal line was able to reach the kidney and engraft into proximal tubules of glycerol-induced ARF-mouse kidneys. Furthermore, the engrafted cells displayed apical expression of megalin, suggesting that they had differentiated to proximal tubule cells. The results also showed no evidence of cell engraftment into non target organs, such as the lung, spleen and liver, in the ARF-induced mice, and there was no evidence that the H6 cells were capable of forming tumours. However, the presence of H6 EGFP⁺ cells in the injured kidneys

did not reduce the levels of BUN and serum creatinine, and although the presence of H6 cells appeared to increase tubular cell proliferation in the initial stages of injury, the number of BrdU⁺ and PCNA⁺ cells in injured kidneys was not significantly higher in the cell-inoculated group compared to controls.

7.3 Discussion

The nephrogenic ability of the H6 clonal line was investigated *in vivo* using a mouse model of acute renal failure (ARF), which was induced by intramuscular injection of glycerol into the hind limb muscles. In this work it was decided to inoculate 8×10^5 H6 EGFP⁺ cells into the tail vein of ARF-induced mice at the peak of renal injury (Zager et al., 2001; Bussolati et al., 2005; Perin et al., 2010; Hauser et al., 2010; Bruno, University of Torino, personal communication), with the aim of seeing whether the cells were able to engraft into their target organ, the kidney, differentiate appropriately and improve kidney function following an acute insult. Immunohistochemical staining and cytofluorimetric analysis demonstrated that H6 EGFP⁺ cells were able to reach the kidney, engraft into proximal tubules and display a correct spatial expression of megalin, which was found on the apical surface of the tubules. The cells were detected at the latest time point investigated (9 days following inoculation) and were not detected in non-target organs, such as the lung, spleen and liver, suggesting that engraftment only occurred in the kidney. Kidney functionality analysis suggested that the H6 clonal line was not able to accelerate the recovery of the kidney throughout the period studied, compared with PBS-injected animals. In addition, the

number of proliferating kidney tubular cells did not significantly increase following H6 EGFP⁺ cell engraftment. Last but not least, the H6 clonal line did not show any tumorigenic activity when subcutaneously injected for 6 weeks into healthy mice.

Intramuscular injection of glycerol induces an acute renal tubular damage due to rhabdomyolysis and the consequent release of myoglobin from muscles. In this work it was initially decided to induce ARF in male CD1 mice by intramuscular injection of 8.5 ml/Kg/body weight of glycerol, as previously reported by Zager and colleagues in a study carried out on the same mouse strain (Zager et al., 2001). However, I observed that this dose of glycerol failed to induce ARF in the animals used, as both blood urea nitrogen (BUN) and creatinine levels measured in ARF-induced mice were similar with those of healthy animals. It was therefore decided to increase the dose of glycerol to 9 ml/Kg/body weight, a condition already assessed (Zager et al., 2008). I documented that the increased dose of glycerol could induce ARF in male CD1 mice, as shown by both morphological and functional studies. However, I also observed that the CD1 mouse strain was particularly sensitive to the increased dose of glycerol, as two main problems were encountered: firstly, the functional studies demonstrated that the renal damage was highly variable, with some animals being only slightly damaged and others being strongly affected. Secondly, a high mortality rate was observed, as 25% of the animals used in this study died following glycerol injection. Most of the deaths occurred within 5 days from the injection of glycerol, which approximately corresponded with the peak of renal injury. Since the animals were housed according with standard conditions and the induction of the damage was carried out using well-established protocols, in this work it was not

possible to find out what caused such a large variation in the degree of the renal damage among different animals. Nevertheless, this variability has been already observed by Zager and colleagues in two earlier studies (Zager et al., 2001; Zager et al., 2008), which suggests that the CD1 mouse strain might not represent the ideal genetic background to study the effects of glycerol-induced acute renal failure. It has also been postulated that the age of mice might influence the severity of renal damage following glycerol injection. In fact 3-4 week old male CD1 mice appeared to be more resistant to glycerol-induced ARF than 9-10 week old mice. Interestingly, 5-6 week old mice, that represented an intermediate time frame between the injury-resistant phenotype and the injury-sensitive phenotype, displayed the greatest variability in the severity of renal damage, compared with the other two age groups (Zager et al., 2008). Given that in the present study 5-8 week old mice were used, it is possible that some of the mice were more sensitive to glycerol injection and showed a higher variability of the degree of renal damage than other animals. The high mortality rate may be due to the strong insult given by the intramuscular injection of glycerol, which not only induces ARF but also causes a serious muscular injury. Indeed, in some cases, the animals died within 6 hours after the injection of glycerol, suggesting that either the muscular injury or the anaesthesia, or the combined effect of these two agents, might have been the main cause of death, as renal function would not be greatly affected at this time point. Due to the seriousness of the glycerol treatment, in future a different strategy to induce acute renal failure in mice might be preferred. The folic acid (FA) model, for instance, might represent a valid alternative since following intraperitoneal injection, it induces transient ARF which also progresses to chronic kidney disease (Long et al., 2008). In

addition, folic acid appears to induce a more reproducible kidney injury than glycerol, which is accompanied by a very low mortality rate of < 5% (Long et al., 2001).

The ability to engraft into a target organ or tissue represents a critical feature for a stem/progenitor cell population. In this work it was decided to inoculate 8×10^5 H6 EGFP⁺ cells, as it represented a number very close to the single injection of 7.5×10^5 of adult human CD24⁺ CD133⁺ renal progenitor cells inoculated by Ronconi and colleagues in SCID mice (Ronconi et al., 2009). The animals were inoculated at the peak of renal injury, as it was decided to follow a protocol which had been well-established in the laboratory where these studies were carried out. I observed that following inoculation into the circulatory system of ARF-induced mice, the H6 clonal line was able to reach the kidney and engraft mostly, if not exclusively, into proximal tubules for up to 9 days (the latest time point tested), as immunohistochemical staining for EGFP and megalin demonstrated. Engrafted cells expressed megalin on the apical surface of proximal tubules, thus showing a correct spatial expression of this receptor (Zhai et al., 2000). Flow cytometry analysis confirmed the engraftment of H6 EGFP⁺ cells into ARF-induced kidneys 2 days after cell inoculation, with the percentage of integration ranging from 0.15% to 3.88%. Interestingly, the highest and the lowest percentages of cell engraftment were found in the most injured and less injured animals, respectively. Although these results confirmed the presence of H6 cells in ARF-induced kidneys, it cannot be concluded that in the animal model studied the cell engraftment increases as the renal damage worsens. In fact flow cytometry showed that also kidneys injected with PBS gave an unspecific EGFP signal which ranged between 0.67% and 1.92%. Since this

variable background signal was most likely due to the presence of dead host cells and/or host cell debris within the cell suspension analysed by flow cytometry, it is conceivable that such variable background also affected the analysis of cell-inoculated ARF-induced kidneys.

As expected, no EGFP-expressing cells were found inside glomeruli. This was most likely due to the fact that the ARF model used in this study did not damage or alter the glomerular structure (Perin et al., 2010). Moreover, the absence of H6 EGFP⁺ cells within ARF-induced mouse lung, spleen and liver confirms the lack of unspecific cell engraftment and hints that the H6 clonal line might be fully committed to engraft into the kidney. This represents a remarkable feature of the H6 clonal line, as the engraftment into a non-target organ might induce the cells to differentiate into distinct cell lineages with the consequent formation of ectopic tissues that can compromise organ functionality. Since no EGFP-expressing cells were found within organ sections analysed by immunohistochemical staining, in order to confirm the absence of non-specific H6 cell engraftment in future it would be important to analyse these organs by performing PCR for the EGFP sequence. These findings, together with the chimera formation assay and the *in vitro* functional studies, strongly support the assumption that a fraction of the H6 clonal line exhibited a proximal tubular cell-like phenotype, which could therefore be committed to contribute to kidney proximal tubule regeneration after injury. Further analysis may elucidate the percentage of inoculated cells that can engraft into kidney proximal tubules of ARF-induced mice; besides, it would be of great interest to investigate how long the cells can persist into the kidney.

As reported in section 1.3.2, several stem/progenitor cell populations, both from human and mouse origin, have shown the ability to improve the recovery of mouse kidney with acute tubular failure following engraftment into damaged tubules (Morigi et al., 2004; Herrera et al., 2004; Sagrinati et al., 2006; Lazzeri et al., 2007; Lee et al. 2010; Perin et al., 2010). Although the H6 clonal line was able to reach the kidney and engraft into proximal tubules, as cytofluorimetric analysis and immunohistochemical staining show, it was observed that the presence of H6 EGFP⁺ cells could not appear to improve the recovery of damaged kidneys, compared with animals injected with PBS. It might be hypothesized that the H6 clonal line was able to induce some beneficial effects on injured kidneys, however these effects might have been masked by the high variability of the severity of renal damage. Recently, Perin and colleagues documented that hAFSC were capable of improving renal function of ARF-induced immunocompromised mice when injected into the renal cortex a few hours after the induction of renal damage. Interestingly, these authors observed that hAFSC did not have any renoprotective effect when mice were treated at the peak of renal injury, thus demonstrating that the timing of cell inoculation was critical (Perin et al., 2010). It might therefore be speculated that the timing of H6 EGFP⁺ cell inoculation into male CD1 mice was crucial as well, and that the H6 clonal line might not be able to induce any functional improvement when inoculated at the peak of injury, a condition characterized by extensive renal tubular damage. Nevertheless, the cells might be able to exert a renoprotective effect when administered in ARF-induced mice concurrently at the induction of the renal damage. It would therefore be of great interest to investigate these aspects in future by treating the mice with the cells contemporaneously with the induction of renal

damage. In the present study the effect of the H6 clonal line on ARF-induced mouse kidneys was assessed on the basis of two biochemical parameters only, BUN and serum creatinine concentrations. In order to better understand the effect of H6 cells on ARF-induced mouse kidneys, besides assessing the renal function, in future it would be important to perform a morphological analysis of injured kidneys by using histochemical parameters (Long et al., 2008).

The injury model used in this study allowed the investigation of the short-term renoprotective effects of a given stem/progenitor cell population on injured kidneys. In fact my Thesis and earlier studies (Zager et al., 2001; Perin et al. 2010) showed that mouse kidneys nearly completely recovered from acute injury 12-14 days after glycerol injection. It cannot be ruled out that the H6 cells might be able to exert a long-term renoprotective effect on injured kidney, a question that cannot be answered by the injury model used here. For this reason, in future it would be of great interest to investigate the ability of the H6 clonal line to confer a long-term renoprotective effect in a mouse model of chronic kidney injury.

In this work it was observed that tubular cell proliferation, assessed by immunohistochemical staining for BrdU and PCNA, decreased throughout the period studied. These data, together with the reduction of both BUN and creatinine levels observed during the same period, demonstrated that the kidney physiology resolved back to normal 12 days after the induction of acute tubular injury. However, it was also noticed that the presence of H6 EGFP⁺ cells within ARF-induced mouse kidney proximal tubules did not significantly increase the number of proliferating tubular cells, compared with PBS-injected ARF-induced mice. As

postulated before, a possible increment in the number of proliferating tubular cells, due to the presence of H6 cells engrafted into damaged tubules, might have been veiled by the high variability of the degree of renal damage. The results presented in this chapter cannot rule out that the H6 clonal line might exert a positive effect on kidney regeneration following acute tubular injury. For example, the H6 clonal line might contribute to reduce tubular proteinuria by expressing the megalin receptor, which is involved in the reabsorption of proteins present in the glomerular ultrafiltrate (Nielsen and Christensen, 2010). Since the excess of protein is potentially harmful for distal tubules (Nielsen and Christensen, 2010) the H6 clonal line might be able to protect the distal segments of the nephron from inflammation, fibrosis and development of chronic kidney disease by reducing proteinuria.

Finally, the tumorigenic ability of the H6 clonal line was investigated by subcutaneous injection of 2×10^6 H6 EGFP⁺ cells into healthy mice. Six weeks after cell inoculation none of the animals treated with the cells presented the appearance of any tumour at the site of injection, thus strongly suggesting the absence of tumorigenic bias for the H6 clonal line.

Overall these findings demonstrated that the H6 clonal line was able to engraft into damaged proximal tubules but did not appear to promote recovery of the induced renal injury. Since H6 cells showed several features of stem cells and appeared to be able to engraft into its target organ only, the kidney, it would be of great interest to investigate the long-term renoprotective capability of these cells in a model of chronic kidney injury. In addition, due to their ability to generate podocyte-like cells in culture, in future it would be very interesting to investigate whether the H6 clonal line

is able to generate podocytes *in vivo* and exert a renoprotective effect in a mouse model of glomerular injury.

CHAPTER 8

8.1 Final discussion

In mammals the functional kidney, the metanephros, develops through a series of complex reciprocal interactions between two embryonic tissues, the ureteric bud (UB) and the metanephric mesenchyme (MM) (see section 1.1.2.3) (Saxén, 1987). It has been demonstrated that all cell types present in the mature nephron, the functional unit of the adult kidney, derive from the cap mesenchyme, which constitutes a domain of the MM adjacent to the ureteric bud tips (Kobayashi et al., 2008). Since several studies have already demonstrated the presence of stem/progenitor cells in adult kidney, both from rodent and human origin (Bussolati et al., 2005, Challen et al., 2006; Dekel et al., 2006; Gupta et al., 2006; Maeshima et al., 2006; Oliver et al., 2009; Ronconi et al., 2009; Lee et al., 2010), it is conceivable that a fraction of MM cells might remain undifferentiated as the kidney develops, in order to give rise to the resident stem/progenitor cells present in the adult organ. It has been demonstrated that, unlike mammals, lower vertebrates, such as adult teleost and cartilaginous fish, are able to form new nephrons following kidney injury in a process that resembles nephrogenesis (Elger et al., 2003). Although these findings suggest that the nephrogenic mesenchyme might be a direct source for stem cells resident in the adult organ, this hypothesis has yet to be proven. Fate mapping experiments using Cre-loxP lines, crossed with Rosa26 mice (Soriano, 1999), might unveil whether a stem cell population in the adult kidney is derived from the metanephric mesenchyme. For instance, this strategy has been adopted by Kobayashi and colleagues who demonstrated that all cell types of the main body of the nephron are derived from a population of Six2⁺ cells present

within the mesenchymal pool of kidney primordium as early as E10.5 (Kobayashi et al., 2008). However, this approach would not be able to unveil whether adult kidney stem cells were direct derivatives of the MM or, alternatively, whether adult kidney stem cells derived from a more differentiated population of cells present in the kidney that had been able to undergo a process of de-differentiation in response to specific stimuli.

The rationale of the present study was that the kidney-derived stem cell H6 clonal line might represent a MM-like cell population present in the postnatal mouse kidney. This hypothesis was investigated by comparing the expression profile and nephrogenic potential of the H6 clonal line, originally derived from postnatal mouse kidney (Fuente Mora, 2009), with those of mouse MM cells following *in vitro* culture. A similar expression profile and nephrogenic ability between *in vitro* cultured MM cells and H6 cells would suggest that the H6 clonal line was a remnant of the MM that could escape differentiation during nephrogenesis. Since the uninduced, non-immortalized MM rapidly undergoes apoptosis when cultured in the absence of ureteric bud or heterologous inducers (Saxén, 1987; Dudley et al., 1999; Kuure et al., 2007), in the first part of this study it became critical to develop culture conditions that could support the expansion of MM cells *in vitro* for several days and, contemporaneously, maintain a MM-like phenotype. The results demonstrate for the first time that MM cells could undergo expansion by approximately 15-fold in 7 days of culture when cultured in the presence of 25 ng/ml BMP7 and 100 ng/ml FGF2, on plastic tissue culture dishes, rather than on nucleopore membrane filter (Dudley et al., 1999). Moreover, these conditions allowed MM cells to retain a MM-like phenotype up to passage 1 (and 8 days in culture), as demonstrated by the

expression of many MM-specific markers, such as *Wt1*, *Osr1*, *Sall1*, *Gdnf* and vimentin. However, it was observed that the expression of the MM- and UB-specific marker *Pax2* was lost when the cells were cultured longer than 24 hours. The results showed that at second passage MM cells could not undergo further expansion and started to lose their MM-like phenotype, as indicated by the downregulation of *Gdnf* and *Sall1*. These markers are required for normal kidney development (Nishinakamura and Takasato, 2005; Costantini and Shakya, 2006). It was then hypothesized that the inability of the cells to undergo further expansion beyond passage 1 and retain a MM-like phenotype at passage 2 might be due to the lack of *Pax2* expression and the downregulation of *Sall1* and *Gdnf*. Since RT-PCR and immunostaining demonstrated that MM cell expression profile did not change following 96 hours of culture, in this work it was decided to investigate the nephrogenic ability of MM cells following 4 days of *in vitro* culture.

In the developing metanephros the ureteric bud induces the surrounding metanephric mesenchyme to undergo tubulogenesis (Saxén, 1987). The ability of MM cells to undergo induction and form developing nephron-like structures following 4 days of *in vitro* culture, was initially assessed by co-stimulation with the embryonic spinal cord, a well known heterologous inducer for the metanephric mesenchyme (Saxén, 1987). The results demonstrated that following 24 hours of *in vitro* culture MM could undergo induction and form developing glomeruli and renal tubules, whereas following 48 hours of culture, MM were unable to form cells of the glomerulus, but only a few distal tubules. The ability of the mesenchyme to undergo induction was completely lost when the cells were cultured longer than 48 hours. Several

studies have suggested that tubulogenesis is regulated by Wnt signalling through the β -catenin canonical pathway, with Wnt4 and Wnt9b playing pivotal roles in this process (Herzinger, 1994; Kispert et al., 1998; Kuure et al., 2007; Park et al., 2007). Since Pax2 can activate the expression of Wnt4 both *in vitro* and *in vivo* (Torban et al., 2006), in this work it was hypothesized that MM cells failed to undergo tubulogenesis when cultured longer than 48 hours because of the lack of Pax2 expression, which occurred in MM cells cultured for more than 24 hours. In the attempt to induce tubulogenesis in MM cultured for more than 2 days, it was decided to bypass the lack of Pax2 signalling and activate the canonical pathway by inhibiting glycogen synthase kinase-3 β (GSK-3 β), a downstream target of Wnt signalling (Schmidt-Ott and Barasch, 2008), using a synthetic GSK-3 inhibitor (BIO) (Kuure et al., 2007). It was observed that the mesenchyme responded only partially better to BIO stimulation than to spinal cord induction, as MM cultured for 48 hours could undergo complete induction and form developing glomeruli and renal tubules. However, the presence of BIO did not stimulate MM cells to undergo tubulogenesis when cultured for more than 48 hours. It might be plausible that the presence of Wnt4-like signalling was not sufficient to trigger nephron formation in MM cultured for more than 2 days, and that other factors were most likely required to initiate tubulogenesis. Interestingly, in the presence of BIO a higher proportion of developing distal tubules formed than in the presence of spinal cord. Under normal circumstances, glomeruli and proximal tubules form earlier during development, whereas distal tubules develop later (Dorup and Maunsbach, 1982). Cheng and colleagues demonstrated that Notch signalling regulates the proximodistal patterning of developing nephrons. In the absence of Notch

signalling distal tubules still form whereas podocyte, glomerular capillaries and proximal tubules do not develop (Cheng et al., 2007). Fujimura and collaborators suggested the existence of a positive loop in which Notch2 activates *Wnt4* and inhibit the maintenance of *Six2*-positive renal progenitor cells within the mesenchyme (Fujimura et al., 2010). Since Notch signalling requires cell-cell contact (Jeffries and Capobianco, 2000), in this Thesis I speculated that the development of more distal convoluted tubules in BIO-stimulated MM compared with samples induced by spinal cord might be explained by the absence of direct contact between the MM and its inducer, which determined a downregulation of Notch signalling.

To investigate if the ability of MM cells cultured for more than 48 hours to become induced was irreversible, the ability of the cells to retain a nephrogenic potential and form developing renal structures was tested using the chimera formation assay (Unbekandt and Davies, 2010). Since this technique allows the formation of chimeras by simply mixing reaggregated rudiments with an exogenous cell population, in the present study it was decided to adopt the chimera formation assay to investigate whether 4 days cultured MM cells were still able to participate to the formation of developing nephrons. The results indicated that following recombination with E11.5 reaggregated kidney rudiments, cultured MM could maintain a nephrogenic potential and integrate into nephron-like developing structures at a comparable rate to that of freshly isolated MM, which represented a positive control for cell integration. Like freshly isolated MM, cultured MM did not integrate into the ureteric bud, which is in agreement with *in vivo* studies showing that MM give rise to all cell types of the nephron, but not ureteric bud derivatives (Kobayashi

et al., 2008). Interestingly, following recombination with reaggregated rudiments, both freshly isolated and cultured MM were capable of expressing Pax2, which suggested that factors released from the ureteric bud cells present within the chimera allowed MM cells to maintain or reactivate the expression of Pax2. It was also observed that several QD-labelled MM cells were found within the stroma, which is considered a domain of the chimera that neither give rise to developing nephrons, nor contains ureteric bud structures. Nevertheless, it cannot be ruled out that the cells present within the stroma might still play a role in the chimera development. Hatini and colleagues provided evidence that stromal cells seem to control kidney development. These authors showed that embryos lacking *Foxd1*, a marker for stromal progenitor cells, displayed impaired nephrogenesis (Hatini et al., 1996). Shan and collaborators demonstrated that during nephrogenesis, the first developing nephrons are only vestigial, since they rapidly degenerate following formation and constitute part of the stromal compartment (Shan et al., 2010). It is plausible that at least some of the QD-labelled MM cells present within the stroma might be a remnant of the very early presumptive developing nephrons that had undergone degeneration, therefore it is conceivable that these cells might still play a role in the regulation of the nephrogenesis process. However, it might also be plausible that during the chimera formation, some MM cells were not close enough to the developing UB to receive the inductive signal, therefore they were unable to participate to nephron formation and ended up within the stromal compartment as uninduced MM.

Having optimized culture conditions that allowed MM cells to maintain a MM-like phenotype and a nephrogenic potential

following several days of *in vitro* culture, in the second part of this work the expression profile and nephrogenic potential of the kidney-derived stem cell H6 clonal line was compared with those of MM cells following 4 days of *in vitro* culture. A similar phenotype between the H6 clonal line and cultured MM cells would suggest that H6 cells represented a MM-like population resident in the postnatal kidney. As explained before, the H6 clonal line was originally derived from 2-6 day old mouse kidney (Fuente Mora, 2009). The cells were isolated from a postnatal organ because, unlike in human, nephrogenesis in mouse continues after birth until around postnatal day 7 (Dickinson et al., 2005). It was therefore hypothesized that kidney-derived stem cells might be found in greater number in the postnatal kidney, when nephrogenesis is still ongoing, than in the adult organ when nephrons are no longer formed. The H6 clonal line exhibited limitless proliferative capacity, with a population doubling time of approximately 25 hours, and the ability to generate renal-like cells in culture, such as podocyte-like cells and proximal tubular-like cells. Gene expression profiling revealed that H6 cells expressed the progenitor cell markers *Msi1* and *Msi2*, and the same set of MM-specific genes already found in freshly isolated MM and cultured MM, such as *Wt1*, *Osr1*, *Gdnf* and *Vim*. Furthermore, like freshly isolated and cultured MM cells, H6 cells did not express *Pax2*. These findings showed that the H6 clonal line shared some of the same characteristics as MM. The expression of many stem and progenitor cell markers, such as *Sca-1*, *CD24*, *CD29*, *CD44* and *CD73*, normally found in renal progenitor cells of both mouse and human origin (Bussolati et al., 2005; Dekel et al., 2006; Sagrinati et al., 2006; Ronconi et al., 2009), indeed suggested a stem cell phenotype for the H6 clonal line. Interestingly, H6 cells expressed several markers of fully differentiated renal cells, such

as the podocyte marker synaptopodin (Shankland et al., 2007) and the proximal tubular markers Aqp1 and megalin (Gburek et al., 2003; Georgas et al., 2008), which suggested that a subset of the H6 clonal line could spontaneously generate podocyte-like and tubular-like cells in culture. The ability to continuously generate the aforementioned cell types in culture might be of great importance and clinical relevance, since the H6 clonal line might become a useful tool to investigate cell responses to injury, elucidate cell repair mechanisms and might serve to identify innovative, stem cell-based therapies to replenish damaged kidney tissues.

Besides the ability to give rise to renal-like cell types, the H6 clonal line could also give rise to non-renal cell types, such as osteocytes and adipocytes, when cultured under appropriate differentiating conditions. The findings of my study unveiled important similarities between the H6 clonal line and a population of adult human CD24⁺ CD133⁺ renal progenitor cells resident at the urinary pole of the Bowman's capsule (Sagrinati et al., 2006; Ronconi et al., 2009). In fact, the results from this Thesis suggested that the H6 clonal line, like CD24⁺ CD133⁺ renal progenitor cells, could generate podocyte-like and tubular-like cells in culture. In addition, both cell populations were able to differentiate into osteocytes and adipocytes when cultured under appropriate differentiating culture conditions.

If the H6 clonal line was a remnant of the embryonic MM, then it would be able to retain a nephrogenic potential and form organotypic renal structures when recombined with reaggregated kidney rudiments. The chimera formation assay showed that H6 cells could maintain a nephrogenic potential *in vitro* and revealed intriguing similarities between the H6 clonal line and MM cells

following 4 days of *in vitro* culture. In fact the results showed that H6 cells could integrate into nephron-like developing structures at a comparable rate to that of cultured MM cells, and were able to activate the expression of Pax2. It might be hypothesized that the chimera likely provides an environment capable of directing the differentiation of MM and H6 cells toward renal-specific cell types. In addition, like the embryonic MM, the H6 clonal line did not integrate into the ureteric bud. The ability of H6 cells to form nephron-like developing structures rules out a UB-derived origin for the H6 clonal line, as the metanephric mesenchyme gives rise to all cell types present in the nephron (Kobayashi et al., 2008). However, I observed that the H6 clonal line integrated at a lower rate into developing nephrons than freshly isolated MM. This result could be due to the fact that freshly isolated MM represents a more undifferentiated and homogeneous cell population compared with the H6 clonal line, therefore it might retain a higher nephrogenic potential than that of the kidney-derived H6 cells. The chimera formation assay also demonstrated that the H6 clonal line was able to integrate into developing glomeruli and proximal tubules. These results are in agreement with previous findings from this study showing that the H6 clonal line expressed podocyte and proximal tubular markers. Altogether these findings indeed strongly suggest that H6 cells might be a postnatal kidney-resident MM-like cell population and underline paramount similarities between the H6 clonal line and adult human CD24⁺ CD133⁺ renal progenitor cells (Ronconi et al., 2009), as both cell populations seem to be able to generate cells present within the initial part of the nephron. In future, it would be interesting to extend the chimera culture period to allow the formation of distal tubular-like structures with the purpose to investigate whether H6

cells are also able to give rise to distal tubular cells following recombination with reaggregated kidney rudiments.

The presence of the proximal tubular markers Aqp1 and megalin, together with their ability to participate in the formation of developing proximal tubules, prompted the question of whether the H6 clonal line could generate functional proximal tubular-like cells in culture. Kidney proximal tubules play a main role in the reabsorption of water and a vast variety of inorganic and organic molecules present in the glomerular ultrafiltrate (Masereeuw et al., 1999; Christensen and Gburek, 2004, Kobayashi et al., 2005). These compounds are reabsorbed as a complex with megalin and cubulin, two endocytic receptors expressed in proximal tubules, along with the cooperating protein amnionless (Nielsen and Christensen, 2010). In the present study it was decided to investigate whether the H6 clonal line comprised functional proximal tubular-like cells by using a megalin functionality assay, already described by Zhai and colleagues in opossum kidney proximal tubular cells (Zhai et al., 2000). In this Thesis I demonstrated that a subset of the H6 clonal line showed *in vitro* functionality for megalin, since only megalin-expressing cells were able to uptake fluorescent bovine serum albumin, a known ligand for megalin (Nielsen and Christensen, 2010). Endocytosis of fluorescent albumin could be almost completely blocked in the presence of either receptor-associated protein (RAP) or unlabelled albumin, two structurally unrelated ligands for megalin, thus confirming that the uptake of fluorescent albumin was megalin-mediated. Besides reabsorption, kidney proximal tubules eliminate a wide spectrum of organic anion and cations, from the blood into the urine, through organic anion transporters (OATs) and organic cation transporters (OCTs), respectively (Sweet, 2005; Sweet et

al., 2006). The functionality of OATs can be assayed *in vitro* by looking at the OAT-mediated uptake of the anionic molecule 6-carboxyfluorescein (6-CF), into presumptive proximal tubules of embryonic tissues (Rosines et al., 2007). The ability of the H6 clonal line to uptake 6-CF *via* OATs was assessed by recombination with E11.5 reaggregated kidney rudiments, using the chimera formation assay (Unbekandt and Davies, 2010). The results indicated that H6 cells were not able to uptake 6-CF since the OAT genes *Oat1*, *Oat2*, *Oat3* and *Oat5*, normally expressed in mouse kidney (Van Wert et al., 2010), were not expressed in the H6 clonal line. These findings appeared to conflict with the fact that some cells within the H6 clonal line population showed a proximal tubular-like phenotype. However, in the kidney, megalin is mainly expressed within the S1 segment of the proximal tubule, which is a portion of the tubule adjacent to the glomerulus that mediates most of the ultrafiltrate reabsorption (Casarett et al., 2007; Russo et al., 2007; Nielsen and Christensen, 2010); OATs, instead, are principally expressed within the S2 segment of the proximal tubule, which mediates most of the tubular secretion (Anzai et al., 2005; Casarett et al., 2007; Hwang et al., 2010). It is therefore plausible that the H6 clonal line might represent a stem cell population which seems capable of spontaneously giving rise to cells present within the first part of the proximal tubules, that show *in vitro* megalin functionality, but no OAT expression. The chimera environment failed to induce the expression of OATs in H6 cells, which indeed hints that the H6 clonal line might only be able to give rise to S1 segment-derived cells.

Besides important similarities, the results from the present study also highlighted some intriguing differences between MM and the H6 clonal line. In fact it was demonstrated that H6 cells were able

to undergo extensive self-renewal, whereas uninduced MM cells had a limited ability to proliferate in culture, as MM cells could only be expanded up to 7 days (and 1 passage). Moreover, H6 cells were clonogenic, whereas the clonogenic ability of MM cells still has to be proven. Altogether, these results suggest that, while the embryonic MM represents a progenitor cell population, the H6 clonal line displays a stem cell phenotype.

In the last part of this work the renoprotective effect of the H6 clonal line was investigated *in vivo* in a mouse model of acute renal tubular failure (ARF), induced by intramuscular injection of glycerol. ARF is a condition characterized by an abrupt decline of kidney function due to an extensive damage of kidney tubules. The kidney has the striking capability to regenerate from acute insults and the recovery seems to be accomplished by intrinsic tubular epithelial cells that undergo rapid proliferation, following tubular injury, with the purpose to replenish damaged tubular cells (Humphreys et al., 2008). Despite these remarkable regenerative capacities, in some circumstance kidney recovery appears inadequate and ARF might progress to chronic kidney disease (Schiffli, 2010) which might ultimately lead to renal failure. The ability of a stem cell population to confer a renoprotective effect from acute renal failure is clearly of great importance and might have clinical relevance as well. Previous studies have shown that renal progenitor cells, both of human and mouse origin, could ameliorate renal function following acute tubular injury in mouse models of ARF (Sagrinati et al., 2006; Ronconi et al., 2009; Lee et al., 2010). In the present study, H6 cells, constitutively expressing enhanced green fluorescent protein (H6 EGFP⁺ cells), were inoculated into the tail vein of a mouse model of ARF (ARF-induced mice), at the peak of renal damage, with the aim to see

whether the cells could confer a renoprotective effect and contribute to the recovery of kidney function following injury. In this model, tubular damage is induced by intramuscular injection of glycerol, which causes extensive rhabdomyolysis and release of myoglobin, which in turn determines necrosis of epithelial tubular cells (Bussolati et al., 2005; Ronconi et al., 2009; Perin et al., 2010). The results highlighted that, following glycerol injection, ARF-induced mouse kidneys were able to recover within 12 days. When inoculated into the circulatory system of ARF-induced mice, H6 EGFP⁺ cells were capable of reaching the kidney and engrafting mostly, if not exclusively, into proximal tubules. Moreover, engrafted cells showed normal localization of megalin, as it was expressed on the apical surface of kidney proximal tubules (Zhai et al., 2000). The ability to engraft only into the kidney was an important feature of the H6 clonal line, as the cells did not show unspecific engraftment into ARF-induced mouse lung, spleen or liver. These findings indeed strongly support the assumption that the H6 clonal line might be a stem cell population which comprises proximal tubular-like cells that have the capability to engraft into damaged kidney proximal tubules following acute tubular failure. Since CD24⁺ CD133⁺ adult human renal progenitor cells are able to replenish damaged tubular cells in a mouse model of ARF (Ronconi et al., 2009), the results presented in this study highlight further intriguing similarities between the H6 clonal line and CD24⁺ CD133⁺ human renal progenitor cells.

Kidney functionality studies revealed that H6 cells were not able to confer a renoprotective effect from acute insults, as the recovery of cell-inoculated ARF-induced mouse kidneys was comparable with that of ARF-induced mice injected with PBS. In addition, the H6 clonal line did not significantly increase the number of

proliferating tubular epithelial cells, compared with control animals. One of the main problems encountered in this work was the response of the particular mouse strain used in this study to glycerol injection. As already explained in section 7.2.1.2, male CD1 mice were initially injected with 8.5 ml/Kg/body weight of glycerol, a dose that has been used in a previous study (Zager et al., 2001). Since this dose was not sufficient to induce acute renal tubular failure, in the current study the amount of glycerol was increased to 9 ml/Kg/body weight, a condition already tested in a previous study (Zager et al., 2008). In my work I found that the degree of renal damage was considerably variable among different animals, as kidney functionality was badly compromised in some mice, whereas in others it was only slightly affected. In addition, approximately 25% of mice used in this study died as a consequence of glycerol injection. Most of the deaths occurred within 5 days of the induction of the damage, thus indicating that the peak of renal injury corresponded with the most critical period for the animals. Because of this variability, it cannot be concluded that the H6 cells did not exert any beneficial effect on damaged kidneys: in fact, if a renoprotective effect was present, it might have been masked by the high variability of the animal response to glycerol treatment. Furthermore, because of the variability and the presence of a background signal that affected cytofluorimetric analyses, it was not possible to conclude that tubular cell engraftment increased as renal damage worsened.

It could also be speculated that the timing of cell inoculation into ARF-induced mice might be critical to obtain a renoprotective effect. Perin and colleagues demonstrated that human amniotic fluid stem cells (hAFSC) could deliver a renoprotective effect only when inoculated into ARF-induced mice a few hours after the

induction of renal damage. No renoprotective effect was observed when mice were treated with hAFSC at the peak of renal injury, three days after glycerol injection (Perin et al., 2010). These results suggest that also the timing of H6 cell inoculation might be crucial and that a renoprotective effect might be obtained if the cells were inoculated concomitantly with the induction of the renal damage. However, the lack of improvement of kidney functionality following cell inoculation cannot exclude that the H6 clonal line exerted some beneficial effects on injured kidneys. For instance, H6 cells might act as scaffold for endogenous tubular epithelial cells to help them to reconstitute damaged tubules. Further studies are required to clarify a possible role for the H6 clonal line in this process.

Since it was observed that 12 days after glycerol injection ARF-induced mouse kidneys recovered and were functionally indistinguishable from those of healthy animals, in this study ARF-induced mice were killed no later than 12 days after glycerol injection. It cannot be ruled out that the H6 clonal line might be able to exert a long-term renoprotective effect. Clearly, the model used in this study was not suitable to answer this question; therefore, in future it would be of great relevance to investigate the renoprotective role of the H6 clonal line in a mouse model of chronic kidney disease. In the search for an appropriate experimental system, the folic acid model might represent a suitable solution. In fact, intraperitoneal injection of folic acid induces transient acute kidney injury, which then progresses to chronic kidney disease (Long et al., 2008).

In conclusion, this work provides evidence that the kidney-derived stem cell H6 clonal line might represent a MM-like cell population

resident in the postnatal mouse kidney. The H6 clonal line seems to act as a bi-potent stem cell population, as it is able to undergo unlimited cell proliferation and can spontaneously generate podocyte-like cells and proximal tubular-like cells in culture.

The use of stem cell-based therapies as alternative to dialysis and kidney transplantation is very attractive, however it might be limited by the complexity of the kidney. As discussed in sections 1.3.2.1, 1.3.2.2 and 1.3.2.3, many kidney stem cell populations have been found in different *niches* of the adult organ. This might postulate the lack of a kidney-derived stem cell population which is capable of giving rise to all cell types present in the kidney; instead, the adult organ might contain different kidney stem cell populations already committed to give rise to distinct renal cell types. It has also been observed that some renal and non-renal stem cell populations have been able to exert a renoprotective effect following kidney injury; on the other hand, other stem cell populations do not appear to exert a beneficial effect on injured kidney. A critical requisite for a stem cell population to be used for renal replacement therapies is that the cells should be present in the organism after birth and their *niche(s)* easily accessible. Moreover, the possibility to isolate the cells in great number certainly represents a further favourable feature.

Bone marrow-derived mesenchymal stem cells (MSC) might represent a possible source of stem cells for renal replacement therapies. It has been shown that MSC appear to be able to improve renal function in animal models of acute kidney injury; additionally, MSC can be obtained from autologous sources in large amounts (Morigi et al., 2004; Herrera et al., 2004; Togel et al., 2005; Herrera et al., 2007). However, the risk of fibrosis and

formation of ectopic tissues due to MSC injection still has to be fully investigated (Sagrinati et al., 2008).

Many stem cell populations resident in the adult kidney have been able to ameliorate renal function following tubular or glomerular injury (Dekel et al., 2006; Sagrinati et al., 2006; Ronconi et al., 2009; Lee et al., 2010). These kidney-derived stem cell populations represent serious candidates for autologous renal replacement therapies, even though their isolation might require more invasive techniques compared with MSC. A better understanding of the characteristics and renoprotective abilities of kidney-derived stem cells would be important to determine which stem cell population represents the most suitable source for treating a particular kidney disease. Ideally, kidney-derived stem cells would be isolated from the healthy part of the kidney, therefore an early diagnosis of kidney injury is certainly paramount to have access to unimpaired stem cells *niches*.

The possibility of reprogramming fully differentiated cells to a pluripotent state by retroviral transfection of four factors, namely *Oct3/4*, *Sox2*, *Klf4* and *c-Myc*, thus generating induced pluripotent stem (iPS) cells (Takahashi and Yamanaka, 2006), might have the potential to revolutionize regenerative medicine (Kaji et al., 2009). iPS cells might be differentiated into a defined cell type with the aim to use these cells for autologous stem cell-based therapies. However, the presence of viral vectors and exogenous genes has raised several concerns regarding the safety of iPS cells for regenerative medicine. More recently, Kaji and colleagues have attempted to overcome this problem by developing a non-viral transfection protocol to obtain iPS cells in which the exogenous genes are eliminated once the reprogramming is completed (Kaji

et al., 2009). If iPS cells were to be used for regenerative medicine, the main challenge for renal replacement therapies would be to develop culture conditions that could induce iPS cells to differentiate only into desired renal cell types. Studies conducted on animal models of acute and chronic kidney diseases will be strongly encouraged to evaluate the feasibility of using iPS cells for renal replacement therapies.

Human amniotic fluid stem cells (hAFSC) (Hauser et al., 2010; Perin et al., 2010) and human umbilical cord (UB)-derived MSC (Morigi et al., 2010) have proven to be able to ameliorate renal function following injury, and the interest regarding the use of these cells for renal replacement therapies has recently been raised. However, UB-MSC and hAFSC are frozen at or before birth, respectively, and usually many years may pass until they might be required for the treatment of renal disease. Therefore, it might become prominent to investigate whether the karyotype and phenotype of hAFSC and UB-MSC remain unchanged after being frozen for decades.

To conclude, several stem cell types might be appropriate candidates for stem cell-based treatments of renal diseases. Further studies carried out on animal models will be required to unveil which stem cell population is the most suitable one for renal replacement therapies. Nevertheless, it should be taken into account that different stem cell populations might be required for the treatment of distinct renal pathologies.

8.2 Future works

The results presented in this Thesis strongly suggest that the postnatal mouse kidney contains a population of kidney-derived stem cells that could possibly be a remnant of the embryonic metanephric mesenchyme that was capable of escaping complete differentiation during kidney development. This Thesis highlights that the kidney-derived stem cells H6 clonal line shares important features with the metanephric mesenchyme and behaves like a bi-potent stem cells population which is able to give rise spontaneously to proximal tubule-like and podocyte-like cells.

However, several questions still remain open and need to be addressed in future in order to fully comprehend the renoprotective effects of the H6 clonal line. As described in chapter 7, the glycerol-induced acute renal failure mouse model used in this study presented several problems, such as a high mortality rate following the induction of renal damage, a high variability of the degree of renal damage among different animals and the impossibility to look at the long-term effects of H6 cell inoculation on renal function. With the aim of overcoming these problems, a different mouse model of renal injury might be used: for instance, the folic acid model (FA) of renal injury might represent a suitable choice because FA induces a very reproducible acute renal injury which is characterized by a low mortality rate (Long et al., 2008). Importantly, the long-term effects of the H6 cells might be investigated using this renal injury model, because following transient acute renal failure, FA administration leads to chronic kidney disease (Long et al., 2008). Since the H6 cells spontaneously generate podocyte-like cells in culture and

participate in the formation of developing glomeruli in the chimera formation assay, another important issue to be addressed in future would be to investigate the ability of the H6 clonal line to replenish damaged podocytes in a mouse model of glomerular injury. The adriamycin model of induced glomerular injury (Ronconi et al., 2009) might therefore be used for this purpose.

Previous studies have demonstrated that the timing of cell inoculation into a mouse model of induced renal injury might be critical (Perin et al., 2010; Prof. Paola Romagnani, University of Firenze, personal communication). In future it would be worth inoculating the H6 clonal line concomitantly with the induction of renal damage, rather than at its peak, with the aim of seeing whether the cells can confer a renoprotective effect. This strategy might be easily applied to both the FA-induced renal injury model and the adriamycin-induced glomerular nephritis model.

In this Thesis the renoprotective effect of the H6 clonal line was evaluated using blood urea nitrogen and serum creatinine concentrations, two biochemical parameters that reflect renal function. In future it would be tremendously useful to evaluate the morphology of cell-inoculated kidney using morphological parameters, in order to ascertain whether the cells were capable of improving the morphology of damaged kidneys. Besides, since the H6 clonal line expressed megalin and engrafted mostly into proximal tubules, they might be able to replenish damaged tubular cells and, in turn, increase absorptive functions of damaged kidney, thus reducing proteinuria. Therefore, the evaluation of this parameter would also be of great importance.

As previously explained, the H6 clonal line was derived from the postnatal mouse kidney because at this stage of development the nephrogenesis was not completed yet; therefore, it was postulated that the postnatal organ might contain more stem/progenitor cells

compared with the adult kidney. It has been suggested that the embryonic kidney is a source for stem/progenitor cells (Kim et al., 2007). In future, using the same strategy followed to isolate the H6 clonal line, it would be interesting to attempt to isolate stem/progenitor cells from kidney rudiments from late-stage embryos, and compare the expression profile and nephrogenic potential of these cells with those of the H6 clonal line.

The very long-term goal of this project is to isolate kidney-derived stem cells from adult human kidney that have the ability to replenish damaged kidney tissues and therefore might be used for stem cell-based renal replacement therapies.

REFERENCES

Alvarez-Dolado M, Pardal R, Garcia-Verdugo JM, Fike JR, Lee HO, Pfeffer K, Lois C, Morrison SJ, Alvarez-Buylla A. Fusion of bone-marrow-derived cells with Purkinje neurons, cardiomyocytes and hepatocytes. *Nature* 425: 968- 973, 2003.

Anzai N, Jutabha P, Enomoto A, Yokoyama H, Nonoguchi H, Hirata T, Shiraya K, He X, Cha SH, Takeda M, Miyazaki H, Sakata T, Tomita K, Igarashi T, Kanai Y, Endou H. Functional Characterization of Rat Organic Anion Transporter 5 (*Slc22a19*) at the Apical Membrane of Renal Proximal Tubules. *The Journal of Pharmacology and Experimental Therapeutics* 315: 534-544, 2005.

Arighi E, Borrello MG, Sariola H. RET tyrosine kinase signalling in development and cancer. *Cytokine and Growth Factor Reviews* 16: 441-467, 2005.

Aros C and Remuzzi G. The rennin-angiotensin system in progression, remission and regression of chronic nephropathies. *Journal of Hypertension* 20: S45-S53, 2002.

Artavanis-Tsakonas S, Rand MD, Lake RJ. Notch signalling: cell fate and signal interaction in development. *Science* 284: 770-776, 1999.

Baer PC, Tunn UW, Nunez G, Scherberich JE, Geiger H. Transdifferentiation of distal but not proximal tubular epithelial cells from human kidney in culture. *Experimental Nephrology* 7: 306-313, 1999.

Barasch J, Qiao J, McWilliams G, Chen D, Oliver JA, Herzlinger D. Ureteric bud cells secrete multiple factors, including bFGF, which rescue renal progenitors from apoptosis. *American Journal of Physiology: Renal Physiology* 273: 757-767, 1997.

Barasch J, Yung J, Ware CB, Taga T, Yoshida K, Erdjument-Bromage H, Tempst P, Parravicini E, Malach S, Aranoff T, Oliver JA. Mesenchymal to epithelial conversion in rat metanephros is induced by LIF. *Cell* 99: 377-386, 1999.

Bouchard M. Transcriptional control of kidney development. *Differentiation* 72: 295-306, 2004.

Bouchard M, Souabni A, Mandler M, Neubuser A, Busslinger M. Nephric lineage specification by Pax2 And Pax8. *Genes and Development* 16: 2958-2970, 2002.

Boyle S, de Caestecker M. Role of transcriptional networks in coordinating early events during kidney development. *American Journal of Physiology: Renal Physiology* 291: F1-F8, 2006.

Brenner B. Brenner and Rector's The Kidney. *Philadelphia-London-Toronto-Montreal-Sidney-Tokyo.* W.B. Saunders Company 2000.

Brodbeck S, Englert C. Genetic determination of nephrogenesis: the Pax/Eya/Six gene network. *Pediatric Nephrology* 19: 249-255, 2004.

Brophy PD, Ostrom L, Lang KM, Dressler GR. Regulation of ureteric bud outgrowth by Pax2-dependent activation of the glial derived neurotrophic factor gene. *Development* 128: 4747-4756, 2001.

Buijs TJ, Henriquez NV, van Overveld PGM, van der Horst G, Que I, Schwaninger R, Rentsch C, ten Dijke P, Cleton-Jansen A, Driouch K, Lidereau R, Bachelier R, Vukicevic S, Cle'zardin P, Papapoulos SE, Cecchini MG, Lo'wik CWGM, van der Pluijm G. Bone morphogenetic protein 7 in the development and treatment of bone metastases from breast cancer. *Cancer Research* 67: 8742-8751, 2007.

Bush KT, Vaughn DA, Li X, Rosenfeld MG, Rose DW, Mendoza SA, Nigam SK. Development and differentiation of the ureteric bud into the ureter in the absence of a kidney collecting system. *Developmental Biology* 298: 571-584, 2006.

Bussolati B, Bruno S, Grange C, Buttiglieri S, Deregibus MC, Cantino D, Camussi G. Isolation of renal progenitor cells from adult human kidney. *American Journal of Pathology* 166: 545-555, 2005.

Bussolati B, Bruno S, Grange C, Ferrando U, Camussi G. Identification of a tumor-initiating stem cell population in human renal carcinoma. *The FASEB Journal* 22: 3696-3705, 2008.

Cai Q, Dimitrieva N, Ferraris JD, Brooks HL, van Balkom BWM, Burg M. Pax2 expression occurs in renal medullary epithelial cells *in vivo* and in cell culture, is osmoregulated, and promotes osmotic tolerance. *Proceeding of the National Academy of Sciences of the United States of America* 102: 503-508, 2005.

Casarett LJ, Klaassen CD, Doull J. Casarett and Doull's toxicology: the basic science of poison. *McGraw-Hill Medical*, 7th Edition, 2008.

Cebrian C, Borodo K, Charles N, Herzlinger DA. Morphometric index of the developing murine kidney. *Developmental Dynamics* 231: 601-608, 2004.

Challen GA, Bertocello I, Deane JA, Ricardo SD, Little MH. Kidney side population reveals multilineage potential and renal functional capacity but also cellular heterogeneity. *Journal of the American Society of Nephrology* 17: 1896-1912, 2006.

Cheng HT, Kim M, Todd Valerius M, Surendran K, Schuster-Gossler K, Gossler A, McMahon AP, Kopan R. Notch2, but not Notch1, is required for proximal fate acquisition in the mammalian nephron. *Development* 134: 801-811, 2007.

Christensen EI, Birn H. Megalin and cubulin: synergistic endocytic receptors in renal proximal tubules. *American Journal of Physiology: Renal Physiology* 280: F562-F573, 2001

Christensen EI and Gburek J. Protein reabsorption in renal proximal tubules – function and dysfunction in kidney pathophysiology. *Pediatric Nephrology* 19: 714-721, 2004.

Clarke JC, Patel SR, Raymond RM Jr, Andrew S, Robinson BG, Dressler GR, Brophy PD. Regulation of *c-Ret* in the developing kidney is responsive to *Pax2* gene dosage. *Human Molecular Genetics* 15: 3420-3428, 2006.

Costantini F, Shakya R. GDNF/Ret signaling and the development of the kidney. *Bioessays* 28: 117-127, 2006.

Cullen-McEwen LA, Caruana G, Bertram JF. The where, what and why of the developing renal stroma. *Experimental Nephrology* 99: e1-e8, 2005.

Dantal J, Souillou JP. Immunosuppressive drugs and the risk of cancer after organ transplantation. *New England Journal of Medicine* 352: 1371-1373, 2005.

Davies JA and Garrod DR. Induction of early stage of kidney tubule differentiation by lithium ions. *Developmental Biology* 167: 50-60, 1995.

De Coppi P, Bartsch GJ, Siddiqui MM, Xu T, Santos CC, Perin L, Mostoslavsky G, Serre AC, Snyder EY, Yoo JJ, Furth ME, Soker S, Atala A. Isolation of amniotic stem cell lines with potential for therapy. *Nature Biotechnology* 25: 100-106, 2007.

Dekel B, Burakova T, Arditti FD, Reich-Zeliger S, Milstein O, Aviel-Ronen S, Rechavi G, Friedman N, Kaminski N, Passwell JH, Reisner Y. Human and porcine early kidney precursors as a new source for transplantation. *Nature Medicine* 9: 53-60, 2003.

Dekel B, Zangi L, Shezen E, Reich-Zeliger S, Eventov-Friedman S, Katchman H, Jacob-Hirsch J, Amariglio N, Rechavi G, Margalit R, Reisner Y. Isolation and characterization of non-tubular Sca-1⁺ Lin⁻ multipotent stem/progenitor cells from adult mouse kidney. *Journal of the American Society of Nephrology* 17: 3300-3314, 2006.

Dickinson H, Walker DW, Cullen-McEwen L, Wintour EM, Moriz K. The spiny mouse (*Acomys cahirinus*) completes nephrogenesis before birth. *American Journal of Physiology: Renal Physiology* 289: F273-F279, 2005.

Donovan MJ, Natoli TA, Sainio K, Amstutz A, Jaenisch R, Sariola H, Kreidberg JA. Initial differentiation of the metanephric mesenchyme is independent of Wt1 and the ureteric bud. *Developmental Genetics* 24: 252-262, 1999.

Dorup J and Maunsbach AB. The ultrastructural development of distal nephron segments in the human fetal kidney. *Anatomy and Embryology* 164: 19-41, 1982.

Dressler GR. Mouse development: patterning, morphogenesis, and organogenesis. *Tam P and Rossant J. (eds) New York: Academic Press: 395-420, 2002.*

Dressler GR. The cellular basis of kidney development. *The Annual Review of Cell and Developmental Biology* 22: 509-529, 2006.

Dressler GR. Advances in early kidney specification, development and patterning. *Development* 136: 3863-3874, 2009.

Dressler GR. The specification and maintenance of renal cell types by epigenetic factors. *Organogenesis* 5: 73-82, 2009.

Dudley AT, Robertson EJ. Overlapping expression domain of bone morphogenetic protein family members potentially account for limited tissue defect in BMP7 deficient embryos. *Developmental Dynamics* 208: 349-362, 1997.

Dudley AT, Godin RE, Robertson EJ. Interaction between FGF and BMP signaling pathways regulates development of metanephric mesenchyme. *Genes and Development* 13: 1601-1613, 1999.

Elger M, Hentschel H, Litteral J, Wellner M, Kirsch T, Luft FC, Haller H. Nephrogenesis is induced by partial nephrectomy in the elasmobranch *Leucoraja erinacea*. *Journal of the American Society of Nephrology* 14: 1506-1518, 2003.

Evans MJ, Kaufman MH. Establishment in culture of pluripotent cells from mouse embryos. *Nature* 292: 154-156, 1981.

Fang TC, Alison MR, Cook HT, Jeffery R, Wright NA, Poulson R. Proliferation of bone marrow-derived cells contributes to regeneration after folic acid-induced acute tubular injury. *Journal of the American Society of Nephrology* 16: 1723-1732, 2005.

Fortun J, Martin-Davila P, Pascual J, Cervera C, Moreno A, Gavalda J, Aguado JM, Pereira P, Gurgu M, Carratala J, Fogueda M, Montejo M, Blasco F, Bou G, Torre-Cisneros J, RESITRA Transplant Network. Immunosuppressive therapy and infection after kidney transplantation. *Transplant Infectious Disease* Jun 11, 2010 (Epub ahead of print).

Fuente Mora C. Isolation and characterization of a novel population of potential kidney stem cells from postnatal mouse kidney. PhD Thesis, 2009.

Fujimura S, Jiang Q, Kobayashi C, Nishinakamura R. Notch2 activation in the embryonic kidney depletes nephron progenitors. *Journal of the American Society of Nephrology* 21: 803-810, 2010.

Galli R, Gritti A, Bonfanti L, Vescovi AL. Neural stem cells: an overview. *Circulation Research* 92: 598-608, 2003.

Garovic V, Wagner SJ, Petrovic LM, Gray CE, Hall P, Sugimoto H, Kalluri R, Grande JP. Glomerular expression of nephrin and synaptopodin, but not podocin, is decreased in kidney sections from women with preeclampsia. *Nephrology and Dialysis Transplantation* 22: 1136-1143, 2007.

Gburek J, Birn H, Verroust PJ, Goj B, Jacobsen C, Moestrup SK, Willnow TE, Christensen EI. Renal uptake of myoglobin is mediated by the endocytic receptors megalin and cubulin. *American Journal of Physiology: Renal Physiology* 285: F451-F458, 2003.

Georgas K, Rumballe B, Wilkinson L, Chiu HS, Lesieur E, Gilbert T, Little MH. Use of dual section mRNA in situ hybridisation/immunohistochemistry to clarify gene expression patterns during the early stages of nephron development in the embryo and in the mature nephron of the adult mouse kidney. *Histochemistry and Cell Biology* 130: 927-942, 2008.

Gilbert S. Developmental biology. *Sinauer Associates, Inc. Massachusetts, USA*, 2006.

Grobstein C. Morphogenetic interaction between embryonic mouse tissues separated by a membrane filter. *Nature* 272: 896-871, 1953.

Grobstein C. Inductive interaction in the development of the mouse metanephros. *Journal of Experimental Zoology* 130: 319-340, 1955.

Guillaume R, Bressan M, Herzlinger D. Paraxial mesoderm contributes stromal cells to the developing kidney. *Developmental Biology* 329: 169-175, 2009.

Gupta S, Verfaillie C, Chmielewski D, Kren S, Eidman K, Connaire J, Heremans Y, Lund T, Blackstad M, Jiang Y, Luttun A, Rosenberg ME. Isolation and characterization of kidney-derived stem cells. *Journal of the American Society of Nephrology* 17: 3028-3040, 2006.

Hatini V, Huh SO, Herzlinger D, Soares VC, Lai E. Essential role of stromal mesenchyme in kidney morphogenesis revealed by targeted disruption of Winged Helix transcription factor *BF-2*. *Genes and Development* 10: 1467-1478, 1996.

Hauser P, De Fazio R, Bruno S, Sdei S, Grange C, Bussolati B, Benedetto C, Camussi G. Stem cells derived from human amniotic fluid contribute to acute kidney injury recovery. *American Journal of Pathology* 177: 2010 (copy posted online ahead of print publication).

Herrera MB, Bussolati B, Bruno S, Fonsato V, Romanazzi GM, Camussi G. Mesenchymal stem cells contribute to the renal repair of acute tubular epithelial injury. *International Journal of Molecular Medicine* 14: 1035-1041, 2004.

Herrera MB, Bussolati B, Bruno S, Morando L, Mauriello-Romanazzi G, Sanavio F, Stamenkovic I, Biancone L, Camussi G. Exogenous mesenchymal stem cells localize to the kidney by means of CD44 following acute tubular injury. *Kidney International* 72: 430-441, 2007.

Herzlinger D, Qiao J, Cohen D, Ramakrishna N, Brown AMC. Induction of kidney epithelial morphogenesis by cells expressing *Wnt-1*. *Developmental Biology* 166: 815-818, 1994.

Humphreys BD, Todd Valerius M, Kobayashi A, Mugford JW, Soeung S, Duffield JS, McMahon AP, Bonventre JB. Intrinsic epithelial cells repair the kidney after injury. *Cell Stem Cell* 2: 284-291, 2008.

Humphreys BD, Lin SL, Kobayashi A, Hudson TE, Nowlin BT, Bonventre JV, Todd Valerius M, McMahon AP, Duffield JS. Fate tracing reveals the pericyte and not epithelial origin of myofibroblast in kidney fibrosis. *American Journal of Pathology* 176: 85-97, 2009.

Hwang JS, Park EY, Kim WY, Yang CW, Kim J. Expression of Oat1 and Oat3 in differentiating proximal tubules of the mouse kidney. *Histology and Histopathology* 25: 33-44, 2010.

Imberti B, Morigi M, Tomasoni S, Rota C, Corna D, Longaretti L, Rottoli D, Valsecchi F, Benigni A, Wang J, Abbate M, Zoja C, Remuzzi G. Insulin-like growth factor-1 sustains stem cell-mediated renal repair. *Journal of the American Society of Nephrology* 18: 2921-2928, 2007.

James RG, Kamei CN, Wang Q, Jiang R, Schultheiss TM. Odd-kipped related 1 is required for development of the metanephric kidney and regulates formation and differentiation of kidney precursor cells. *Development* 133: 2995-3004, 2006.

James MT, Hemmelgarn BR, Tonelli M. Early recognition and prevention of chronic kidney disease. *Lancet* 375: 1296-1309, 2010.

Jeffries S and Capobianco AJ. Neoplastic transformation by Notch requires nuclear localization. *Molecular and Cellular Biology* 20: 3928-3941, 2000.

Jessberger S, Clemenson GD Jr, Gage FH. Spontaneous fusion and nonclonal growth of adult neural stem cells. *Stem Cells* 25: 871-874, 2007.

Kaji K, Norrby K, Paca A, Mileikovsky M, Mohseni P, Woltjen K. Virus-free induction of pluripotency and subsequent excision of reprogramming factors. *Nature* 458: 771-776, 2009.

Kalyesubula R, Perazella MA. HIV-related drug nephrotoxicity in sub-saharan Africa. *The Internet Journal of Nephrology* 6: 2010.

Kim SS, Park HJ, Han J, Gwak S, Park HM, Song KW, Rhee YH, Chung HM, Kim B. Improvement of kidney failure with fetal kidney precursor cell transplantation. *Transplantation* 83: 1249-1258, 2007.

Kim SS, Gwak SJ, Han J, Park HJ, Park MH, Song KW, Cho SW, Rhee YH, Chung HM, Kim B. Kidney tissue reconstruction by fetal kidney cell transplantation: effect of gestation stage of fetal kidney cells. *Stem Cells* 25: 1393-1401, 2007.

Kim SS, Gwak SJ, Han J, Park MY, Song KW, Kim BS. Regeneration of kidney tissue using *in vitro* cultured fetal kidney cells. *Experimental and Molecular Medicine* 40: 361-369, 2008.

Kirschstein R, Skirboll LR. Scientific progress and future research directions. *Report prepared by the National Institute of Health*, 2001.

Kispert A, Vainio S, McMahon AP. *Wnt-4* is a mesenchymal signal for epithelial transformation of metanephric mesenchyme in the developing kidney. *Development* 125: 4225-4234, 1998.

Kitamura S, Yamasaki Y, Kinomura M, Sugaya T, Sugiyama H, Maeshima Y, Makino H. Establishment and characterization of renal progenitor like cells from S3 segment of nephron in rat adult kidney. *The FASEB Journal* 19: 1789-1797, 2005.

Knauf F and Aronson PS. ESRD as a window into America's cost crisis in health care. *Journal of the American Society of Nephrology* 20: 2093-2097, 2009.

Kobayashi A, Kwan KM, Carroll TJ, McMahon AP, Mendelsohn CL, Behringer RR. Distinct and sequential tissue-specific activities of the LIM-class homeobox gene *Lim1* for tubular morphogenesis during kidney development. *Development* 132, 2809-2823, 2005.

Kobayashi Y, Ohbayashi M, Kohyama N, Yamamoto T. Mouse organic anion transporter 2 and 3 (mOAT2/3[Slc22a7/8]) mediates the renal transport of bumetanide. *European Journal of Pharmacology* 524: 44-48, 2005.

Kobayashi A, Valerius MT, Mugford JM, Carroll TJ, Self M, Oliver G, McMahon AP. *Six2* defines and regulates a multipotent progenitor cell population in the developing kidney. **Kobayashi H, Kawakami K, Asashima M, Nishinakamura M.** *Six1* and *Six4* are essential for *Gdnf* expression in the metanephric mesenchyme and ureteric bud formation, while *Six1*-deficiency alone causes mesonephric-tubule defects. *Mechanisms of Development* 124: 290-303, 2007.

Kobayashi A, Todd Valerius M, Mugford JW, Carroll TJ, Self M, Oliver G, McMahon AP. Six2 Defines and Regulates a Multipotent Self-Renewing Nephron Progenitor Population throughout Mammalian Kidney Development. *Cell Stem Cell* 3: 169-181, 2008.

Koopman P, Gubbay J, Vivian N, Goodfellow P, Lovell-Badge R. Male development of chromosomally female mice transgenic for *Sry*. *Nature* 351: 117-121, 1991.

Kumar S, Kimberling WJ, Weston MD, Schaefer BG, Berg MA, Marres HA, Cremers CW. Identification of three novel mutations in human EYA1 protein associated with brachio-oto-renal syndrome. *Human Mutation* 11: 443-449, 1998.

Kuure S, Vuolteenhao R, Vainio S. Kidney morphogenesis: cellular and molecular regulation. *Mechanisms of Development* 92: 31-45, 2000.

Kuure S, Popsueva A, Jakobson M, Sainio K, Sariola H. Glycogen Synthase Kinase-3 inactivation and stabilisation of β -catenin induce nephron differentiation in isolated mouse and rat kidney mesenchymes. *Journal of the American Society of Nephrology* 18: 1130-1139, 2007.

Lazzeri E, Crescioli C, Ronconi E, Mazzinghi B, Sagrinati C, Netti GS, Angelotti ML, Parente E, Ballerini L, Cosmi L, Maggi L, Gesualdo L, Rotindi M, Annunziato F, Maggi E, Lasagni L, Serio M, Romagnani S, Vannelli GB, Romagnani P. Regenerative potential of embryonic renal multipotent progenitors in acute renal failure. *The Journal of the American Society of Nephrology* 18: 3128-3138, 2007.

Lee PT, Lin HH, Jiang ST, Lu PJ, Chou KJ, Fang HC, Chiou YY, Tang MJ. Mouse kidney progenitor cells accelerate renal regeneration and prolong survival after ischemic injury. *Stem Cells* 28: 573-584, 2010.

Liu E, Morimoto M, Kitajima S, Koike T, Yu Y, Shiiki H, Nagata M, Watanabe T, Fan J. Increased Expression of Vascular Endothelial Growth Factor in Kidney Leads to Progressive Impairment of Glomerular Functions. *Journal of the American Society of Nephrology* 18: 2094-2104, 2007.

Long DA, Woolf AS, Suda T, Yuan HT. Increased renal angiotensin-1 expression in folic acid-induced nephrotoxicity in mice. *Journal of the American Society of Nephrology* 12: 2721-2731, 2001.

Long DA, Price KL, Ioffe E, Gannon CM, Gnudi L, White KE, Yancopoulos GD, Rudge JS, Woolf AS. Angiotensin-1 therapy enhances fibrosis and inflammation following folic acid-induced acute renal injury. *Kidney International* 74: 300-309, 2008.

Macconi D, Abbate M, Morigi M, Angioletti S, Mister M, Buelli S, Bonomelli M, Mundel P, Endlich K, Remuzzi A, Remuzzi G. Permselective dysfunction of podocyte-podocyte contact upon angiotensin II unravels the molecular target for renoprotective intervention. *American Journal of Pathology* 168: 1073–1085, 2006.

Maeshima A, Sakurai H, Nigam SK. Adult kidney tubular cell population showing phenotypic plasticity, tubulogenic capacity, and integration capability into developing kidney. *Journal of the American Society of Nephrology* 17: 188-198, 2006.

Maeshima A, Sakurai H, Choi Y, Kitamura S, Vaughn DA, Tee JB, Nigam SK. Glial cell-derived neurotrophic factor-independent ureteric bud outgrowth from the Wolffian duct. *Journal of the American Society of Nephrology* 18: 3147-3155, 2007.

Martin G. Isolation of a pluripotent cell line from early mouse embryos cultured in medium conditioned by teratocarcinoma stem cells. *Proceeding of the National Academy of Sciences of the United States of America* 78: 7634-7638, 1981.

Masereeuw R, Moons MM, Toomey BH, Russel FGM, Miller DS. Active lucifer yellow secretion in renal proximal tubule: evidence for organic anion transport system crossover. *The Journal of Pharmacology and Experimental Therapeutics* 289: 1104-1111, 1999.

Maurer ME and Cooper JA. Endocytosis of megalin by visceral endoderm cells requires the Dab2 adaptor protein. *Journal of Cell Science* 118: 5345-5355, 2005.

Mendes S, Robin C, Dzierzak E. Mesenchymal progenitor cells localize within hematopoietic sites through ontogeny. *Development and disease* 132: 1127-1136, 2004.

Mikesch JH, Steffen B, Berdel WE, Serve H, Muller-Tidow C. The emerging role of Wnt signaling in the pathogenesis of acute myeloid leukemia. Role of Wnt signaling in the pathogenesis of AML. *Leukemia* 21: 1638-1647, 2007.

Moore KA, Lemisckha IR. Stem cells and their niches. *Science* 311: 1880-1885, 2006.

Morigi M, Imberti B, Zoja C, Corna D, Tomasoni S, Abbate M, Rottoli D, Angioletti S, Benigni A, Perico N, Alison M, Remuzzi G. Mesenchymal stem cells are renotropic, helping to repair the kidney and improve function in acute renal failure. *Journal of America Society of Nephrology* 15: 1794-1804, 2004.

Morigi M, Rota C, Montemurro T, Montelatici E, Lo Cicero V, Imberti B, Abbate M, Zoja C, Cassis P, Longaretti L, Rebulli P, Introna M, Capelli C, Benigni A, Remuzzi G, Lazzari L. Life-sparing Effect of Human Cord-Blood Mesenchymal Stem Cells in Experimental Acute Kidney Injury. *Stem Cells* 28: 513-522, 2010.

Mugford JW, Sipila P, McMahon JA, McMahon AP. Osr1 expression demarcates a multi-potent population of intermediate mesoderm that undergoes progressive restriction to an Osr1-dependent nephron progenitor compartment within the mammalian kidney *Developmental Biology* 324: 88-98, 2008.

Mundel P, Reisner J, Kriz W. Induction of differentiation in cultured rat and human podocytes. *Journal of the American Society of Nephrology* 8: 697-705, 1997.

Murray PA, Vasilev K, Fuente-Mora C, Ranghini E, Tensaout H, Rak-Raszewska A, Wilm B, Edgar D, Short RD, Kenny SE. The potential of small chemical functional groups for directing the differentiation of kidney stem cells. *Biochemical Society Transactions* 38: 1062-1066, 2010.

Nagai A, Kim WK, Lee HJ, Jeong HS, Kim KS, Hong SH, Park IH, Kim SU. Multilineage Potential of Stable Human Mesenchymal

Nagy A and Quaggin SE. Stem cell therapy for the kidney: a cautionary tale. *Journal of the American Society of Nephrology* 21: 1070-1072, 2010.

Nielsen R and Christensen EI. Proteinuria and events beyond the slit. *Pediatric Nephrology* 25: 813-822, 2010.

Nishinakamura R. Kidney development conserved over species: essential role of *Sall1*. *Seminars in Cell & Developmental Biology* 14: 241-247, 2003.

Nishinakamura R, Takasato M. Essential roles of *Sall1* in kidney development. *Kidney International* 68: 1948-1950, 2005.

Oliver JA, Barasch J, Yang J, Herzlinger D, Al-Aqwati Q. Metanephric mesenchyme contains embryonic renal stem cells. *American Journal of Physiology: Renal Physiology* 283: F799-809, 2002.

Oliver JA, Maarouf O, Cheema FH, Martens TP, Al-Awqati Q. The renal papilla is a niche for adult kidney stem cells. *The Journal of Clinical Investigation* 114: 795-804, 2004.

Oliver JA, Klinakis A, Cheema FH, Friedlander J, Sampogna RV, Martens TP, Liu C, Efstratiadis A, Al-Awqati Q. Proliferation and migration of label-retaining cells of the kidney papilla. *Journal of the American Society of Nephrology* 20: 2315-2327, 2009.

Osafune K, Tasakato M, Kispert A, Asashima M, Nishinakamura R. Identification of multipotent progenitors in the embryonic mouse kidney by a novel colony-forming assay. *Development* 133: 151-161, 2006.

Park JS, Valerius MT, McMahon AP. Wnt/ β -catenin signaling regulates nephron induction during mouse kidney development. *Development* 134: 2533-2539, 2007.

Pavlova A, Sakurai H, Leclercq B, Beier DR, Yu ASL, Nigam SK. Developmentally regulated expression of organic ion transporters NKT (OAT1), OCT1, NLT (OAT2), and Roct. *American Journal of Physiology: Renal Physiology* 278: F635-F643, 2000.

Pedersen A, Skjong C, Shawlot W. *Lim-1* is required for nephric duct extension and ureteric bud morphogenesis. *Developmental Biology* 288: 571-581, 2005.

Pepicelli CV, Kispert A, Rowitch DH, McMahon AP. GDNF induces branching and increases cell proliferation in the ureter of the mouse. *Developmental Biology* 192: 193-198, 1997.

Perantoni AO, Dove L, Karavanova I. Basic fibroblast growth factor can mediate the early inductive events in renal development. *Proceeding of the National Academy of Sciences of the United States of America* 92: 4696-4700, 1995.

Perin L, Sedrakyan S, Giuliani S, De Sacco S, Carraro G, Shiri L, Lemley KV, Rosol M, Wu S, Atala A, Warburton D, De Filippo RE. Protective effect of human amniotic fluid stem cells in an immunodeficient mouse model of acute tubular necrosis. *PLoS One* 5: 1-16, 2010.

Piggott K, Deng J, Warrington K, Younge B, Kubo, JT, Desai M, Goronzy JJ, Weyand CM. Blocking the NOTCH Pathway Inhibits Vascular Inflammation in Large-Vessel Vasculitis. *Circulation* 123: 309-318, 2011.

Poladia DP, Kish K, Kutay B, Hains D, Kegg H, Zhao H, Bates CM. Role of fibroblast growth factor receptors 1 and 2 in the metanephric mesenchyme. *Developmental Biology* 291: 325-339, 2006.

Popsueva A, Poteryaev D, Arighi E, Meng X, Angers-Loustau A, Kaplan D, Saarma M, Sariola H. GDNF promotes tubulogenesis of GFRalpha 1-expressing MDCK cells by Src-mediated phosphorylation of Met receptor tyrosine kinase. *The Journal of Cell Biology* 161: 119-129, 2003.

Poteryaev D, Titievsky A, Sun YF, Thomas-Crusells J, Lindahl M, Billaud M, Arumae U, Saarma M. GDNF triggers a novel ret-independent Src kinase family-coupled signalling via a GPI-linked GDNF receptor alpha 1. *FEBS Letters* 463: 63-66, 1999.

Price KL, Long DA, Jina N, Liapis H, Hubank M, Woolf AS, Winyard PJD. Microarray interrogation of human metanephric mesenchymal cells highlights potentially important molecules *in vivo*. *Physiological Genomics* 28: 193-202, 2007.

Qiao J, Cohen D, Herzlinger D. The metanephric blastema differentiates into collecting system and nephron epithelia *in vitro*. *Development* 121: 3207-3214, 1995.

Rak-Raszewska A. Investigating the nephrogenic potential of mouse embryonic stem cells and their derivatives. PhD Thesis, 2010.

Risbud MV, Schaer TP, Shapiro IM. Toward an understanding of the role of notochordal cells in the adult intervertebral disc: from discord to accord. *Developmental Dynamics* 239: 2141-2148, 2010.

Romio L, Wright V, Price K, Winyard PJD, Donnai D, Porteous ME, Franco B, Giorgio G, Malcolm S, Woolf AS, Feather SA. *OFD1*, the gene mutated in oral-facia-digital syndrome type 1, is expressed in the metanephros and in human embryonic renal mesenchymal cells. *Journal of the American Society of Nephrology* 14: 680-689, 2003.

Ronconi E, Sagrinati C, Angelotti ML, Lazzeri E, Mazzinghi B, Ballerini L, Parente E, Becherucci F, Gacci M, Carini M, Maggi E, Serio M, Vannelli GB, Lasagni L, Romagnani S, Romagnani P. Regeneration of glomerular podocytes by human renal progenitors. *Journal of the American Society of Nephrology* 20: 322-332, 2009.

Rose RA, Jiang H, Wang X, Helke S, Tsoporis JN, Gong N, Keating SCJ, Parker TG, Backx PH, Keating A. Bone marrow-derived mesenchymal stromal cells express cardiac-specific markers, retain the stromal phenotype, and do not become functional cardiomyocytes in vitro. *Stem Cells* 26: 2884-2892, 2008.

Rosen AB, Kelly DJ, Schuldt AJT, Lu J, Potapova IA, Doronin SV, Robichaud KJ, Robinson RB, Rosen MR, Brink PR, Gaudette GR, Cohen IS. Finding fluorescent needles in the cardiac haystack: tracking human mesenchymal stem cells labeled with quantum dots for quantitative in vivo three-dimensional fluorescence analysis. *Stem Cells* 25: 2128-2138, 2007.

Rosines E, Sampogna RV, Johkura K, Vaughn DA, Choi Y, Sakurai H, Shah, MM, Nigam SK. Staged *in vitro* reconstitution and implantation of engineered rat kidney. *Proceeding of the National Academy of Sciences of the United States of America* 104: 20938-20943, 2007.

Russo LM, Del Re E, Brown D, Lin HY. Evidence for a role of transforming growth factor (TGF)- β 1 in the induction of postglomerular albuminuria in diabetic nephropathy. Amelioration by soluble TGF- β type II receptor. *Diabetes* 56: 380-388, 2007.

Sagrinati C, Netti GS, Mazzinghi B, Lazzeri E, Liotta F, Frosali F, Ronconi E, Meini C, Gacci M, Squecco R, Carini M, Gesualdo L, Francini F, Maggi E, Annunziato F, Lasagni L, Serio M, Romagnani S, Romagnani P. Isolation and characterization of multipotent progenitor cells from the Bowman's capsule of adult human kidneys. *Journal of the American Society of Nephrology* 17, 2443-2456, 2006.

Sagrinati C, Ronconi E, Lazzeri E, Lasagni L, Romagnani P. Stem-cell approaches for kidney repair: choosing the right cells. *Trends in Molecular Medicine* 14: 277-285, 2008.

Sainio K, Suvanto P, Davies J, Wartiovaara J, Wartiovaara K, Saarma M, Arume U, Meng X, Lindahl M, Pachnis V, Sariola H. Glial-cell-line-derived neurotrophic factor is required for bud initiation from ureteric epithelium. *Development* 124: 4077-4087, 1997.

Sajithlal G, Zou D, Silvius D, Xu PX. Eya1 acts as a critical regulator for specifying the metanephric mesenchyme. *Developmental Biology* 284: 323-336, 2005.

Saxén L. Organogenesis of the kidney. *Cambridge University Press, Cambridge-London-New York-Melbourne-Sydney* 173, 1987.

Saxén L, Lethonen E, Karkinen-Jaaskelainen M, Nordling S, Wartiovaara J. Are morphogenetic tissue interactions mediated by transmissible signals substances or through cell contacts? *Nature* 259: 662-663, 1976.

Schiff H. The dark side of high-intensity renal replacement therapy of acute kidney injury in critically ill patients. *International Urology and Nephrology* 42: 435-440, 2010.

Schmidt-Ott KM, Chen X, Paragas N, Levinson RS, Mendelsohn CL, Barasch J. c-kit delineates a distinct domain of progenitors in the developing kidney. *Developmental Biology* 299: 238-249, 2006.

Schmidt-Ott KM and Barasch J. WNT/ β -catenin signaling in nephron progenitors and their epithelial progeny. *Kidney International* 74: 1004-1008, 2008.

Schmidt-Ott KM, Masckauchan TNH, Chen X, Hirsh BJ, Sarkar A, Yang J, Paragas N, Wallace VA, Dufort D, Pavlidis P, Jagla B, Kitajewski J, Barasch J. β -catenin/TCF/Lef controls a differentiation-associated transcriptional program in renal epithelial progenitors. *Development* 134: 3177-3190, 2007.

Self M, Lagutin OV, Bowling B, Hendrix J, Cai, Y, Dressler GR, Oliver G. *Six2* is required for suppression of nephrogenesis and progenitor renewal in the developing kidney. *The EMBO Journal* 25: 5214-5228, 2006.

Shah M, Tee JB, Meyer T, Meyer-Schwesinger C, Choi C, Sweeney DE, Gallegos TF, Johkura K, Rosines E, Kouznetsova V, Rose DW, Bush KT, Sakurai H, Nigam SK. The instructive role of metanephric mesenchyme in ureteric bud patterning, sculpting, and maturation and its potential ability to buffer ureteric bud branching defects. *The American Journal of Physiology: Renal Physiology* 297: F1330-F1341, 2009.

Shan J, Joleka T, Skovorodkin I, Vainio S. Mapping of the fate of cell line ages generated from cells that express the *Wnt4* gene by time-lapse during kidney development. *Differentiation* 79: 57-64, 2010.

Shankland SJ. The podocyte's response to injury: role in proteinuria and glomerulosclerosis. *Kidney International* 69: 2131-2147, 2006.

Shankland SJ, Pippin JW, Reiser J, Mundel P. Podocytes in culture: past, present, and future. *Kidney International* 72: 26-36, 2007.

Shmelkov SV, Butler JM, Hooper AT, Hormigo A, Kushner J, Milde T, St. Clair R, Baljevic M, White I, Jin DK, Chadburn A, Murphy AJ, Valenzuela DM, Gale NW, Thurston G, Yancopoulos GD, D'Angelica M, Kemeny N, Lyden D, Rafii S. CD133 expression is not restricted to stem cells, and both CD133⁺ and CD133⁻ metastatic colon cancer cells initiate tumors. *The Journal of Clinical Investigation* 118: 2111-2120, 2008.

Siegel N, Rosner M, Unbekandt M, Fuchs C, Slabina N, Dolzing H, Davies JA, Lubec G, Hengstschlager M. Contribution of human amniotic fluid stem cells to renal tissue formation depends on mTOR. *Human Molecular Genetics* 19, 3320-3331, 2010.

Slack JMW. Origin of stem cells in organogenesis. *Science* 322: 1498-1501, 2008.

Smoyer WE and Mundel P. Regulation of podocyte structure during the development of nephrotic syndrome. *Journal of Molecular Medicine* 76: 172-183, 1998.

Solanki A, Kim J, Lee K. Nanotechnology for regenerative medicine: nanomaterials for stem cell imaging. *Nanomedicine* 3: 567-578, 2008.

Soriano P. Generalized lacZ expression with the ROSA26 Cre reporter strain. *Nature Genetics* 21: 70-71, 1999.

Stark K, Vainio S, Vassileva G, McMahon AP. Epithelial transformation of metanephric mesenchyme in the developing kidney regulated by *Wnt-4*. *Nature* 372: 679-683, 1994.

Stem Cell Line Derived from Fetal Marrow. *PLoS One* 12: 1-18, 2007.

Sugiyama-Nakagiri Y, Akiyama M, Shibata S, Okano H, Shimizu H. Expression of RNA-Binding Protein Musashi in Hair Follicle Development and Hair Cycle Progression. *American Journal of Pathology* 168: 80-92, 2006.

Sullivan S, Egli D, Akutsu H, Melton DA, Eggan K, Cowan CA. Derivation of human embryonic stem cells. Human embryonic stem cells, *John Wiley & Sons*, 2007.

Sweet DH. Organic anion transporter (Slc22a) family members as mediators of toxicity. *Toxicology and Applied Pharmacology* 204: 198-205, 2005.

Sweet DH, Eraly SA, Vaughn DA, Bush KT, Nigam SK. Organic anion and cation transporter expression and function during embryonic kidney development and in organ culture models. *Kidney International* 69, 837-845, 2006.

Takahashi M. The GDNF/RET signaling pathway and human diseases. *Cytokine and Growth Factor Reviews* 12: 361-373, 2001.

Takahashi K, Yamanaka S. Induction of pluripotent stem cells from mouse embryonic and adult fibroblast cultures by defined factors. *Cell* 126: 663-676, 2006.

Terada N, Hamazaki T, Oka M, Hoki M, Mastalerz DM, Nakano Y, Meyer EM, Morel L, Petersen BE, Scott EW. Bone marrow cells adopt the phenotype of other cells by spontaneous cell fusion. *Nature* 416: 542-545, 2002.

Thadhani R, Pascual M, Bonventre JV. Acute renal failure. *The New England Journal of Medicine* 334: 1448-1460, 1996.

Thirabanjasak D, Tantiwongse K, Thorner PS. Angiomyeloproliferative lesions following autologous stem cell therapy. *Journal of the American Society of Nephrology* 21: 1218-1222, 2010.

Togel F, Hu Z, Welss K, Isaac J, Lange C, Westenfelder C. Administered mesenchymal stem cells protect against ischemic acute renal failure through differentiation-independent mechanisms. *American Journal of Physiology: Renal Physiology* 289, F31-F42, 2005.

Togel F, Welss K, Yang Y, Hu Z, Zhang P, Westenfelder C. Vasculotropic, paracrine actions of infused mesenchymal stem cells are important to the recovery from acute kidney injury. *American Journal of Physiology: Renal Physiology* 292: F1626-F1635, 2007.

Torban E, Dziarmaga A, Iglesias D, Chu LL, Vassilieva T, Little M, Eccles M, Discenza M, Pelletier J, Goodyer P. Pax2 activates Wnt4 expression during mammalian kidney development. *The Journal of Biological Chemistry* 281: 12705-12712, 2006.

Torres M, Gomez-Pardo E, Dressler GR, Gruss P. Pax2 controls multiple steps of urogenital development. *Development* 121: 4057-4065, 1995.

Trupp M, Scott R, Whittemore SR, Ibanez CF. Ret-dependent and independent mechanisms of glial-cell-line derived neurotrophic factor signaling in neuronal cells. *The Journal of Biological Chemistry* 274: 20885-20894, 1999.

Tsang TE, Shawlot W, Kinder SJ, Kobayashi A, Kwan KM, Schughart K, Kania A, Jessell TM, Behringer RR, Tam PP. Lim1 activity is required for intermediate mesoderm differentiation in the mouse embryo. *Developmental Biology* 223: 77-90, 2000.

Ueda S, Mizuki M, Ikeda H, Tsujimura T, Matsumura I, Nakano K, Daino H, Honda Zi Z, Sonoyama J, Shibajama H, Sugahara H, Machii T, Kanakura Y. Critical roles of c-Kit tyrosine residues 567 and 719 in stem cell factor-induced chemotaxis: contribution of src family kinase and PI3-kinase on calcium mobilization and cell migration. *Blood* 99: 3342-3349, 2002.

Unbekandt M and Davies JA. Dissociation of embryonic kidney followed by reaggregation allows the formation of renal tissues. *Kidney International* 77: 407-416, 2010.

Van Wert AL, Gionfriddo MR, Sweet DH. Organic anion transporters: discovery, pharmacology, regulation and roles in pathophysiology. *Biopharmaceutics and Drug Disposition* 31: 1-71, 2010.

Vize P, Woolf A, Bard J. The kidney, from normal development to congenital disease. *Academic Press Amsterdam-Boston-London-New York-Oxford-Paris-San Diego-San Francisco-Singapore-Sydney-Tokyo* 519, 2003.

Wagers AJ, Weissman IL. Plasticity of adult stem cells. *Cell* 116: 639-648, 2004.

Wagner KD, Wagner N, Schedl A. The complex life of Wt1. *Journal of Cell Science* 116: 1653-1658, 2003.

Wartiovaara J, Lehtonen E, Saxén L. Do membrane filters prevent cell contacts? *Nature* 238: 407-408, 1972.

Wartiovaara J, Nordling S, Lethonen E, Saxén L. Transfilter induction in kidney tubules: correlation with cytoplasmic penetration into Nucleopore filters. *Journal of Embryology and Experimental Morphology* 31: 667-682, 1974.

Weissman IL. Stem cells: units of development, units of regeneration, and units in evolution. *Cell* 100: 157-168, 2000.

Wellik DM, Hawkes PJ, Capecchi MR. *Hox11* paralogous genes are essential for metanephric kidney induction. *Genes & Development* 16: 1423-1432, 2002.

Widera D, Zander C, Heidbreder M, Kasperek Y, Noll T, Seitz O, Saldamli B, Sudhoff H, Sader R, Kaltschmidt C, Kaltschmidt B. Adult palatum as a novel source of neural crest-related stem cells. *Stem cells* 27: 1899-1910, 2009.

Xu PX, Adams J, Peters H, Brown MC, Heaney S, Maas R. *Eya1*-deficient mice lack ears and kidneys and show abnormal apoptosis of organ primordia. *Nature Genetics* 23: 113-117, 1999.

Xu PX, Zheng W, Huang L, Maire P, Laclef C, Silviu D. *Six1* is required for the early organogenesis of mammalian kidney. *Development* 130: 3085-3094, 2003.

Ying QL, Nichols J, Evans EP, Smith AG. Changing potency by spontaneous fusion. *Nature* 416: 545-548, 2002.

Yokoo T, Ohashi T, Shen JS, Sakurai K, Miyazaki Y, Utsunomiya Y, Takahashi M, Terada Y, Eto Y, Kawamura T, Osumi, N, Hosoya T. Human mesenchymal stem cells in rodent whole-embryo culture are reprogrammed to contribute to kidney tissues. *Proceeding of the National Academy of Sciences of the United States of America* 102: 3296-3300, 2005.

Zager RA, Andoh T, Bennett WM. Renal cholesterol accumulation. A durable response after acute and subacute renal insults. *American Journal of Pathology* 159: 743-752, 2001.

Zager RA, Johnson ACM, Naito M, Lund SR, Kim N, Bomsztyk K. Growth and development alter susceptibility to acute renal injury. *Kidney International* 74: 674-678, 2008.

Zeisberg M, Shah AA, Kalluri R. Bone morphogenic protein-7 induces mesenchymal to epithelial transition in adult renal fibroblasts and facilitates regeneration of injured kidney. *The Journal of Biochemical Chemistry* 280:8094-8100, 2005.

Zhai XY, Nielsen R, Birn H, Drumm K, Mildenerger S, Freudinger R, Moestrup SK, Verroust PJ, Christensen EI, Gelke M. Cubilin- and megalin-mediated uptake of albumin in cultured proximal tubule cells of opossum kidney. *Kidney International* 58: 1523-1533, 2000.

Zoccali C, Kramer A, Jager KJ. Chronic kidney disease and end-stage renal disease-a review produced to contribute to the report "the status of health in the European union: toward a healthier Europe". *Nephrology Dialysis and Transplantation* 3: 213-224, 2010.